GCAT
TACG
GCAT genes

Special Issue Reprint

Advanced Research in Forensic Genetics

Edited by
Mauro Pesaresi

mdpi.com/journal/genes

MDPI

Advanced Research in Forensic Genetics

Advanced Research in Forensic Genetics

Guest Editor

Mauro Pesaresi

MDPI

Basel • Beijing • Wuhan • Barcelona • Belgrade • Novi Sad • Cluj • Manchester

Guest Editor
Mauro Pesaresi
Department of Biomedical
Sciences and Public Health
Polytechnic University
of Marche
Ancona
Italy

Editorial Office
MDPI AG
Grosspeteranlage 5
4052 Basel, Switzerland

This is a reprint of the Special Issue, published open access by the journal *Genes* (ISSN 2073-4425), freely accessible at: https://www.mdpi.com/journal/genes/special_issues/D54IML41IZ.

For citation purposes, cite each article independently as indicated on the article page online and as indicated below:

Lastname, A.A.; Lastname, B.B. Article Title. *Journal Name* **Year**, *Volume Number*, Page Range.

ISBN 978-3-7258-8845-0 (Hbk)
ISBN 978-3-7258-8846-7 (PDF)
https://doi.org/10.3390/books978-3-7258-8846-7

Contents

About the Editor

Mauro Pesaresi

Mauro Pesaresi is affiliated with the Section of Legal Medicine within the Department of Biomedical Sciences and Public Health at the Polytechnic University of Marche, Ancona, Italy. His core research interests encompass legal medicine, forensic pathology, and the investigation of sudden death, with a specific focus on sudden unexpected death in epilepsy (SUDEP) and sudden cardiac death (SCD). In the field of advanced forensics, his scientific work drives projects centered on nuclear and mitochondrial DNA polymorphisms, DNA persistence, and forensic DNA phenotyping for individual identification. Active research endeavors also target contemporary challenges in legal contexts, particularly activity level propositions and the application of probabilistic genotyping to complex biological traces. His academic achievements include pioneering multidisciplinary methodologies that bridge molecular biology with traditional post-mortem investigations, thereby establishing robust interpretative frameworks to enhance the reliability of genetic evidence within the modern justice system.

Preface

The field of forensic genetics is undergoing a profound transformation driven by rapid technological innovation and increasing interpretative complexity. This Reprint gathers the latest methodological developments, emerging challenges, and future perspectives in contemporary forensic science. The primary aim and purpose of this scientific work is to provide a comprehensive and multidimensional overview of modern forensic genetics, focusing on critical topics such as population diversity, kinship analysis, DNA transfer dynamics, complex and degraded sample analysis, and predictive approaches like forensic DNA phenotyping.

The motivation for compiling this scientific work stems from the crucial need for robust interpretative frameworks that can match the heightened sensitivity of new analytical techniques. As tools like next-generation sequencing and probabilistic genotyping become standard in laboratories, the demand for specialized, shared knowledge becomes vital to ensure that biological evidence is accurately evaluated within legal contexts.

This Reprint is addressed to a broad audience, including forensic biologists, geneticists, medical examiners, legal professionals, and researchers who wish to stay informed about the cutting edge of forensic science.

Mauro Pesaresi
Guest Editor

genes

Editorial

Advanced Research in Forensic Genetics

Mauro Pesaresi * and Alessia Bernini Di Michele

Section of Legal Medicine, Department of Biomedical Sciences and Public Health, Polytechnic University of Marche, Via Tronto, 60126 Ancona, Italy; a.bernini@pm.univpm.it
* Correspondence: m.pesaresi@univpm.it

This Special Issue on advanced research in forensic genetics aims to showcase recent methodological developments, emerging challenges, and future perspectives in a field that is rapidly evolving under the pressure of technological innovation and increasing interpretative complexity. Modern forensic genetics encompasses population genetics, kinship analysis, DNA transfer dynamics, complex and degraded sample analysis and predictive approaches such as forensic DNA phenotyping. The contributions collected in this Special Issue reflect this multidimensional evolution, emphasizing both the opportunities and the critical need for robust interpretative frameworks. This Special Issue brought together six original research articles and two reviews that collectively highlight both the advances and persistent challenges in contemporary forensic genetics.

At the population level, K. Alkaraki et al. [1] provided a clear example of how genetic markers can inform both forensic databases and anthropological interpretation. By analyzing Y-chromosome variation in Jordanian Bedouin and Fellahin groups, the authors demonstrated how social structure, mobility, and cultural practices shape paternal genetic diversity.

A similar concern with interpretation emerges in the work of Kruijver [2], which focused on identity-by-descent (IBD) segments to distinguish biological relationships. This study investigated the evidential value obtained for discriminating between common pedigree relationships if IBD is observed continuously across the autosomal genome without error. In the continuous case, the evidential value is limited only by the pedigree relationship and recombination rates. This highlighted a recurring issue in forensic genetics: as analytical sensitivity increases, so does the complexity of interpreting results within a probabilistic framework.

Another complex field in forensic genetics concerns DNA transfer. The experimental study by Lee et al. [3] demonstrated that secondary DNA transfer between items stored in the same evidence package is far from negligible. Even without direct contact, DNA can transfer in a significant proportion of cases, sometimes influencing forensic interpretation.

These findings align with the broader discussion presented in the review by Bini et al. [4], which examined the role of domestic animals as vectors of human DNA. Pets can act as reservoirs and intermediaries of genetic material, enabling both primary and secondary transfer across multiple steps. Together, these studies emphasize that DNA evidence cannot be interpreted in isolation from mechanisms of transfer and the context in which biological traces are deposited.

The challenge of interpreting DNA evidence is compounded when dealing with complex or degraded samples. The contributions focusing on formalin-fixed, paraffin-embedded (FFPE) tissues illustrated the technical limitations of current methodologies (Lisman et al. [5]). Although improved extraction kits, such as the Maxwell® RSC Xcelerate system, allowed the recovery of relatively high quantities of DNA, the quality of the genetic

material often remained insufficient for complete STR profiling. These findings underlined the need for alternative approaches, such as miniSTRs, SNP panels, and next-generation sequencing, particularly in cases where FFPE samples represent the only available source of DNA.

The use of FFPE tissue is also common in post-mortem analyses, particularly when these blocks represent the only available biological material. This is illustrated by the study conducted by Bernini et al. [6], which investigated genetic variation by analyzing both blood and FFPE tissue samples using NGS techniques. The aim was to identify variants in cardiac genes associated with sudden unexpected death in epilepsy (SUDEP).

Another highly studied topic in advanced research in forensic genetics is forensic DNA phenotyping (FDP). The review by Sessa et al. [7] outlines the current state of the art, with particular attention paid to low-template DNA and the integration of machine learning models to enhance predictive accuracy. However, the authors also stress the importance of addressing ethical considerations and population biases, reminding us that technological innovation must be accompanied by responsible implementation.

González-Ortiz et al. [8] evaluated the performance of FDP using the ForenSeq™ Imagen kit on a Mexican mestizo population. Phenotype prediction was performed using the HIrisPlex-S model, while ancestry inference relied on principal component analysis. The results showed that ancestry, hair and skin color, and sex prediction were generally robust, even under suboptimal DNA conditions. However, eye color prediction was significantly affected by the dropout of key SNPs, leading to reduced accuracy. Overall, the study highlights that FDP performance strongly depends on the presence of specific high-impact genetic markers rather than overall genotype completeness.

Taken together, the contributions in this Special Issue illustrate a field that is rapidly evolving toward greater sensitivity and sophistication. However, they also make clear that progress in forensic genetics is not solely a matter of technological advancement; equally crucial is the development of robust interpretative frameworks that account for population diversity, DNA transfer dynamics, sample quality, and probabilistic reasoning. Bridging these aspects will be essential in ensuring that DNA evidence continues to serve as a reliable and scientifically grounded tool within the justice system.

Conflicts of Interest: The authors declare no conflicts of interest.

References

1. Alkaraki, A.K.; Alsliman, M.B.; Twait, M.M.; Alfonso-Sánchez, M.A.; Peña, J.A. Genetic Diversity of 27 Y-STRs in Two Jordanian Subpopulations: Bedouins and Fellahin. *Genes* **2026**, *17*, 194. [CrossRef] [PubMed]
2. Kruijver, M. An Upper Bound on the Power of DNA to Distinguish Pedigree Relationships. *Genes* **2025**, *16*, 492. [CrossRef] [PubMed]
3. Lee, Y.S.; Syn, C.K.-C. DNA Transfer between Items within an Evidence Package. *Genes* **2025**, *16*, 894. [CrossRef] [PubMed]
4. Bini, C.; Trasatti, A.; Giorgetti, A.; Amurri, S.; Fazio, G.; Pelotti, S. A Mini Narrative Review on Human DNA Transfer Involving Dogs and Cats and Their Role in Forensic Investigation. *Genes* **2026**, *17*, 423. [CrossRef] [PubMed]
5. Lisman, D.; Ossowski, A.; Tołoczko-Grabarek, A.; Kozłowski, M.; Cymbaluk-Płoska, A. Forensic DNA Recovery from FFPE Tissue Using the Maxwell® RSC Xcelerate Kit: Optimization, Challenges, and Limitations. *Genes* **2025**, *16*, 1074. [CrossRef] [PubMed]
6. Bernini Di Michele, A.; Onofri, V.; Melchionda, F.; Fiordelmondo, L.; Ciarimboli, E.; Palpacelli, M.; Sablone, S.; Turchi, C.; Pesaresi, M. Cardiac Genetic Variants in Sudden, Unexpected Death in Epilepsy: From Challenging DNA Extraction Methods to Updated NGS Panels for Improved Genetic Analysis. *Genes* **2025**, *16*, 1272. [CrossRef] [PubMed]

https://doi.org/10.3390/genes17050582

7. Sessa, F.; Dervišević, E.; Esposito, M.; Francaviglia, M.; Chisari, M.; Pomara, C.; Salerno, M. Predicting Physical Appearance from Low Template: State of the Art and Future Perspectives. *Genes* **2026**, *17*, 59. [CrossRef] [PubMed]
8. González-Ortiz, N.; Guardado-Estrada, M.; Zepeta-Flores, N.; Moreno-Ortiz, J.M.; Ramírez-de-Arellano, A.; Rangel-Villalobos, H.; Muñoz-Valle, J.F.; Aguilar-Velázquez, J.A. Performance of the ForenSeqTM Imagen Kit for Forensic DNA Phenotyping under Partial Genotyping Conditions. *Genes* **2026**, *17*, 354. [CrossRef] [PubMed]

https://doi.org/10.3390/genes17050582

genes

MDPI

Review

A Mini Narrative Review on Human DNA Transfer Involving Dogs and Cats and Their Role in Forensic Investigation

Carla Bini, Alessia Trasatti, Arianna Giorgetti *, Sara Amurri, Giulia Fazio and Susi Pelotti *

Section of Legal Medicine, Department of Medical and Surgical Sciences, University of Bologna, 40126 Bologna, Italy; carla.bini@unibo.it (C.B.); alessia.trasatti@studio.unibo.it (A.T.); sara.amurri4@unibo.it (S.A.); giulia.fazio2@unibo.it (G.F.)

* Correspondence: arianna.giorgetti@unibo.it (A.G.); susi.pelotti@unibo.it (S.P.); Tel.: +39-0512088354 (A.G.)

Abstract

Background/Objectives: The potential role of domestic animals in DNA transfer, persistence, prevalence and recovery (TPPR) warrants careful consideration in forensic contexts. This mini narrative review aims to provide an updated overview of human DNA transfer involving household dogs and cats as vectors, to clarify their forensic relevance, and to identify key considerations for the design of future experimental research. Methods: A narrative review was conducted using multiple electronic databases as search engines without restriction related to the timing of publication. Results: Experimental evidence shows that dogs and cats readily acquire human DNA following even brief contact, acting as reservoirs for primary DNA transfer. Once acquired, human DNA can be redistributed via secondary transfer to a wide range of substrates, such as gloved hands, vehicle interiors, clothing, and surfaces. Moreover, multi-step and higher-order transfer events have been documented, highlighting the complexity of DNA transfer involving household animals. Conclusions: The sampling on pets may be included in certain scenarios and may contribute to building a Bayesian network together with the experimental data. To deal with uncertainty during probability assignment, more experimental data, especially addressing the main variables impacting DNA TPPR involving pets, should be generated and are highly needed to assist in activity level evaluation.

Keywords: human DNA transfer; domestic animals; crime scene investigation

1. Introduction

In recent years, increasing attention has been directed toward the factors influencing DNA transfer, persistence, prevalence, and recovery (TPPR) in forensic contexts [1,2]. A persistent limitation lies in the availability of experimental data under conditions relevant to criminal cases even if an increasing number of publications dealing with these issues was observed [3].

As the prevalence of companion animals in domestic settings continues to increase, their potential role in human DNA transfer warrants careful consideration, especially in crime investigation where pets could be vectors of biological evidence.

The sustained and intimate contact between humans and their pets, as well as the interaction of companion animals with intruders and criminal offenders [4] creates favorable conditions for the deposition, accumulation, and persistence of human biological material on animals and on items with which they interact. From a forensic genetics' perspective, these dynamics raise important considerations regarding DNA transfer mechanisms and evidence interpretation in forensic casework [5].

Recent studies have demonstrated that both dogs and cats can harbor detectable quantities of human DNA, predominantly originating from individuals within the household, although contributions from non-household members are also frequently observed [6]. Companion animals may act not only as passive carriers of human DNA, but also as intermediates facilitating its transfer between individuals, objects, and environments [7].

The aim of the present mini narrative review is to provide an updated overview of human DNA transfer involving household pets as vectors, particularly examining the experimental approaches employed in existing studies and evaluating the feasibility and extent of primary, secondary or higher-order transfer. By conducting a methodological synthesis of the published articles on the topic, and considering the multiple variables involved in DNA TPPR, we also aim to identify potential research gaps which may need further investigation, and to discuss the implications of the experimental results for activity level propositions.

Finally, by synthesizing current evidence, the present work aims to enhance understanding of the forensic relevance of companion animals in criminal investigation and to identify key considerations for the design of future experimental research in this emerging field.

2. Materials and Methods

A narrative review was conducted until the end of February 2026 using multiple electronic databases as search engines, particularly PubMed, Scopus, and Web of Science, including articles exploring the topic of DNA transfer using household pets. Search terms used were "forensic", "DNA transfer" combined with "pet", "dog", "cat", "domestic animal". No restriction related to the timing of publication was applied. Only articles published in English were considered, while book chapters were not included.

References to the included articles were cross-checked for inclusion.

From the included articles, the following data were extracted: authors and year of publication, type of article, whether original article or short communication/conference proceedings, experimental design, technical characteristics, including sampling methods, DNA extraction, quantification and amplification, and main findings of the study. Experimental design and main findings of the studies were briefly summarized by the authors.

The screening of the databases was conducted by multiple reviewers, and disagreements were managed to uniform the terminology, deciding to adopt the authors' one. No gray literature was included because it was missing.

3. Results

The present mini review identified a limited number (n = 6) of articles specifically addressing human DNA transfer involving pet and household animals, summarized in Table 1.

Among these, three studies focus on dogs, two on cats, and one included both. The emergence of the research topic of human DNA transfer involving domestic animals as vectors appears recent, since all articles were published from 2022 onwards [5].

https://doi.org/10.3390/genes17040423

Table 1. Summary of the studies reviewed, including authors, year of publication and type of article (Ref.), experimental design, technical procedures and main findings.

Ref.	Experimental Design	Technical Procedures	Main Findings
Monkman H. et al. 2022 [5] Short communication	A total of 20 cats from 15 households - **Samples on cats**: from the right side. - Reference samples from every person in household. Questionnaires on cats' behaviors, living environment and recent human contacts.	Double swabbing technique. Extraction: DNA IQ System (Promega, Madison, WI, USA). Quantification: Quantifiler® Trio system (Life Technologies, Carlsbad, CA, USA). DNA Amplification: PowerPlex® 21 system (Promega, Madison, WI, USA).	- **Samples on cats**: 80% of samples showed detectable human DNA (average 0.22 ng). Interpretable profile in 70% of samples. - In 66.7% of interpretable profiles, one person from the household was detected. The last person to contact the cat was detected as the major or single source contributor. - DNA from unknowns was observed in 8/18 of interpretable profiles.
Monkman H. et al. 2023 [8] Original article	A total of 20 dogs, 9 samples per dog: - **Indirect transfer**: gloves after scratching and patting the dog and plastic floor after pet walking. - **Samples on dogs**: chest, head, back, left side under the fur and right-side surface of the fur, stomach. - **Direct transfer**: sample from dog neck after scratching with bare hand. Questionnaire to the primary carer of the dog regarding living conditions, interactions, and grooming. Reference samples: dog's owners and residents of the household.	Wet–dry swabbing technique using viscose swabs. Extraction: DNA IQ System (Promega, Madison, WI, USA). Quantification: Quantifiler® Trio. DNA system (Life Technologies, Carlsbad, CA, USA). DNA Amplification: PowerPlex® 21 System (Promega, Madison, WI, USA).	- **Indirect transfer**: human detectable DNA on 19/20 occasions of secondary transfer to gloves (median 0.09 ng) and 9/20 to simulated floor (median 0.0 ng). - **Samples on dogs**: human detectable DNA in 70.8% (median 0.06 ng). Best recovery from the surface of the fur, head and back than under the fur. - Of 120 samples, in 61.7% the MNC was assigned (49 samples with two persons mixture, 7 samples, three persons mixture and 18 single source). - Of 120 profiles, 39.2% showed human DNA from unknown sources. - **Direct transfer** (from bare hands patting the dogs): occurred in 50% of cases.
Monkman H. et al. 2025 [9] Original article	A total of 20 cats, 6 samples per cat: - **Background samples**: the top of the fur cat's head, back and right side, left side skin base of the fur. - **Secondary transfer**: palm and fingers of glove after scratching and patting the cat. - **Direct transfer**: cat's chest and neck after scratching with bare dominant hand. Questionnaire to the carer of the cat regarding living conditions, habits, interactions and grooming.	Wet–dry double swabbing technique using viscose swabs. Extraction: DNA IQ System (Promega, Madison, WI, USA). Quantification: Quantifiler® Trio DNA (Applied Biosystems, Waltham, MA, USA). DNA Amplification: PowerPlex® 21 System (Promega, Madison, WI, USA).	- **Background samples**: detectable DNA from 69% of samples. Highest DNA yields from back fur (mean 0.36 ng), head fur (0.33 ng), right fur (0.22 ng), and skin at the base of the fur (0.06 ng). - In total, 29% did not produce a profile; 54% generated a profile with more than 4 alleles, of which 79% showed the owner's profile. - DNA from an unknown source was detected in 47% of samples with more than 4 alleles. - **Secondary transfer** (from the cat to gloves) occurred in 80% of trials, yielding quantifiable DNA in 16 of 20 glove samples (mean 0.18 ng). DNA typing showed the owner profile in 12/14 of samples with more than 4 alleles. - **Direct transfer** (following brief patting with bare hands): 75% samples showed quantifiable DNA with a mean recovered amount of 0.11 ng. Donor DNA was transferred to the cat in 25% of the 20 samples collected.

https://doi.org/10.3390/genes17040423

Table 1. *Cont.*

Ref.	Experimental Design	Technical Procedures	Main Findings
Monkman H. et al. 2025 [10] Original article	A total of 5 dogs, visitors drove to the dog's household, interacted for 5 min with the dog, patting and playing, returned to the car and drove home, where they were instructed to make tea. - DNA samples collected from the **first 5 surfaces** contacted **in the car** by visitors prior to home return. - DNA samples from the **first 3 items** touched by visitors on arrival at home. - DNA samples collected from the **kettle, mug** and **visitor's hands** at home. - DNA samples collected from two areas where the dogs spent time post-interaction. - **Samples on dogs**: left side of the body, right side of the body, top of the head, top of the back. Questionnaire to the carer of the dog regarding the visitor's living conditions, number of housemates and frequency of visitors.	Wet–dry double swabbing technique using viscose swabs. Extraction: DNA IQ System (Promega, Madison, WI, USA). Quantification: Quantifiler® Trio DNA (Applied Biosystems, Waltham, MA, USA). DNA Amplification: PowerPlex® 21 System (Promega, Madison, WI, USA).	- From the **first 5 surfaces** contacted **in the car** by visitors, the average DNA quantity was 4.25 ng. A DNA profile was generated from all surfaces. The dog owner's DNA was detected in 33% of samples. - From the **first 3 items** touched by visitors at home, the average DNA recovered was 3.54 ng. 93% of samples generated a DNA profile. The dog owner was excluded from all of these samples. - From the **kettle and mug**, average DNA recovered was 1.37 and 2.70 ng, respectively. The dog owner profile was detected in 30% of these samples. - From the **visitor's hands**, the average DNA recovery was 5.4 ng from dominant hand and 4.1 ng from a non-dominant hand. The dog owner profile was detected in 80% of these samples. - **Samples on dogs**: From the two areas where the dogs spent time post-interaction, average recovered DNA was 2.3 ng not showing the visitor's profile. From the dog's head, back or sides, quantifiable DNA was recovered in all samples (average 1.4 ng) and in 50% of samples the visitor's or visitor's related person was transferred.
Oefelein R. et al. 2025 [6] Short communication	A total of 10 domestic pets (5 canines and 5 felines) - **Background samples:** back, ears/head, nose/mouth. - **Secondary transfer**: 3 samples on a smooth plastic card rubbed on the animal's same areas. LR calculation following propositions: (H1): Primary Pet Owner + N-1 Unknowns/ (H2): N Unknowns.	Single swabbing—cotton swab for pets. Double swabbing—wet and dry cotton swab for card samples. Extraction: Maxwell™ FSC DNA IQ™ Casework Kit with Promega Casework Extraction Kit (Promega, Madison, WI, USA). Quantification: PowerQuant® System (Promega, Madison, WI USA). DNA Amplification: Powerplex Fusion 6C system (Promega, Madison, WI, USA).	- **Background samples:** canines presented higher levels of background DNA (average 0.98 ng) than cats (average 0.11 ng). - In total, 53% of background feline samples and 80% of background canine samples were suitable for amplification. - In total, 31% of background samples were suitable for comparison supporting H 1 in 16/19 samples and H2 in 3/19. - **Secondary transfer**: human DNA was detected with an average DNA of 0.01 ng. - In total, 13% of secondary transfer feline samples and none of canine were suitable for amplification. - No sample produced DNA profiles suitable for comparison.

https://doi.org/10.3390/genes17040423

Table 1. *Cont.*

Ref.	Experimental Design	Technical Procedures	Main Findings
Monkman H. et al. 2026 [7] Original article	A total of 5 dogs, 5 cars, 1 holder, different shirt worn per experiment. Simulated dog-theft involving brief lifting and transporting by a handler, placing in an unfamiliar car (20 min), and return home by lifting and holding - **Background samples from cars** not associated with the dogs. - **Samples on dogs**: 1 h after simulated theft, 4 samples per dog (head, neck, sides). - **Samples from car** 4 h **after the simulated theft.** - **Samples of the holder's t-shirt**: left, right arms, abdomen, chest worn by the holder the day after (n = 20). - DNA reference samples from the dog owners, car owners, car users and the holder. Questionnaires to owners on number of owners, preferred locations of the dog in house, regular activities. Bayesian network built.	Wet–dry double swabbing technique using viscose swabs and sterile water. Extraction: DNA IQ System (Promega, Madison, WI, USA). Quantification: Quantifiler® Trio DNA (Applied Biosystems, USA) Quantifiler Kit on a 3500xL Genetic Analyser, GeneMapper™ ID-X Software v1.6Amplification: PowerPlex® 21 System (Promega, Madison, WI, USA).	- **Background samples from the car**: in 9 samples DNA in quantity range 0.12–3.420 ng. - **Samples on dogs**: average DNA 0.79 ng, the least (av 0.36) from the left side. DNA profile from the owner (s) 85% of samples. DNA from the holder in 40%. Unknown DNA in 70% of the samples. - **Samples from car** 4 h **after the simulated theft:** DNA recovery on 18/19 samples of car (average quantity 1.81 ng). DNA of car owners in 47% of samples. DNA of dog owners in 35% of samples. DNA of the holder in 35% of samples and in 13% excluding the car belonging to the holder. - **Samples of the holder's t-shirt:** DNA present in all the 20 samples (average 1.51 ng). DNA of car owners in 5% of samples (1 of 20) as minor contributor. DNA of dog owners in 10% of samples as minor contributor. The holder was detected in 85% of samples as sole or major contributor. At least one unknown contributor was detected in 75% of the samples as single source or minor contributor. Bayesian Network analysis demonstrated that dog-derived DNA can be useful for activity level propositions.

4. Discussion

The recent concentration of publications on human DNA transfer involving domestic animals suggests an increasing awareness of the potential forensic relevance of primary and secondary DNA transfer involving domestic animals, particularly in indoor environments. On the other hand, the limited number of studies and their recent publication dates highlight the preliminary nature of this research field and underline the need for further investigation to better characterize the human DNA transfer via household pets, as recommended by the authors in the forensic context.

4.1. Experimental Design

The experimental designs described in the reviewed studies involved a sample size between 5 and 20 animals and were based on a common framework of either background (naturalistic) conditions or controlled or semi-controlled models simulating typical human–domestic animal interactions. In the latter, dogs and cats were involved in contact scenarios with owners, household members, external individuals, and selected surfaces or objects to assess human DNA transfer.

Sampling was primarily focused on fur-covered areas, with samples collected immediately after contact or at short post-contact intervals. The presence and origin of background human DNA on domestic cats was first assessed in a preliminary study published in 2022, involving naturalistic conditions of 15 households [5]. In this study, sampling was limited to the cat's right side, with no further specification. In the following study of Monkman H et al., 2023, both the surface of the fur and the skin beneath it were sampled, demonstrating higher human DNA quantities from the former [8]. This may be explained by the fact that the fur of animals is more exposed to the environment and is therefore more likely to come

https://doi.org/10.3390/genes17040423

into contact with humans and their surrounding surfaces, compared to the inner surface, which is protected by fur [9]. The top of the fur is thus recommended for sampling to recover human DNA.

Multiple sites of sampling were analyzed in four studies, two involving dogs, one cat and one both, with head and back providing the best human DNA recovery both for dogs [8] and cats [9]. These areas are thus suggested for recovery of human touch DNA on companion animals. Interestingly, although domestic animals also use to ingest and lick the fur on the stomach area, significantly less DNA was recovered on dogs from this area compared to other sampling areas on fur [8], so that the sampling from stomach area is not suggested for future studies on dogs.

The characteristics of the fur, e.g., length and porosity, the shedding abilities of the owners and animals as well as differences between indoor and outdoor pets, to the best of the authors knowledge, have not been extensively investigated in experimental studies yet. Fur length, classified as short, medium, or long, was mentioned in the 2022 study involving cats, but no significant difference in the amount of human DNA was found depending on this characteristic [5]. Similarly, the dog breeds and the fur length were specified for dogs in the most recent study, but these variables were not used for correlation analysis [7].

Factors that certainly influence the amount of DNA recovered, and should thus be considered in an experimental design, include washing time frames and human proximity and interactions [8], with particular reference to the nature of a pat, where limited force is applied as opposed to the force typically applied when a person uses an item [11].

Brief contacts with holders or patters or scratchers were mostly simulated in the experiments, while persistence of human DNA has not been thoroughly investigated yet [7].

Moreover, scenarios with variable connections between pet owner and offender, different environmental and dog transportation conditions are suggested, especially in relationship to animal kidnapping cases [7].

4.2. Technical Issues

Five out of six articles included in our review (83%) involved a double wet–dry swabbing method, although no experimental comparison of DNA recovery efficiency between different swab types has been conducted on domestic animals. The double-swab technique has been indicated as preferable for DNA recovery from complex surfaces [12], especially in the case of touch DNA [13].

For background samples collection, among our series, Oefelein R. et al. was the only study using cotton swabs for human DNA collection from pets back, ears/head and nose/mouth [6], and showed lower DNA recovery from cats (average 0.11 ng) compared to other studies (median 0.22 ng [5], 0.36–0.33 ng on back and head [9]). On the other hand, human DNA recovered from dogs (average 0.98 ng [6]) was higher than the median reported by Monkman et al. (median 0.06, from 0 to 1.26 ng [8]), making it complex to clearly establish a preferred sampling strategy, as expected for the influence of the variables in the experimental design.

A recent study on wildlife specimens compared the effectiveness of human DNA touch recovery methods, particularly cotton swabs (used as wet swabs followed by a second dry swab), flocked swabs and foam swabs (both used as a single swab, with one wetted side followed by the dry side), as well as minitapes, showing that foam swabs significantly yielded higher DNA recovery for antelope fur [14]. In the absence of pet-specific validation studies, one might also consider extrapolating the best recovery method from research on human hair. To the best of the authors' knowledge, there is no consensus on the optimal approach for recovering exogenous human DNA from human hair [15]. A study showed that the moistened swab, compared to other cleaning methods, was the most

https://doi.org/10.3390/genes17040423

effective way to obtain both the hair and exogenous DNA from a human hair stained with biological material [16]. Nevertheless, findings from studies on pet fur may provide useful methodological insights for humans, rather than the reverse [15].

4.3. Background Human DNA and Profiles

The first study on background DNA on companion animals involved cats. The presence of human DNA was assessed on the right side of the pet in 80% of samples, with an average amount of 0.22 ng (range from 0 to 1.32 ng) [5].

A slightly lower percentage of samples with detectable quantities of human DNA (70.8%) was reported in the study of Monkman H. et al. on dogs [8]. Average amounts were lower, with a median of 0.06 ng, although this might be due to the multiple different sites sampled on dogs, including the stomach. Indeed, also when sampling multiple areas of cats, 69% of background samples provided detectable human DNA [9], highlighting the influence of anatomical sites on DNA deposition and recovery. When comparing background DNA on cats and dogs, Oefelein R. et al. found higher amounts on dogs (0.98 ng vs. 0.11 ng) and higher percentage of samples suitable for amplification (80% vs. 53%), and this was attributed to the available surfaces for sampling or different behavior of pets [6].

Nevertheless, washing the fur of the animal, as well as the characteristics of the shampoo and fur, could impact the presence and persistence of human DNA on household pets, similarly to hand cleaning that impacts the recovery of touch DNA from humans [17]. However, in the study by Monkman H. et al., the washing time frames, considered to interpret the results of DNA amount on dogs, did not impact the DNA recovery [8].

Variability in recovered DNA among different pets might additionally be related to different interactions between the owner and the pet, which also vary by the size of dogs, with smaller dogs having usually more intense contacts [8].

Other factors apparently did not impact the amount of human DNA recovered from pets, including the number of house occupants and amount of time spent with the pet, although the limited small dataset of the studies does not allow us to draw firm conclusions [8]. In most of the studies, persons from the household were detected in the majority of interpretable profiles, both on dogs [8] and cats, ranging in the latter from 66.7% to 79% [5,9], and up to 16 of 19 samples (84.2%) considering both pets [6].

In the first study by Monkman H. et al., although there was no significant difference between the amount of DNA present on the cat and the time since the cat was last contacted, the last person to touch the cat was mostly detected as the major or single source contributor [5]. Nevertheless, as suggested by the presence of a different number of contributors in two cats living in the same household, direct contact might not be the most impacting factor on human DNA presence. Other factors including the shedder status and the behavior of the cat, could be relevant for human DNA presence [5]. Again, in another study involving cats, the last person to have contact with the cat was detected in 61% of the samples [9].

Contrarily, considering dogs, the last person to contact the pet, as emerged from a questionnaire compiled by the carer of the dog, was only detected in 35% of samples, and higher DNA recovery was yielded from areas that were not the most recently contacted [8].

The observed dissimilarities between cats and dogs may be explained by differences between the typical cat–human and dog–human interaction: cats generally show limited active physical interaction with their owners, usually choose specific locations to rest and a preferred person to spend time with. In most cases, this preferred owner was also the last person to have contact with the animal prior to sampling, which could explain the greater accumulation of that individual's DNA. Contrarily, dogs are closer and interact more with all their owners [9,18].

https://doi.org/10.3390/genes17040423

It is interesting to note that, despite reference profiles being obtained from the owner as well as from the other residents of the household in all studies, DNA from unknown sources was commonly observed in 47% of samples with five or more alleles in one study on cats [9], in 44.4% of interpretable profiles on cats in another study [5], and in 39.2% of interpretable profiles on dogs [8]. This was additionally confirmed in the simulated dog-theft experiment, where 70% of samples provided unknown DNA, with a total of 17 unknown donors detected across 14 samples out of 20, as already well-known from touch DNA and DNA transfer studies [7]. The high prevalence of unknown profiles could arise from the close interaction with the environment and with potentially contaminated surfaces usually contacted by pets, such as the floor [8]. Future research should investigate the role of realistic environmental factors, to minimize the gap between experimental and real-world scenarios relevant for forensic purposes.

4.4. Primary Transfer to Animals

The studies included in the present mini review demonstrated that human DNA transfer could occur to dogs [7,8] and cats [9], even after a single contact, especially if it consists of scratching/patting the animal. An example of primary transfer or direct transfer is shown in Figure 1.

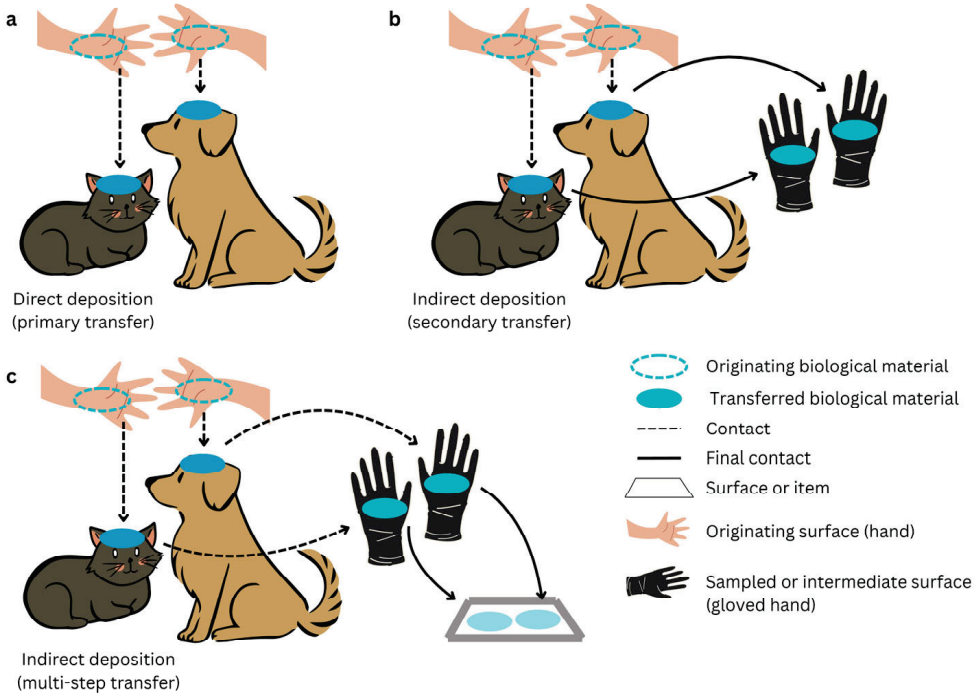

Figure 1. (**a**) An example of direct deposition or primary transfer. (**b**) An example of indirect deposition or secondary transfer. (**c**) An example of indirect deposition with multi-step transfer.

After a single scratch on the necks of dogs, median amounts of human DNA transferred were 0.09 ng, with a maximum of 0.4 ng, and 70.8% of samples showing human detectable DNA. In this case, 50% profiles matched the individual patting the dog [8].

A short one-time patting on cats, chosen to simulate a possible contact between an offender and the animal in a potential crime scene, did not always result in the detection of the patter's DNA. Although quantifiable DNA was recovered from 75% of cats after contact with bare hands, the transfer from the patter to the cat was only detected in 25% of samples [9].

Higher percentages of transfer rate were observed in another recent experimental study, where holders were asked to pick up dogs and put them in a car, simulating a

https://doi.org/10.3390/genes17040423

"dog—napping" scenario: the profile of the holder was identified in 40% of samples on dog [7]. The transfer of holders' DNA occurred with contact of approximately 2 min, suggesting that the duration of the contact, as expected, influences the human TPPR [7]. Another possible influencing factor was hypothesized as the area of contact, since larger dogs had to be "secured" by the holder for transportation, and these dogs corresponded to the ones carried for longer times [7].

In another study, Monkman H. et al. [10] investigated the persistence and transfer of human DNA following brief human–dog interactions. After a five-minute pat-and-play interaction, DNA from the visitors or their housemate was recovered from the dog's head, back, or sides in 50% of samples (10/20) one hour after contact. Visitor-associated DNA was never the major contributor, appearing only as a minor component in 35% of samples (7/20). Notably, DNA from a visitor's housemate, who had no direct contact with the dog, was detected in 15% of samples (3/20), all of which originated from the same animal [10].

4.5. Secondary Transfer from Animals to Other Surfaces

A figure with an example of indirect or secondary transfer is shown in Figure 1. Detectable human DNA was transferred via dogs, used as vectors, to gloved hands scratching the animal on 95% of cases in the study of Monkman H. et al. DNA recovery on gloves ranged from 0.0 to 2.0 ng, with a median of 0.09 ng. Generated profiles mostly reflected the mixture of individuals found on the dogs' fur [8].

In a study on cats, detectable and quantifiable DNA was found in 80% of samples collected from the gloves after contacting, with a recovery ranging between 0.0 and 0.72 ng. Even if not statistically significant, it emerged that cats with a higher level of background DNA were able to transfer higher amounts of DNA to the gloves. In most cases, the DNA belonged to the cat's owner, consistent with cats' tendency to prefer a specific owner and spend more time with them [9].

On the contrary, a maximum DNA amount of 0.4 ng was obtained from plastic sheets simulating the floor upon which dogs walked. This lower DNA amount might reflect DNA loss while walking, the small areas of paws contacting the floor, the background DNA on the plastic sheets simulating the floor or an area-related lower DNA persistence compared to other dogs' surfaces, e.g., in the hypothesis of greater washing and licking of the paws by the dog, or extraction inhibition due to the dirt [8].

The secondary transfer on another plastic surface as plastic card, rubbed against the back, ears/head and nose/mouth of cats and dogs in the study by Oefelein R. et al. [6], showed very low DNA amounts (average 0.01 ng) and no profiles suitable for comparisons. The authors hypothesized that this result was due to use of a smooth surface, while other rough surfaces might be investigated.

In the "dog—napping" simulation, DNA of both the dog owners (35% detection rate) and of the dog holders (13% detection rate) was recovered from the surfaces of the car in which the dog was placed after the dog occupation, most likely indicating indirect transfer via the dogs [7]. The transfer of dog owners' DNA was considered rather high compared to previous studies exploring indirect human DNA transfer under uncontrolled conditions [19,20]. The higher DNA transfer could be related to the higher shedder status of the participants even if not assessed in the study or to differences in activities involved, as reported by authors [7]. It is well known that the shedder status is one of the most important variables impacting the quantity of DNA deposited, with several papers demonstrating differences between good and bad shedder. The profile of good shedder has been found even on objects they never handled [2].

In the same experiment, indirect transfer from the dog owner to the shirt of the dog holders also occurred, with dogs acting as vectors, with a detection in 10% of the samples.

https://doi.org/10.3390/genes17040423

Interestingly, one of the dog owners' DNA was detected on dog, on the car where the dog was placed after pick up, and on the shirt of the dog holder, suggesting multi-step DNA transfer, considering that the study was performed under controlled conditions: the owner had not previously contacted the car or the holder on the t-shirt [7].

The study of Monkman H. et al. [10] investigating the impact of a five-minute pat-and-play interaction between humans and dogs demonstrated that dog owner DNA was transferred from the animal to the visitor, and subsequently to the visitor's secondary touched surfaces in 33% of samples from the car and in 30% from kettle and mug touched by visitors at home. However, analysis of car surfaces contacted immediately after the visit revealed visitor's DNA profile on all five car items as the major or predominant contributor and on the kettle and mug in 60% of the samples.

Data generated with similar experimental designs involving transfer events, as in the simulated "dog—napping" of Monkman H. et al. [7], were tested in only one study with a Bayesian network, but appeared to be informative for the DNA activity level evaluation.

Actually, nowadays the activity level evaluation represents a significant challenge for forensic genetics, which has shifted attention from the answer to the 'Who?' question to the 'How?' one. The application of Bayesian networks to inference problems involving the results of DNA analyses provides the likelihood of DNA findings given competing propositions of interest with respect to the activities aware of variables impacting DNA TPPR [2]. Improving the knowledge on TPPR through investigation and experimental data presentation may assist evaluation of evidence under propositions considering DNA transfer mechanism.

5. Conclusions and Future Perspectives

This review summarizes current evidence supporting the forensic relevance of domestic pets in primary and secondary human DNA transfer. Despite most studies involving a limited number of replicates, they provided data from various experimental designs simulating forensic scenarios and foundational methodologies for larger cohort studies.

The studies showed that household animals create multiple opportunities for direct but also multi-step indirect transfer of human biological material, with the need to differentiate between criminal activity-related transfer and innocent contacts. Overall, the complex dynamic of DNA transfer shows potential implications for the interpretation of forensic evidence in crime scenes. Actually, evaluation of a DNA profile from human biological traces requires us to determine the diagnostic value of findings given activity level propositions [21] that should consider the mechanisms of DNA TPPR able to impact the findings.

Recently, the novel term of contextual sampling was introduced to indicate the targeted collection of additional samples from the surroundings of crime-related items to assign probabilities on prevalence and background based on case-relevant data [21]. The sampling on pets may be included in certain scenarios within the contextual sampling and may contribute to some nodes of a Bayesian network, together with the experimental data informing additional nodes.

Notably, only one study within the reviewed literature implemented a Bayesian network approach to model transfer dynamics at the activity level, illustrating the potential of a probabilistic framework to account for competing propositions. Building on this approach, to deal with uncertainty during probability assignment, more experimental data should be generated and are highly needed to assist in activity level evaluation. Actually, variables can be combined in a Bayesian network to evaluate evidence with regard to the relevant activities at stake [22]. Further studies should follow The ReAct (Recovery, Activity) project, an ENFSI (European Network of Forensic Science Institutes) initiative with

https://doi.org/10.3390/genes17040423

the primary purpose to design experiments simulating typical casework circumstances; collect data and to implement Bayesian networks to assess the value (i.e., likelihood ratio) of DNA results given activity level propositions [23]. As highlighted by the present mini review, future research should explore the main variables impacting DNA TPPR when pets are involved, as, among others, the transfer of primary touch DNA after different time periods, the awareness of general levels of background DNA [2] and also consider factors such as sampling method, prevalence and persistence of DNA, the influence of behavior of pets, environmental contamination, shedding status of the participants, and human–animal interactions in pet-involved crimes.

Author Contributions: Conceptualization, S.P. and C.B.; methodology, A.G.; formal analysis, A.T.; data curation, S.A. and G.F.; writing—original draft preparation, A.T. and A.G.; writing—review and editing, C.B. and A.G.; supervision, S.P. All authors have read and agreed to the published version of the manuscript.

Funding: This research received no external funding.

Institutional Review Board Statement: Not applicable.

Informed Consent Statement: Not applicable.

Data Availability Statement: No new data were created or analyzed in this study.

Conflicts of Interest: The authors declare no conflicts of interest.

References

1. van Oorschot, R.R.A.H.; Szkuta, B.; Meakin, G.E.; Kokshoorn, B.; Goray, M. DNA transfer in forensic science: A review. *Forensic Sci. Int. Genet.* **2019**, *38*, 140–166. [CrossRef]
2. van Oorschot, R.A.H.; Meakin, G.E.; Kokshoorn, B.; Goray, M.; Szkuta, B. DNA Transfer in Forensic Science: Recent Progress towards Meeting Challenges. *Genes* **2021**, *12*, 1766. [CrossRef] [PubMed]
3. Kokshoorn, B.; Aarts, L.H.J.; Ansell, R.; Connolly, E.; Drotz, W.; Kloosterman, A.D.; McKenna, L.G.; Szkuta, B.; van Oorschot, R.A.H. Sharing data on DNA transfer, persistence, prevalence and recovery: Arguments for harmonization and standardization. *Forensic Sci. Int. Genet.* **2018**, *37*, 260–269. [CrossRef] [PubMed]
4. Monkman, H.; van Oorschot, R.A.H.; Goray, M. Video analysis of human and animal interactions for possible use in forensic human DNA identification. *Aust. J. Forensic Sci.* **2024**, *56*, 84–86. [CrossRef]
5. Monkman, H.; van Oorschot, R.A.H.; Goray, M. Is there human DNA on cats. *Forensic Sci. Int. Genet. Suppl. Ser.* **2022**, *8*, 145–146. [CrossRef]
6. Oefelein, R.; Cresswell, S.; Matheson, C. Transfer and persistence of owner DNA on domestic pets. *Sci. Justice* **2025**, *65*, 83–91. [CrossRef]
7. Monkman, H.; van Oorschot, R.A.H.; Luke, V.; Goray, M. Investigation of human DNA transfer during mock dog-napping. *Forensic Sci. Int.* **2026**, *378*, 112724. [CrossRef]
8. Monkman, H.; Szkuta, B.; van Oorschot, R.A.H. Presence of Human DNA on Household Dogs and Its Bi-Directional Transfer. *Genes* **2023**, *14*, 1486. [CrossRef]
9. Monkman, H.; van Oorschot, R.A.H.; Goray, M. The role of cats in human DNA transfer. *Forensic Sci. Int. Genet.* **2025**, *74*, 103132. [CrossRef]
10. Monkman, H.; van Oorschot, R.A.H.; Goray, M. Paws for a moment: Investigation of bi-directional transfer of human DNA during a short human-dog interaction and subsequent indirect transfers. *Sci. Justice* **2025**, *65*, 101312. [CrossRef]
11. Atkinson, K.; Arsenault, H.; Taylor, C.; Volgin, L.; Millman, J. Transfer and persistence of DNA on items routinely encountered in forensic casework following habitual and short-duration one-time use. *Forensic Sci. Int. Genet.* **2022**, *60*, 102737. [CrossRef]
12. Hedman, J.; Jansson, L.; Akel, Y.; Wallmark, N.; Gutierrez Liljestrand, R.; Forsberg, C.; Ansell, R. The double-swab technique versus single swabs for human DNA recovery from various surfaces. *Forensic Sci. Int. Genet.* **2020**, *46*, 102253. [CrossRef]
13. Verdon, T.J.; Mitchell, R.J.; van Oorschot, R.A. Swabs as DNA collection devices for sampling different biological materials from different substrates. *J. Forensic Sci.* **2014**, *59*, 1080–1089. [CrossRef]
14. Thomas, A.; McColl, S.; Rae, R.; Ogden, R.; Gibson, L.; Dawnay, N. Human DNA recovery in the context of wildlife crime: Comparison of trace DNA collection methods from wildlife specimens. *Forensic Sci. Int. Genet.* **2026**, *81*, 103361. [CrossRef] [PubMed]

https://doi.org/10.3390/genes17040423

15. Woollacott, C.; Goray, M.; van Oorschot, R.A.H.; Taylor, D. The Transfer, Prevalence, Persistence, and Recovery of DNA from Body Areas in Forensic Science: A Review. *Forensic Sci.* **2025**, *5*, 9. [CrossRef]
16. Naue, J.; Sänger, T.; Lutz-Bonengel, S. Get it off, but keep it: Efficient cleaning of hair shafts with parallel DNA extraction of the surface stain. *Forensic Sci. Int. Genet.* **2020**, *45*, 102210. [CrossRef]
17. Bini, C.; Giorgetti, A.; Fazio, G.; Amurri, S.; Pelletti, G.; Pelotti, S. Impact on touch DNA of an alcohol-based hand sanitizer used in COVID-19 prevention. *Int. J. Leg. Med.* **2023**, *137*, 645–653. [CrossRef]
18. Joosten, P.; Van Cleven, A.; Sarrazin, S.; Paepe, D.; De Sutter, A.; Dewulf, J. Dogs and Their Owners Have Frequent and Intensive Contact. *Int. J. Environ. Res. Public Health* **2020**, *17*, 4300. [CrossRef]
19. Cahill, A.; Volgin, L.; van Oorschot, R.A.H.; Taylor, D.; Goray, M. Where did it go? A study of DNA transfer in a social setting. *Forensic Sci. Int. Genet.* **2024**, *73*, 103101. [CrossRef]
20. Zacher, M.; van Oorschot, R.A.H.; Handt, O.; Goray, M. Transfer and persistence of intruder DNA within an office after reuse by owner. *Forensic Sci. Int. Genet.* **2024**, *73*, 103130. [CrossRef]
21. Goedhart, Y.R.; de Koeijer, J.A.; Aarts, L.H.J.; de Poot, C.J.; Kokshoorn, B. Contextual DNA samples in evaluations given activity level propositions. *Forensic Sci. Int. Genet.* **2026**, *84*, 103452. [CrossRef]
22. Taroni, F.; Biedermann, A.; Bozza, S.; Garbolino, P.; Aitken, C.G.G. *Bayesian Networks for Probabilistic Inference and Decision Analysis in Forensic Science*, 2nd ed.; John Wiley & Sons: Hoboken, NJ, USA, 2014.
23. Gill, P.; Fonneløp, A.E.; Hicks, T.; Xenophontos, S.; Cariolou, M.; van Oorschot, R.; Buckel, I.; Sukser, V.; Papić, S.; Merkaš, S.; et al. The ReAct project: Analysis of data from 23 different laboratories to characterise DNA recovery given two sets of activity level propositions. *Forensic Sci. Int. Genet.* **2025**, *76*, 103222. [CrossRef]

https://doi.org/10.3390/genes17040423

genes

Article

Performance of the ForenSeq™ Imagen Kit for Forensic DNA Phenotyping Under Partial Genotyping Conditions

Nayeli González-Ortiz [1,2], Mariano Guardado-Estrada [3], Nahum Zepeta-Flores [3], José Miguel Moreno-Ortiz [4], Adrián Ramírez-de-Arellano [5], Héctor Rangel-Villalobos [6], José Francisco Muñoz-Valle [7] and José Alonso Aguilar-Velázquez [1,*]

[1] Laboratorio de Ciencias Morfológico Forenses y Medicina Molecular, Departamento de Morfología, Centro Universitario de Ciencias de la Salud, Universidad de Guadalajara, Guadalajara 44340, Jalisco, Mexico
[2] Doctorado en Genética Humana, Departamento de Biología Molecular y Genómica, Centro Universitario de Ciencias de la Salud, Guadalajara 44340, Jalisco, Mexico
[3] Laboratorio de Genética, Escuela Nacional de Ciencias Forenses, Universidad Nacional Autónoma de México, Ciudad de México 04510, Mexico
[4] Instituto de Genética Humana "Dr. Enrique Corona Rivera", Departamento de Biología Molecular, Centro Universitario de Ciencias de la Salud, Universidad de Guadalajara, Guadalajara 44340, Jalisco, Mexico
[5] Instituto de Investigación en Cáncer e Infecciones, Departamento de Microbiología y Patología, Centro Universitario de Ciencias de la Salud, Universidad de Guadalajara, Guadalajara 44340, Jalisco, Mexico
[6] Instituto de Investigación en Genética Molecular, Departamento de Ciencias Médicas y de la Vida, Centro Universitario de la Ciénega, Universidad de Guadalajara, Ocotlán 47810, Jalisco, Mexico
[7] Instituto de Investigación en Ciencias Biomédicas, Centro Universitario de Ciencias de la Salud, Universidad de Guadalajara, Guadalajara 44340, Jalisco, Mexico
* Correspondence: ja.aguilarvelazquez@gmail.com

Abstract

Background: Forensic DNA phenotyping (FDP) enables the inference of externally visible characteristics (EVCs) and biogeographic ancestry when conventional STR profiling is inconclusive. The ForenSeq™ Imagen kit (107 SNPs) integrates phenotype-, ancestry-, and Y-SNPs markers; however, its performance under partial genotyping conditions has not been systematically evaluated. Methods: Ninety-four samples from a Mexican mestizo population were analyzed using the ForenSeq™ Imagen kit on the MiSeq FGx™ platform. Due to incomplete genotype recovery, 41 samples with >60% locus detection were selected for downstream analyses. Phenotype prediction was performed using the HIrisPlex-S model, and ancestry inference was assessed through principal component analysis. In silico simulations were conducted to evaluate locus-specific dropout effects. Results: Eye color prediction showed both reduced feasibility (68.3%) and lower overall accuracy (56.1%), primarily driven by systematic prediction failure when rs12913832 (*HERC2*) was absent, although accuracy among successfully predicted samples remained high (82.1%). In contrast, hair and skin color inference remained feasible in >97% and 100% of evaluable samples, respectively; however, classification accuracy was moderate (70% for hair and 61% for skin), improving substantially when allowing adjacent-category concordance (90.2% for skin). Ancestry inference was robust when at least 27 aiSNPs were detected, and Y-SNPs reliably distinguished male and female samples. In silico analyses confirmed the critical contribution of rs12913832 to eye color model operability. Conclusions: FDP performance under partial genotyping reflects a trade-off between prediction feasibility and accuracy and depends on locus-specific integrity rather than overall genotype completeness. The ForenSeq™ Imagen kit shows robustness for ancestry, sex, hair, and skin prediction, although with variable accuracy, whereas eye color inference remains structurally vulnerable to drop out of high-impact variants. Evaluating FDP systems under realistic non-ideal conditions is essential to define their true operational limits and ensure scientifically robust and responsible implementation.

Keywords: forensic DNA phenotyping; ForenSeq imagen kit; performance; prediction

1. Introduction

Since their introduction into forensic genetics, short tandem repeats (STRs) have become the markers of choice for human identification. Their high polymorphism and strong discriminatory power have enabled reliable individualization across a broad range of forensic contexts. Nevertheless, despite their extensive utility, STR-based approaches present important limitations. These include reduced performance in cases involving degraded or low-quality template DNA, susceptibility to stochastic effects such as allele drop-out, and limited applicability in scenarios where no reference samples are available for comparison, as is frequently the case in unidentified human remains or investigative casework [1].

In such contexts, single nucleotide polymorphisms (SNPs) have emerged as valuable complementary markers. Due to their biallelic nature and short amplicon size, SNPs are particularly suitable for degraded DNA samples. Moreover, depending on their genomic location and functional relevance, certain SNPs enable the inference of biogeographic ancestry (ancestry-informative SNPs, aiSNPs) as well as externally visible characteristics (phenotype-informative SNPs, piSNPs), including eye, hair, and skin color, among other externally visible characteristics (EVCs) [2].

The inference of EVCs from DNA, commonly referred to as Forensic DNA Phenotyping (FDP), has gained increasing relevance in forensic investigations where conventional identification methods are insufficient. FDP is particularly useful when physical descriptors of the DNA donor are unavailable, such as in cases involving highly decomposed remains or when STR profiles obtained from crime scene samples fail to generate database matches. In these situations, FDP can provide investigative leads by narrowing the pool of potential contributors and guiding casework prioritization [1].

Several SNP-based systems have been developed specifically for FDP. Early examples include IrisPlex for eye color prediction [3], followed by HIrisPlex, which expanded phenotype inference to include hair color [4], and HIrisPlex-S, which further incorporates skin color prediction [5]. As the number of markers required for comprehensive phenotype inference increased, massively parallel sequencing (MPS) technologies were introduced to forensic genetics, enabling the simultaneous analysis of large SNP panels across multiple samples within a single assay [6]. Currently, the most widely used MPS platforms in forensic research are Ion Torrent (Thermo Fisher Scientific, Waltham, MA, USA) and the MiSeq (Illumina, San Diego, CA, USA) platforms [2].

Several commercial MPS-based kits for FDP have been validated and implemented in forensic research and practice. Among these, the ForenSeq™ DNA Signature Prep Kit with DNA Primer Set B (DPSB) enables the inference of eye and hair color phenotypes and has been extensively evaluated across diverse populations, with studies consistently reporting high prediction accuracy for blue and brown eye color, as well as blond and red hair color [7–10].

More recently, the ForenSeq™ Imagen kit (Illumina, San Diego, CA, USA) was developed as an integrated genomic system comprising 107 SNPs distributed across three marker panels: (i) 41 piSNPs for eye, hair, and skin color inference; (ii) 56 aiSNPs for biogeographic ancestry estimation; and (iii) 14 Y-SNPs for sex determination. Despite its potential forensic utility, there are currently no comprehensive validation studies assessing the kit's performance for its intended forensic applications. The only published study involving this system explored its use for predicting EVCs beyond the scope for which

https://doi.org/10.3390/genes17030354

the kit was designed [11] and has been subject to substantial methodological criticism regarding study design and result interpretation [12,13].

The evaluation and implementation of FDP technologies such as the ForenSeq™ Imagen kit are particularly relevant in countries like Mexico, where forensic identification faces significant challenges. According to official records, as of September 2023, a total of 294,297 cases have been documented, including 111,516 (37.9%) missing persons and 182,781 (62.1%) located individuals since 1962 [14]. A considerable proportion of unidentified individuals remain unresolved due to degraded biological material or the absence of first-degree relatives for comparative genetic analysis, thereby limiting the effectiveness of conventional STR-based identification approaches [15].

In this context, the ForenSeq™ Imagen kit represents a promising MPS-based tool that integrates multiple informative SNP panels within a single assay. The present study aims to evaluate the applicability and operational performance of this system in a Mexican population, with particular emphasis on its accuracy for forensic DNA phenotyping under conditions of partial genotype recovery. By assessing its performance in realistic forensic laboratory conditions, this work seeks to contribute to the implementation of FDP technologies as complementary tools for human identification and to help reduce the current backlog of unidentified human remains.

2. Materials and Methods

2.1. Population Sample

A total of 94 genomic DNA samples were obtained from unrelated adult volunteers residing in Jalisco, Mexico. Participants ranged in age from 18 to 38 years and included 72 males and 22 females. Written informed consent was obtained from all individuals prior the enrollment. The study was conducted in accordance with established ethical standards for research involving human subjects and was approved by the Research Ethics Committee (Comité de Ética en Investigación (CEI) from the Centro Universitario de Ciencias de la Salud of the Universidad de Guadalajara; approved code CI-06824).

2.2. Reference Phenotype Assignment

High-resolution digital photographs were obtained using a Canon EOS Rebel T6 camera (Canon Inc., Tokyo, Japan). Images included close-up photographs of the iris, the posterior scalp for hair color assessment, and the forearm for skin pigmentation evaluation. All images were compiled into a standardized Microsoft Excel for Microsoft 365 (Microsoft Corporation, Redmond, WA, USA) database.

Three independent analysts evaluated each volunteer's phenotype based on the photographic documentation. Phenotypic categories were assigned according to classification schemes compatible with the HIrisPlex-S prediction system. Phenotypes were categorized as follows: (A) Eye color: blue, intermediate (green, hazel, and yellowish tones), and brown. (B) Hair color: blond, red, brown, and black, with light or dark shades. (C) Skin color: Fitzpatrick phototypes I (very pale), II (pale), III (intermediate), IV (dark), and V (very dark/black). Consensus was achieved in all cases across the three evaluators. These assigned phenotypes were used as reference data for subsequent assessments of prediction accuracy.

2.3. DNA Extraction and Quantification

Genomic DNA was extracted from peripheral blood using a CTAB/DTAB method based on the protocol described by Miller [16]. This protocol employs the cationic detergents cetyltrimethylammonium bromide (CTAB) and dodecyltrimethylammonium bromide (DTAB) to lyse cells, remove proteins and other contaminants, and selectively

https://doi.org/10.3390/genes17030354

precipitate high-molecular-weight DNA. The resulting DNA was stored at −20 °C until further analysis. Extracted DNA was quantified by fluorometric analysis using the Qubit™ 4 Fluorometer (Thermo Fisher Scientific, Waltham, MA, USA), following the manufacturer's instructions.

2.4. Library Preparation and Massively Parallel Sequencing

Genomic libraries were prepared using the ForenSeq™ Imagen kit (Verogen Inc., San Diego, CA, USA) according to the manufacturer's protocol. Library preparation began with an input of 125 pg of genomic DNA. Target regions were amplified and tagged during an initial PCR step, followed by a second enrichment PCR incorporating Unique Dual Index (UDI) sequences and sequencing adapters.

Following amplification, libraries were purified enzymatically using magnetic bead-based cleanup procedures to remove residual primers and reaction components. Libraries were subsequently normalized to achieve equimolar concentrations before pooling. Equal volumes of each normalized library were combined to generate a pooled library mixture.

The initial 94 libraries were pooled, diluted in hybridization buffer, and heat-denatured before being loaded onto the MiSeq FGx micro flow cell for a single run (Verogen Inc., San Diego, CA, USA). Sequencing was performed according to the MiSeq FGx™ System Reference Guide (Verogen Inc., San Diego, CA, USA). The sequencing run included both positive and negative controls to monitor amplification performance and potential contamination.

2.5. Evaluation of Sequencing Run Quality

Sequencing run quality was assessed using post-sequencing performance and quality metrics generated by the MiSeq FGx™ platform. The following parameters were evaluated to determine overall sequencing efficiency and data reliability. First, cluster density was examined and expressed as the number of clusters per square millimeter (K/mm^2). For the Forensic Imagen kit, the recommended optimal range is between 400 and 1650 K/mm^2, which reflects appropriate library loading and cluster generation efficiency. Second, clusters passing filters (PFs) were evaluated as the percentage of total clusters that met Illumina's quality filtering criteria. This metric reflects the proportion of clusters with sufficient signal intensity and base-calling reliability. A PF value of $\geq$80% was considered indicative of acceptable sequencing performance.

Third, phasing and prephasing rates were assessed as indicators of synchronization efficiency during the sequencing-by-synthesis process. Phasing represents the percentage of DNA molecules within a cluster that lags the current sequencing cycle due to incomplete nucleotide incorporation, whereas prephasing corresponds to the proportion of strands that advance of the cycle because of premature incorporation events. In accordance with the manufacturer's recommendations, acceptable thresholds were defined as $\leq$0.25% for phasing and $\leq$0.15% for prephasing.

In addition, overall read quality was evaluated using Illumina's per-cycle quality score visualization, which summarizes average base-call quality across sequencing cycles using a color-coded system. In this system, green indicates that the mean quality scores fall within the expected performance range, whereas orange denotes deviations from optimal sequencing quality. These metrics were used to evaluate the technical quality of each sequencing run to ensure data reliability before genotyping and phenotype inference analyses.

2.6. Definition of Partial Genotypes and Profile Inclusion Criteria

A partial genotype was defined as a genetic profile in which one or more marker sets failed to produce complete SNP data but retained sufficient genetic information to support phenotype or ancestry inference. Profiles were considered suitable for downstream

https://doi.org/10.3390/genes17030354

analyses when genotype data allowed for successful processing within the HIrisPlex-S prediction framework or ancestry assessment via principal component analysis (PCA). Samples lacking sufficient genotype information to generate any phenotype or ancestry inference were excluded from performance evaluations but retained for overall sequencing outcome reporting.

2.7. Genotype Processing and Data Management

Genotype data generated by the MiSeq FGx™ instrument were processed using Verogen's Universal Analysis Software (UAS) version 1.3 (Verogen Inc., San Diego, CA, USA). Genotyping results, sequencing metrics, and locus-level information were exported in Microsoft Excel format for subsequent analyses. Missing SNP calls were retained as missing data and were not imputed or manually corrected. Downstream predictive analyses were performed using the genotype information available for each sample, without additional filtering or data inference.

2.8. Forensic DNA Phenotyping Analysis

Phenotype prediction was performed using the HIrisPlex-S web-based tool developed by Erasmus Medical Center (https://hirisplex.erasmusmc.nl/, accessed on 12 February 2025). This system predicts eye, hair, and skin color using validated SNP panels and a prediction model trained on diverse continental populations [3–5]. The R script provided by the EMC platform was used to convert piSNP output files generated by UAS into the required input format for phenotype prediction. Predictions were generated for all samples that met the profile inclusion criteria.

Predicted phenotypes were compared with reference phenotypes assigned from photographic analysis. Prediction performance was assessed by calculating the percentage of correctly classified samples for each phenotypic trait. Additionally, the number of SNPs contributing to successful phenotype prediction and the number of genotypes producing interpretable predictions were recorded to evaluate system performance under conditions of partial genotype recovery and incomplete marker representation.

To evaluate the relative contribution of individual eye color SNPs to prediction feasibility, an in silico dropout analysis was performed using the HIrisPlex-S online platform (Erasmus Medical Center). Complete genotype profiles were systematically modified by artificially removing one SNP at a time from the IrisPlex eye color panel while retaining all remaining loci. Six independent simulations were conducted, each corresponding to the exclusion of a different eye color SNP. The modified datasets were reanalyzed to determine whether phenotype prediction remained viable in the absence of each specific marker. This approach allowed for the assessment of locus-specific sensitivity within the predictive model under controlled virtual dropout conditions.

2.9. Biogeographic Ancestry Analysis

Biogeographic ancestry inference was evaluated by visual inspection of sample clustering patterns in the principal component analysis (PCA) generated by the Universal Analysis Software (UAS) v2.x software (Verogen, San Diego, CA, USA). Samples were assessed based on their relative positions within PCA space and their proximity to reference population clusters included in the analysis. No formal ancestry assignment thresholds were applied.

2.10. Statistical Approach

All analyses were descriptive and were designed to evaluate operational system performance, profile recovery, and interpretability of phenotype and ancestry predictions under partial genotyping conditions. No inferential statistical testing was performed, as

https://doi.org/10.3390/genes17030354

the primary objective was to assess methodological performance in realistic laboratory forensic scenarios.

3. Results

3.1. Sequencing Run Quality

Bioinformatic analysis was performed using UAS v2 with the ForenSeq™ Imagen Geo assay. The sequencing run comprised four reads (Read 1, Index 1, Index 2, and Read 2), totaling 318 cycles. All evaluated run metrics were within the manufacturer's recommended thresholds, indicating appropriate sequence performance and data reliability.

The cluster density was 478 K/mm^2, falling within the optimal recommended range (400–1650 K/mm^2). A total of 98.09% of clusters passed Illumina's quality filter (PF), exceeding the minimum acceptable threshold of 80% and demonstrating high signal quality and base-calling reliability.

Phasing and prephasing values were 0.205% and 0%, respectively, both within the acceptable limits ($\leq$0.25% for phasing and $\leq$0.15% for prephasing), indicating adequate synchronization during the sequencing-by-synthesis process without compromising read accuracy. Per-cycle quality score plots showed mean base-call quality values within the expected (green) performance range across all sequencing cycles. No discordant genotypes were observed across loci, indicating stable assay performance under the evaluated sequencing conditions.

According to the reference manual, the assay can generate up to 50,000 reads per sample. In this run, the number of reads varied substantially across samples, ranging from 148 to 90,000. Given this variability, the performance of the HSC control was considered critical for determining the inclusion of samples with low read counts in subsequent analyses under partial genotyping conditions.

3.2. Genotype Recovery and Profile Completeness

A total of 94 samples were processed using the ForenSeq™ Imagen kit, targeting 41 phenotype-informative SNPs (piSNPs), 56 ancestry-informative SNPs (aiSNPs), and 14 Y-SNPs, for a total of 107 markers. Of these, 53 samples (56.4%) were genotyped for only 5–57 markers and produced between 148–29,000 total reads; consequently, they were excluded from the analyses presented in this study. In contrast, 41 samples (43.6%) achieved a genotyping rate greater than 60% of the total panel and were considered suitable for downstream phenotype and ancestry inference analyses (Tables S1 and 1). Although these samples yielded partial genetic profiles, they retained sufficient marker representation to support phenotype and ancestry inference.

Within the piSNP panel (41 markers), locus recovery varied across trait categories. For the eye color subpanel (6 SNPs), between 3 and 6 loci were successfully genotyped per sample. The rs12913832 (*HERC2*) SNP was successfully genotyped in 28 out of 41 samples (68.3%), while dropout was observed in 13 samples (31.7%). In 13 samples, eye color prediction was not possible. In all of these cases, amplification failure of rs12913832 was observed. Samples 124, 153, and 154 amplified only 4, 4, and 3 eye-related SNPs, respectively. In the remaining 10 samples where prediction was not possible (08, 19, 23, 25, 31, 47, 96, 122, 163, and 303), five SNPs were successfully genotyped; however, rs12913832 was consistently absent. Notably, other samples (e.g., 74 and 88) also showed five successfully genotyped SNPs but retained rs12913832, allowing phenotype prediction. This pattern highlights the critical role and predictive dependency of rs12913832 within the HIrisPlex-S eye color prediction model.

For the hair color panel (22 SNPs), between 12 and 22 loci were successfully genotyped across samples. Phenotype inference was achieved in 40 out of 41 samples (97.6%). Only

https://doi.org/10.3390/genes17030354

sample 147, which presented 11 genotyped SNPs, did not yield a hair color prediction. Regarding the skin color panel (36 SNPs), a minimum of 25 loci were successfully genotyped in all 41 samples. In all cases, sufficient genetic information was available to generate a phenotype prediction (100% prediction feasibility).

Table 1. Number of markers successfully amplified in each panel for every individual in the study population. The numbers of loci included in each panel are indicated in parentheses.

Sample	piSNP				aiSNP (56)	Y-SNP (14)	Total (107)
	Eye (6)	Hair (22)	Skin (36)	Subtotal (41)			
08	5 *	19	31	35	40	F	75
19	5 *	20	31	36	42	11	89
23	5 *	20	31	36	39	F	75
24	6	22	34	39	47	12	98
25	5 *	16	29	32	38	F	70
31	5 *	21	32	37	41	F	78
34	6	20	32	36	42	12	90
47	5 *	19	30	33	40	10	83
66	6	22	35	40	52	14	106
74	5	16	29	32	50	10	92
81	6	22	35	40	54	12	106
82	6	22	35	40	55	14	107
83	6	22	35	40	52	12	104
88	5	17	30	33	47	8	88
89	6	21	32	37	44	F	81
91	6	22	34	39	51	12	102
96	5 *	20	31	36	35	10	81
98	6	22	35	40	51	12	103
103	6	22	35	40	54	14	107
104	6	22	36	41	53	12	106
106	6	21	34	39	48	12	99
107	6	22	35	40	52	12	104
109	6	21	31	37	44	11	92
122	5 *	20	32	37	40	11	88
123	6	21	32	37	44	F	81
124	4 *	14	27	30	36	8	74
134	6	21	33	38	48	11	97
144	6	22	34	39	50	12	101
145	6	22	33	38	42	F	80
147	6	11*	23	24	47	6	77
151	6	22	35	40	52	F	92
152	6	22	35	40	51	F	91
153	4 *	13	25	27	29	7	63
154	3 *	12	25	27	27	6	60
155	6	22	35	40	51	12	103
156	5 *	20	31	36	44	F	80
159	6	22	35	40	53	13	106
160	6	22	35	40	53	12	105
158	6	22	35	40	48	F	88
254	6	22	34	39	49	12	100
303	5 *	15	29	31	36	8	75

F: female sample, no Y-SNPs detected; * samples where no prediction was possible.

For the 56 aiSNPs, at least 27 markers were successfully genotyped per sample, which was sufficient to generate principal component analysis (PCA) plots for ancestry inference in all evaluable cases. Concerning the Y-SNP panel, Y markers were not detected in

https://doi.org/10.3390/genes17030354

10 samples, corresponding to female individuals. The presence of at least one Y-SNP was sufficient to determine male sex in the remaining samples.

3.3. Phenotype Prediction Performance Under Partial Genotyping Conditions

Phenotype predictions obtained using the HIrisPlex-S system were compared against the observed phenotypes derived from standardized photographic assessment in the 41 samples that generated partial but interpretable genotypes (Table 2). Performance was evaluated using prediction rate (the proportion of samples for which a prediction was generated), strict classification accuracy, overall accuracy (including failed predictions), and balanced performance across categories.

Eye color prediction was successfully generated in 28 out of the 41 samples (68.3%). In the remaining 13 samples (31.7%), no prediction could be generated due to insufficient marker recovery. Notably, all failed predictions shared the absence of rs12913832, confirming its pivotal role within the HIrisPlex-S model. Among the 28 samples with available predictions, 23 were correctly classified and 5 were misclassified, yielding a strict classification accuracy of 82.1% among the predicted samples. When failed predictions were included, the overall accuracy decreased to 56.1%. Misclassifications primarily involved confusion between blue and brown eye color categories, as well as the assignment of intermediate eye color to the brown category. No extreme or biologically implausible classifications were observed. The relatively high accuracy between predicted samples suggests that once the core SNPs—particularly rs12913832—are recovered, the system retains strong discriminatory capacity even under partial genotyping conditions. However, the reduced prediction rate highlights the sensitivity of eye color inference to locus dropout.

Hair color prediction was achieved in 40 out of 41 samples (97.6%), demonstrating high robustness to partial genotype recovery. Only one sample failed to generate a prediction due to insufficient SNP recovery (11 of 22 loci). Among the 40 predicted samples, 28 were correctly classified, and 12 were misclassified, corresponding to a strict classification accuracy of 70.0% and an overall accuracy of 68.3%. Most discrepancies occurred between adjacent pigmentation categories, particularly between black and dark brown, and between brown and blond. Importantly, the single red-haired individual was correctly predicted, consistent with the high discriminatory performance of the red hair-associated markers. The lower accuracy relative to eye color likely reflects the polygenic complexity of hair pigmentation and the continuous variation observed in admixed populations, where categorical classification may oversimplify biological reality. Balanced performance across hair color categories revealed reduced sensitivity in distinguishing dark shades, suggesting that partial marker recovery may disproportionately affect the resolution of closely related pigmentation phenotypes.

Skin color prediction was successfully generated in all 41 samples (100% prediction rate), indicating strong resilience of the 36-marker panel to partial genotype conditions. Strict classification accuracy was 61.0% (25/41). However, when allowing a one-category deviation (e.g., phototype II predicted as III), concordance increased substantially to 90.2% (37/41). No extreme misclassifications were observed. Most discrepancies occurred between adjacent phototypes (II–III and III–IV), consistent with the continuous distribution of pigmentation in admixed populations. These findings suggest that although categorical precision may decrease under partial genotyping, the system maintains high biological plausibility and practical utility for investigative purposes.

https://doi.org/10.3390/genes17030354

Table 2. Observed and predicted phenotypes, including their corresponding area under the curve (AUC) values. The following categories were considered: eye color (brown, blue, or intermediate); hair color (brown, black, blond, or red); and skin color classified as very pale or phototype I (FI), pale or phototype II (FII), intermediate or phototype III (FIII), dark or phototype IV (FIV), and black or phototype V (FV). NA was used for non-generated data.

	Eye Color			Hair Color			Skin Color		
Sample	**Observed**	**Predicted (p)**	**AUC**	**Observed**	**Predicted (p)**	**AUC**	**Observed**	**Predicted (p)**	**AUC**
8	Brown	NA	0.9460	Brown	Black (0.5194)	0.8592	F-III	F-III (0.9432)	0.7833
19	Brown	NA	0.9460	Brown	Black (0.5886)	0.8592	F-III	F-III (0.9998)	0.7833
23	Intermediate	NA	0.9460	Brown	Black (0.7216)	0.8592	F-II	F-III (0.4844)	0.7833
24	Brown	Brown (0.9909)	0.9460	Brown	Brown (0.8201)	0.7410	F-III	F-III (0.9999)	0.7833
25	Brown	NA	0.9460	Brown	Blond (0.5128)	0.8132	F-II	F-III (0.7337)	0.7833
31	Brown	NA	0.9460	Brown	Blond (0.5020)	0.8132	F-II	F-III (0.9995)	0.7833
34	Brown	Brown (0.9946)	0.9460	Black	Black (0.6699)	0.8592	F-IV	F-III (0.9952)	0.7833
47	Brown	NA	0.9460	Black	Brown (0.4771)	0.7410	F-III	F-III (0.9543)	0.7833
66	Brown	Brown (0.9930)	0.9460	Black	Brown (0.6974)	0.7410	F-III	F-III (0.9992)	0.7833
74	Brown	Brown (0.9784)	0.9460	Black	Brown (0.5391)	0.7410	F-III	F-V (0.9540)	0.9934
81	Brown	Brown (0.9117)	0.9460	Brown	Brown (0.6169)	0.7410	F-III	F-III (0.9996)	0.7833
82	Brown	Brown (0.7758)	0.9460	Blond	Brown (0.6294)	0.7410	F-I	F-III (0.5864)	0.7833
83	Brown	Brown (0.9978)	0.9460	Black	Black (0.6120)	0.6120	F-IV	F-V (0.8312)	0.9934
88	Brown	Brown (0.9945)	0.9460	Black	Black (0.8595)	0.8592	F-III	F-III (0.9216)	0.7833
89	Intermediate	Brown (0.5474)	0.9460	Brown	Brown (0.6221)	0.7410	F-II	F-III (0.9999)	0.7833
91	Brown	Brown (0.9972)	0.9460	Black	Black (0.7683)	0.8592	F-III	F-III (0.9981)	0.7833
96	Brown	NA	0.9460	Black	Black (0.8780)	0.8592	F-II	F-III (0.9965)	0.7833
98	Brown	Brown (0.7667)	0.9460	Brown	Brown (0.5531)	0.7410	F-II	F-III (0.6326)	0.7833
103	Brown	Brown (0.9972)	0.9460	Black	Black (0.7915)	0.8592	F-IV	F-III (0.9981)	0.7833
104	Brown	Brown (0.9857)	0.9460	Black	Black (0.5666)	0.8592	F-III	F-III (0.9998)	0.7833
106	Brown	Brown (0.9930)	0.9460	Brown	Brown (0.5052)	0.7410	F-III	F-III (0.9952)	0.7833
107	Brown	Brown (0.9377)	0.9460	Red	Red (0.8363)	0.9289	F-II	F-III (0.5412)	0.7833
109	Brown	Brown (0.9822)	0.9460	Black	Brown (0.5415)	0.7410	F-III	F-III (0.9989)	0.7833
122	Brown	NA	0.9460	Black	Brown (0.4889)	0.7410	F-III	F-III (0.89117)	0.7833
123	Brown	Brown (0.9930)	0.9460	Brown	Brown (0.7204)	0.7410	F-II	F-III (0.8211)	0.7833

https://doi.org/10.3390/genes17030354

Table 2. *Cont.*

	Eye Color			Hair Color			Skin Color		
Sample	**Observed**	**Predicted (p)**	**AUC**	**Observed**	**Predicted (p)**	**AUC**	**Observed**	**Predicted (p)**	**AUC**
124	Brown	NA	0.9460	Black	Black (0.4559)	0.8592	F-III	F-III (0.9968)	0.7833
134	Brown	Brown (0.9426)	0.9460	Blond	Brown (0.4957)	0.7410	F-I	F-III (0.9999)	0.7833
144	Brown	Brown (0.9978)	0.9460	Black	Black (0.8555)	0.8592	F-IV	F-III (0.9377)	0.7833
145	Brown	Blue (0.8478)	0.9460	Black	Blond (0.7053)	0.8132	F-III	F-II (0.6178)	0.7627
147	Brown	Brown (0.9565)	0.9460	Black	NA	0.9289	F-III	F-III (0.9506)	0.7833
151	Brown	Brown (0.9946)	0.9460	Black	Brown (0.5491)	0.7410	F-II	F-III (0.8482)	0.7833
152	Brown	Brown (0.9815)	0.9460	Brown	Brown (0.6806)	0.7410	F-II	F-III (0.8618)	0.7833
153	Intermediate	NA	0.9460	Brown	Black (0.7481)	0.8592	F-III	F-III (0.8618)	0.7833
154	Brown	NA	0.9460	Black	Black (0.5126)	0.8592	F-III	F-III (0.9969)	0.7833
155	Brown	Blue (0.9150)	0.9460	Black	Blond (0.6323)	0.8132	F-II	F-III (0.9991)	0.7833
156	Brown	NA	0.9460	Brown	Brown (0.3984)	0.7410	F-II	F-III (0.9780)	0.7833
159	Blue	Brown (0.9767)	0.9460	Blond	Black (0.5478)	0.8592	F-I	F-III (0.9980)	0.7833
160	Brown	Brown (0.7667)	0.9460	Black	Brown (0.5418)	0.7410	F-III	F-III (0.9389)	0.7833
158	Brown	Brown (0.9780)	0.9460	Brown	Brown (0.6362)	0.7410	F-III	F-III (0.9559)	0.7833
254	Intermediate	Blue (0.6498)	0.9460	Brown	Brown (0.5865)	0.7410	F-III	F-III (0.7663)	0.7833
303	Brown	NA	0.9460	Brown	Brown (0.5604)	0.7410	F-III	F-V (0.6829)	0.9934

3.4. In Silico Sensitivity Assessment of the IrisPlex Eye Color Panel

Considering the eye color prediction failures observed under partial genotyping conditions, an additional in silico sensitivity analysis was conducted to evaluate the relative contribution of each SNP within the IrisPlex eye color panel to model operability.

Six independent simulation assays were performed using the HIrisPlex-S online platform. For each assay, complete genotype datasets were artificially modified to introduce systematic locus-specific dropout across all individuals. In the first simulation, genotypes at rs12913832 were removed for the entire sample set. In subsequent simulations, dropout was sequentially introduced at rs1800407 and each of the remaining IrisPlex eye color SNPs, one at a time, while keeping all other loci intact. This approach allowed the isolated evaluation of each marker's contribution to prediction feasibility.

The simulations demonstrated that eye color prediction remained possible for all individuals as long as rs12913832 was retained in the genotype profile. In contrast, artificial removal of rs12913832 resulted in complete prediction failure across the dataset, regardless of the presence of the remaining SNPs. Dropout of any other individual marker did not prevent the generation of eye color predictions.

These findings confirm that rs12913832 functions as the primary driver of model operability within the IrisPlex system. Its absence compromises the algorithm's capacity to compute posterior probabilities, explaining the systematic prediction failures observed in

https://doi.org/10.3390/genes17030354

the empirical partial genotypes described above. The in silico results, therefore, provide mechanistic support for the experimental data and highlight the disproportionate weight of rs12913832 in eye color inference.

3.5. Comparative Robustness Across Traits

When comparing performance metrics across traits, clear differences in robustness under partial genotyping conditions were observed. Skin color inference demonstrated the highest resilience, with a 100% prediction rate and high adjacent-category concordance. Hair color prediction also showed high feasibility (97.6%), although with moderate classification accuracy. In contrast, eye color prediction was the most sensitive to marker dropout, primarily driven by the absence of rs12913832, resulting in the lowest prediction rate (68.3%) despite high accuracy among successfully predicted samples. These results indicate that the predictive stability of the ForenSeq™ Imagen kit under partial genotyping conditions is trait-dependent and strongly influenced by the relative weight of individual SNPs within each predictive model.

3.6. Biogeographic Ancestry Inference

All 41 samples yielded sufficient aiSNP recovery (≥27 of 56 loci) to generate interpretable principal component analysis (PCA) clustering patterns. The observed distributions revealed four predominant ancestry patterns (Figure 1): (a) centroid with predominantly American ancestry (admixed); (b) slightly inclined towards the East Asian population, probably showing higher Native American ancestry; (c) slightly inclined towards the European sample; and (d) highly inclined towards the European sample, showing individuals with high European ancestry. Interestingly, samples with the European pattern were the most frequent (46.3%), while the East Asian/Native American pattern was the least frequent (7.3%). Partial genotype recovery did not preclude ancestry inference in any sample, indicating that the aiSNP panel retains analytical stability even when full marker recovery is not achieved.

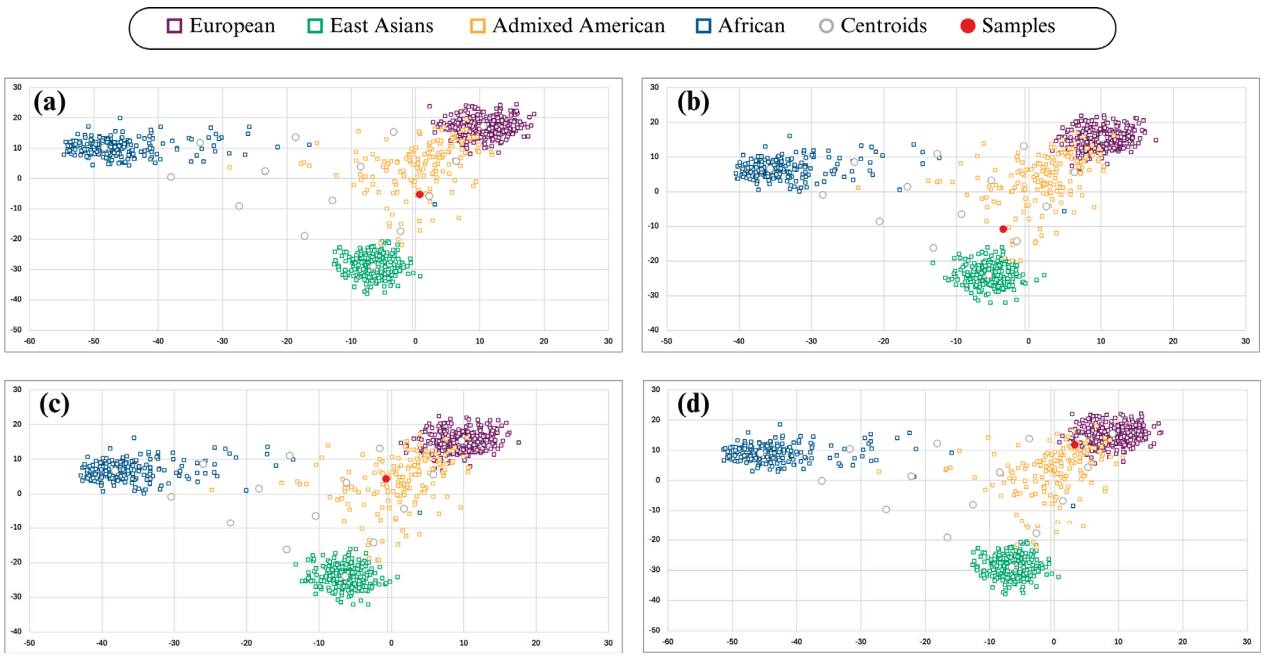

Figure 1. Distribution of ancestry patterns in 41 samples analyzed using the ForenSeq™ IMAGEN kit. The following groups were observed: (**a**) centroid pattern of American Mestizos; (**b**) pattern slightly shifted toward East Asian ancestry; (**c**) pattern with a slight shift toward European ancestry; and (**d**) pattern strongly shifted toward European ancestry.

https://doi.org/10.3390/genes17030354

4. Discussion

4.1. Technical Performance Under Partial Genotyping Conditions

This study, to our knowledge, provides the first independent evaluation of the ForenSeq™ Imagen kit under partial genotyping conditions, offering insight into system behavior beyond ideal validation settings. Although complete genotype recovery was not achieved across all samples, the partial profiles generated allowed for the assessment of the operational tolerance of phenotype and ancestry inference models when confronted with incomplete genetic information—an increasingly realistic scenario in forensic casework involving degraded or limited DNA [1].

A considerable proportion of samples exhibited locus-specific dropout across different marker panels. Importantly, the results demonstrate that prediction feasibility is not directly proportional to the overall percentage of recovered loci. Instead, model operability depends disproportionately on retaining specific high-impact variants. This distinction is critical: global genotyping success rates may appear acceptable while phenotype prediction fails due to the absence of a single pivotal marker.

The spatial clustering of dropout events across the sequencing plate suggested a technical origin associated with multichannel pipetting variability during library preparation. Recurrent amplification failure in samples occupying the same channel position supports the hypothesis of uneven reagent dispensing. Such pre-analytical variability is consistent with high-throughput MPS workflows and has been recognized as a source of locus imbalance in forensic MPS applications [7]. These findings suggest that the incomplete genotype recovery observed in this study likely reflects workflow-related variability rather than intrinsic limitations of the ForenSeq™ Imagen kit chemistry. Studies evaluating related MPS-based forensic workflows have also reported locus imbalance and variable marker recovery when analyzing degraded or otherwise challenging DNA samples, particularly under degraded conditions [17]. Nonetheless, the downstream interpretive consequences remain operationally relevant.

An additional factor that may have contributed to the observed variability in genotyping performance is the absence of a human-specific DNA quantification method. In forensic NGS workflows, qPCR-based quantification assays targeting human DNA are critical to accurately estimate the amount of amplifiable template. Non-specific quantification methods may overestimate DNA concentration in the presence of degradation, non-human DNA, or inhibitors, potentially leading to suboptimal library input and increased allele dropout. Therefore, the incomplete genotype recovery observed in this study may be partially explained by limitations in DNA quantification, in addition to stochastic and technical factors during library preparation.

Importantly, the overall sequencing run quality metrics were well within the manufacturer's recommended thresholds, including optimal cluster density, high percentages of clusters passing filters, and acceptable phasing and prephasing rates. Per-cycle quality plots confirmed stable base-calling performance throughout the run. These findings indicate that the locus-specific dropout observed in this study cannot be attributed to suboptimal sequencing chemistry or instrument performance, reinforcing the interpretation that pre-analytical workflow variability is the primary contributing factor.

4.2. Phenotype Prediction Robustness and Marker-Specific Sensitivity

Eye color prediction was critically dependent on the presence of rs12913832. Both empirical observations and in silico dropout simulations consistently showed that its absence led to systematic prediction failure, even when the remaining IrisPlex markers were successfully genotyped. This behavior is consistent with the design of the HIrisPlex-S

https://doi.org/10.3390/genes17030354

model, which does not generate eye color predictions when rs12913832 is missing [5]. In contrast, dropout affecting other individual SNPs did not prevent phenotype inference.

The relatively high frequency of rs12913832 dropout observed in this study further explains the reduced feasibility of eye color prediction under partial genotyping conditions. This dependency reflects the biological and statistical architecture of pigmentation models. The rs12913832 variant, located within an intronic enhancer region of HERC2, regulates OCA2 expression and exerts a major effect on blue versus brown eye pigmentation [3,18,19]. Its strong predictive weight explains why HIrisPlex-S operability collapses when this marker is absent. Thus, the observed sensitivity does not represent dataset-specific instability but rather an inherent structural characteristic of the model.

Intermediate eye colors showed greater variability, consistent with previous IrisPlex validation studies reporting reduced accuracy for non-binary pigmentation categories [3,5]. This limitation is particularly relevant in admixed populations such as Mexican mestizos, whose tri-hybrid ancestry components (European, Native American, and African) generate continuous ancestry and pigmentation gradients that challenge models trained predominantly on European reference datasets [3,5,20,21].

In contrast, hair and skin color prediction exhibited greater resilience under partial genotype recovery. Hair prediction remained feasible in over 97% of samples despite recovery ranging from 12 to 22 SNPs, while skin color inference was successful with as few as 25 of 36 loci. The polygenic architecture of these traits, involving distributed effect sizes across multiple loci [5], likely confers greater tolerance to partial genotype loss compared with the near single-locus dependency observed for eye color.

4.3. Ancestry and Y-SNP Inference Stability

Biogeographic ancestry inference demonstrated notable robustness. All samples with at least 27 aiSNPs produced interpretable PCA clustering patterns. This resilience likely reflects the multivariate structure of ancestry inference, where population differentiation signals are distributed across numerous loci rather than concentrated in a single variant [1]. Unlike eye color prediction, which can collapse with the loss of a critical SNP, ancestry inference relies on cumulative allele frequency patterns across populations.

Similarly, Y-SNP detection reliably distinguished male and female samples, as no Y-SNPs were detected in female individuals. The presence of even a single Y-SNP was sufficient for sex determination, confirming analytical specificity despite incomplete recovery. The utility of Y-linked markers for sex determination in forensic genetics has been widely established [22].

4.4. Comparison with Previous Mexican MPS-Based FDP Studies

Previous studies conducted in Mexican populations using the ForenSeq™ DNA Signature Prep kit (DPSB configuration) reported high accuracy in eye color prediction, particularly for brown phenotypes (>96%), and variable performance for hair color depending on the analytical tool used. Those studies, however, were performed under conditions of near-complete genotype recovery [10,23].

The present work extends these findings by examining system behavior under incomplete marker recovery. While the previous works demonstrated the feasibility of FDP in Mexican mestizo cohorts, they did not explicitly evaluate the impact of locus-specific dropout on prediction operability. Our results indicate that even modest marker loss may critically impair prediction if high-impact loci such as rs12913832 are absent.

Moreover, the predominance of brown eyes and dark hair in Mexican cohorts [10,23] may inflate classification accuracy for majority phenotypes while limiting the evaluation

https://doi.org/10.3390/genes17030354

of rarer categories. Under partial genotyping conditions, these structural dependencies become more evident.

Compared to exploratory analyses of the ForenSeq™ Imagen kit for additional phenotypes [11], which focused on trait expansion rather than operational robustness, the present study provides performance-based evidence regarding genotype completeness thresholds and marker dependency, an aspect essential for real forensic implementation.

4.5. Practical Implications for Forensic Casework

An important operational insight emerging from this study is that the reliability of phenotype prediction cannot be inferred solely from overall genotyping percentages. Instead, locus-specific integrity must be evaluated. Laboratories implementing MPS-based forensic DNA phenotyping systems should monitor marker-level recovery metrics and transparently report missing high-impact loci.

Although the strong association between rs12913832 and eye color is well-established [3,18,19], the present results highlight an important operational implication for forensic DNA phenotyping workflows. When genotype profiles are incomplete, the absence of this single high-impact SNP can prevent reliable eye color prediction, even if most other loci are successfully recovered. Therefore, locus-level quality assessment becomes critical during data interpretation. Laboratories implementing MPS-based FDP systems should explicitly verify and report the recovery of key predictive markers such as rs12913832 when presenting phenotype inference results derived from partial genotype profiles.

In countries such as Mexico, where large numbers of unidentified remains persist, and reference samples are often unavailable [24], FDP may provide valuable investigative leads. However, predictions derived from incomplete profiles must be interpreted with caution. Overinterpretation of predictions in the absence of critical markers should be avoided to ensure the responsible application of forensic analysis.

4.6. Study Limitations and Future Directions

This study has some limitations that should be considered when interpreting the results. First, the analyses were performed using reference samples under controlled laboratory conditions rather than typical forensic casework material. Consequently, the DNA analyzed in this study does not fully replicate the range of degradation patterns commonly encountered in forensic investigations. In this context, the genotype loss observed across some samples likely reflects technical variability during library preparation rather than environmental DNA damage or other common forensic challenges. Additionally, the number of evaluable partial genotypes was moderate, and genotype loss was not systematically evaluated using controlled degradation or low-template DNA experiments. Therefore, quantitative thresholds for minimum DNA input or degradation tolerance could not be defined.

Another limitation concerns the ancestry inference analysis. In this study, population structure was explored using principal component analysis (PCA), and ancestry patterns were interpreted based on visual clustering of the samples relative to reference populations. While PCA is widely used as an exploratory tool in population genetics, this approach does not provide probabilistic ancestry assignment, admixture proportions, or formal classification accuracy estimates. Consequently, the ancestry interpretations presented here should be considered descriptive rather than definitive.

Future research should incorporate probabilistic ancestry inference approaches, such as admixture-based models or assignment tests, to provide quantitative estimates of ancestry proportions and classification probabilities. However, this task appears to be difficult in the short-term, as no databases of Mexican Native American groups have been reported

https://doi.org/10.3390/genes17030354

that are compatible with the aiSNPs included in this kit, a prerequisite for determining percentages of ancestry and genetic admixture [25].

Additionally, future studies should incorporate controlled degradation models, low-template DNA experiments, and samples containing potential inhibitors to better simulate realistic forensic conditions. Replicate library preparations could also be performed to assess technical reproducibility, and quantitative analyses should be implemented to determine the minimum number of loci required for stable phenotype and ancestry prediction across traits.

5. Conclusions

Collectively, these findings demonstrate that the ForenSeq™ Imagen kit retains practical utility under partial genotyping conditions, particularly for hair color, skin color, ancestry, and sex inference. However, eye color prediction exhibits structural vulnerability due to its dependence on rs12913832, a locus consistently identified as the principal determinant in IrisPlex-based systems. Evaluating forensic DNA phenotyping systems under realistic non-ideal conditions is essential to define their true operational limits and ensure scientifically robust and responsible implementation.

Supplementary Materials: The following supporting information can be downloaded at: https://www.mdpi.com/article/10.3390/genes17030354/s1, Table S1: Genotype and sequencing quality data for the 107 SNPs included in the ForenSeq IMAGEN Kit (Illumina), used for the prediction of eye, hair, and skin color, as well as biogeographic ancestry, were analyzed in 41 samples from Mexican individuals.

Author Contributions: Conceptualization, N.G.-O. and J.A.A.-V.; data curation, N.G.-O., J.M.M.-O., and J.A.A.-V.; formal analysis, N.G.-O., M.G.-E., and N.Z.-F.; funding acquisition, J.A.A.-V.; methodology, N.G.-O., N.Z.-F., M.G.-E., J.M.M.-O., and A.R.-d.-A.; project administration, H.R.-V., J.F.M.-V.; resources, H.R.-V., J.F.M.-V., and J.A.A.-V.; supervision, J.A.A.-V.; writing—original draft, N.G.-O., and J.A.A.-V.; writing—review and editing, N.G.-O., J.M.M.-O., A.R.-d.-A., H.R.-V., J.F.M.-V., and J.A.A.-V. All authors have read and agreed to the published version of the manuscript.

Funding: This study was supported by the Mexican Government's Secretaría de Ciencia, Humanidades, Tecnología e Innovación (SECIHTI), to José Alonso Aguilar-Velázquez (project CF-2023-G-536).

Institutional Review Board Statement: This project received ethical approval from Comité de Ética en Investigación (CEI) from the Centro Universitario de Ciencias de la Salud of the Universidad de Guadalajara (approved code CI-06824; date of approval: 8 October 2024). All analyses were performed in accordance with the relevant guidelines and regulations, and all participants provided informed consent for research involvement. The study was conducted in accordance with the Declaration of Helsinki.

Informed Consent Statement: Informed consent was obtained from all subjects involved in the study.

Data Availability Statement: The genotype dataset reported in this paper is reported as Supplementary Materials.

Acknowledgments: The authors would like to thank the Mexican Government's Secretaría de Ciencia, Humanidades, Tecnología e Innovación (SECIHTI) for the financial support granted to José Alonso Aguilar-Velázquez in the Ciencia de Frontera 2024 competition (project CF-2023-G-536). We also thank SECIHTI for the doctoral fellowship awarded to Nayeli González-Ortiz. Finally, the authors acknowledge QIAGEN for partial financial support through the provision of the ForenSeq™ Imagen sequencing kit used in this study.

Conflicts of Interest: The authors declare no conflicts of interest.

https://doi.org/10.3390/genes17030354

References

1. Kayser, M. Forensic DNA phenotyping: Predicting human appearance from crime scene material for investigative purposes. *Forensic Sci. Int. Genet.* **2015**, *18*, 33–48. [CrossRef]
2. Terrado-Ortuño, N.; May, P. Forensic DNA phenotyping: A review on SNP panels, genotyping techniques, and prediction models. *Forensic Sci. Res.* **2025**, *10*, owae013. [CrossRef]
3. Walsh, S.; Liu, F.; Ballantyne, K.N.; van Oven, M.; Lao, O.; Kayser, M. IrisPlex: A sensitive DNA tool for accurate prediction of blue and brown eye colour in the absence of ancestry information. *Forensic Sci. Int. Genet.* **2011**, *5*, 170–180. [CrossRef]
4. Walsh, S.; Liu, F.; Wollstein, A.; Kovatsi, L.; Ralf, A.; Kosiniak-Kamysz, A.; Branicki, W.; Kayser, M. The HIrisPlex system for simultaneous prediction of hair and eye colour from DNA. *Forensic Sci. Int. Genet.* **2013**, *7*, 98–115. [CrossRef]
5. Chaitanya, L.; Breslin, K.; Zuñiga, S.; Wirken, L.; Pośpiech, E.; Kukla-Bartoszek, M.; Sijen, T.; de Knijff, P.; Liu, F.; Walsh, S.; et al. The HIrisPlex-S system for eye, hair and skin colour prediction from DNA: Introduction and forensic developmental validation. *Forensic Sci. Int. Genet.* **2018**, *35*, 123–135. [CrossRef]
6. Carratto, T.; Moraes, V.; Recalde, T.; de Oliveira, M.; Mendes-Junior, C. Applications of massively parallel sequencing in forensic genetics. *Genet. Mol. Biol.* **2022**, *45*, e20220077. [CrossRef] [PubMed]
7. Jäger, A.C.; Alvarez, M.L.; Davis, C.P.; Guzmán, E.; Han, Y.; Way, L.; Walichiewicz, P.; Silva, D.; Pham, N.; Caves, G.; et al. Developmental validation of the MiSeq FGx Forensic Genomics System for target sequencing of forensically relevant SNPs and STRs. *Forensic Sci. Int. Genet.* **2017**, *28*, 52–70. [CrossRef] [PubMed]
8. Frégeau, C. Validation of the Verogen ForenSeq™ DNA Signature Prep kit/Primer Mix B for phenotypic and biogeographical ancestry predictions using the Micro MiSeq® Flow Cells. *Forensic Sci. Int. Genet.* **2021**, *53*, 102533. [CrossRef]
9. Salvo, N.; Janssen, K.; Kirsebom, M.; Meyer, O.; Berg, T.; Olsen, G. Predicting eye and hair colour in a Norwegian population using Verogen's ForenSeq™ DNA Signature Prep kit. *Forensic Sci. Int. Genet.* **2021**, *56*, 102620. [CrossRef]
10. Aguilar-Velázquez, J.; Llamas-De-Dios, B.; Córdova-Mercado, M.; Coronado-Ávila, C.; Salas-Salas, O.; López-Quintero, A.; Ramos-González, B.; Rangel-Villalobos, H. Accuracy of eye and hair color prediction in Mexican mestizos from Monterrey City based on ForenSeq™ DNA Signature Prep. *Genes* **2023**, *14*, 1120. [CrossRef] [PubMed]
11. Elkins, K.M.; Garloff, A.T.; Zeller, C.B. Additional predictions for forensic DNA phenotyping of externally visible characteristics using the ForenSeq™ and IMAGEN kits. *J. Forensic Sci.* **2023**, *68*, 608–613. [CrossRef] [PubMed]
12. Wendt, F.R. Commentary on: Additional predictions for forensic DNA phenotyping using the ForenSeq and IMAGEN kits. *J. Forensic Sci.* **2023**, *68*, 1089–1091. [CrossRef] [PubMed]
13. Kayser, M. Commentary on: Additional predictions for forensic DNA phenotyping using the ForenSeq and IMAGEN kits. *J. Forensic Sci.* **2024**, *69*, 739–740. [CrossRef]
14. Registro Nacional de Personas Desaparecidas y No Localizadas (RNPED). Government of Mexico. Available online: https://www.gob.mx/sesnsp/acciones-y-programas/registro-nacional-de-datos-de-personas-extraviadas-o-desaparecidas-rnped (accessed on 17 October 2025).
15. Manera-Scliar, G.; Hernández, S.; Martín-López, M.; Gomes, C. Difficulties in kinship analysis for victims' identification in armed conflicts. *Genealogy* **2023**, *7*, 31. [CrossRef]
16. Miller, S.A.; Dykes, D.D.; Polesky, H.F. A simple salting out procedure for extracting DNA from human nucleated cells. *Nucleic Acids Res.* **1988**, *16*, 1215. [CrossRef]
17. Fattorini, P.; Previderé, C.; Carboni, I.; Marrubini, G.; Sorçaburu-Cigliero, S.; Grignani, P.; Bertoglio, B.; Vatta, P.; Ricci, U. Performance of the ForenSeqTM DNA Signature Prep kit on highly degraded samples. *Electrophoresis* **2017**, *38*, 1163–1174. [CrossRef]
18. Visser, M.; Kayser, M.; Palstra, R.J. HERC2 rs12913832 modulates human pigmentation through regulation of OCA2 expression. *Hum. Mol. Genet.* **2012**, *21*, 245–255. [CrossRef]
19. Meyer, O.S.; Andersen, J.D.; Simonsen, K.P.; Morling, N. Evaluation of rs12913832 as a single predictive marker for eye colour. *Forensic Sci. Int. Genet.* **2021**, *50*, 102405. [CrossRef]
20. Rubí-Castellanos, R.; Martínez-Cortés, G.; Muñoz-Valle, J.F.; González-Martín, A.; Cerda-Flores, R.M.; Anaya-Palafox, M.; Rangel-Villalobos, H. Pre-Hispanic Mesoamerican demography approximates the present-day ancestry of mestizos throughout the territory of Mexico. *Am. J. Phys. Anthropol.* **2009**, *139*, 284–294. [CrossRef]
21. Moreno-Estrada, A.; Gignoux, C.R.; Fernández-López, J.C.; Zakharia, F.; Sikora, M.; Contreras, A.V.; Acuña-Alonzo, V.; Sandoval, K.; Eng, C.; Romero-Hidalgo, S.; et al. The genetics of Mexico recapitulates Native American substructure and affects biomedical traits. *Science* **2014**, *344*, 1280–1285. [CrossRef] [PubMed]
22. Jobling, M.A.; Tyler-Smith, C. Human Y-chromosome variation in the genome-sequencing era. *Nat. Rev. Genet.* **2017**, *18*, 485–497. [CrossRef] [PubMed]

https://doi.org/10.3390/genes17030354

23. Aguilar-Velázquez, J.A.; García-Aceves, M.E.; Córdova-Mercado, M.F.; Guardado-Estrada, M.; Peña-Durán, E.; Villavicencio-Queijeiro, A.; Salas-Salas, O.; Coronado-Ávila, C.E.; Cárdenas-Monroy, C.A.; Ramos-González, B.; et al. Choice between DNA primer sets (A or B) of the ForenSeq kit: Forensic evaluation in a Mexican admixed population sample. *Int. J. Legal Med.* **2025**, *139*, 983–993. [CrossRef] [PubMed]
24. Quinto-Sanchez, M.; Huerta-Pacheco, N.S. Missing persons patterns from Mexico: Evidence of a forensic emergency crisis. *Forensic Sci. Res.* **2023**, *8*, 288–294. [CrossRef] [PubMed]
25. Jobling, M.A.; Hurles, M.E.; Tyler-Smith, C. *Human Evolutionary Genetics: Origins, Peoples and Disease*; Garland Science: New York, NY, USA, 2004.

https://doi.org/10.3390/genes17030354

genes

MDPI

Article

Genetic Diversity of 27 Y-STRs in Two Jordanian Subpopulations: Bedouins and Fellahin

Almuthanna K. Alkaraki [1,*], Mohammad B. Alsliman [1], Mohammad M. Twait [1], Miguel A. Alfonso-Sánchez [2] and Jose A. Peña [2]

[1] Department of Biological Sciences, Faculty of Science, Yarmouk University, Irbid 21163, Jordan; alsalman411@gmail.com (M.B.A.); mohammadspecial021@gmail.com (M.M.T.)
[2] Department of Genetics, Physical Anthropology and Animal Physiology, Faculty of Science and Technology, University of the Basque Country (UPV/EHU), Barrio Sarriena s/n, 48940 Leioa, Bizkaia, Spain; malfonsan@gmail.com (M.A.A.-S.); joseangel.pena@ehu.eus (J.A.P.)
* Correspondence: alkaraki@yu.edu.jo

Abstract

Background/Objectives: The Bedouins (nomads) and the Fellahin (farmers) of Jordan represent two distinct subpopulations, characterized by unique lifestyles, settlement patterns, and linguistic features. This study aims to estimate the frequency of 27 Y-STRs in these two Jordanian subpopulations, along with various forensic parameters and paternal lineage comparisons with neighboring populations. Methods: Twenty-seven Y-STRs were typed in two major Jordanian subpopulations: Bedouin nomads (n = 101) and Fellahin farmers (n = 98). The forensic and paternal genetic lineage parameters and Y-haplogroup predictions were estimated. In addition, we conducted multidimensional scaling (MDS) and centroid analyses based on the Fst distance matrix to compare the sampled communities with neighboring populations from the MENA region, East Africa, Southeast Europe, and South Asia. Results: The Y-haplogroup predictions revealed differences in the predicted lineage composition based on the Y-STR profiles. The predicted J1a2a1a2 haplogroup predominated among the Bedouins (74.3%), whereas the Fellahin displayed a more heterogeneous profile, with notable frequencies of J1 (40%) and J2 (17.3%). Furthermore, the Fellahin exhibited remarkable genetic diversity and significant gene flow, providing plausible evidence of kinship with neighboring Levantine and Arabian groups. In contrast, the Bedouins showed consistently lower diversity across multiple loci, indicating long-term tribal isolation and, therefore, the potential effects of genetic drift. The MDS and centroid analyses positioned the Fellahin among the genetically interconnected Middle Eastern populations, while the Bedouins were clustered with the Arabian Peninsula populations. Conclusions: Overall, the contrasting genetic signatures of the two Jordanian subpopulations reflect their settlement patterns and sociocultural practices. In addition, the Y-STR dataset generated in this study enhances the Jordanian forensic database and to extends our understanding of paternal lineage structures in the West Asian/Levantine region.

Keywords: Y-STRs; Bedouins; Fellahin; population genetics; Jordan

1. Introduction

The Y chromosome constitutes a cornerstone of human evolutionary genetics; its paternal mode of inheritance and the lack of meiotic recombination in the male-specific region make it a powerful tool for forensic identification, tracing paternal ancestry, and reconstructing migration routes of past human populations [1,2]. Among its most informative features are short

tandem repeats (Y-STRs), which provide insights into phylogenetic relationships and kinship patterns in both forensic and anthropological contexts [3–5]. The worldwide distribution of Y-STR variation has revealed evolutionary footprints of historical events, regional population expansions, nomadic mobility, and settlement processes [5–9].

Despite Jordan's geographical position at the crossroads of Asia, Africa, and Europe [10], and the presence of diverse subpopulations and ethnic groups [11], genetic data from the Jordanian population remain limited.

Within Jordan, the Bedouins (nomads) and the Fellahin (farmers) represent the core of the original Trans-Jordan population, predating the major influxes of refugees during the 19th and 20th centuries as a result of political conflicts and regional wars [12–15]. These two socioculturally defined groups are distinguished by their lifestyles, settlement patterns, and linguistic features [16].

Bedouins (al-Badu) refers to the term Badawi, which means people who live in the Badia (desert) and belong to a qabila (tribe) as an inherent relationship [17]. A tribe embodies an assemblage of individuals forming a societal, cultural, economic, and political structure, typically inhabiting a singular geographic entity either of their volition or due to the influence of intertribal conflicts or external compulsion [18]. The Bedouins' main activity is the farming of livestock like camels and sheep, and their basic diet depends on meat, fermented/dried dairy products, wheat, and imported dates [19]. On the other hand, the Fellahin's livelihood depends mainly upon agricultural activity and small-scale animal husbandry including sheep, goats, and chickens. Generally, the Fellahin reside within villages in stone or mud houses, either with their immediate family or within an extended familial context (hamula/clan); the Fellahin's life revolves around this fundamental connection to the land [20]. Linguistically, the Fellahin speak a distinct Arabic dialect that is characterized by several phonetic features, such as using "Ani" instead of "Ana" for I am, and the addition of the phonetic sound of the letter "H" when addressing females. Moreover, they tend to pronounce the Arabic letter (ق, Gaf), as "g" in "big", which is similar to Yemini and some Bedouins' dialect, contrasting with the Druze (strongly articulated GAF), urban Levantine (pronounced as A), or Westbank Palestinians (pronounced as Kaf) [21]. In contrast, the Jordanian Bedouins' dialect is somehow like that the Arabian Peninsula and retains many features of classical Arabic [22–24].

This study aims to estimate the frequency of 27 Y-STRs in two Jordanian subpopulations: Bedouins (nomads) and Fellahin (farmers). The findings are expected to provide new data for a Jordanian forensic Y-chromosome database and to refine the understanding of Y-STR and predicted Y haplogroups among both studied Jordanian subgroups, and in comparison with adjacent populations.

2. Materials and Methods

All scientific and experimental procedures followed the tenets of the Declaration of Helsinki and the Belmont Report for the protection of human subjects. The initial scientific proposal was carefully reviewed by the Institutional Review Board at Yarmouk University (IRB) to make sure it adhered to the standards' ethical codes and the local cultural values (approval reference number: IRB/2023/13). Participation was voluntary, and all volunteers provided written informed consent before blood collection. The research team explained the study objectives and procedures in accessible language and shared the principal investigator's contact information to safeguard the right to withdraw at any stage. The blood donors were randomly recruited from unrelated, healthy individuals aged 18–60 years. Sampling was conducted in the spring of 2023 (2 April to 29 May). The donors were classified according to their dialect, locality of residence, and family narrative history. The use of the terms

https://doi.org/10.3390/genes17020194

Fellahin (farmers) and Bedouins (nomads) as descriptive categories aligns with Jordanian cultural norms and is regarded as a positive marker of local heritage, raising no ethical concerns regarding discrimination. The Fellahin samples were collected from subjects residing in the northern Jordanian governorates (Irbid, Jerash, and Ajloun), whereas the Bedouin samples were collected from the three administratively defined (virtual) Bedouin regions (northern, central, and southern). Three subjects with ambiguous backgrounds were excluded, which accounted for 0.014% of the initial recruitment pool. The exclusion criteria included individuals of non-Trans-Jordanian paternal ancestry who did not self-identify as Arab and therefore could not be assigned to either studied subgroup. In total, 3 mL of venous blood was collected in EDTA tubes from 199 Jordanian males, comprising 98 Fellahin and 101 Bedouins. Donor privacy was protected by coding all the samples, and access to the genomic and demographic data was restricted to the principal investigator.

The genomic DNA was extracted from the blood samples with a Monarch® Genomic DNA Purification Kit (New England Biolabs, Ipswich, MA, USA), following the manufacturer's instructions. The DNA quantity and quality was measured using a commercial "Investigator Quantiplex Pro Kit" (Qiagen, Venlo, The Netherlands) according to the manufacturer recommendations. Twenty-seven Y-STR loci were amplified using a Yfiler™ Plus PCR Amplification Kit (Applied Biosystems, Waltham, MA, USA). Capillary electrophoresis was performed on a 3500XL Genetic Analyzer, and alleles were assigned with GeneMapper™ ID-X Software v1.6 (Thermo Fisher Scientific, Waltham, MA, USA), based on the allelic ladder provided by the kit. After experimental optimization, a total of 10 random samples were genotyped twice to ensure quality assurance along with performing standardization of known samples as a control.

Allele frequencies for each locus were calculated by using IBM SPSS Statistics v25. Gene diversity (formula: D = (n/n − 1) × (1 − ∑pi2)) was computed manually for each locus. NEVGEN Haplogroup Predictor (Y-DNA Haplogroup Predictor—NEVGEN.ORG) was used to predict Y haplogroups. Genetic distances (Fst) and centroid analyses were performed with GenoCline software package [25]. Multidimensional scaling (MDS) and neighbor joining (NJ) analyses were conducted using PAST program [26]. In order to establish population clusters, series of iterations were performed with Structure [27] for different values of K. Results were analyzed with structure Harvester [28] to determine most plausible number of clusters.

3. Results

3.1. Allele Frequencies and Genetic Diversity

The data on 27 Y-STR loci were obtained from 199 Jordanian males (Supplementary Materials Table S1). The allele frequencies and genetic diversity (GD) indices were calculated for the single-copy markers (23 Y-STRs) in the Fellahin (Supplementary Materials Table S2) and Bedouin (Supplementary Materials Table S3) subpopulations. The GD values ranged from 0.114 (DYS392) to 0.833 (DYS458) in the Bedouins, and from 0.305 (DYS392) to 0.880 (DYS458) in the Fellahin. The number of alleles per locus varied from 3 (DYS389I) in both subpopulations to 14 (DYS449) in the Fellahin and 11 (DYS458) in the Bedouins. Both the Fellahin and Bedouins showed high GD values (>0.750) at DYS576, DYS627, DYS481, and DYS518. Conversely, the Bedouins exhibited very low GD (<0.300) at DYS392, DYS437, and DYS533, while the Fellahin showed relatively low GD (0.300–0.500) at DYS437, DYS389I, and YGATAH4. Overall, the Fellahin displayed greater GD in 19 STRs, whereas the Bedouins showed higher diversity in 4 STRs.

An analysis of multi-copy loci (Supplementary Materials Table S4) revealed extensive allelic variation in both groups. At the DYS385 locus, 33 allelic combinations were identified in the Fellahin compared to 24 in the Bedouins. At DYS387S1, the Fellahin exhibited 23 allelic

https://doi.org/10.3390/genes17020194

patterns, while the Bedouins showed 13. Both loci (DYS385 and DYS387S1) demonstrated high GD in the Fellahin (>0.850), highlighting their strong power of discrimination among unrelated male lineages. Similarly, the Bedouins displayed high GD at DYS385 (0.866), whereas the GD at DYS387S1 was comparatively lower (0.806).

The heterogeneity between the two subpopulations in Jordan (Bedouin and Fellahin) was analyzed. It was found that they were significantly different (Mann–Whitney U-test: $z = 2.91$; $p < 0.01$).

3.2. Y Haplogroups

Twenty-three of the twenty-seven markers were used to predict the Y haplogroups with the NEVGEN Y-DNA Haplogroup Predictor online tool. The analysis identified 17 distinct haplogroups belonging to eight macro-haplogroups in the Fellahin subpopulation, compared to 15 distinct haplogroups within eight macro-haplogroups in the Bedouin subpopulation (Table 1). The predominant haplogroup in the Bedouins was J1a2a1a2, accounting for 74.3% of sampled individuals. The same haplogroup was also detected in the Fellahin, but at a lower frequency (40%). Haplogroup J2 was present in 17.3% of Fellahin compared to only 3.9% of Bedouins. Haplogroup E occurred in 17% of Fellahin and 4.9% of Bedouins. Haplogroup A showed comparable frequencies in both groups (3%). All other haplogroups were observed at frequencies below 5% in both populations. Additionally, the predictor classified one sample from each subpopulation as belonging to an unsupported subclade.

Table 1. Frequencies of predicted haplogroups in Jordanian Fellahin and Bedouin populations.

Fellahin		Bedouins	
Predicted Haplogroup	**Frequency**	**Predicted Haplogroup**	**Frequency**
A0a	0.010204	A1b1b2b	0.029703
A1b1b2b	0.020408	E1a	0.009901
E1a	0.010204	E1b1b	0.039604
E1b1b	0.173469	G2a	0.019802
G2a1	0.010204	G2a2b1	0.009901
G2a2b1	0.030612	G2b	0.019802
H1a1a	0.010204	H1a1a	0.009901
I2a2a	0.010204	J1a	0.009901
J1a	0.010204	J1a2a1a2	0.742574
J1a2a1a2	0.408163	J2a1	0.039604
J1b	0.010204	L1a	0.009901
J2a1	0.142857	R1a	0.009901
J2b2a	0.020408	R1b	0.009901
J2b2b	0.010204	R2	0.009901
R1a	0.05102	T	0.019802
R1b	0.020408		
T	0.040816		

A database was compiled containing the allele and haplogroup frequencies from populations in nearby regions, including the Middle East [29–39], North Africa [40], East Africa [41], Southeast Europe [36], and South Asia [42–44]. A comparative analysis with

https://doi.org/10.3390/genes17020194

these populations indicated that the genetic diversity of the Jordanian Bedouins (Jordan-B) is relatively low (Figure 1).

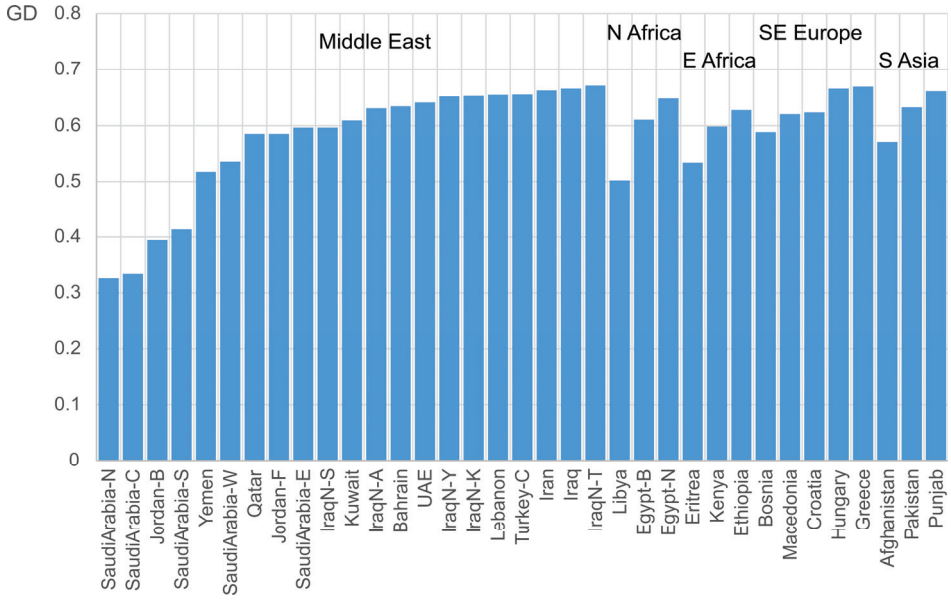

Figure 1. Genetic diversity observed in a series of populations from the Middle East, North Africa, East Africa, Southeast Europe, and South Asia for a group of STRs on the Y chromosome. Population labels: N (North), E (East), S (South), SE (Southeast), W (West), Jordan-B (Jordanian Bedouins), Jordan-F (Jordanian Fellahin), IraqN-S (Northern Iraqi Syriacs), IraqN-A (Northern Iraqi Arabs), IraqN-Y (Northern Iraqi Yazidis), IraqN-K (Northern Iraqi Kurds), IraqN-T (Northern Iraqi Turkmens), Turkey-C (Central Turkey), Egypt-B (Egypt Berbers), and Egypt-N (Northern Egyptians).

Indeed, it ranks among the lowest values recorded, comparable to those observed in several populations across Saudi Arabia (north, center, and south). Conversely, the value observed in the Fellahin population (Jordan-F) is higher and approximates the average of the populations considered in this study. The MDS plot derived from the Fst distances based on the allele frequencies is shown in Figure 2. The populations from South Asia (fuchsia), Europe (green), and North and East Africa (brown) are primarily distributed along the positive segment of Axis 1. Within this distribution, the South Asian populations are positioned at the top of the graph, the European populations occupy a central position, and the African populations are located at the bottom. Afghanistan, Eritrea, and Libya are the most distant from these clusters. Afghanistan lies at the positive end of Axis 1, Eritrea at the negative end of Axis 2, and Libya is relatively close to the populations of the Arabian Peninsula. The Berbers of Egypt (Egypt-B) are separated from the Arab populations and positioned among those of East Africa. Most Middle Eastern populations cluster around the centroid, including the Fellahin of Jordan (red). The most distant populations within this group are the Turks (Turkey-C) and the Syriacs of Iraq (IraqN-S), located at the positive end of Axis 2. At the negative end of Axis 1 are three Saudi Arabian populations (north, center, and south) together with the Bedouins of Jordan. This cluster of populations exhibits the lowest genetic diversity (Figure 1).

The centroid analysis (Figure 3) reveals a large cluster of populations with similar features, characterized by high heterozygosity (H) and low heterogeneity (Ri) values. These findings suggest a substantial level of gene flow among them, and the Fellahin population of Jordan is included in this cluster. The Eritreans and Egyptian Berbers exhibit both high heterogeneity and heterozygosity, likely reflecting gene flow from populations not represented in the database. In contrast, three Saudi Arabian populations (north, center,

https://doi.org/10.3390/genes17020194

and south), together with the Bedouins of Jordan, display very low heterozygosity and average heterogeneity values, indicating a high degree of population isolation.

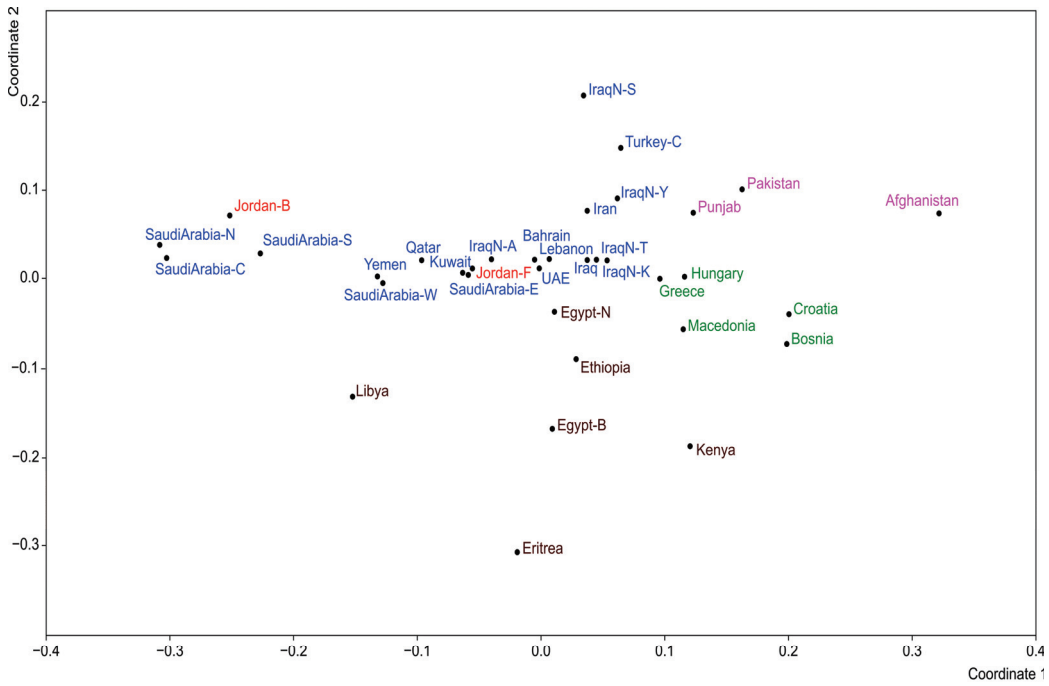

Figure 2. MDS on FST distance matrix based on allele frequencies. Populations of South Asia are identified in fuchsia, those of Europe in green, those of North and East Africa in brown, those of Middle East in blue, and those of Jordan in red.

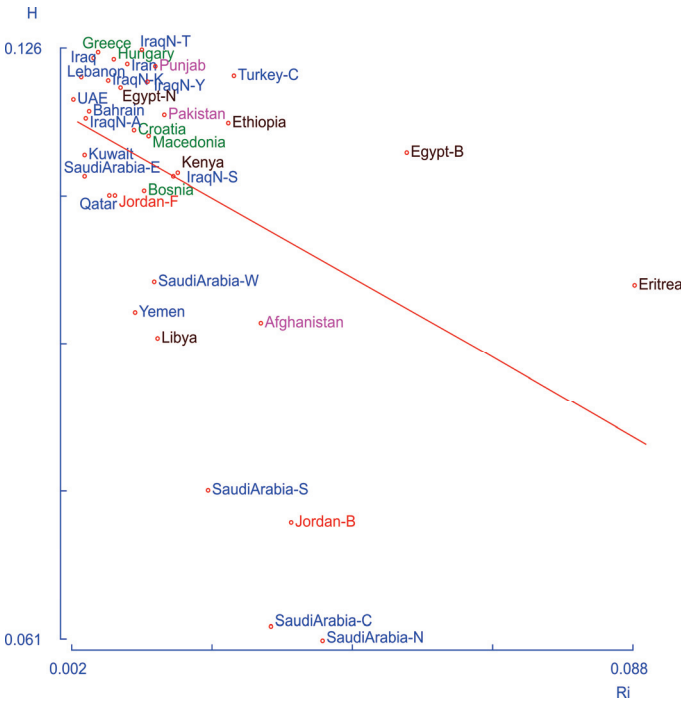

Figure 3. Centroid analysis of a group of populations from South Asia, the Middle East, Europe, and northeast Africa. Populations of South Asia are identified in fuchsia, those of Europe in green, those of North and East Africa in brown, those of Middle East in blue, and those of Jordan in red. The line represents the expected relationship between heterozygosity and Ri.

https://doi.org/10.3390/genes17020194

A series of analyses were performed using Structure with different values of K and several repetitions. The results were analyzed using Structure Harvester, which found that the best fit was obtained for K = 3. An NJ tree was also obtained from the FST distance matrix using Past (Figure 4). The population labels are colored according to the most important Structure component in each population. The groupings are distributed consistently. One group (brown) includes populations from North and East Africa, with the exception of Libya, which has an Arab origin. A second group (green) includes European populations, populations from South Asia, and some populations from the Middle East. The third group (blue) finally includes most of the populations of the Arabian Peninsula and Libya.

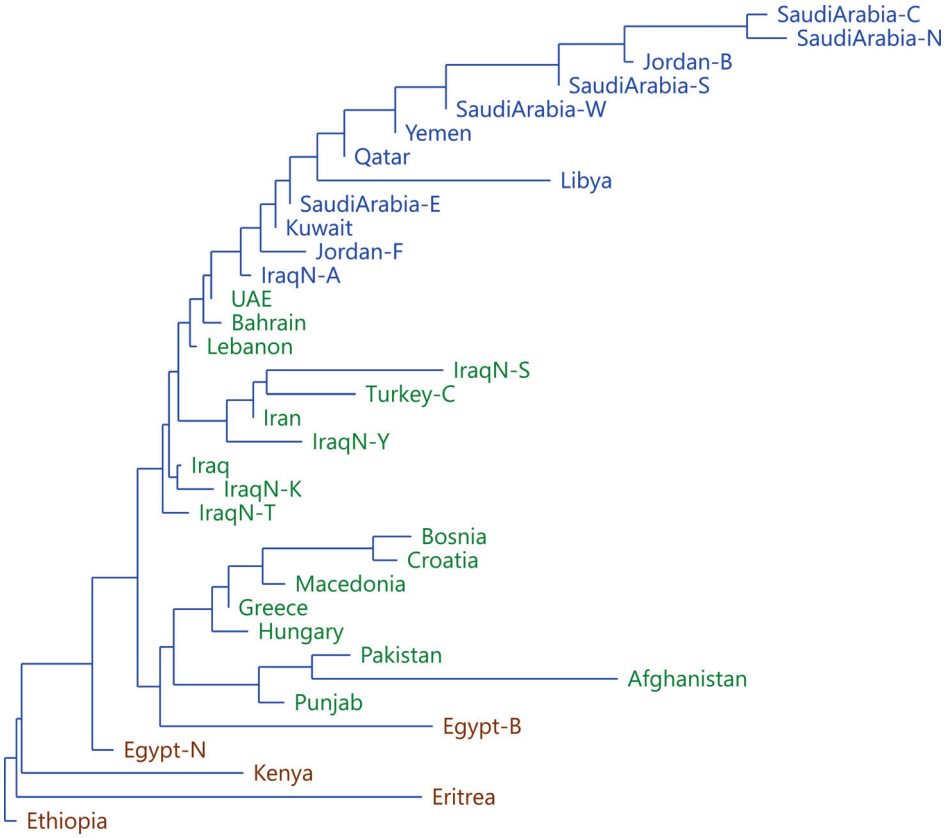

Figure 4. NJ on FST distance matrix based on allele frequencies. Populations are colored according to the predominant component in Structure for K = 3. Group 1 is colored green, group 2 blue, and group 3 brown.

An MDS analysis was also performed using the haplogroup frequencies for the same set of populations (Figure 5). The results closely parallel those emerging from the allele frequencies. Axis 1 distributes the South Asian populations (fuchsia), European populations (green), and North and East African populations (brown) toward one end, corresponding in this case to negative values. In this analysis, however, Afghanistan does not appear significantly differentiated from Punjab and Pakistan. The Fellahin of Jordan again occupy an intermediate position, clustering with a large group of Middle Eastern populations. Finally, the northern, central, and southern Saudi Arabian populations, together with the Bedouins of Jordan, are located at the opposite end of Axis 1, once again standing out for their distinct genetic profile.

https://doi.org/10.3390/genes17020194

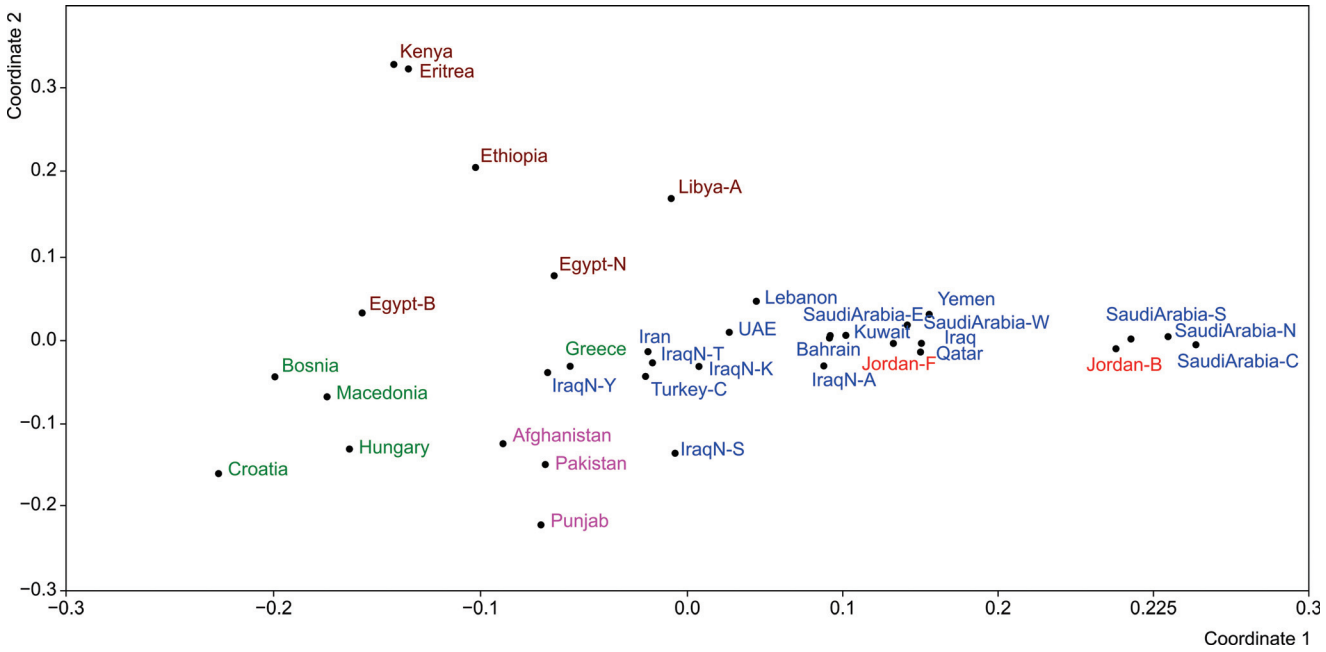

Figure 5. MDS on FST distance matrix based on haplogroup frequencies. Populations of South Asia are identified in fuchsia, those of Europe in green, those of North and East Africa in brown, those of Middle East in blue, and those of Jordan in red.

4. Discussion

The present study provides a comprehensive overview of Y-STR diversity in the Fellahin and Bedouin subpopulations of Jordan. Historically, the studied subgroups are considered as the main native population of Trans-Jordan before the multi-waves of refuges, such as Arab (Palestinians, Iraqi, and Syrians) and non-Arab refuges (Chechen, Circassian, and Armenian).

The obtained results clearly demonstrate a difference between the Bedouins and Fellahin in the predicted Y-STR haplogroups. These differences reflect a contrasting paternal demographic history shaped by the settlement patterns, social organization, and acceptance of others within agricultural communities vs. the restricted tribal organization associated with Bedouin culture.

The predicted predominant haplogroup J1 observed in the Jordanian Bedouins supports a paternal lineage continuity with the Arabian Peninsula, particularly the J1-P58 branch, which is associated with Semitic-speaking pastoral tribes and underwent major expansion during the Holocene [45]. In addition, higher frequency of such predicted haplogroups has been reported in Saudi Arabia, Yemen, and the Gulf area, often linked with a tribal founder effect [34,35]. Compared to the Bedouins, the predicted haplogroups in the Fellahin show a more balanced composition (J1, J2, and E), indicating an acceptable gene flow within the Fellahin subpopulation. The J2 haplogroup is associated with Neolithic agricultural expansion from the Fertile Crescent, while the reported haplogroup E reflects the gene flow between north/east Africa and the Levant area, likely facilitated by climate-driven migration or trade routes [40,46]. Other minor haplogroups reported in the Fellahin reflect admixture and ongoing gene flow.

The lower GD observed among the Bedouin subpopulation across many loci is consistent with tribal structures and paternal lineage-based stratifications. Tribal Bedouins favor the expansion of a limited number of male founders and reduce the male ancestral size, resulting in amplified genetic drift. A similar reduction in Y-chromosome diversity can be

https://doi.org/10.3390/genes17020194

noticed in the Arabian Peninsula populations, where tribal identity and consanguineous marriages shaped the tribal structure to depend on the paternal lineage [34,35]. Moreover, low Y-STRs diversity is always associated with closed/isolated populations with strong genealogical continuity traced through the male lineage [7].

In contrast, the observed higher diversity in the Fellahin subgroup reflects a more heterogeneous paternal composition and a more diverse gene pool. Historically, agricultural communities engaged in trade, urban interactions, and intercommunity marriages, all of which promote male-mediated gene flow. Comparable Y-STR diversity patterns have been reported in Levantine communities with long-term settlement, including Syrian, Lebanese, and Mesopotamian groups [32,33,47,48].

The two studied subpopulations were analyzed within a broad geographical framework, considering comparative data from Asia, Europe, and Africa to explore potential genetic affinities. The multidimensional scaling based on both alleles and predicted haplogroups groups the Fellahin with other Levantine populations and broader Middle Eastern populations, while the Bedouins are aligned more closely with Arabian Peninsula groups. Thus, the male lineages of the Fellahin exhibit a greater genetic diversity level within the ranks of the analyzed population set. This pattern points to a complex demographic history involving admixture events and long-term gene flow with neighboring communities. Their agricultural tradition has kept them rooted to the land and sharing in the demographic processes that have unfolded in the region over time. Jordan's geographical position at the intersection of Africa, Asia, and Europe has made the region a historical arena for numerous transformative events, including major migratory movements since the out-of-Africa dispersal. It is further acknowledged as one of the principal centers of origin of agriculture and animal husbandry, practices that subsequently diffused from the Middle East into Europe and, likely, into North and East Africa and southwest Asia. The Middle East was among the few regions where cattle domestication occurred. Nevertheless, both agriculture and pastoralism underwent a substantial decline as a result of widespread aridification. The conclusion of the African Humid Period precipitated the rapid desertification of the Sahara and the Arabian Peninsula [49,50] with profound consequences, including the collapse of the Akkadian Empire [51] and the Old Kingdom in Egypt [52] around 4300 years ago.

It has been argued that the aridification of the Arabian Peninsula may have precipitated a subsistence crisis, which was alleviated through the domestication of the camel [53]. The demographic pressures arising from the depletion of agricultural and pastoral resources, combined with the low population densities inherent to resource-poor environments, represent two plausible drivers of the pronounced genetic drift observed in populations that persisted in desert contexts, such as the Bedouins. The imprint of this drift is evident in the markedly low genetic diversity and high genetic heterogeneity relative to neighboring populations, as demonstrated by the multidimensional scaling (MDS) analyses of both allele and haplotype frequencies.

From a forensic point of view, the higher haplotype diversity among the Fellahin increases the discriminatory power; meanwhile, the reduced diversity among the Bedouins may increase haplotype sharing among different individuals belonging to the same tribal background. This pattern is recognized in forensic interpretations of endogamous populations.

5. Conclusions

This study generated a comprehensive dataset of 27 Y-chromosomal markers in two Jordanian subpopulations, the Bedouins and the Fellahin. The genetic relationships observed between both groups and with neighboring populations are congruent with the geographic, linguistic, and cultural frameworks that have historically shaped the region. No-

https://doi.org/10.3390/genes17020194

tably, the Bedouin haplotypes reflect reduced Y-STR haplotype diversity consistent with limited paternal lineage variability, whereas admixture, gene flow, and demographic complexity are reflected in the Fellahin subpopulation. The Y-STR profiles obtained for both subpopulations not only enhance the resolving power of the Jordanian forensic database, but also contribute to the reconstruction of paternal lineages, the refinement of our understanding of population structure, and the enrichment of the evolutionary narrative of Middle Eastern and Levantine groups.

Supplementary Materials: The following supporting information can be downloaded at: https://www.mdpi.com/article/10.3390/genes17020194/s1, Table S1: Raw data for the 27 Y-STRs in both Jordanian Bedouins and Fellahin subpopulations. Table S2: Allele frequencies and genetic diversity (GD) for single-copy marker in Fellahin Jordanian population. Table S3: Allele frequencies and genetic diversity (GD) for single-copy marker in Bedouin Jordanian population. Table S4: Allele frequencies and genetic diversity (GD) for Multi-copy marker in Fellahin and Bedouin Jordanian population.

Author Contributions: Conceptualization, A.K.A. and M.B.A.; methodology, M.B.A. and M.M.T.; software, M.A.A.-S., M.B.A. and J.A.P.; validation, A.K.A., J.A.P. and M.A.A.-S.; formal analysis, A.K.A., M.B.A., M.M.T., M.A.A.-S. and J.A.P.; investigation, A.K.A., M.B.A. and M.M.T.; resources, A.K.A. and J.A.P.; data curation, M.B.A. and M.M.T.; writing—original draft preparation, A.K.A., M.B.A. and M.M.T.; writing—review and editing, A.K.A., M.B.A., M.M.T., M.A.A.-S. and J.A.P.; visualization, M.A.A.-S.; supervision, A.K.A. and J.A.P.; project administration, A.K.A.; funding acquisition, A.K.A. All authors have read and agreed to the published version of the manuscript.

Funding: This research was funded by the Deanship of Scientific Research and Graduate Studies at Yarmouk University, grant number 74/2022.

Institutional Review Board Statement: The study was conducted in accordance with the Declaration of Helsinki and approved by the Institutional Review Board Committee of Yarmouk University (YU/IRB/2023/13, 23 January 2023).

Informed Consent Statement: Informed consent was obtained from all subjects involved in the study.

Data Availability Statement: The original contributions presented in this study are included in the article/Supplementary Materials. Further inquiries can be directed to the corresponding author.

Conflicts of Interest: The authors declare no conflicts of interest.

References

1. Jobling, M.A.; Tyler-Smith, C. Human Y-chromosome variation in the genome-sequencing era. *Nat. Rev. Genet.* **2017**, *18*, 485–497. [CrossRef] [PubMed]
2. Calafell, F.; Larmuseau, M.H.D. The Y chromosome as the most popular marker in genetic genealogy benefits interdisciplinary research. *Hum. Genet.* **2017**, *136*, 559–573. [CrossRef] [PubMed]
3. Balanovsky, O. Toward a consensus on SNP and STR mutation rates on the human Y-chromosome. *Hum. Genet.* **2017**, *136*, 575–590. [CrossRef] [PubMed]
4. Kayser, M. Forensic use of Y-chromosome DNA: A general overview. *Hum. Genet.* **2017**, *136*, 621–635. [CrossRef]
5. Costa, R.; Fadoni, J.; Amorim, A.; Cainé, L. Y-STR Databases-Application in Sexual Crimes. *Genes* **2025**, *16*, 484. [CrossRef]
6. Claerhout, S.; Vandenbosch, M.; Nivelle, K.; Gruyters, L.; Peeters, A.; Larmuseau, M.H.D.; Decorte, R. Determining Y-STR mutation rates in deep-routing genealogies: Identification of haplogroup differences. *Forensic Sci. Int. Genet.* **2018**, *34*, 1–10. [CrossRef]
7. de Knijff, P. On the Forensic Use of Y-Chromosome Polymorphisms. *Genes* **2022**, *13*, 898. [CrossRef]
8. Navarro-López, B.; Granizo-Rodríguez, E.; Palencia-Madrid, L.; Raffone, C.; Baeta, M.; de Pancorbo, M.M. Phylogeographic review of Y chromosome haplogroups in Europe. *Int. J. Leg. Med.* **2021**, *135*, 1675–1684. [CrossRef]
9. Hodișan, R.; Zaha, D.C.; Jurca, C.; Petchesi, C.D.; Bembea, M. A Review of Genetic Diversity Based on the Y Chromosome in the Romanian Population. *Cureus* **2024**, *16*, e67593. [CrossRef]

10. Rowold, D.J.; Luis, J.R.; Terreros, M.C.; Herrera, R.J. Mitochondrial DNA geneflow indicates preferred usage of the Levant Corridor over the Horn of Africa passageway. *J. Hum. Genet.* **2007**, *52*, 436–447. [CrossRef]
11. Central Intelligence Agency. The World Factbook: Jordan. 2025. Available online: https://www.cia.gov/the-world-factbook/countries/jordan/ (accessed on 23 October 2025).
12. Alduraidi, H.; Waters, C.M. Health-related quality of life of Palestinian refugees inside and outside camps in Jordan. *Nurs. Outlook* **2017**, *65*, 436–443. [CrossRef]
13. Alduraidi, H.; Aqel, A.A.; Saleh, Z.; Almansour, I.; Darawad, M. UNRWA's role in promoting health outcomes of Palestinian refugees in Jordan: A systematic literature review. *Public Health Nurs.* **2021**, *38*, 692–700. [CrossRef] [PubMed]
14. Simadi, F.A.; Nahar, G.S. Refugees in Jordan: Sociological perspective. *Soc. Responsib. J.* **2009**, *5*, 257–264. [CrossRef]
15. Chatelard, G. Jordan: A Refugee Haven. 2010. Available online: https://www.migrationpolicy.org/article/jordan-refugee-haven (accessed on 23 October 2025).
16. Abo-Zaied Arar, E.; Tannenbaum, M. Pride, shame, and guilt: Socio-emotional aspects of the encounter between the Bedouin and Fellahi dialects. *Int. J. Biling. Educ. Biling.* **2021**, *24*, 1232–1246. [CrossRef]
17. Marx, E. Economic change among pastoral nomads in the Middle East. In *Settling the Desert*; Routledge: London, UK, 1981; pp. 133–190.
18. Khazanov, A.M. *Nomads and the Outside World*; Gellner, E., Ed.; Crookenden, J., Translator; University of Wisconsin Press: Madison, WI, USA, 1984; p. 382.
19. Cole, D.P. Where have the Bedouin gone? *Anthropol. Q.* **2003**, *76*, 235–267. [CrossRef]
20. Mazarib, T. *From Desert to Town: The Integration of Bedouin into Arab Fellahin Villages and Towns in the Galilee, 1700–2020*; Liverpool University Press: Liverpool, UK, 2021.
21. Naïm, S. Dialects of the Levant. In *The Semitic Languages: An International Handbook*; De Gruyter Mouton: Berlin, Germany, 2011; pp. 220–237.
22. Al Huneety, A.; Mashaqba, B.; abu Hula, R.; Thnaibat, B.K. Phonological aspects of al-Issa Arabic, a Bedouin dialect in the north of Jordan. *Heliyon* **2021**, *7*, e07405. [CrossRef]
23. Suleiman, S.M. *Jordanian Arabic Between Diglossia and Bilingualism*; John Benjamins Publishing Company: Amsterdam, The Netherlands, 1985.
24. Migdadi, F.; Jarbou, S. Compliments in Fellahi Jordanian Arabic. In *Grazer Linguistische Studien*; Department of Linguistics University of Graz: Graz, Austria, 2007.
25. Peña, J.A.; Gómez-Pérez, L.; Alfonso-Sánchez, M.A. On the Trail of Spatial Patterns of Genetic Variation. *Evol. Biol.* **2022**, *49*, 84–91. [CrossRef]
26. Hammer, Ø.; Harper, D.A.T. Past: Paleontological statistics software package for educaton and data anlysis. *Palaeontol. Electron.* **2001**, *4*, 1.
27. Pritchard, J.K.; Stephens, M.; Donnelly, P. Inference of population structure using multilocus genotype data. *Genetics* **2000**, *155*, 945–959. [CrossRef]
28. Earl, D.A.; vonHoldt, B.M. STRUCTURE HARVESTER: A website and program for visualizing STRUCTURE output and implementing the Evanno method. *Conserv. Genet. Resour.* **2012**, *4*, 359–361. [CrossRef]
29. Al-Shoba, K.; Al-Hamadi, N.; Almohammed, E.K.; Hadi, S.; Goodwin, W.; Lazim, H. The Yemeni genetic structure revealed by the Y chromosome STRs. *Forensic Sci. Med. Pathol.* **2025**, *21*, 1196–1212. [CrossRef]
30. Al-Snan, N.R.; Messaoudi, S.A.; Khubrani, Y.M.; Wetton, J.H.; Jobling, M.A.; Bakhiet, M. Geographical structuring and low diversity of paternal lineages in Bahrain shown by analysis of 27 Y-STRs. *Mol. Genet. Genom.* **2020**, *295*, 1315–1324. [CrossRef] [PubMed]
31. Alakoc, Y.D.; Gokcumen, O.; Tug, A.; Gultekin, T.; Gulec, E.; Schurr, T.G. Y-chromosome and autosomal STR diversity in four proximate settlements in Central Anatolia. *Forensic Sci. Int. Genet.* **2010**, *4*, e135–e137. [CrossRef] [PubMed]
32. Almohammed, E.K.; Hadi, A.; Al-Asmakh, M.; Lazim, H. The Qatari population's genetic structure and gene flow as revealed by the Y chromosome. *PLoS ONE* **2023**, *18*, e0290844. [CrossRef]
33. Dogan, S.; Gurkan, C.; Dogan, M.; Balkaya, H.E.; Tunc, R.; Demirdov, D.K.; Ameen, N.A.; Marjanovic, D. A glimpse at the intricate mosaic of ethnicities from Mesopotamia: Paternal lineages of the Northern Iraqi Arabs, Kurds, Syriacs, Turkmens and Yazidis. *PLoS ONE* **2017**, *12*, e0187408. [CrossRef] [PubMed]
34. Elliott, K.S.; Haber, M.; Daggag, H.; Busby, G.B.; Sarwar, R.; Kennet, D.; Petraglia, M.; Petherbridge, L.J.; Yavari, P.; Heard-Bey, F.U.; et al. Fine-Scale Genetic Structure in the United Arab Emirates Reflects Endogamous and Consanguineous Culture, Population History, and Geography. *Mol. Biol. Evol.* **2022**, *39*, msac039. [CrossRef]
35. Khubrani, Y.M.; Wetton, J.H.; Jobling, M.A. Extensive geographical and social structure in the paternal lineages of Saudi Arabia revealed by analysis of 27 Y-STRs. *Forensic Sci. Int. Genet.* **2018**, *33*, 98–105. [CrossRef]

https://doi.org/10.3390/genes17020194

36. Purps, J.; Siegert, S.; Willuweit, S.; Nagy, M.; Alves, C.; Salazar, R.; Angustia, S.M.; Santos, L.H.; Anslinger, K.; Bayer, B.; et al. A global analysis of Y-chromosomal haplotype diversity for 23 STR loci. *Forensic Sci. Int. Genet.* **2014**, *12*, 12–23. [CrossRef]
37. Sayyari, M.; Salehzadeh, A.; Tabatabaiefar, M.A.; Abbasi, A. Profiling of 17 Y-STR loci in Mazandaran and Gilan provinces of Iran. *Turk. J. Med. Sci.* **2019**, *49*, 1277–1286. [CrossRef]
38. Taqi, Z.; Alenizi, M.; Alenizi, H.; Ismael, S.; Dukhyil, A.A.B.; Nazir, M.; Sanqoor, S.; Al Harbi, E.; Al-Jaber, J.; Theyab, J.; et al. Population genetics of 23 Y-STR markers in Kuwaiti population. *Forensic Sci. Int. Genet.* **2015**, *16*, 203–204. [CrossRef]
39. Zeyad, T.; Adam, A.; Alghafri, R.; Iratni, R. Study of 27 Y-STR markers in United Arab Emirates population. *Forensic Sci. Int. Rep.* **2020**, *2*, 100057. [CrossRef]
40. D'Atanasio, E.; Iacovacci, G.; Pistillo, R.; Bonito, M.; Dugoujon, J.M.; Moral, P.; El-Chennawi, F.; Melhaoui, M.; Baali, A.; Cherkaoui, M.; et al. Rapidly mutating Y-STRs in rapidly expanding populations: Discrimination power of the Yfiler Plus multiplex in northern Africa. *Forensic Sci. Int. Genet.* **2019**, *38*, 185–194. [CrossRef]
41. Iacovacci, G.; D'Atanasio, E.; Marini, O.; Coppa, A.; Sellitto, D.; Trombetta, B.; Berti, A.; Cruciani, F. Forensic data and microvariant sequence characterization of 27 Y-STR loci analyzed in four Eastern African countries. *Forensic Sci. Int. Genet.* **2017**, *27*, 123–131. [CrossRef] [PubMed]
42. Adnan, A.; Rakha, A.; Noor, A.; van Oven, M.; Ralf, A.; Kayser, M. Population data of 17 Y-STRs (Yfiler) from Punjabis and Kashmiris of Pakistan. *Int. J. Leg. Med.* **2018**, *132*, 137–138. [CrossRef] [PubMed]
43. Ikram, M.S.; Mehmood, T.; Rakha, A.; Akhtar, S.; Khan, M.I.M.; Al-Qahtani, W.S.; Safhi, F.A.; Hadi, S.; Wang, C.C.; Adnan, A. Genetic diversity and forensic application of Y-filer STRs in four major ethnic groups of Pakistan. *BMC Genom.* **2022**, *23*, 788. [CrossRef]
44. Lacau, H.; Bukhari, A.; Gayden, T.; La Salvia, J.; Regueiro, M.; Stojkovic, O.; Herrera, R.J. Y-STR profiling in two Afghanistan populations. *Leg. Med.* **2011**, *13*, 103–108. [CrossRef] [PubMed]
45. Sahakyan, H.; Margaryan, A.; Saag, L.; Karmin, M.; Flores, R.; Haber, M.; Kushniarevich, A.; Khachatryan, Z.; Bahmanimehr, A.; Parik, J.; et al. Origin and diffusion of human Y chromosome haplogroup J1-M267. *Sci. Rep.* **2021**, *11*, 6659. [CrossRef]
46. Cruciani, F.; Trombetta, B.; Massaia, A.; Destro-Bisol, G.; Sellitto, D.; Scozzari, R. A revised root for the human Y chromosomal phylogenetic tree: The origin of patrilineal diversity in Africa. *Am. J. Hum. Genet.* **2011**, *88*, 814–818. [CrossRef]
47. Zalloua, P.A.; Platt, D.E.; El Sibai, M.; Khalife, J.; Makhoul, N.; Haber, M.; Xue, Y.; Izaabel, H.; Bosch, E.; Adams, S.M.; et al. Identifying genetic traces of historical expansions: Phoenician footprints in the Mediterranean. *Am. J. Hum. Genet.* **2008**, *83*, 633–642. [CrossRef]
48. Al-Zubaidi, M.M.; Sabbah, M.A.; Mahmood, H.K. Molecular diversity of 23-YSTR markers in Iraqi populations. *Gene* **2023**, *872*, 147440. [CrossRef]
49. McGee, D.; de Menocal, P.B.; Winckler, G.; Stuut, J.B.W.; Bradtmiller, L.I. The magnitude, timing and abruptness of changes in North African dust deposition over the last 20,000yr. *Earth Planet. Sci. Lett.* **2013**, *371–372*, 163–176. [CrossRef]
50. Armitage, S.J.; Bristow, C.S.; Drake, N.A. West African monsoon dynamics inferred from abrupt fluctuations of Lake Mega-Chad. *Proc. Natl. Acad. Sci. USA* **2015**, *112*, 8543–8548. [CrossRef]
51. Cullen, H.M.; deMenocal, P.B.; Hemming, S.; Hemming, G.; Brown, F.H.; Guilderson, T.; Sirocko, F. Climate change and the collapse of the Akkadian empire: Evidence from the deep sea. *Geology* **2000**, *28*, 379–382. [CrossRef]
52. Welc, F.; Marks, L. Climate change at the end of the Old Kingdom in Egypt around 4200 BP: New geoarchaeological evidence. *Quat. Int.* **2014**, *324*, 124–133. [CrossRef]
53. Alkaraki, A.K.; Alfonso-Sánchez, M.A.; Peña, J.A.; Abuelezz, A.I. Lactase persistence in the Jordanian population: Potential effects of the Arabian Peninsula and Sahara's aridification. *Heliyon* **2024**, *10*, e33455. [CrossRef]

genes

MDPI

Review

Predicting Physical Appearance from Low Template: State of the Art and Future Perspectives

Francesco Sessa [1,*,†], Emina Dervišević [2,†], Massimiliano Esposito [3], Martina Francaviglia [4], Mario Chisari [3], Cristoforo Pomara [4,‡] and Monica Salerno [4,*,‡]

1 Department of Psychology and Health Sciences, Faculty of Human Sciences, Education, and Sports, Pegaso University, 80143 Naples, Italy
2 Department of Forensic Medicine, Faculty of Medicine, University of Sarajevo, 71000 Sarajevo, Bosnia and Herzegovina; emina.dervisevic@mf.unsa.ba
3 Faculty of Medicine and Surgery, "Kore" University of Enna, 94100 Enna, Italy; massimiliano.esposito@unikore.it (M.E.); mario.chisari@unikore.it (M.C.)
4 Department of Medical, Surgical and Advanced Technologies "G.F. Ingrassia", University of Catania, 95121 Catania, Italy; martinafrancaviglia95@gmail.com (M.F.); cristoforo.pomara@unict.it (C.P.)
* Correspondence: francesco.sessa@unipegaso.it (F.S.); monica.salerno@unict.it (M.S.)
† These authors contributed equally to the study.
‡ These authors share last authorship.

Abstract

Background/Objectives: Forensic DNA phenotyping (FDP) enables the prediction of externally visible characteristics (EVCs) such as eye, hair, and skin color, ancestry, and age from biological traces. However, low template DNA (LT-DNA), often derived from degraded or trace samples, poses significant challenges due to allelic dropout, contamination, and incomplete profiles. This review evaluates recent advances in FDP from LT-DNA, focusing on the integration of machine learning (ML) models to improve predictive accuracy and operational readiness, while addressing ethical and population-related considerations. **Methods**: A comprehensive literature review was conducted on FDP and ML applications in forensic genomics. Key areas examined include SNP-based trait modeling, genotype imputation, epigenetic age estimation, and probabilistic inference. Comparative performance of ML algorithms (Random Forests, Support Vector Machines, Gradient Boosting, and deep learning) was assessed using datasets such as the 1000 Genomes Project, UK Biobank, and forensic casework samples. Ethical frameworks and validation standards were also analyzed. **Results**: ML approaches significantly enhance phenotype prediction from LT-DNA, achieving AUC > 0.9 for eye color and improving SNP recovery by up to 15% through imputation. Tools like HIrisPlex-S and VISAGE panels remain robust for eye and hair color, with moderate accuracy for skin tone and emerging capabilities for age and facial morphology. Limitations persist in admixed populations and traits with polygenic complexity. Interpretability and bias mitigation remain critical for forensic admissibility. **Conclusions**: L integration strengthens FDP from LT-DNA, offering valuable investigative leads in challenging scenarios. Future directions include multi-omics integration, portable sequencing platforms, inclusive reference datasets, and explainable AI to ensure accuracy, transparency, and ethical compliance in forensic applications.

Keywords: forensic DNA phenotyping (FDP); low template DNA (LT-DNA); machine learning (ML); externally visible characteristics (EVC); SNP-based prediction; forensic genomics

1. Introduction

The forensic application of genetic data has evolved from a tool of straightforward identity verification to a complex system capable of predicting human phenotypes from biological traces, a field known as Forensic DNA Phenotyping (FDP) [1,2]. This paradigm shift is driven by technological advances in genomics, particularly genome-wide association studies (GWAS), next-generation sequencing (NGS), and increasingly sophisticated computational modeling [3]. FDP allows investigators to derive investigative leads from crime scene DNA by predicting externally visible characteristics (EVCs) such as eye, hair, and skin color, biogeographic ancestry, and chronological age, even in the absence of a known reference profile [4].

The idea of forensic DNA intelligence is to extract any information from DNA that can help guide criminal investigations, especially when no match exists in short tandem repeat (STR) databases [5]. Of practical importance are clues to the physical phenotype, due to the high heritability of human appearance traits [6]. While early forensic genetics relied on STR profiling for identity matching, STR markers are neutral and do not provide phenotypic information [7]. FDP has thus emerged as an essential tool in cases involving unidentified perpetrators, cold cases, mass disasters, or heavily degraded biological remains [8].

The notion that physical features can be "read" from DNA began to gain scientific credibility in the early 2000s with the publication of large-scale GWAS that identified single nucleotide polymorphisms (SNPs) associated with human pigmentation and morphology. Early SNP-based systems such as IrisPlex and HIrisPlex-S demonstrated the feasibility of predicting eye and hair color with moderate to high accuracy. As understanding of complex trait genetics expanded, FDP broadened to include traits like freckles, hair structure, male pattern baldness, and tall stature, as well as subcontinental ancestry and age from multiple tissues [1].

A major challenge in FDP is the prediction of complex traits, which are polygenic and often influenced by environmental and developmental factors. Traits like facial morphology or skin tone involve many small-effect variants, requiring big data approaches and machine learning (ML) models trained on large, diverse reference datasets (Figure 1). For simpler traits with high heritability, targeted analysis of a limited number of markers using massively parallel sequencing (MPS) has proven effective. However, achieving universal genomic predictors for all traits will require the construction of much larger databases derived from whole-genome sequencing (WGS), including rare variants that may influence phenotypes. Furthermore, for accurate appearance prediction, age estimation must be considered; this can be derived from epigenetic modifications, particularly DNA methylation markers, which reflect biological age [3].

Technological limitations persist, especially in cases involving LT-DNA or degraded skeletal remains, which are common in real-world forensics. LT-DNA samples, often collected from trace biological material such as epithelial cells, touched objects, or aged remains, are susceptible to allelic dropout, amplification errors, and partial genotyping. Despite these challenges, tools like the Ion AmpliSeq™ HIrisPlex-S panel, validated using Ion Torrent MPS technology, have shown remarkable resilience. In a study analyzing 63 bone samples aged up to 80 years, full pigmentation profiles could be recovered from over 55% of cases, with successful eye and hair color predictions made from partial profiles in many others. Nonetheless, certain SNPs, especially those relevant to skin color, showed consistent underperformance, highlighting the need for primer redesign in future iterations of the panel [9].

https://doi.org/10.3390/genes17010059

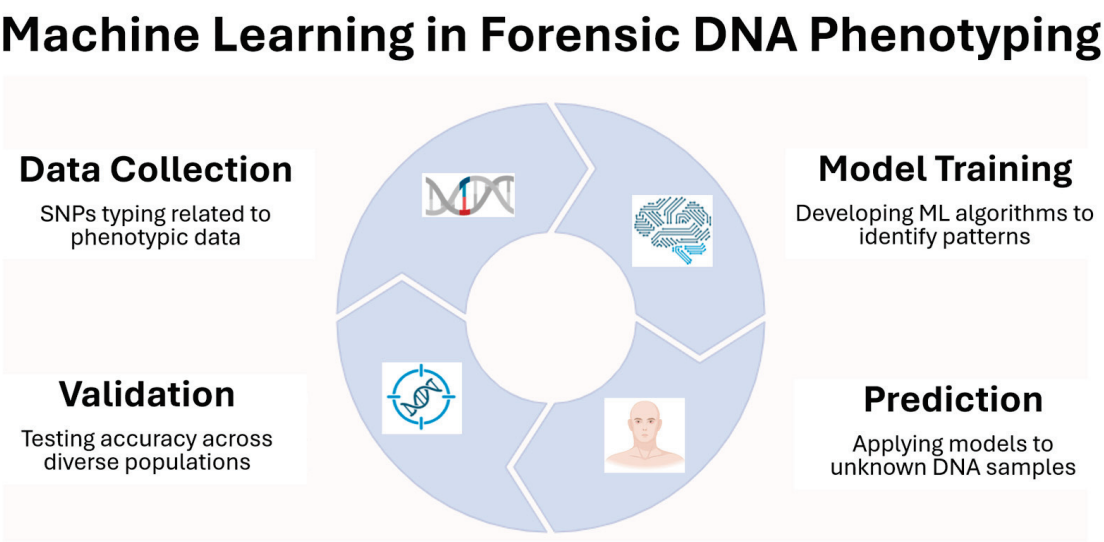

Figure 1. The integration of ML with FDP has significantly enhanced the ability to extract meaningful information from LT-DNA, though the accuracy of predictions remains fundamentally tied to data quality, genetic coverage, and technological sensitivity (created with BioRender, https://www.biorender.com).

Importantly, the correctness and utility of forensic phenotyping are fundamentally tied to data quality, genetic coverage, and technological sensitivity. As shown by the example of paleoanthropology, where DNA is extracted from highly degraded remains, there is potential for adapting high-throughput, low-input genomic methods to forensic contexts. The slow pace of their forensic adoption, however, is due in part to technical, regulatory, and funding constraints [10–14].

This review explores the scientific and technological advances that are reshaping the field of FDP, with particular emphasis on the application of ML for predicting physical appearance from LT-DNA. It begins by defining LT-DNA and outlining the unique challenges it presents in forensic investigations. The development of FDP is then examined, from its early use in identity testing to its current application in predicting (EVCs), biogeographic ancestry, and chronological age. Particular attention is given to the integration of ML approaches, which have become essential for modeling complex traits from partial or degraded genetic data. The review also addresses the practical and technical limitations associated with compromised samples and highlights how recent technological and computational advancements aim to mitigate these issues. Finally, it discusses future perspectives in the field, including the integration of multi-omics data, the expansion of reference databases to enhance predictive accuracy across diverse populations, and the ethical considerations surrounding the forensic use of predictive genetic information.

2. Low Template DNA: Challenges and Opportunities

2.1. Definition and Characteristics

LT-DNA represents a critical category of forensic genetic evidence characterized by a minute quantity of recoverable DNA, typically considered to be below 100 picograms (pg), or fewer than approximately 15–20 human diploid cells [15]. Such low-level samples are frequently encountered in crime scene investigations involving biological trace, including touch DNA, aged stains, shed hairs, or severely degraded tissue [16]. The forensic utility of LT-DNA lies in its potential to provide investigative leads in cases where standard DNA profiling techniques may fail due to insufficient template quantity, stochastic effects, or contamination risks [17].

https://doi.org/10.3390/genes17010059

A defining feature of LT-DNA analysis is its susceptibility to stochastic variation during PCR amplification, leading to challenges such as allelic dropout (failure to detect one allele of a heterozygous locus), allelic drop-in (spurious alleles introduced during amplification), and peak imbalance in electropherograms [18]. These artifacts compromise interpretation reliability, necessitating both technical rigor and statistical caution in forensic applications. To address these limitations, laboratories have developed specialized protocols and technologies aimed at maximizing the information recovered from low-level DNA while minimizing noise and erroneous profiles [19].

One of the central technical questions in processing LT-DNA is whether to concentrate the available extract into a single amplification or split it across replicates. A decision-theoretical study investigating this dilemma demonstrated that performing two replicates yields a higher expected net gain (ENG) than a single amplification, provided that the DNA quantity is sufficient to produce peak heights as low as 43 relative fluorescence units (RFU) on average. This finding underscores the benefit of replicate analyses in enhancing the reliability and information content of LT-DNA profiles, particularly when operating near the analytical sensitivity threshold of current instrumentation [20].

Analytical threshold (AT) determination is another key factor in managing LT-DNA profiles. Given the low signal intensity and high background noise often observed in such samples, accurate AT setting becomes crucial for distinguishing true alleles from spurious peaks. Research has shown that baseline signal patterns are influenced by reagent kits, laboratory conditions, instrument calibration, and the number of amplification cycles. In response, some laboratories now calculate the AT dynamically using baseline signal distributions from negative control profiles. One study proposed a comparative framework for evaluating AT methods and introduced a real-time analysis tool that allows forensic analysts to tailor ATs to specific experimental conditions, improving data accuracy while preserving true allele signals in most LT-DNA scenarios, though challenges persist in extremely low-template and high-cycle cases [21,22] (Figure 2).

Beyond analytical thresholds, optimizing amplification strategies is essential when dealing with limited or degraded DNA. A study involving 155 forensic case samples with DNA concentrations between 5 and 14.3 pg/μL revealed that samples exceeding 10 pg/μL and with a degradation index below 3 (a ratio indicating the relative amplification success of short versus long DNA fragments, used to assess sample degradation) were significantly more likely to yield informative profiles. Applying empirically derived thresholds for DNA quantity and quality, researchers found that forensic laboratories could reduce analytical workload by 32% while retaining 83% of usable profiles, offering a pragmatic approach to resource allocation in high-throughput forensic contexts [23].

Recent developments in post-PCR processing have also demonstrated promises for improving allele recovery from low template and trace DNA samples. A study evaluating the Amplicon RX post-PCR clean-up method found significant improvements in allele recovery and signal intensity when compared to standard 29- and 30-cycle protocols using the GlobalFiler amplification kit. Particularly at DNA concentrations as low as 0.001 ng/μL (i.e., 1 pg/μL), the Amplicon RX method yielded superior results, reinforcing its value in analyzing extremely low-template and degraded samples. While all methods struggled at the lowest tested concentration (0.0001 ng/μL), the clean-up procedure still outperformed traditional protocols, emphasizing the need for continued innovation in post-amplification refinement techniques [24].

https://doi.org/10.3390/genes17010059

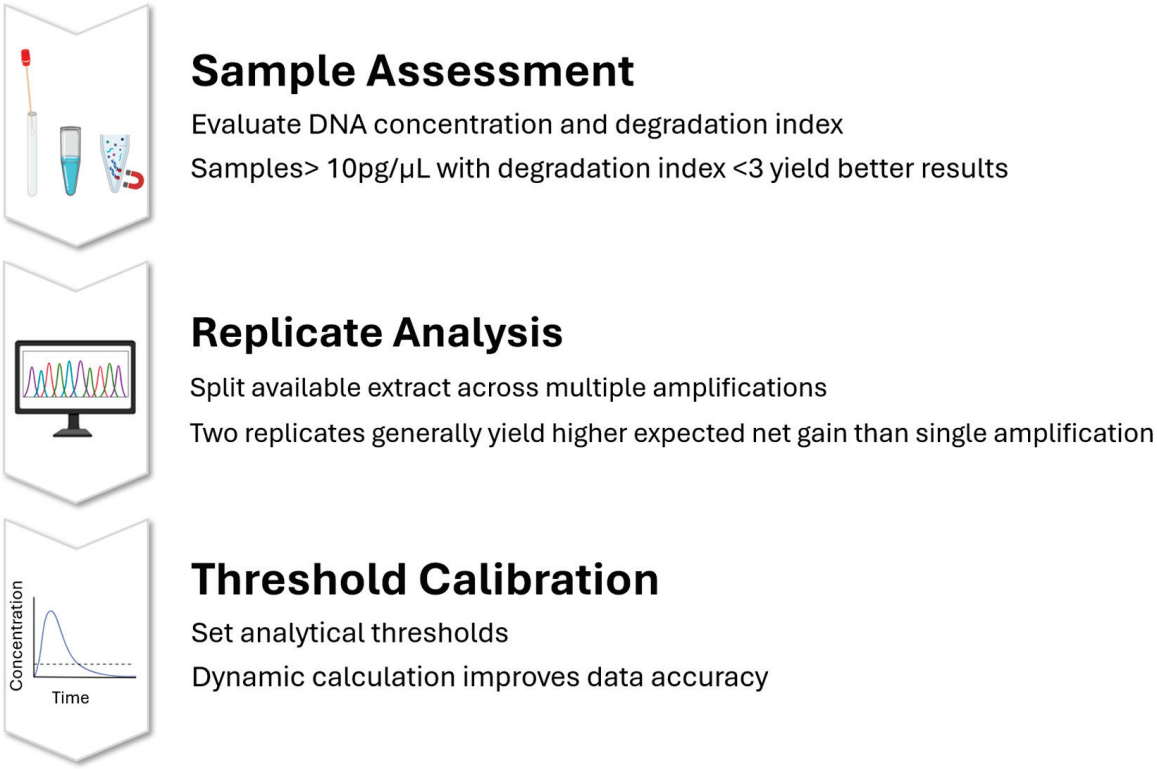

Figure 2. Optimized workflow for LT-DNA analysis in forensic laboratories. Key steps include: (1) sample assessment for DNA concentration and degradation index; (2) replicate analysis to improve reliability and ENG; and (3) dynamic threshold calibration based on baseline signal distributions. (Created with BioRender: www.biorender.com).

Despite these methodological advances, significant limitations remain in working with LT-DNA. The inherent stochasticity of low-copy amplification, variability in laboratory-specific workflows, and the impact of environmental factors such as temperature and humidity all contribute to result uncertainty [25,26]. Additionally, inter-laboratory standardization for defining what constitutes "low template" remains inconsistent, although the commonly cited threshold of 100 pg has become widely accepted as a working guideline [27]. Importantly, successful profiling from LT-DNA is not solely a function of DNA quantity, but rather a balance of factors including degradation, inhibition, locus-specific amplification efficiency, and the effectiveness of downstream analysis tools [28].

In conclusion, LT-DNA represents both a challenge and an opportunity in forensic genetics. Its successful analysis requires careful consideration of DNA quantity, quality, amplification strategies, threshold calibration, and post-PCR treatment. The body of evidence now supports the use of multi-replicate strategies, adaptive thresholding, and optimized amplification-clean-up protocols as key methods to enhance the reliability of LT-DNA profiling. As technological advancements in sequencing sensitivity and forensic assay design continue to evolve, it is anticipated that the definition and analytical handling of LT-DNA will become increasingly standardized and robust, improving the evidentiary value of this critical class of forensic samples.

2.2. Sources of LT-DNA

LT-DNA is frequently obtained from minute or degraded samples encountered in forensic casework, including touch DNA, shed or rootless hair shafts, trace biological fluids, and skeletal remains such as aged bone and teeth. While these sources can be pivotal in linking a suspect to a crime scene or identifying unknown remains, they each

https://doi.org/10.3390/genes17010059

present distinct challenges related to DNA quantity, degradation, contamination risk, and extraction complexity [29,30].

Touch DNA, or transfer DNA, is one of the most common sources of LT-DNA in forensic casework. It consists of DNA deposited via skin contact on surfaces, items, or human skin. The DNA is primarily derived from shed epithelial cells (corneocytes), which are often anucleated or contain degraded nuclear material. Studies have shown that to recover a full STR profile using direct PCR, at least 40 buccal cells or 4000 corneocytes are needed from touch samples collected via swab or tape lift. When extracted using conventional workflows, 8000 or more corneocytes may be required to obtain comparable results [31]. Collection methods significantly impact DNA recovery, though no single swabbing technique has proven superior. The widely used double-swab method showed modest improvement in DNA yield (average 13.7% more DNA) but not necessarily in STR recovery [32]. Further complicating touch DNA analysis is the indirect transfer of human DNA into the environment, onto dust, furniture, or air particles, raising the possibility of retrieving DNA from individuals who were merely present in a room, not necessarily involved in a criminal act [33].

Hair shafts, especially shed or rootless hairs, are another key yet problematic source of LT-DNA. Hair shafts contain highly degraded and fragmented nuclear DNA, often in insufficient quantities for STR profiling, particularly when subjected to environmental stress such as UV exposure or chemical treatment [34]. While mitochondrial DNA (mtDNA) can be recovered more consistently from hair shafts, hair nuDNA typing has been improved by massively parallel sequencing (MPS) platforms, which enable simultaneous analysis of mtDNA, STRs, SNPs, and Amelogenin markers [35]. DNA extraction methods, such as the Investigator and MinElute protocols, significantly affect outcomes; the Investigator method has shown superior results in terms of depth of coverage, SNP genotyping success, and lower dropout rates [35]. Additionally, telogen hair roots, those not in active growth phase, have historically yielded poor DNA results. However, using Hematoxylin staining to quantify nuclear content before selecting roots for testing has been shown to double the success rate of DNA profiling, from 32% to 69% [36].

Trace biological fluids such as saliva, sweat, and dried blood smears are also common sources of LT-DNA. These samples often contain small quantities of nucleated cells, and the DNA yield varies widely. Fluids such as urine and sweat yield the least DNA due to their low cellular content, whereas blood and semen typically contain higher concentrations of nucleated cells and are more amenable to traditional STR analysis [37]. Identification and proper collection of such fluids, especially when partially degraded or exposed, are essential to ensure successful analysis. Innovative strategies using fluorescent nucleic acid dyes have enhanced the visualization and targeted collection of cellular material, improving downstream processing success rates [38].

Skeletal remains, including bones and teeth, are routinely encountered in forensic investigations involving long postmortem intervals or extreme environmental exposure. These matrices are inherently challenging due to the degradation of DNA over time by temperature, humidity, microbial activity, and pH. Among skeletal elements, the petrous part of the temporal bone has demonstrated the highest DNA yield, up to 30 times that of other bones, due to its dense structure and protective anatomy. Several studies have confirmed that petrous bones outperform femurs, metacarpals, and even teeth in terms of STR profile completeness and reduced dropout rates [39,40]. Similarly, teeth remain a viable DNA source even when exposed to harsh environmental or chemical conditions, such as prolonged submersion in acids, due to their resilient enamel structure. Full or partial DNA profiles can still be recovered from teeth exposed to sulfuric, hydrochloric, or nitric acids for up to 120 h [41].

https://doi.org/10.3390/genes17010059

Aged or degraded skeletal samples require optimized pre-analytical strategies, including the use of decalcification agents, silica-based extraction protocols, and automated systems such as the Maxwell FSC DNA IQ platform. These methods improve yield and reduce handling time, though the success of DNA recovery still largely depends on selecting the most suitable skeletal elements and applying strict contamination controls [42].

In conclusion, LT-DNA is obtained from a wide range of forensic materials, each presenting unique challenges that must be addressed through tailored extraction, quantification, and amplification protocols. The advent of MPS technologies, nuclear content screening, and enhanced collection methods has significantly expanded the ability to recover probative genetic information from even the most limited and compromised DNA sources. Continued innovation in these areas, combined with better triage methods and decision thresholds, will be essential for maximizing the utility of LT-DNA in forensic casework.

2.3. Current Forensic Approaches for LT-DNA Analysis

LT-DNA analysis involves working with very small amounts of DNA, and presents a series of challenges related to sensitivity, reproducibility, and interpretation. Despite these limitations, significant advances in molecular techniques and analytical strategies have allowed forensic scientists to maximize the evidentiary value of minimal and degraded DNA samples, which are increasingly encountered in real-world forensic contexts.

One of the central technical approaches in LT-DNA analysis is the increase in PCR cycle numbers during STR amplification to enhance sensitivity. By extending the amplification process beyond the standard 28–30 cycles to 34 or more, low levels of DNA can be more effectively amplified, increasing the likelihood of detecting alleles that would otherwise remain below analytical thresholds. However, this approach is not without drawbacks. Stochastic effects, including allelic and locus drop-out, allelic drop-in, and peak imbalance, become more pronounced as the DNA quantity decreases and amplification cycles increase. These artifacts can compromise the reliability of the resulting profiles, especially in mixed samples or degraded material. Nonetheless, validation studies have demonstrated that replicate testing, even at very low template levels (e.g., 10–100 pg), can produce reliable single-source profiles when a consensus approach is used. Such strategies have helped forensic laboratories implement protocols that balance sensitivity with interpretive robustness, even in high-stakes criminal investigations [43].

In addition to replicating testing, alternative strategies for improving the quality of LT-DNA results have gained traction. Among these is single-cell DNA (scDNA) analysis, which offers a solution to the limitations of traditional "bulk" extraction methods used for mixed samples. In conventional workflows, crime scene stains containing multiple contributors are extracted en masse, producing a homogenized mixture that complicates deconvolution. In contrast, scDNA approaches involve subsampling individual cells from the mixture before DNA extraction, thereby enabling the generation of highly probative, single-source DNA profiles. This technique is particularly advantageous in resolving complex mixtures, such as those involving relatives with similar genetic profiles, or when detecting low-level contributors who may be masked in standard bulk analysis. Although scDNA techniques are still in development and face technical hurdles related to sensitivity, contamination risk, and cost, they represent a promising direction for the future of LT-DNA analysis and forensic genomics as a whole [15].

Beyond individual technical innovations, forensic laboratories are also integrating probabilistic genotyping software (PGS) to enhance interpretation of low-template or complex DNA profiles. These software platforms employ statistical modeling to assign likelihood ratios to competing hypotheses about DNA contributors, incorporating drop-out probabilities, stutter modeling (stutter refers to minor PCR artifacts where a small peak ap-

https://doi.org/10.3390/genes17010059

pears one repeat unit shorter than the true allele, caused by slippage during amplification), and peak height variability. In LT-DNA contexts, where traditional binary interpretation methods often fall short, PGS allows analysts to extract meaningful conclusions from incomplete or uncertain data. Probabilistic genotyping is now considered the best practice in the analysis of complex mixtures and degraded samples and is increasingly used in courtrooms worldwide [44].

Another major advancement supporting LT-DNA analysis is the implementation of NGS, which enables massively parallel processing of STRs, SNPs, and other markers from minimal input DNA. NGS offers several advantages over capillary electrophoresis (CE)-based STR analysis, including the ability to detect additional sequence variation within STR alleles, improved resolution of mixture components, and simultaneous analysis of mitochondrial and nuclear DNA. In LT-DNA contexts, NGS improves both the quantity and quality of data recovered from challenging samples, such as aged bones, hair shafts, or trace skin cells. However, NGS is not yet universally adopted in forensic laboratories due to its cost, complexity, and validation requirements. Continued technological refinement and standardization will be essential for widespread implementation in routine casework.

Despite these technical advances, LT-DNA analysis is not without controversy. Ethical and legal debates persist regarding the admissibility and interpretation of low-level DNA evidence. Concerns about contamination, false inclusions, and the risk of overstating the probative value of partial profiles have led courts and scholars to scrutinize the scientific reliability and legal fairness of LT-DNA testimony. Furthermore, as forensic DNA analysis becomes more powerful and intrusive, especially with the rise in familial searching, phenotyping, and investigative genetic genealogy, important questions arise about privacy, consent, and the potential infringement of civil liberties. Drawing on historical parallels from the early days of DNA profiling, some commentators argue that current advances must be met with a renewed commitment to protecting individual rights and ensuring transparent, accountable use of forensic science [43].

Looking ahead, the future of LT-DNA analysis lies in the integration of multidisciplinary approaches. As highlighted by the INTERPOL Forensic Science Managers Symposium, the field is advancing through the convergence of technologies such as rapid DNA testing, lineage marker analysis, microhaplotypes, proteomics, and epigenetic clocks for age prediction. These methods are being combined with enhanced extraction protocols, automation, and increasingly sophisticated bioinformatic tools to overcome the inherent limitations of low-template samples. Quality assurance remains a top priority, with over 70 new international guidance documents published in recent years to standardize procedures, enhance reliability, and promote cross-laboratory reproducibility [44].

In conclusion, current forensic approaches in LT-DNA analysis represent a dynamic and rapidly evolving area of forensic science. Through the combined use of increased PCR cycles, replicate consensus profiling, probabilistic modeling, single-cell analysis, and NGS technologies, laboratories are increasingly capable of obtaining meaningful results from the smallest and most degraded samples. At the same time, the legal and ethical frameworks surrounding these technologies must evolve in parallel to ensure that forensic innovations serve justice while respecting fundamental rights.

3. From Genotype to Phenotype: The Rise in FDP

The emergence of FDP marks a paradigm shift in modern forensic science. Where traditional DNA profiling has long been limited to identifying individuals through STR markers, FDP opens the possibility of predicting EVCs directly from genetic material, particularly in human remains [45]. By bridging the gap between genotype and phenotype, FDP enables investigators to infer aspects of an unknown person's physical appearance,

https://doi.org/10.3390/genes17010059

ancestry, and even age from DNA found at a crime scene [46]. This approach offers valuable investigative leads, especially in cases where conventional methods reach a dead end [1].

FDP currently focuses on a defined but gradually expanding set of traits, each with its own level of scientific maturity and predictive accuracy. Eye color, for instance, is among the most reliable phenotypic traits to be predicted from DNA, thanks to well-characterized variants in genes such as *HERC2* and *OCA2* [47,48]. In contrast, traits like skin pigmentation and hair color are more genetically complex, influenced by multiple genes and moderated by environmental factors. While red and black hair can be predicted with reasonable confidence, intermediate hair shades and skin tones remain more difficult to assess, particularly in admixed or non-European populations [49–51].

Secondary traits such as freckling and sun sensitivity can further refine a DNA-based appearance profile, though they are typically used in conjunction with primary pigmentation traits [52]. A more ambitious goal is the prediction of facial morphology, which remains one of the most challenging areas due to its highly polygenic nature and sensitivity to non-genetic influences like age, nutrition, and development. Although some genetic variants (e.g., in *PAX3* or *EDAR*) have been associated with facial shape, practical applications in forensic casework are still in the early stages [53].

In parallel, advancements in epigenetics have introduced the possibility of estimating chronological age from DNA, using methylation markers at specific CpG sites. Though age is not a fixed phenotype in the genetic sense, these DNA methylation-based "epigenetic clocks" offer promising tools for narrowing suspect or victim pools, particularly when traditional identifiers are absent [54]. Moreover, biogeographical ancestry inference provides essential context for phenotype prediction, as genetic variant frequencies differ across populations [55].

Tools like IrisPlex, HIrisPlex, and HIrisPlex-S panels, as well as the VISible Attributes through GEnomics (VISAGE) Enhanced Tool, have made FDP more accessible in forensic settings, allowing for targeted genotyping of key SNPs related to eye, hair, and skin color. Genotyping 24 genetic markers (SNPs and indels) enables rapid and reliable prediction of eye and hair color using the HIrisPlex system; the inclusion of 17 additional markers extends this capability to skin color prediction through the HIrisPlex-S system. While these panels show strong performance under ideal laboratory conditions, their predictive accuracy often diminishes in real-world scenarios involving degraded, mixed, or low-template DNA. As a result, integrating FDP into investigations requires not only scientific rigor but also careful consideration of its limitations and the probabilistic nature of the predictions it offers [56–59]. It is important to note that current forensic prediction panels (IrisPlex, HIrisPlex-S, VISAGE) primarily employ multinomial logistic regression for trait inference. These models are interpretable and validated for forensic use but differ fundamentally from ML approaches discussed later, which aim to capture complex genotype–phenotype relationships using non-linear, high-dimensional methods.

3.1. Forensic Eye Color Prediction from DNA: Insights from Genetic Markers

In forensic science, biological traces such as blood, saliva, semen, or epithelial cells recovered from crime scenes are primarily used for human identification through DNA profiling. However, recent advances have enabled the use of DNA to predict EVCs [60].

Eye color prediction is based on the analysis of specific SNPs associated with pigmentation genes [47]. These SNPs influence melanin synthesis and distribution in the iris, which, despite being covered by the transparent cornea, exhibits color variation due to both pigment concentration and structural light scattering in the stroma. The variation in iris color is primarily determined by the number and distribution of stromal melanocytes and the type of melanin, especially eumelanin, present [61].

https://doi.org/10.3390/genes17010059

Eye color is a polygenic trait, with multiple genes contributing to its expression [57]. Among these, the SNP rs12913832 in the *HERC2* gene has the most significant impact, particularly in European populations. Although located in an intronic region of *HERC2*, this SNP regulates the expression of the *OCA2* gene, which encodes a protein essential for melanin transport. Individuals with the AA genotype at rs12913832 typically have blue eyes, GG genotype correlates with brown eyes, and AG heterozygotes often exhibit intermediate shades such as green or hazel [62,63].

Other genes, such as *SLC24A4*, *SLC45A2*, *TYR*, *TYRP1*, *ASIP* or *IRF4*, also contribute to eye color variation, especially for intermediate phenotypes. However, their predictive power is generally lower and may vary across populations. Polymorphisms in these genes, while informative, are often population-specific and less conserved than the *HERC2-OCA2* regulatory axis [64–66].

To operate these genetic insights, the IrisPlex system was developed. This forensic tool uses a panel of six SNPs (Table 1) to predict eye color using a multinomial logistic regression model. The system outputs probabilities for three eye color categories: blue, brown, and intermediate. A prediction is considered reliable when the highest probability exceeds a threshold of 0.7. For example, a prediction of 0.89 for blue, 0.08 for brown, and 0.03 for intermediate would be interpreted as blue eyes [58].

Table 1. This table summarizes six SNPs located on various chromosomes, each associated with genes involved in eye color prediction.

SNP ID	Gene	Chromosome	Position	Reference Genome
rs12913832	*HERC2*	15	28120472	GRCh38 38.1/141
rs1800407	*OCA2*	15	27985172	GRCh38 38.1/142
rs12896399	*LOC105370627*	14	92307319	GRCh38 38.1/141
rs16891982	*SLC45A2*	5	33951588	GRCh38 38.1/141
rs1393350	*TYR*	11	89277878	GRCh38 38.1/141
rs12203592	*IRF4*	6	396321	GRCh37 37.1/131

Validation studies have demonstrated that IrisPlex achieves over 90% accuracy for blue and brown eyes in European populations. However, prediction accuracy for intermediate eye colors remains lower (around 73%), with sensitivity as low as 1.1%, reflecting the complex genetic architecture of these phenotypes [58].

As detailed in Section 2.3, LT-DNA introduces stochastic effects and allelic dropout that may compromise prediction accuracy. Future challenges in iris color prediction lie in integrating newly identified genetic markers to enhance predictive accuracy. A recent publication highlighted that whole-exome sequencing of 150 individuals has uncovered 27 previously unreported variants associated with eye color, offering promising new targets for prediction models. Notably, the SNP rs2253104 in the *ARFIP2* gene emerged as a key predictor, selected by multiple feature selection methods and contributing to the most accurate regression models. These findings suggest that expanding SNP panels with newly validated variants could significantly improve prediction outcomes, especially when working with degraded or limited DNA samples where maximizing the information from each locus is crucial. Validating and adapting these new markers for use in mini-amplicon assays could be a key step forward in applying iris prediction to challenging forensic samples [47].

Additionally, high-sensitivity genotyping platforms, including MassARRAY (MALDI-TOF mass spectrometry for multiplex SNP genotyping), NGS/MPS (parallel sequencing of multiple loci), and real-time PCR (using allele-specific probes or high-resolution melting

https://doi.org/10.3390/genes17010059

analysis), have enhanced the precision and robustness of SNP detection [51,67]. Replicate testing and consensus genotyping further mitigate random amplification errors by allowing analysts to identify consistent results across multiple runs. Moreover, the integration of probabilistic models into prediction tools enables the communication of uncertainty levels, helping to avoid overinterpretation of marginal or ambiguous profiles. Enforcing strict quality control thresholds, such as minimum allele calling criteria and prediction probability cutoffs (e.g., >0.7), also ensures that only high-confidence phenotype predictions are reported. Nevertheless, certain limitations remain. Intermediate eye colors, for instance, continue to be difficult to predict accurately due to their polygenic inheritance patterns and relatively low heritability. Furthermore, variations in allele frequencies across populations can influence prediction outcomes, highlighting the necessity of validating predictive models in diverse genetic backgrounds to ensure their broader applicability and forensic reliability [68].

While eye color is generally considered a low-risk trait in terms of privacy, its use in FDP must adhere to ethical standards and legal frameworks. Misinterpretation of probabilistic predictions, especially in cases with low confidence or ambiguous results, can lead to investigational bias. Therefore, careful communication of FDP findings to law enforcement is crucial to avoid wrongful suspicion [11,69].

3.2. Hair Color Prediction from Biological Traces

When biological traces are collected, forensic experts apply extraction protocols designed to preserve DNA quality even from degraded or low template samples [70]. Following DNA isolation and quantification, molecular techniques are used to identify SNPs associated with hair pigmentation [71].

Specific DNA regions are involved in the production, distribution, and degradation of melanin, the pigment primarily responsible for hair, eye, and skin coloration [56]. Hair color is determined by the type and quantity of melanin in the hair shaft: eumelanin (black/brown pigment) and pheomelanin (red/yellow pigment). The balance between these two types of melanin, regulated by a network of genes and genetic variants, gives rise to the wide spectrum of human hair colors, from black and brown to blond and red [72].

Hair color is a complex trait shaped by the combined influence of many genes and their interactions, each contributing in different ways to the final pigmentation phenotype. Among these, *MC1R* (Melanocortin 1 Receptor) plays a particularly prominent role. Variants in this gene are closely linked to red hair, as *MC1R* controls the switch between the production of eumelanin (dark pigment) and pheomelanin (red/yellow pigment). When *MC1R* function is disrupted by specific genetic variants, the balance shifts toward pheomelanin, leading to the characteristic red or auburn hair tones [73–75].

Other genes also contribute significantly to hair color diversity. *HERC2* and *OCA2*, which are more widely recognized for their role in determining eye color, also influence melanin synthesis in the hair, particularly affecting the variations observed in blond and brown shades [48].

Genes such as *SLC24A4*, *SLC45A2*, and *TYR* further support the pigmentation process by regulating melanosome function and the activity of tyrosinase, an enzyme critical for melanin biosynthesis. Variants in these genes are commonly associated with lighter hair tones [76].

Lastly, *IRF4* has emerged as another important contributor. This gene influences pigmentation through its regulatory functions in melanocyte biology. Not only is it associated with lighter hair colors, but it is also implicated in age-related changes in pigmentation, such as the gradual transition to gray hair [77].

https://doi.org/10.3390/genes17010059

The HIrisPlex system, developed as an extension of the earlier IrisPlex model for eye color prediction, integrates both eye and hair color SNPs into a single assay. As summarized in Table 2, the system uses 24 SNPs across multiple pigmentation genes [56].

Table 2. This table summarizes twenty-four SNPs located on various chromosomes, each associated with genes involved in eye and hair color prediction.

SNP ID	Gene	Chromosome	Position	Reference Genome
rs312262906 (rs796296176)	*MC1R*	16	89919342	GRCh38.p7 38.3/149
rs11547464	*MC1R*	16	89919683	GRCh38 38.1/141
rs885479	*MC1R*	16	89919746	GRCh38 38.1/141
rs1805008	*MC1R*	16	89919736	GRCh38 38.1/141
rs1805005	*MC1R*	16	89919436	GRCh38 38.1/141
rs1805006	*MC1R*	16	89919510	GRCh38 38.1/141
rs1805007	*MC1R*	16	89919709	GRCh38 38.1/141
rs1805009	*TUBB3*	16	89920138	GRCh38 38.1/141
rs201326893	*MC1R*	16	89919714	GRCh38 38.1/141
rs2228479	*MC1R*	16	89919532	GRCh38 38.1/141
rs1110400	*MC1R*	16	89919722	GRCh38 38.1/141
rs28777	*SLC45A2*	5	33958854	GRCh38 38.1/141
rs16891982	*SLC45A2*	5	33951588	GRCh38 38.1/141
rs12821256	*KITLG*	12	88934558	GRCh38 38.1/141
rs4959270	*LOC105374875*	6	457748	GRCh37.p5 37.3/135
rs12203592	*IRF4*	6	396321	GRCh37 37.1/131
rs1042602	*TYR*	11	89178528	GRCh38 38.1/141
rs1800407	*OCA2*	15	27985172	GRCh38 38.1/142
rs2402130	*SLC24A4*	14	92334859	GRCh38 38.1/141
rs12913832	*HERC2*	15	28120472	GRCh38 38.1/141
rs2378249	*PIGU*	20	34630286	GRCh38.p7 38.3/151
rs12896399	*LOC105370627*	14	92307319	GRCh38 38.1/141
rs1393350	*TYR*	11	89277878	GRCh38 38.1/141
rs683	*TYRP1*	9	12709305	GRCh38 38.1/141

The model outputs probability for each color, allowing forensic experts to assess the likely hair color of the DNA donor. A prediction is usually accepted when one color category exceeds a predefined probability threshold (e.g., >70%). For example, a sample yielding 0.82 probability for brown, 0.10 for black, 0.06 for blond, and 0.02 for red would result in a brown hair color prediction [78].

The predictive accuracy of hair color varies by color category and population group. For example, red hair can be predicted with over 80–90% accuracy, primarily due to the strong effect of *MC1R* variants [79]. Blond and brown hair predictions are also relatively reliable (75–85%) but may show variation across different ethnic backgrounds. Black hair, being the most common worldwide, is typically predicted with high sensitivity but may have slightly lower specificity due to overlapping SNP effects [80].

https://doi.org/10.3390/genes17010059

Prediction models have been validated in European populations, where hair color diversity is greatest. However, performance in non-European populations can differ due to allele frequency differences and additional contributing variants. Ongoing research continues to expand databases and improve prediction accuracy across ancestrally diverse groups [81].

The utility of hair color prediction from biological traces hinges on the ability to generate accurate genotypes from compromised samples [82].

In cases involving severely degraded DNA, MPS-based typing offers advantages by enabling parallel analysis of multiple short DNA fragments and improving coverage at key SNP sites [67,83,84]. Still, probabilistic interpretation remains essential, particularly when prediction confidence falls below threshold values [82].

Although hair color is a relatively non-sensitive trait in forensic terms, the use of predictive models still raises questions about genetic privacy, the potential for profiling, and public trust. Moreover, probabilistic results should be presented with appropriate caveats, particularly when based on partial or degraded DNA samples [83].

3.3. Skin Pigmentation Prediction in Forensic Science from Biological Traces

The HIrisPlex-S model further incorporates skin color prediction and uses a total of 41 SNPs (Table 3), enabling a broader EVC profile from a single DNA sample. This comprehensive approach improves the informative value of FDP in real-world investigations [84].

Table 3. This table summarizes forty-one SNPs located on various chromosomes, each associated with genes involved in eye and hair color prediction.

SNP ID	Gene	Chromosome	Position	Reference Genome
rs312262906 (rs796296176)	*MC1R*	16	89919342	GRCh38.p7 38.3/149
rs11547464	*MC1R*	16	89919683	GRCh38 38.1/141
rs885479	*MC1R*	16	89919746	GRCh38 38.1/141
rs1805008	*MC1R*	16	89919736	GRCh38 38.1/141
rs1805005	*MC1R*	16	89919436	GRCh38 38.1/141
rs1805006	*MC1R*	16	89919510	GRCh38 38.1/141
rs1805007	*MC1R*	16	89919709	GRCh38 38.1/141
rs1805009	*TUBB3*	16	89920138	GRCh38 38.1/141
rs201326893	*MC1R*	16	89919714	GRCh38 38.1/141
rs2228479	*MC1R*	16	89919532	GRCh38 38.1/141
rs1110400	*MC1R*	16	89919722	GRCh38 38.1/141
rs28777	*SLC45A2*	5	33958854	GRCh38 38.1/141
rs16891982	*SLC45A2*	5	33951588	GRCh38 38.1/141
rs12821256	*KITLG*	12	88934558	GRCh38 38.1/141
rs4959270	*LOC105374875*	6	457748	GRCh37.p5 37.3/135
rs12203592	*IRF4*	6	396321	GRCh37 37.1/131
rs1042602	*TYR*	11	89178528	GRCh38 38.1/141
rs1800407	*OCA2*	15	27985172	GRCh38 38.1/142
rs2402130	*SLC24A4*	14	92334859	GRCh38 38.1/141

https://doi.org/10.3390/genes17010059

Table 3. *Cont.*

SNP ID	Gene	Chromosome	Position	Reference Genome
rs12913832	*HERC2*	15	28120472	GRCh38 38.1/141
rs2378249	*PIGU*	20	34630286	GRCh38.p7 38.3/151
rs12896399	*LOC105370627*	14	92307319	GRCh38 38.1/141
rs1393350	*TYR*	11	89277878	GRCh38 38.1/141
rs683	*TYRP1*	9	12709305	GRCh38 38.1/141
rs3114908	*ANKRD11*	16	89317317	GRCh38.p14
rs1800414	*OCA2*	15	27951891	GRCh38 38.1/141
rs10756819	*BNC2*	9	16858086	GRCh38 38.1/141
rs2238289	*HERC2*	15	28208069	GRCh38 38.1/141
rs17128291	*SLC24A4*	14	92416482	GRCh38.p14
rs6497292	*HERC2*	15	28251049	GRCh38.p14
rs1129038	*HERC2*	15	28111713	GRCh38 38.1/141
rs1667394	*HERC2*	15	28285036	GRCh38 38.1/141
rs1126809	*TYR*	11	89284793	GRCh38 38.1/141
rs1470608	*OCA2*	15	28042975	GRCh38.p14
rs1426654	*SLC24A5*	15	48134287	GRCh38 38.1/141
rs6119471	*ASIP*	20	34197406	GRCh38.p14
rs1545397	*OCA2*	15	27942626	GRCh38.p14
rs6059655	*RALY*	20	34077942	GRCh38.p7 38.3/151
rs12441727	*OCA2*	15	28026629	GRCh38.p14
rs3212355	*MC1R*	16	89917970	GRCh38.p14
rs8051733	*DEF8*	16	89957798	GRCh38.p14

While the SNP tables provide a comprehensive overview of markers used in FDP, performance varies significantly across panels and traits, especially under degraded-DNA conditions. The HIrisPlex-S system, which integrates eye, hair, and skin color prediction, has demonstrated robust performance in forensic contexts, including aged bone samples, ref. [59] with successful recovery of pigmentation profiles in over 55% of cases [9]. However, certain SNPs associated with skin tone (e.g., rs1426654 in *SLC24A5* and rs12913832 in *HERC2*) show reduced amplification success in highly degraded samples, leading to underperformance in intermediate pigmentation categories. VISAGE panels, designed for massively parallel sequencing, offer improved sensitivity and multiplexing, enabling better SNP recovery from LT-DNA and degraded skeletal remains. Inter-laboratory validation studies [59] confirm that VISAGE achieves higher reproducibility and lower dropout rates compared to HIrisPlex-S, particularly for skin color and ancestry inference. Nonetheless, both panels exhibit population-specific limitations: predictive accuracy is highest in European cohorts and declines in admixed populations, underscoring the need for inclusive reference datasets and ongoing calibration.

Skin pigmentation prediction from biological traces is an emerging and powerful facet of FDP, allowing forensic scientists to infer EVCs of unknown individuals when conventional identification techniques are unfeasible. Alongside eye and hair color, skin

https://doi.org/10.3390/genes17010059

pigmentation provides essential descriptive features that can generate investigative leads from DNA alone. This is particularly relevant in cases involving unknown perpetrators, unidentified human remains, or degraded biological evidence [85].

Biological traces recovered from crime scenes can contain sufficient nuclear DNA to permit genotyping, and in such cases, the typing of SNPs associated with pigmentation traits [44]. Human skin color is primarily determined by the quantity and type of melanin produced by melanocytes in the basal layer of the epidermis. The density, distribution, and synthesis of melanin granules, regulated by a network of pigmentation genes, are key factors in determining skin tone [86]. These processes are influenced by several genes that affect melanosome formation, melanocyte biology, and melanin biosynthesis pathways [87]. Numerous genes have been associated with variations in skin pigmentation, many of which have been included in forensic prediction panels. Furthermore, skin color is a continuous trait influenced by both genetic and environmental factors (i.e., sun exposure, tanning behavior, and age can affect observed skin tone) [88]. Its prediction from DNA is complex due to its polygenic nature, wide variation across populations, and the influence of evolutionary history. Despite this, robust predictive models have been developed, especially those designed to distinguish between broad pigmentation categories (light, intermediate, dark) across major global ancestries [89]. This classification system simplifies the continuous nature of skin tone into practical categories for forensic investigation. The model utilizes logistic regression trained on a large reference dataset that includes individuals from diverse ancestral backgrounds [90].

In validation studies, HIrisPlex-S demonstrated high accuracy, particularly in predicting light and dark pigmentation. Intermediate skin tones are more challenging due to greater phenotypic and genetic diversity and less clear boundaries between categories. The prediction accuracy is also influenced by the genetic background of the individual: for example, predictions are more reliable in populations of European or sub-Saharan African descent, and less so in admixed or South Asian populations [81].

The prediction of skin color from LT-DNA is a promising yet complex frontier in forensic genetics. LT-DNA samples are inherently prone to degradation and contamination [70]. These factors can compromise the integrity of genetic markers, particularly SNPs used in pigmentation prediction models such as HIrisPlex-S. Indeed, LT-DNA samples frequently result in incomplete genetic profiles, which limits the number of informative SNPs available for analysis. This can hinder the statistical confidence of phenotype predictions, especially in individuals with intermediate or admixed ancestry, where subtle genetic variations play a significant role in pigmentation. Advanced probabilistic models and imputation techniques are being developed to address these limitations, but their effectiveness remains contingent on the quality and completeness of the input DNA [9].

Despite these challenges, LT-DNA-based skin color prediction remains a valuable tool in forensic investigations. When used responsibly, it can provide critical leads in otherwise unsolvable cases, offering a glimpse into the physical appearance of unknown individuals and narrowing suspect pools in a scientifically grounded manner.

3.4. Freckles and Sun Sensitivity Prediction in Forensic Science from Biological Traces

Among the suite of the prediction of EVCs from biological traces, freckles and sun sensitivity may seem minor at first glance, but they can contribute meaningfully to the construction of a biogeographic and phenotypic profile of an unknown individual [91]. Freckles (ephelides) are small, pigmented macules that typically appear on sun-exposed areas of fair skin. Sun sensitivity refers to a person's susceptibility to burning rather than tanning upon UV exposure, typically resulting from lower eumelanin levels and higher pheomelanin content [86]. These traits, rooted in pigmentation biology, are closely

https://doi.org/10.3390/genes17010059

associated with genes involved in melanin synthesis and regulation, particularly the *MC1R* gene, located on chromosome 16 [92]. Several common *MC1R* variants (e.g., R151C, R160W, D294H) are collectively referred to as "R alleles" and are associated with the red hair color (RHC) phenotype, but also contribute independently to freckling and UV sensitivity, even in individuals without red hair [93]. Other genes, such as *ASIP*, *TYR*, and *IRF4*, may modulate freckling and pigmentation patterns, although their effects are smaller and often population-specific [94].

With appropriate genetic analysis, forensic scientists can derive probabilistic predictions about whether an individual is likely to have freckled skin and/or increased sensitivity to sunlight. The relative SNPs are included in comprehensive forensic phenotyping tools such as HIrisPlex-S [85]. These models use multinomial logistic regression or ML classifiers trained on large, multi-ethnic datasets [51,95]. For freckles, individuals are categorized as likely or unlikely to have them based on the presence of specific MC1R variants and other associated SNPs [3,96–99]. For sun sensitivity, prediction involves assessing genetic profiles associated with reduced melanin production and increased burn tendency (high likelihood of sunburn with minimal tanning, moderate sensitivity, low sensitivity/likely to tan) [100].

Prediction accuracy for freckles and sun sensitivity is generally good when the relevant SNPs are reliably genotyped, and the individual belongs to a well-represented population in the model's training data (typically of European ancestry) [51]. For instance, freckle prediction can reach accuracies above 75–80%, particularly when individuals carry two or more non-functional MC1R alleles. Sun sensitivity prediction is somewhat more variable due to the continuous nature of the phenotype and its interaction with environmental factors (e.g., lifetime sun exposure, behavior, geography) [101].

However, there are several limitations: -polygenic complexity: many small-effect genes and gene-environment interactions contribute to these traits; -environmental influence: freckling can be influenced by UV exposure history, making it a dynamic, rather than strictly genetically determined, trait; -population bias: predictive models perform best in individuals of European ancestry, where pigmentation variation is highest and best studied; accuracy drops in admixed or underrepresented populations; -LT-DNA [100].

3.5. Facial Morphology Prediction in Forensic Science from Biological Traces

In the field of FDP, the prediction of facial morphology, the shape and structure of the human face, represents a frontier with considerable scientific promise and complex challenges [102]. While traits like eye, hair, and skin color have reached relatively high predictive reliability, facial morphology prediction is more intricate due to the polygenic and multifactorial nature of facial features. However, recent advances in genomics, 3D facial imaging, and ML models are progressively transforming facial prediction from a speculative vision into an emerging forensic tool. The ability to reconstruct aspects of a person's facial structure from biological traces such as blood, saliva, or touch DNA could significantly support investigations, particularly when no biometric or documentary information is available [102,103].

Facial morphology is a highly heritable trait governed by the interaction of hundreds of genes and regulatory elements. GWAS have identified dozens of loci associated with specific facial traits, including: facial width and height, nasal bridge length and tip projection, lip thickness, chin prominence, brow ridge shape, mandibular and maxillary dimensions [6,104].

Key genes such as *PAX3*, *EDAR*, *DCHS2*, *RUNX2*, and *PRDM16* have been linked to facial development, often through their role in craniofacial growth, tissue differentiation, and skeletal patterning. Variants in these genes influence the position and projection of facial landmarks that define individual appearance. Notably, the expression of these traits

https://doi.org/10.3390/genes17010059

is further modulated by age, sex, ancestry, and environmental influences (e.g., nutrition, trauma), which makes prediction from DNA alone inherently probabilistic [105,106].

In addition to genotyping, the ancestry and sex of the donor are determined, as both play pivotal roles in shaping facial morphology. Ancestry informs baseline structural patterns common in different populations (e.g., nasal breadth, cheekbone prominence), while sex influences sexually dimorphic traits such as jaw angle and brow thickness [107].

To transform genetic data into facial predictions, researchers apply ML techniques trained on large databases of paired genotype and 3D facial imaging data. These datasets often consist of thousands of individuals with detailed facial scans and genome-wide SNP data. Key modeling approaches include partial least squares regression (PLSR) to link SNPs to principal components of facial variation; convolutional neural networks (CNNs) to analyze facial geometry from genetic and demographic inputs; deep generative models (e.g., variational autoencoders or GANs) to create realistic 3D face renderings from DNA data [108].

Recent examples include the FaceBase project, VisiGen, and research from the Penn State Forensic Anthropology Lab, which has shown that genetic data can explain 10–20% of the variance in certain facial traits, modest but meaningful progress toward practical forensic use [109,110]. Despite promising advances, current models explain only a modest proportion of facial trait variance, typically between 10–20%, with substantial limitations in predicting features influenced by environmental and developmental factors. Traits such as facial asymmetry, age-related changes, and expression dynamics remain poorly captured by genotype-based models. This modest predictive power underscores that current models are research-grade and unsuitable for operational forensic deployment.

The predictive power of facial trait modeling is strongest when combined with known ancestry, sex, and age estimates, particularly in young adults, whose facial structures are relatively stable. Nonetheless, these models often lack precision at the individual level and are more effective at generating composite depictions or narrowing demographic search pools than at identifying exact facial characteristics. Reproducibility remains a major challenge in facial morphology prediction. Variability in imaging techniques, SNP panels, and population structure can lead to inconsistent results across studies. Moreover, the lack of standardized validation protocols and limited availability of forensic-grade datasets restrict the generalizability of current models. According to recent publications, the highest predictability is observed for traits such as nose width, facial width, intercanthal distance (the distance between the eyes), and lip thickness. Moderate predictability applies to features like brow ridge prominence, chin shape, and nasal tip projection. In contrast, traits such as facial asymmetry, expression-related features, and age-related morphological changes exhibit low predictability [46,111].

In forensic contexts, these predictions are used as investigative leads rather than as confirmatory evidence. Reproducibility remains limited due to variability in imaging protocols, SNP panels, and population structure. Most data sets are European-biased, reducing generalizability and increasing misclassification risk in admixed populations. Future efforts should focus on expanding training datasets to include diverse populations, integrating multi-omics data to capture non-genetic influences, and establishing standardized pipelines for model development and validation to enhance reproducibility and forensic reliability. For example, in cold cases, a predicted facial image may be released to the public to generate tips. In mass disaster scenarios, facial predictions can assist in identifying unknown victims when traditional methods, such as fingerprinting or dental records, are unavailable. Similarly, in cases involving unidentified remains, predicted facial features can complement skeletal reconstructions and ancestry estimations, enhancing the overall identification process.

https://doi.org/10.3390/genes17010059

Facial prediction from LT-DNA represents a cutting-edge intersection of forensic genetics and computational modeling. Facial predictions derived from LT-DNA are probabilistic rather than definitive and are best used to generate investigative leads rather than serve as conclusive evidence [3,102]. Indeed, despite promising advances, current models explain only 10–20% of variance in facial traits, which is insufficient for individual-level reconstruction. These outputs remain research-grade and are not forensically deployable. Reproducibility is constrained by differences in imaging protocols, SNP panels, and population structure. Beyond technical limitations, predicting facial morphology raises significant ethical concerns. Unlike eye, hair, and skin color, facial features are closely linked to ancestry and identity, making them particularly sensitive. Generated facial composites risk being misinterpreted as accurate likenesses, potentially leading to investigational bias or discrimination. These challenges underscore the need for transparent communication of uncertainty, strict governance, and clear disclaimers when using such predictions as investigative leads rather than confirmatory evidence.

3.6. Age Prediction in Forensic Science Based on Biological Traces

Estimating chronological age from biological traces has become a valuable forensic tool, particularly when conventional identifiers are unavailable [112]. Unlike skeletal assessments, molecular approaches rely on biomarkers that change predictably over time [113]. Among these, DNA methylation at specific CpG sites is the most reliable indicator of age, outperforming earlier methods based on telomere length or mtDNA mutations, which showed high variability and limited forensic utility [114–116].

Epigenetic clocks exploit methylation changes at selected loci to predict age with high accuracy. Forensic models prioritize simplicity and robustness for degraded or LT-DNA. A widely used approach by Bekaert et al. employs four CpG sites in genes such as *ELOVL2*, *FHL2*, *KLF14*, and *TRIM59*, achieving mean absolute deviations of about 3–4 years in blood samples. *ELOVL2* is particularly informative due to its consistent methylation increase across tissues, including blood, saliva, and buccal cells [117]. The VISAGE Consortium has further advanced this field by creating multiplex assays compatible with NGS, enabling sensitive and robust age estimation from trace DNA. *ELOVL2*, in particular, has emerged as a key biomarker due to its consistent methylation increase with age across multiple tissue types, including blood, saliva, and buccal cells [118].

One of the strengths of DNA methylation-based age prediction is its applicability across various forensic sample types [119]. Blood and saliva are most commonly used due to their higher DNA yield and stable methylation profiles. Semen requires tissue-specific models, as methylation patterns vary significantly between tissues. Touch DNA, derived from epithelial cells, presents greater challenges due to low DNA quantities, but ongoing research is improving its feasibility. Even skeletal remains can be analyzed for methylation-based age estimation, offering valuable insights in cold cases or mass grave investigations [112,120].

In forensic casework, age prediction serves multiple roles. It can assist in suspect profiling when no known individual is linked to the biological evidence, providing an estimated age range to guide investigations. In victim identification, especially in cases involving unidentified remains, age estimates help correlate findings with missing persons databases. Additionally, age prediction is sometimes used in legal and immigration contexts to determine whether individuals are minors, although this application remains ethically and legally contentious [121,122].

Technological platforms for methylation analysis include pyrosequencing, quantitative PCR, and NGS. Pyrosequencing remains popular for targeted assays because of its cost-effectiveness and compatibility with forensic workflows, while NGS offers higher sen-

https://doi.org/10.3390/genes17010059

sitivity and multiplexing for degraded samples. Recent VISAGE Consortium developments integrate methylation-based age estimation into multiplex panels, enabling simultaneous prediction of age and other traits from trace DNA [123,124].

Despite these advances, LT-DNA poses challenges such as allelic dropout and incomplete methylation profiles, which can reduce accuracy [125]. Optimized assays using short amplicons, replicate testing, and probabilistic models help mitigate these issues [126]. When combined with strict quality control and robust statistical frameworks, methylation-based age prediction provides actionable investigative leads, even from compromised samples [127].

3.7. Ancestry Prediction in Forensic Science from Biological Traces

Ancestry prediction from biological traces has become a powerful tool in forensic science, offering critical insights into the biogeographical origins of unknown individuals when traditional identification methods are unavailable [128]. This approach is particularly valuable in criminal investigations, mass disasters, and the identification of unidentified remains, where DNA evidence may be the only clue. Unlike cultural or self-reported ethnicity, forensic ancestry inference relies on genetic markers that reflect population-level differences shaped by evolutionary history, migration, and genetic drift. These markers, primarily SNPs, are distributed across the genome and exhibit frequency patterns that vary among continental and subcontinental populations [129].

The foundation of ancestry prediction lies in the analysis of ancestry-informative markers (AIMs), SNPs selected for their high allele frequency differences between populations. Panels such as the SNPforID 34-plex or others, such as the Precision ID Ancestry Panel, include hundreds of AIMs optimized for forensic use. These panels can distinguish major continental ancestries (e.g., African, European, East Asian, Native American, South Asian) and, in some cases, provide finer resolution within regions [130,131]. The VISAGE Consortium has developed advanced multiplex assays compatible with MPS, enabling ancestry inference from degraded or LT-DNA samples commonly encountered in forensic contexts [59,132].

Despite the promise of ancestry prediction, several challenges must be addressed, particularly when working with LT-DNA. However, recent advances in sequencing sensitivity and bioinformatic tools have improved the robustness of ancestry inference from trace samples. Probabilistic models and ML algorithms can now integrate partial genotypes and assign ancestry with high confidence, even from compromised DNA [90,133].

In forensic casework, ancestry prediction serves multiple purposes. It can help narrow suspect pools by providing investigators with information about the likely population background of an unknown individual. In missing persons cases, ancestry estimates can guide comparisons with databases and assist in facial reconstruction efforts. In mass disaster scenarios, ancestry inference can support victim identification when other biological or contextual information is lacking. Importantly, ancestry prediction is not intended to identify individuals directly but to provide investigative leads that complement other forensic evidence [134].

The accuracy of ancestry prediction depends on several factors, including the number and informativeness of SNPs used, the diversity of reference populations, and the complexity of individual genetic backgrounds. Admixed individuals, those with ancestry from multiple populations, pose particular challenges, as their genetic profiles may not align neatly with reference categories. To address this, modern forensic tools incorporate admixture analysis and ancestry deconvolution, estimating proportional ancestry contributions from different populations. These methods enhance the interpretability of results and reduce the risk of misclassification [135].

https://doi.org/10.3390/genes17010059

As forensic genomics continues to evolve, ancestry prediction from biological traces, especially LT-DNA, will play an increasingly important role in investigative workflows. With ongoing improvements in marker panels, sequencing technologies, and computational methods, the ability to infer ancestry from even the most challenging samples is becoming more accurate and accessible, offering valuable insights in the pursuit of justice.

4. Integrating ML with LT-DNA in FDP

The integration of ML into FDP represents a transformative advancement in the ability to predict EVCs from genetic material, particularly in challenging cases involving LT-DNA. LT-DNA samples, often recovered from trace biological material such as touch DNA or degraded remains, contain minimal quantities of DNA and are prone to allelic dropout, contamination, and stochastic effects. These limitations pose significant challenges for traditional statistical models, which often rely on complete and high-quality genotypic data. ML, with its capacity to handle high-dimensional, noisy, and incomplete datasets, offers a powerful solution for enhancing phenotype prediction from LT-DNA [95,136]. It is important to clarify that we define ML as a class of algorithms capable of learning complex, often non-linear relationships from data without relying on pre-specified parametric forms. Examples include Random Forests, Support Vector Machines, Gradient Boosting, and deep neural networks. In contrast, traditional statistical models, such as logistic regression, assume a fixed functional form and are widely used in operational FDP systems (e.g., IrisPlex, HIrisPlex-S, VISAGE). While logistic regression is sometimes grouped under supervised learning, it is not considered ML in the contemporary sense of high-dimensional, non-linear modeling.

4.1. Common ML Algorithms and Their Forensic Applications

ML models are particularly well-suited to forensic genomics due to several key factors: the high dimensionality of genomic data, the complex and non-linear relationships between SNPs and phenotypic traits, and the need to integrate diverse data types, including genotype, gene expression, and epigenetic modifications such as DNA methylation. Commonly used ML algorithms in FDP include Random Forests (RFs), which are valued for their robustness and interpretability; Support Vector Machines (SVMs), which perform well with small sample sizes and high-dimensional data; Gradient Boosting Machines (GBMs), which often outperform RFs in accuracy; and deep learning models such as neural networks (NNs), which are capable of modeling intricate genotype–phenotype relationships. Simple models like k-nearest neighbors (KNN) can also be effective in small datasets, particularly when combined with feature selection techniques [137,138]. Recent comparative studies provide quantitative evidence of ML performance in FDP. Katsara et al. [95] evaluated RFs, SVMs, and GBMs for eye color prediction using HIrisPlex SNPs in 1200 individuals. RF achieved an AUC of 0.93 for blue/brown classification, outperforming SVMs (AUC = 0.91) and logistic regression (AUC = 0.89) under 10-fold cross-validation. For skin color prediction, Zaorska et al. [91] applied neural networks to a Polish cohort (n = 800), reporting precision = 0.82 and recall = 0.79 for light pigmentation, compared to RF precision = 0.78 and recall = 0.75. VISAGE validation studies further demonstrated that ML-based genotype imputation improved SNP recovery from LT-DNA samples by 12–15%, enabling phenotype prediction from partial profiles. These findings underscore the advantage of ML in handling incomplete and noisy data, particularly in LT-DNA contexts (Table 4).

https://doi.org/10.3390/genes17010059

Table 4. Performance of ML algorithms for FDP traits across datasets.

Trait	Algorithm	Dataset	AUC	Precision	Recall	Reference
Eye color	Random Forest	HIrisPlex SNPs	0.93	0.90	0.88	[95]
Eye color	SVM	HIrisPlex SNPs	0.91	0.88	0.86	[95]
Skin color	Neural Network	Polish cohort	--- (*)	0.82	0.79	[91]
Skin color	Random Forest	Polish cohort	--- (*)	0.78	0.75	[91]

* AUC not reported for skin color in Zaorska et al. [91].

While deep learning models achieved slightly higher accuracy for complex traits, their lack of interpretability raises concerns for forensic admissibility, making RF and SVM preferred in operational contexts.

A critical challenge in applying ML to FDP is data imbalance and overfitting. Most training datasets, such as HIrisPlex and VISAGE, are predominantly composed of individuals of European ancestry, which can bias predictions and reduce accuracy in admixed or underrepresented populations [95,139]. Overfitting occurs when models capture noise or population-specific patterns rather than generalizable features, leading to poor performance on forensic casework samples.

To mitigate imbalance and overfitting, strategies such as feature selection (e.g., LASSO, recursive feature elimination) and regularization techniques (ridge regression, dropout layers in neural networks) are employed. These approaches improve generalization and reduce variance when working with high-dimensional genomic data.

These approaches collectively enhance robustness when working with LT-DNA, where incomplete and noisy profiles are common. However, further research is needed to validate these methods across diverse populations and forensic-grade datasets.

To provide a concise overview, Table 5 summarizes commonly used ML algorithms in FDP, their input data types, dataset sizes, predicted traits, and reported performance metrics. These results highlight that Random Forest and Gradient Boosting consistently achieve high AUC values for eye color prediction, while neural networks show promise for complex traits such as skin pigmentation. Deep learning approaches applied to facial morphology explain only a modest proportion of variance (10–20%), underscoring the need for larger and more diverse training datasets. For age estimation, regularized regression models using methylation data achieve mean absolute deviations of approximately 3–4 years, demonstrating their forensic utility.

Table 5. Summary of ML algorithms applied in FDP: input type, dataset size, accuracy, and key references.

Algorithm	Input Type	Dataset Size	Trait(s) Predicted	Reported Accuracy (AUC/Precision/Recall)	Reference
Random Forest	SNP array (HIrisPlex)	~1200 individuals	Eye color (blue/brown)	AUC = 0.93; Precision = 0.90; Recall = 0.88	[95]
SVM	SNP array (HIrisPlex)	~1200 individuals	Eye color	AUC = 0.91; Precision = 0.88; Recall = 0.86	[95]

https://doi.org/10.3390/genes17010059

Table 5. *Cont.*

Algorithm	Input Type	Dataset Size	Trait(s) Predicted	Reported Accuracy (AUC/Precision/Recall)	Reference
Neural Network	SNP array	~800 individuals	Skin color	Precision = 0.82; Recall = 0.79	[91]
Gradient Boosting	SNP array	~1200 individuals	Eye color	AUC = 0.92	[95]
Deep Learning (CNN)	SNP + 3D facial scans	~3000 individuals	Facial morphology	Explains 10–20% variance in facial traits	[7]
Elastic Net	DNA methylation (CpG sites)	~500 individuals	Age estimation	MAD ≈ 3.5 years	[117]

Accuracy metrics vary by population and validation method; most studies used cross-validation. IrisPlex and HIrisPlex-S use logistic regression, not ML in the contemporary sense.

4.2. Logistic Regression vs. Random Forest vs. Deep Learning in FDP: Accuracy, Data Require-Ments, and Admissibility

Operational FDP panels such as IrisPlex, HIrisPlex-S, and VISAGE rely on multinomial logistic regression because of its interpretability, stability under limited SNP sets, and extensive forensic validation. In contrast, RF, SVM, GBM, and deep learning architectures (CNNs, GANs) are increasingly explored in research for modeling complex, non-linear genotype–phenotype relationships and integrating diverse data types, but they remain largely experimental in operational pipelines.

Comparative evidence suggests that ML models can offer incremental accuracy gains under controlled conditions. For example, RF achieved AUC ≈ 0.93 for eye color prediction, outperforming SVM (≈0.91) and logistic regression (≈0.89) in cross-validation on HIrisPlex SNPs [95]. Neural networks reported precision ≈ 0.82 and recall ≈ 0.79 for skin color in a Polish cohort, slightly higher than RF (precision ≈ 0.78, recall ≈ 0.75) [91]. However, these improvements often diminish in LT-DNA casework due to allelic dropout and incomplete profiles. Facial morphology pre-diction remains particularly challenging, with deep learning explaining only 10–20% of variance in research cohorts [7,109–111], insufficient for individual-level reconstruction.

Modeling assumptions differ markedly. Logistic regression assumes a fixed parametric form and works well with modest sample sizes, making it straightforward to validate. RF, SVM, and GBM capture non-linear interactions and tolerate incomplete data but require larger, diverse datasets and careful regularization to avoid overfitting [95]. Deep learning demands thousands of samples and rich paired inputs (e.g., genotype and 3D facial scans), otherwise risking spurious, population-specific signals [7,109–111].

Overfitting and population bias remain critical concerns. FDP training datasets are often European-ancestry-heavy, which can skew predictions and reduce generalizability in admixed populations [95,135]. Cross-validation alone is insufficient; external and inter-laboratory validation on forensic-grade LT-DNA is essential [44,59]. Imputation of missing SNPs using ML can improve completeness but must include uncertainty estimates, and imputed calls should never be reported as hard genotypes [139–141].

Interpretability and admissibility are decisive for forensic use. Courts favor transparent methods with known error rates and peer-reviewed acceptance [14]. Logistic regression meets these standards; RF and GBM can be partially explained using feature importance and SHAP/LIME [136], but these tools are not yet standardized for legal contexts. Deep learning poses greater interpretability challenges, limiting its current admissibility.

https://doi.org/10.3390/genes17010059

Logistic regression remains the operational standard for FDP due to its interpretability and validation history. ML approaches are promising for research but remain experimental until broader validation, inclusive datasets, and courtroom-ready interpretability are achieved.

4.3. Future Directions and Operational Readiness

One of the most critical applications of ML in LT-DNA analysis is genotype imputation. Due to dropout events, many SNPs may be missing in LT-DNA samples. ML-based imputation tools such as Beagle, IMPUTE2, and deep learning-based networks can reconstruct missing genotypes with high accuracy, enabling more complete input data for phenotype prediction. Additionally, ML models are inherently more tolerant of noise and missing data than traditional approaches. Algorithms like RF and GBM can manage incomplete datasets by focusing on the most informative loci, while feature selection methods such as LASSO (Least Absolute Shrinkage and Selection Operator) and recursive feature elimination help reduce dimensionality and improve model performance [140].

Another promising strategy is the use of synthetic data augmentation to enhance model training. Techniques such as Synthetic Minority Oversampling Technique (SMOTE) or Generative Adversarial Networks (GANs) can simulate plausible low-quality or rare-case samples, thereby improving the generalizability of ML models to real-world forensic scenarios. This is particularly valuable in FDP, where the availability of high-quality, annotated training data is often limited [139,141].

The application of ML in FDP is already evident in tools like HIrisPlex and HIrisPlex-S, which use logistic regression and probabilistic models to predict eye, hair, and skin color from SNP panels. However, as FDP expands to include more complex traits such as facial morphology, freckles, sun sensitivity, and age estimation, ML becomes increasingly indispensable. For example, deep learning models trained on large datasets of paired genotype and 3D facial imaging data have shown promise in predicting facial structure, while epigenetic clocks based on DNA methylation patterns use regression models to estimate chronological age with high accuracy, even from degraded or LT-DNA samples [95,142].

To ensure forensic reliability, ML models must be trained and validated on diverse, well-annotated datasets such as the 1000 Genomes Project or the UK Biobank. Cross-validation and external validation using real forensic case data are essential to assess model robustness under practical constraints. Moreover, ethical considerations must guide the deployment of ML in forensic contexts, particularly regarding privacy, consent, and the communication of probabilistic predictions [143].

In summary, the integration of ML with LT-DNA analysis significantly enhances the predictive power and applicability of FDP. By enabling accurate phenotype inference from compromised samples, ML-driven FDP provides valuable investigative leads in cases where traditional methods fall short, marking a new era in forensic science.

5. Ethical Frameworks, Limitations, and Future Directions in FDP from LT-DNA

FDP has emerged as a powerful tool for predicting EVCs such as eye, hair, and skin color, as well as ancestry and age, from biological traces (Figure 3). However, when applied to LT-DNA samples, those containing minimal and often degraded genetic material, FDP faces significant technical, ethical, and interpretive challenges [144]. LT-DNA is particularly vulnerable to allelic dropout, contamination, and stochastic amplification errors, which can compromise the accuracy and reliability of phenotype predictions. These limitations are especially pronounced in complex traits like facial morphology, where prediction models

https://doi.org/10.3390/genes17010059

rely on the integration of hundreds of genetic markers and are sensitive to even minor genotyping errors [1,145].

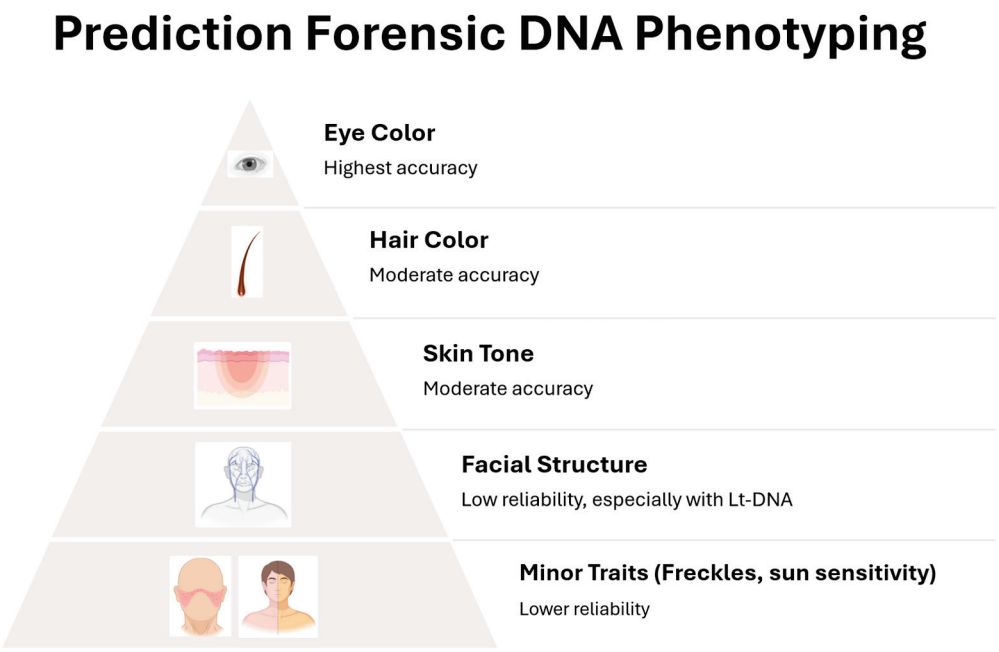

Figure 3. Relative prediction accuracy of EVCs from DNA, ranked by trait complexity. Eye color shows the highest accuracy (AUC > 0.9), followed by hair and skin color. Predictions for facial morphology, freckles, and sun sensitivity are less reliable, especially from LT-DNA. (Created with BioRender: www.biorender.com).

Prediction accuracy varies widely depending on the trait and the quality of the DNA. Eye color prediction remains the most robust, with AUC values exceeding 0.9 in European populations. Hair color and skin tone predictions are moderately accurate, while traits such as facial structure, freckles, and sun sensitivity are more difficult to predict reliably, particularly from LT-DNA. Moreover, most predictive models have been trained on individuals of European ancestry, limiting their applicability and accuracy in admixed or underrepresented populations. This population bias can lead to skewed or misleading results when applied in diverse forensic contexts [135] (Table 6).

Table 6. Comparative prediction accuracies for major traits across populations.

Trait	Category	Accuracy (%)	Notes
Eye color	Blue/Brown	>90	High reliability in Europeans
Eye color	Intermediate	70	Low sensitivity (1–2%)
Hair color	Red	85–90	Strong MC1R effect
Hair color	Blond/Brown	75–85	Moderate accuracy
Skin color	Light/Dark	80–85	Reliable in Europeans/African cohorts
Skin color	Intermediate	<70	Challenging, especially in admixed

Ethical and legal concerns further complicate the use of FDP in LT-DNA scenarios. Privacy remains a central issue, particularly under frameworks such as the EU General Data Protection Regulation (GDPR), which classifies genetic data as a special category requiring strict compliance with principles of lawfulness, purpose limitation, and data minimization.

https://doi.org/10.3390/genes17010059

FDP applications in surveillance or public appeals raise heightened risks because they infer sensitive personal traits—such as ancestry or appearance—from biological material without consent. The secondary use of publicly available genomic data or biobank resources for forensic purposes introduces additional ethical challenges, including unclear consent scope, governance gaps, and potential erosion of public trust. Recent European debates on the European Health Data Space and U.S. discussions around investigative genetic genealogy highlight the tension between investigative utility and individual rights [69,146–148].

Algorithmic bias is another critical concern: ML models trained predominantly on European datasets often underperform for admixed or underrepresented populations, leading to inaccurate or misleading predictions. This bias can amplify inequities and undermine the legitimacy of FDP in diverse forensic contexts. To mitigate these risks, inclusive reference datasets, transparent validation across populations, and clear reporting of limitations are essential [149,150].

Court admissibility standards further demand rigorous attention. Under frameworks such as Daubert and Rule 702 in the U.S., and proportionality principles in Europe, FDP evidence must demonstrate scientific validity, known error rates, and peer-reviewed acceptance. Uncertainty should be communicated explicitly through probabilistic outputs, confidence intervals, and verbal scales, avoiding deterministic language that could mislead investigators or courts. Failure to convey uncertainty risks investigational bias or wrongful suspicion, particularly in high-stakes cases [14,151].

Finally, public perception and informed consent remain pivotal. Surveys and stakeholder interviews in Europe and the U.S. reveal mixed attitudes toward FDP, with concerns about genetic privacy, discrimination, and misuse. Transparent communication of capabilities and limitations, coupled with robust governance and consent frameworks, is essential to maintain trust and ensure that FDP serves justice without compromising fundamental rights [152,153].

To address these concerns, ethical frameworks must evolve alongside technological advancements. Clear guidelines are needed to govern the use of FDP, particularly in cases involving LT-DNA, where the margin for error is higher. Transparency in reporting, including the communication of prediction probabilities and confidence intervals, is essential to prevent misuse or misinterpretation. Additionally, the development of inclusive models trained in diverse populations is critical to ensuring fairness and accuracy across global forensic applications [154].

To ensure that forensic FDP is applied responsibly and transparently, especially in cases involving LT-DNA, it is essential to establish operational safeguards that address both scientific limitations and ethical risks. To operationalize ethical safeguards, we propose the following checklist outlines key considerations for the ethical deployment of FDP in forensic investigations (Figure 4).

Looking ahead, several promising directions are emerging to enhance FDP from LT-DNA. One key area is the integration of multi-omics data, combining genomics with transcriptomics, epigenomics, and proteomics, to enable more dynamic and context-sensitive predictions. For example, integrating DNA methylation profiles can improve age estimation, while gene expression data may offer insights into lifestyle or environmental exposures. Another advantage is the development of portable and rapid phenotyping platforms, such as those based on Oxford Nanopore sequencing and edge-based ML inference, which could allow on-site analysis of LT-DNA in real time [155,156].

https://doi.org/10.3390/genes17010059

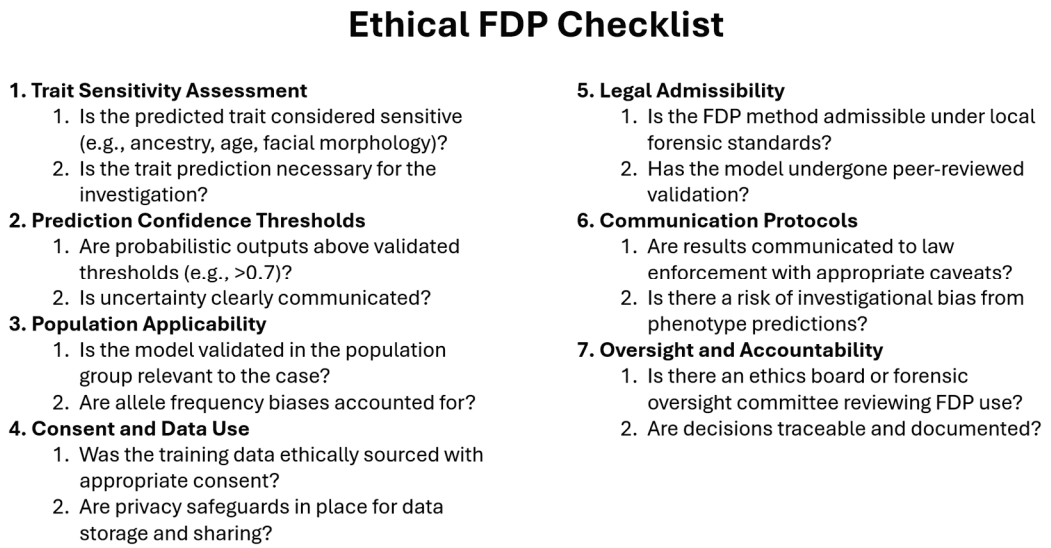

Figure 4. Ethical deployment checklist for FDP. Designed to assist forensic practitioners, legal professionals, and oversight bodies in evaluating scientific validity, privacy safeguards, and procedural accountability of FDP-based predictions.

ML and artificial intelligence AI are also playing an increasingly significant role in FDP. ML models can manage noisy, incomplete data and are well-suited to the imputation of missing genotypes, a common issue in LT-DNA samples. Techniques such as SHAP values and LIME are being explored to improve model interpretability, which is crucial for courtroom credibility. Furthermore, synthetic data generation using generative adversarial networks (GANs) may help augment training datasets, improving model robustness in low-quality scenarios [157–159].

Ultimately, the future of FDP in LT-DNA contexts depends on balancing scientific innovation with ethical responsibility. By addressing current limitations, enhancing model inclusivity, and ensuring transparent communication, forensic science can harness the full potential of DNA phenotyping while safeguarding individual rights and public trust.

6. Conclusions

The intersection of LT-DNA analysis and ML is poised to revolutionize FDP. While ML approaches show promise for improving phenotype prediction from LT-DNA, most operational systems currently rely on logistic regression, which remains the forensic standard due to its interpretability and validation status. By enabling the prediction of EVCs from minimal and often degraded biological material, this integration expands the investigative potential of forensic science beyond traditional identity matching. ML models, with their ability to manage high-dimensional, noisy, and incomplete data, are particularly well-suited to the challenges posed by LT-DNA. They facilitate genotype imputation, enhance trait prediction accuracy, and support probabilistic interpretation of complex phenotypes such as facial morphology and age.

Despite these advances, significant limitations remain. Prediction accuracy varies by trait and is often reduced in LT-DNA due to allelic dropout and partial genotyping. Moreover, the majority of current models are trained on European-ancestry datasets, limiting their generalizability across diverse populations. Ethical concerns, including privacy, consent, and the risk of overinterpreting probabilistic predictions, must be addressed through robust legal and regulatory frameworks.

Looking ahead, the future of FDP in LT-DNA contexts lies in the integration of multi-omics data, the development of portable and rapid sequencing technologies, and the refinement of interpretable ML models. These innovations, coupled with efforts to diversify

https://doi.org/10.3390/genes17010059

training datasets and standardize forensic protocols, will be essential for transitioning FDP from experimental research to routine forensic practice.

To strengthen future research and operational readiness, we recommend the following actions:

- Validation across diverse populations: Systematically validate ML-FDP models on non-European and admixed cohorts to mitigate algorithmic bias and improve global applicability.
- Integration of multi-omics data: Incorporate DNA methylation, transcriptomics, and proteomics into predictive frameworks to enhance accuracy for complex traits such as age and facial morphology.
- Portable sequencing workflows: Develop rapid, field-deployable FDP solutions using portable sequencing platforms (e.g., Oxford Nanopore) combined with edge-based ML inference for on-site analysis.
- Interpretability and transparency: Establish forensic ML interpretability standards using explainable AI tools (e.g., SHAP, LIME) to ensure transparency, accountability, and courtroom admissibility.
- Global collaboration: Promote international initiatives to create inclusive reference datasets and harmonized validation protocols across laboratories, ensuring reproducibility and fairness.

These steps will accelerate the transition of FDP from experimental research to operational forensic practice while safeguarding ethical and legal principles.

Author Contributions: Conceptualization, F.S., E.D., C.P. and M.S.; methodology, F.S., E.D., M.E., M.F., M.C., C.P. and M.S.; validation, F.S., E.D., C.P. and M.S.; formal analysis, F.S., E.D., M.E., M.F., M.C., C.P. and M.S.; writing—original draft preparation, F.S. and E.D.; writing—review and editing, F.S., E.D., M.E., M.F., M.C., C.P. and M.S. All authors have read and agreed to the published version of the manuscript.

Funding: This research received no external funding.

Institutional Review Board Statement: Not applicable.

Informed Consent Statement: Not applicable.

Data Availability Statement: All data were included in the manuscript.

Conflicts of Interest: The authors declare no conflicts of interest.

Abbreviations

The following abbreviations are used in this manuscript:

FDP	Forensic DNA Phenotyping
LT-DNA	Low Template DNA
ML	Machine Learning
EVC	Externally Visible Characteristics
SNP	Single Nucleotide Polymorphism
STR	Short Tandem Repeat
GWAS	Genome-Wide Association Studies
NGS	Next-Generation Sequencing
MPS	Massively Parallel Sequencing
WGS	Whole-Genome Sequencing
PCR	Polymerase Chain Reaction
RFU	Relative Fluorescence Units
AT	Analytical Threshold

https://doi.org/10.3390/genes17010059

scDNA	Single-Cell DNA
PGS	Probabilistic Genotyping Software
AIMs	Ancestry-Informative Markers
CNN	Convolutional Neural Network
GAN	Generative Adversarial Network
SMOTE	Synthetic Minority Oversampling Technique
LASSO	Least Absolute Shrinkage and Selection Operator
PLSR	Partial Least Squares Regression
CpG	Cytosine-phosphate-Guanine (dinucleotide)
MAD	Mean Absolute Deviation
qPCR	Quantitative Polymerase Chain Reaction
VISAGE	VISible Attributes through GEnomics
AI	Artificial Intelligence
SHAP	SHapley Additive exPlanations
LIME	Local Interpretable Model-Agnostic Explanations

References

1. Kayser, M.; Branicki, W.; Parson, W.; Phillips, C. Recent Advances in Forensic DNA Phenotyping of Appearance, Ancestry and Age. *Forensic Sci. Int. Genet.* **2023**, *65*, 102870. [CrossRef] [PubMed]
2. Haidar, M.; Mousawi, F.; Al-Matrouk, A.K. Forensic DNA Phenotyping Using Next-Generation Sequencing. In *Next Generation Sequencing (NGS) Technology in DNA Analysis*; Academic Press: Cambridge, MA, USA, 2024; pp. 289–310. [CrossRef]
3. Pośpiech, E.; Teisseyre, P.; Mielniczuk, J.; Branicki, W. Predicting Physical Appearance from DNA Data—Towards Genomic Solutions. *Genes* **2022**, *13*, 121. [CrossRef]
4. Vajpayee, K.; Shukla, R.K. DNA Phenotyping: The Technique of the Future. In *Handbook of DNA Profiling*; Springer: Singapore, 2022.
5. Ge, J.; Budowle, B. Forensic Investigation Approaches of Searching Relatives in DNA Databases. *J. Forensic Sci.* **2021**, *66*, 430–443. [CrossRef]
6. Richmond, S.; Howe, L.J.; Lewis, S.; Stergiakouli, E.; Zhurov, A. Facial Genetics: A Brief Overview. *Front. Genet.* **2018**, *9*, 462. [CrossRef]
7. Claes, P.; Hill, H.; Shriver, M.D. Toward DNA-Based Facial Composites: Preliminary Results and Validation. *Forensic Sci. Int. Genet.* **2014**, *13*, 208–216. [CrossRef]
8. Ketsekioulafis, I.; Katsos, K.; Kolentinis, C.; Kouzos, D.; Moraitis, K.; Spiliopoulou, C.; Sakelliadis, E.I. Humanitarian Forensic Medicine: A Systematic Review. *Int. J. Leg. Med.* **2025**, *139*, 747–761. [CrossRef]
9. Kukla-Bartoszek, M.; Szargut, M.; Pośpiech, E.; Diepenbroek, M.; Zielińska, G.; Jarosz, A.; Piniewska-Róg, D.; Arciszewska, J.; Cytacka, S.; Spólnicka, M.; et al. The Challenge of Predicting Human Pigmentation Traits in Degraded Bone Samples with the MPS-Based HIrisPlex-S System. *Forensic Sci. Int. Genet.* **2020**, *47*, 102301. [CrossRef]
10. Fleckhaus, J.; Bugert, P.; Al-Rashedi, N.A.M.; Rothschild, M.A. Investigation of the Impact of Biogeographic Ancestry on DNA Methylation Based Age Predictions Comparing a Middle East and a Central European Population. *Forensic Sci. Int. Genet.* **2023**, *67*, 102923. [CrossRef] [PubMed]
11. Zieger, M.; Scudder, N. Ethical and Legal Reflections on Secondary Research Using Genetic Data Acquired for Criminal Investigation Purposes. *Forensic Sci. Int. Genet.* **2025**, *75*, 103178. [CrossRef] [PubMed]
12. Gareau-Léonard, A.; Mousseau, V.; Crispino, F.; Milot, E. Forensic DNA Phenotyping: Examining Knowledge and Operational View from Police Officers. *Forensic Sci. Int.* **2025**, *10*, 100586. [CrossRef]
13. Zieger, M. Forensic DNA Phenotyping in Europe: How Far May It Go? *J. Law Biosci.* **2022**, *9*, lsac024. [CrossRef]
14. Sessa, F.; Chisari, M.; Esposito, M.; Karaboue, M.A.A.; Salerno, M.; Cocimano, G. Ethical, Legal and Social Implications (ELSI) Regarding Forensic Genetic Investigations (FGIs). *J. Acad. Ethics* **2024**, *23*, 617–637. [CrossRef]
15. Huffman, K.; Ballantyne, J. Single Cell Genomics Applications in Forensic Science: Current State and Future Directions. *iScience* **2023**, *26*, 107961. [CrossRef]
16. van Oorschot, R.A.H.; Meakin, G.E.; Kokshoorn, B.; Goray, M.; Szkuta, B. DNA Transfer in Forensic Science: Recent Progress towards Meeting Challenges. *Genes* **2021**, *12*, 1766. [CrossRef]
17. Hicks, T.; Buckleton, J.; Castella, V.; Evett, I.; Jackson, G. A Logical Framework for Forensic DNA Interpretation. *Genes* **2022**, *13*, 957. [CrossRef]
18. Schulte, J.; Marciano, M.A.; Scheurer, E.; Schulz, I. A Systematic Approach to Improve Downstream Single-Cell Analysis for the DEPArray™ Technology. *J. Forensic Sci.* **2023**, *68*, 1875–1893. [CrossRef] [PubMed]

https://doi.org/10.3390/genes17010059

19. Laurin, N.; Boulianne, H.; Frégeau, C. Comparative Analysis of Two Rapid DNA Technologies for the Processing of Blood and Saliva-Based Samples. *Forensic Sci. Int. Genet.* **2023**, *67*, 102928. [CrossRef] [PubMed]
20. Gittelson, S.; Steffen, C.R.; Coble, M.D. Low-Template DNA: A Single DNA Analysis or Two Replicates? *Forensic Sci. Int.* **2016**, *264*, 139–145. [CrossRef]
21. Chen, D.; Tan, M.; Xue, J.; Wu, M.; Song, J.; Wu, Q.; Liu, G.; Zheng, Y.; Xiao, Y.; Lv, M.; et al. Optimizing Analytical Thresholds for Low-Template DNA Analysis: Insights from Multi-Laboratory Negative Controls. *Genes* **2024**, *15*, 117. [CrossRef] [PubMed]
22. Martínez-Gómez, J.; Laso-Izquierdo, S.; Vera-Yánez, A.; Fernández-Serrano, J.J.; Gomes, C. Preliminary Results of Reduced Polymerase Chain Reaction (PCR) Volumes When Analysing Low Template DNA Samples with Globalfiler™ and Yfiler™ Plus Kits. *DNA* **2025**, *5*, 2. [CrossRef]
23. Ido, A.; Kirshenbaum, L.; Waiskopf, O.; Voskoboinik, L. Optimizing Amplification Threshold of Low Template DNA. *J. Forensic Sci.* **2025**, *70*, 1521–1526. [CrossRef]
24. Aljanahi, N.S.; Alketbi, S.K.; Almheiri, M.M.; Alshehhi, S.A.; Sanqoor, A.N.; Alghanim, H.J. Enhancing Trace DNA Profile Recovery in Forensic Casework Using the Amplicon RX Post-PCR Clean-up Kit. *Sci. Rep.* **2025**, *15*, 3324. [CrossRef]
25. Tozzo, P.; Mazzobel, E.; Marcante, B.; Delicati, A.; Caenazzo, L. Touch DNA Sampling Methods: Efficacy Evaluation and Systematic Review. *Int. J. Mol. Sci.* **2022**, *23*, 15541. [CrossRef]
26. Sessa, F.; Pomara, C.; Esposito, M.; Grassi, P.; Cocimano, G.; Salerno, M. Indirect DNA Transfer and Forensic Implications: A Literature Review. *Genes* **2023**, *14*, 2153. [CrossRef]
27. Costa, C.; Figueiredo, C.; Costa, S.; Ferreira, P.M.; Amorim, A.; Prieto, L.; Pinto, N. The Impact of Parameter Variation in the Quantification of Forensic Genetic Evidence. *Sci. Rep.* **2025**, *15*, 2524. [CrossRef] [PubMed]
28. Butler, J.M.; Iyer, H.; Press, R.; Taylor, M.K.; Vallone, P.M.; Willis, S. DNA Mixture Interpretation. 2024. Available online: https://nvlpubs.nist.gov/nistpubs/ir/2024/NIST.IR.8351.pdf (accessed on 10 December 2025).
29. Sessa, F.; Salerno, M.; Bertozzi, G.; Messina, G.; Ricci, P.; Ledda, C.; Rapisarda, V.; Cantatore, S.; Turillazzi, E.; Pomara, C. Touch DNA: Impact of Handling Time on Touch Deposit and Evaluation of Different Recovery Techniques: An Experimental Study. *Sci. Rep.* **2019**, *9*, 9542. [CrossRef]
30. Sessa, F.; Panepinto, E.; Salerno, M.; Chisari, M.; Esposito, M.; Cocimano, G.; Pomara, C. Impact of Liquid Antibacterial Soap and Hand Sanitizer on DNA Transfer in Forensic Investigations: An Experimental Study. *Forensic Sci. Res.* **2025**, *10*, owae068. [CrossRef]
31. Kanokwongnuwut, P.; Martin, B.; Taylor, D.; Kirkbride, K.P.; Linacre, A. How Many Cells Are Required for Successful DNA Profiling? *Forensic Sci. Int. Genet.* **2021**, *51*, 102453. [CrossRef] [PubMed]
32. Kallupurackal, V.; Kummer, S.; Voegeli, P.; Kratzer, A.; Dørum, G.; Haas, C.; Hess, S. Sampling Touch DNA from Human Skin Following Skin-to-Skin Contact in Mock Assault Scenarios—A Comparison of Nine Collection Methods. *J. Forensic Sci.* **2021**, *66*, 1889–1900. [CrossRef] [PubMed]
33. Fantinato, C.; Gill, P.; Fonneløp, A.E. Investigative Use of Human Environmental DNA in Forensic Genetics. *Forensic Sci. Int. Genet.* **2024**, *70*, 10302. [CrossRef]
34. Rayimoglu, G.; Yonar, F.C.; Anılanmert, B. From One Strand Dyed/Undyed Hair With/Without Root to Fast and Successful STR Profiling and Evaluation With Principle Component Analysis. *Electrophoresis* **2025**, *46*, 1292–1307. [CrossRef]
35. Peng, D.; Wang, N.; Zang, Y.; Liu, Z.; Liu, Z.; Geng, J.; Cong, B.; Sun, H.; Wu, R. Concurrent Genotyping of Mitochondrial DNA and Nuclear DNA in Rootless Hair Shafts and Blood Samples for Enhanced Analysis. *Forensic Sci. Int. Genet.* **2025**, *75*, 103176. [CrossRef]
36. Admire, L.; Carson, M.; Crawford, K.; Nguyen, E.; Daniels, T. Hair Root Staining with Hematoxylin: Increasing the Rate of Obtaining DNA Profiles in Forensic Casework. *Forensic Sci. Int.* **2023**, *343*, 111544. [CrossRef] [PubMed]
37. Shrivastava, P.; Kumawat, R.K.; Kushwaha, P.; Rana, M. Biological Sources of DNA: The Target Materials for Forensic DNA Typing. In *Handbook of DNA Profiling*; Springer Nature: Heidelberg, Germany, 2022.
38. Madden, I.; Taylor, D.; Mitchell, N.; Goray, M.; Henry, J. Predicting Probative Levels of Touch DNA on Tapelifts Using Diamond™ Nucleic Acid Dye. *Forensic Sci. Int. Genet.* **2024**, *70*, 103024. [CrossRef] [PubMed]
39. Haarkötter, C.; Vinueza-Espinosa, D.C.; Gálvez, X.; Saiz, M.; Medina-Lozano, M.I.; Lorente, J.A.; Álvarez, J.C. A Comparison between Petrous Bone and Tooth, Femur and Tibia DNA Analysis from Degraded Skeletal Remains. *Electrophoresis* **2023**, *44*, 1559–1568. [CrossRef] [PubMed]
40. Di Stefano, B.; Zupanič Pajnič, I.; Concato, M.; Bertoglio, B.; Calvano, M.G.; Sorçaburu Ciglieri, S.; Bosetti, A.; Grignani, P.; Addoum, Y.; Vetrini, R.; et al. Evaluation of a New DNA Extraction Method on Challenging Bone Samples Recovered from a WWII Mass Grave. *Genes* **2024**, *15*, 672. [CrossRef]
41. Sapan, T.Ü.; Karaboğa, N. Determination of DNA Recovery from Human Teeth Exposed to Various Acids. *Int. J. Leg. Med.* **2025**, *139*, 1453–1463. [CrossRef]
42. Varela Morillas, Á.; Suhling, K.; Frascione, N. Unlocking the Potential of Forensic Traces: Analytical Approaches to Generate Investigative Leads. *Sci. Justice* **2022**, *62*, 310–326. [CrossRef]

https://doi.org/10.3390/genes17010059

43. Oosthuizen, T.; Howes, L.M. The Development of Forensic DNA Analysis: New Debates on the Issue of Fundamental Human Rights. *Forensic Sci. Int. Genet.* **2022**, *56*, 102606. [CrossRef]
44. Butler, J.M. Recent Advances in Forensic Biology and Forensic DNA Typing: INTERPOL Review 2019–2022. *Forensic Sci. Int.* **2023**, *6*, 100311. [CrossRef]
45. Fabbri, M.; Alfieri, L.; Mazdai, L.; Frisoni, P.; Gaudio, R.M.; Neri, M. Application of Forensic DNA Phenotyping for Prediction of Eye, Hair and Skin Colour in Highly Decomposed Bodies. *Healthcare* **2023**, *11*, 647. [CrossRef]
46. Kayser, M. Forensic DNA Phenotyping: Predicting Human Appearance from Crime Scene Material for Investigative Purposes. *Forensic Sci. Int. Genet.* **2015**, *18*, 33–48. [CrossRef]
47. Kukla-Bartoszek, M.; Teisseyre, P.; Pośpiech, E.; Karłowska-Pik, J.; Zieliński, P.; Woźniak, A.; Boroń, M.; Dąbrowski, M.; Zubańska, M.; Jarosz, A.; et al. Searching for Improvements in Predicting Human Eye Colour from DNA. *Int. J. Leg. Med.* **2021**, *135*, 2175–2187. [CrossRef]
48. Brancato, D.; Coniglio, E.; Bruno, F.; Agostini, V.; Saccone, S.; Federico, C. Forensic DNA Phenotyping: Genes and Genetic Variants for Eye Color Prediction. *Genes* **2023**, *14*, 1604. [CrossRef] [PubMed]
49. Carratto, T.M.T.; Guimarães de Oliveira, M.L.; Mendes-Junior, C.T. Forensic DNA Phenotyping in the Next-Generation Sequencing Era. In *Next Generation Sequencing (NGS) Technology in DNA Analysis*; Academic Press: Cambridge, MA, USA, 2023; ISBN 9780323991445.
50. Liu, F.; Wen, B.; Kayser, M. Colorful DNA Polymorphisms in Humans. *Semin. Cell Dev. Biol.* **2013**, *24*, 562–575. [CrossRef]
51. Terrado-Ortuño, N.; May, P. Forensic DNA Phenotyping: A Review on SNP Panels, Genotyping Techniques, and Prediction Models. *Forensic Sci. Res.* **2025**, *10*, owae013. [CrossRef] [PubMed]
52. Kukla-Bartoszek, M.; Pośpiech, E.; Woźniak, A.; Boroń, M.; Karłowska-Pik, J.; Teisseyre, P.; Zubańska, M.; Bronikowska, A.; Grzybowski, T.; Płoski, R.; et al. DNA-Based Predictive Models for the Presence of Freckles. *Forensic Sci. Int. Genet.* **2019**, *42*, 252–259. [CrossRef]
53. Naqvi, S.; Hoskens, H.; Wilke, F.; Weinberg, S.M.; Shaffer, J.R.; Walsh, S.; Shriver, M.D.; Wysocka, J.; Claes, P. Decoding the Human Face: Progress and Challenges in Understanding the Genetics of Craniofacial Morphology. *Annu. Rev. Genom. Hum. Genet.* **2022**, *23*, 383–412. [CrossRef]
54. Bell, C.G.; Lowe, R.; Adams, P.D.; Baccarelli, A.A.; Beck, S.; Bell, J.T.; Christensen, B.C.; Gladyshev, V.N.; Heijmans, B.T.; Horvath, S.; et al. DNA Methylation Aging Clocks: Challenges and Recommendations. *Genome Biol.* **2019**, *20*, 249. [CrossRef] [PubMed]
55. Cheung, E.Y.Y.; Gahan, M.E.; McNevin, D. Prediction of Biogeographical Ancestry from Genotype: A Comparison of Classifiers. *Int. J. Leg. Med.* **2017**, *131*, 901–912. [CrossRef]
56. Chaitanya, L.; Breslin, K.; Zuñiga, S.; Wirken, L.; Pośpiech, E.; Kukla-Bartoszek, M.; Sijen, T.; Knijff, P.d.; Liu, F.; Branicki, W.; et al. The HIrisPlex-S System for Eye, Hair and Skin Colour Prediction from DNA: Introduction and Forensic Developmental Validation. *Forensic Sci. Int. Genet.* **2018**, *35*, 123–135. [CrossRef] [PubMed]
57. Walsh, S.; Liu, F.; Wollstein, A.; Kovatsi, L.; Ralf, A.; Kosiniak-Kamysz, A.; Branicki, W.; Kayser, M. The HIrisPlex System for Simultaneous Prediction of Hair and Eye Colour from DNA. *Forensic Sci. Int. Genet.* **2013**, *7*, 98–115. [CrossRef] [PubMed]
58. Walsh, S.; Liu, F.; Ballantyne, K.N.; Van Oven, M.; Lao, O.; Kayser, M. IrisPlex: A Sensitive DNA Tool for Accurate Prediction of Blue and Brown Eye Colour in the Absence of Ancestry Information. *Forensic Sci. Int. Genet.* **2011**, *5*, 170–180. [CrossRef]
59. Xavier, C.; de la Puente, M.; Mosquera-Miguel, A.; Freire-Aradas, A.; Kalamara, V.; Ralf, A.; Revoir, A.; Gross, T.E.; Schneider, P.M.; Ames, C.; et al. Development and Inter-Laboratory Evaluation of the VISAGE Enhanced Tool for Appearance and Ancestry Inference from DNA. *Forensic Sci. Int. Genet.* **2022**, *61*, 102779. [CrossRef]
60. Bukyya, J.L.; Tejasvi, M.L.A.; Avinash, A.; Chanchala, H.P.; Talwade, P.; Afroz, M.M.; Pokala, A.; Neela, P.K.; Shyamilee, T.K.; Srisha, V. DNA Profiling in Forensic Science: A Review. *Glob. Med. Genet.* **2021**, *08*, 135–143. [CrossRef]
61. Mackey, D.A. What Colour Are Your Eyes? Teaching the Genetics of Eye Colour & Colour Vision. Edridge Green Lecture RCOphth Annual Congress Glasgow May 2019. *Eye* **2022**, *36*, 704–715. [CrossRef]
62. Shapturenko, M.N.; Vakula, S.I.; Kandratsiuk, A.V.; Gudievskaya, I.G.; Shinkevich, M.V.; Luhauniou, A.U.; Borovko, S.R.; Marchenko, L.N.; Kilchevsky, A.V. HERC2 (Rs12913832) and OCA2 (Rs1800407) Genes Polymorphisms in Relation to Iris Color Variation in Belarusian Population. *Forensic Sci. Int. Genet. Suppl. Ser.* **2019**, *7*, 331–332. [CrossRef]
63. Salvo, N.M.; Andersen, J.D.; Janssen, K.; Meyer, O.L.; Berg, T.; Børsting, C.; Olsen, G.H. Association between Variants in the OCA2-HERC2 Region and Blue Eye Colour in HERC2 Rs12913832 AA and AG Individuals. *Genes* **2023**, *14*, 698. [CrossRef] [PubMed]
64. Rafati, A.; Hosseini, S.M.; Far, H.Z. Using the Irisplex System for Eye Color Prediction on Skeletal Remaining from the Past 30 Years. *J. Forensic Sci. Med.* **2023**, *9*, 367–370. [CrossRef]
65. Becher, D.; Jmel, H.; Kheriji, N.; Sarno, S.; Kefi, R. Genetic Landscape of Forensic DNA Phenotyping Markers among Mediterranean Populations. *Forensic Sci. Int.* **2024**, *354*, 111906. [CrossRef]

https://doi.org/10.3390/genes17010059

66. Martinez-Cadenas, C.; Penãa-Chilet, M.; Ibarrola-Villava, M.; Ribas, G. Gender Is a Major Factor Explaining Discrepancies in Eye Colour Prediction Based on HERC2/OCA2 Genotype and the IrisPlex Model. *Forensic Sci. Int. Genet.* **2013**, *7*, 453–460. [CrossRef]
67. Carratto, T.M.T.; Moraes, V.M.S.; Recalde, T.S.F.; de Oliveira, M.L.G.; Mendes-Junior, C.T. Applications of Massively Parallel Sequencing in Forensic Genetics. *Genet. Mol. Biol.* **2022**, *45*, e20220077. [CrossRef]
68. Atwood, L.; Raymond, J.; Sears, A.; Bell, M.; Daniel, R. From Identification to Intelligence: An Assessment of the Suitability of Forensic DNA Phenotyping Service Providers for Use in Australian Law Enforcement Casework. *Front. Genet.* **2021**, *11*, 568701. [CrossRef]
69. Sessa, F. Secondary transfer and its involvement in forensic investigation. *Investig. Predict. DNA* **2026**, 289–300. [CrossRef]
70. Bhoyar, L.; Mehar, P.; Chavali, K. An Overview of DNA Degradation and Its Implications in Forensic Caseworks. *Egypt. J. Forensic Sci.* **2024**, *14*, 15. [CrossRef]
71. Pośpiech, E.; Chen, Y.; Kukla-Bartoszek, M.; Breslin, K.; Aliferi, A.; Andersen, J.D.; Ballard, D.; Chaitanya, L.; Freire-Aradas, A.; van der Gaag, K.J.; et al. Towards Broadening Forensic DNA Phenotyping beyond Pigmentation: Improving the Prediction of Head Hair Shape from DNA. *Forensic Sci. Int. Genet.* **2018**, *37*, 241–251. [CrossRef]
72. van Daal, A. The Genetic Basis of Human Pigmentation. *Forensic Sci. Int. Genet. Suppl. Ser.* **2008**, *1*, 541–543. [CrossRef]
73. Suarez, P.; Baumer, K.; Hall, D. Further Insight into the Global Variability of the OCA2-HERC2 Locus for Human Pigmentation from Multiallelic Markers. *Sci. Rep.* **2021**, *11*, 22530. [CrossRef]
74. Andrade, E.S.; Fracasso, N.C.A.; Strazza Júnior, P.S.; Simões, A.L.; Mendes-Junior, C.T. Associations of OCA2-HERC2 SNPs and Haplotypes with Human Pigmentation Characteristics in the Brazilian Population. *Leg. Med.* **2017**, *24*, 78–83. [CrossRef]
75. Branicki, W.; Brudnik, U.; Wojas-Pelc, A. Interactions between HERC2, OCA2 and MC1R May Influence Human Pigmentation Phenotype. *Ann. Hum. Genet.* **2009**, *73*, 160–170. [CrossRef]
76. Le, L.; Escobar, I.E.; Ho, T.; Lefkovith, A.J.; Latteri, E.; Haltaufderhyde, K.D.; Dennis, M.K.; Plowright, L.; Sviderskaya, E.V.; Bennett, D.C.; et al. SLC45A2 Protein Stability and Regulation of Melanosome PH Determine Melanocyte Pigmentation. *Mol. Biol. Cell* **2020**, *31*, 2687–2702. [CrossRef]
77. Pośpiech, E.; Kukla-Bartoszek, M.; Karłowska-Pik, J.; Zieliński, P.; Woźniak, A.; Boroń, M.; Dąbrowski, M.; Zubańska, M.; Jarosz, A.; Grzybowski, T.; et al. Exploring the Possibility of Predicting Human Head Hair Greying from DNA Using Whole-Exome and Targeted NGS Data. *BMC Genom.* **2020**, *21*, 538. [CrossRef]
78. Branicki, W.; Liu, F.; Van Duijn, K.; Draus-Barini, J.; Pośpiech, E.; Walsh, S.; Kupiec, T.; Wojas-Pelc, A.; Kayser, M. Model-Based Prediction of Human Hair Color Using DNA Variants. *Hum. Genet.* **2011**, *129*, 443–454. [CrossRef]
79. Zorina-Lichtenwalter, K.; Lichtenwalter, R.N.; Zaykin, D.V.; Parisien, M.; Gravel, S.; Bortsov, A.; Diatchenko, L. A Study in Scarlet: MC1R as the Main Predictor of Red Hair and Exemplar of the Flip-Flop Effect. *Hum. Mol. Genet.* **2019**, *28*, 2093–2106. [CrossRef]
80. Kukla-Bartoszek, M.; Pośpiech, E.; Spólnicka, M.; Karłowska-Pik, J.; Strapagiel, D.; Żądzińska, E.; Rosset, I.; Sobalska-Kwapis, M.; Słomka, M.; Walsh, S.; et al. Investigating the Impact of Age-Depended Hair Colour Darkening during Childhood on DNA-Based Hair Colour Prediction with the HIrisPlex System. *Forensic Sci. Int. Genet.* **2018**, *36*, 26–33. [CrossRef]
81. Navarro-López, B.; Baeta, M.; Moreno-López, O.; Olalde, I.; de Pancorbo, M.M.; Suárez-Ulloa, V.; Martos-Fernández, R.; Martínez-Jarreta, B.; Jiménez, S. Exploring Eye, Hair, and Skin Pigmentation in a Spanish Population: Insights from Hirisplex-S Predictions. *Genes* **2024**, *15*, 1330. [CrossRef]
82. Browne, T.N.; Freeman, M. Next Generation Sequencing: Forensic Applications and Policy Considerations. *WIREs Forensic Sci.* **2024**, *6*, e1531. [CrossRef]
83. Cabrejas-Olalla, A.; Athanasiadis, G.; Jørgensen, F.G.; Cheng, J.Y.; Kjærgaard, P.C.; Schierup, M.H.; Mailund, T. Genetic Predictions of Eye and Hair Colour in the Danish Population. *Forensic Sci. Int. Genet.* **2025**, *78*, 103267. [CrossRef]
84. Breslin, K.; Wills, B.; Ralf, A.; Ventayol Garcia, M.; Kukla-Bartoszek, M.; Pospiech, E.; Freire-Aradas, A.; Xavier, C.; Ingold, S.; de La Puente, M.; et al. HIrisPlex-S System for Eye, Hair, and Skin Color Prediction from DNA: Massively Parallel Sequencing Solutions for Two Common Forensically Used Platforms. *Forensic Sci. Int. Genet.* **2019**, *43*, 102152. [CrossRef]
85. Perez Palomeque, G.; Khacha-ananda, S.; Monum, T.; Wunnapuk, K. Prediction of Skin Color Using Forensic DNA Phenotyping in Asian Populations: A Focus on Thailand. *Biomolecules* **2025**, *15*, 548. [CrossRef]
86. Del Bino, S.; Duval, C.; Bernerd, F. Clinical and Biological Characterization of Skin Pigmentation Diversity and Its Consequences on UV Impact. *Int. J. Mol. Sci.* **2018**, *19*, 2668. [CrossRef]
87. D'Mello, S.A.N.; Finlay, G.J.; Baguley, B.C.; Askarian-Amiri, M.E. Signaling Pathways in Melanogenesis. *Int. J. Mol. Sci.* **2016**, *17*, 1144. [CrossRef]
88. Maroñas, O.; Phillips, C.; Söchtig, J.; Gomez-Tato, A.; Cruz, R.; Alvarez-Dios, J.; De Cal, M.C.; Ruiz, Y.; Fondevila, M.; Carracedo, Á.; et al. Development of a Forensic Skin Colour Predictive Test. *Forensic Sci. Int. Genet.* **2014**, *13*, 34–44. [CrossRef]
89. Irving-Pease, E.K.; Muktupavela, R.; Dannemann, M.; Racimo, F. Quantitative Human Paleogenetics: What Can Ancient DNA Tell Us About Complex Trait Evolution? *Front. Genet.* **2021**, *12*, 703541. [CrossRef]
90. Barash, M.; McNevin, D.; Fedorenko, V.; Giverts, P. Machine Learning Applications in Forensic DNA Profiling: A Critical Review. *Forensic Sci. Int. Genet.* **2024**, *69*, 102994. [CrossRef]

https://doi.org/10.3390/genes17010059

91. Zaorska, K.; Zawierucha, P.; Nowicki, M. Prediction of Skin Color, Tanning and Freckling from DNA in Polish Population: Linear Regression, Random Forest and Neural Network Approaches. *Hum. Genet.* **2019**, *138*, 635–647. [CrossRef] [PubMed]
92. Herraiz, C.; Garcia-Borron, J.C.; Jiménez-Cervantes, C.; Olivares, C. MC1R Signaling. Intracellular Partners and Pathophysiological Implications. *Biochim. Biophys. Acta Mol. Basis Dis.* **2017**, *1863*, 2448–2461. [CrossRef] [PubMed]
93. Davies, J.R.; Randerson-Moor, J.; Kukalizch, K.; Harland, M.; Kumar, R.; Madhusudan, S.; Nagore, E.; Hansson, J.; Höiom, V.; Ghiorzo, P.; et al. Inherited Variants in the MC1R Gene and Survival from Cutaneous Melanoma: A BioGenoMEL Study. *Pigment. Cell Melanoma Res.* **2012**, *25*, 384–394. [CrossRef]
94. Jacobs, L.C.; Hamer, M.A.; Gunn, D.A.; Deelen, J.; Lall, J.S.; Van Heemst, D.; Uh, H.W.; Hofman, A.; Uitterlinden, A.G.; Griffiths, C.E.M.; et al. A Genome-Wide Association Study Identifies the Skin Color Genes IRF4, MC1R, ASIP, and BNC2 Influencing Facial Pigmented Spots. *J. Investig. Dermatol.* **2015**, *135*, 1735–1742. [CrossRef]
95. Katsara, M.A.; Branicki, W.; Walsh, S.; Kayser, M.; Nothnagel, M. Evaluation of Supervised Machine-Learning Methods for Predicting Appearance Traits from DNA. *Forensic Sci. Int. Genet.* **2021**, *53*, 102507. [CrossRef] [PubMed]
96. Cha, M.Y.; Choi, J.E.; Lee, D.S.; Lee, S.R.; Lee, S.I.; Park, J.H.; Shin, J.H.; Suh, I.S.; Kim, B.H.; Hong, K.W. Novel Genetic Associations for Skin Aging Phenotypes and Validation of Previously Reported Skin GWAS Results. *Appl. Sci.* **2022**, *12*, 11422. [CrossRef]
97. Fridman, C.; Ferreira, M.A.; Marano, L.A.; Forlenza, B.S. Analysis of Genetic Polymorphisms Associated with the Presence of Freckles for Phenotypic Prediction. *Forensic Sci. Int. Genet. Suppl. Ser.* **2022**, *8*, 26–28. [CrossRef]
98. Elkins, K.M.; Garloff, A.T.; Zeller, C.B. Additional Predictions for Forensic DNA Phenotyping of Externally Visible Characteristics Using the ForenSeq and Imagen Kits. *J. Forensic Sci.* **2023**, *68*, 608–613. [CrossRef]
99. Bastiaens, M.; Ter Huurne, J.; Gruis, N.; Bergman, W.; Westendorp, R.; Vermeer, B.J.; Bavinck, J.N.B. The Melanocortin-1-Receptor Gene Is the Major Freckle Gene. *Hum. Mol. Genet.* **2001**, *10*, 1701–1708. [CrossRef] [PubMed]
100. Walsh, S.; Chaitanya, L.; Breslin, K.; Muralidharan, C.; Bronikowska, A.; Pospiech, E.; Koller, J.; Kovatsi, L.; Wollstein, A.; Branicki, W.; et al. Global Skin Colour Prediction from DNA. *Hum. Genet.* **2017**, *136*, 847–863. [CrossRef] [PubMed]
101. Guida, S.; Guida, G.; Goding, C.R. MC1R Functions, Expression, and Implications for Targeted Therapy. *J. Investig. Dermatol.* **2022**, *142*, 293–302. [CrossRef]
102. Alshehhi, A.; Almarzooqi, A.; Alhammadi, K.; Werghi, N.; Tay, G.K.; Alsafar, H. Advancement in Human Face Prediction Using DNA. *Genes* **2023**, *14*, 136. [CrossRef]
103. Stephan, C.N.; Caple, J.M.; Guyomarc'h, P.; Claes, P. An Overview of the Latest Developments in Facial Imaging. *Forensic Sci. Res.* **2019**, *4*, 10–28. [CrossRef]
104. Weinberg, S.M.; Roosenboom, J.; Shaffer, J.R.; Shriver, M.D.; Wysocka, J.; Claes, P. Hunting for Genes That Shape Human Faces: Initial Successes and Challenges for the Future. *Orthod. Craniofac. Res.* **2019**, *22*, 207–212. [CrossRef]
105. Navarro-López, B.; Wilke, F.; Suárez-Ulloa, V.; Baeta, M.; Martos-Fernández, R.; Moreno-López, O.; Olalde, I.; Martínez-Jarreta, B.; Jiménez, S.; Walsh, S.; et al. Exploring the Association between SNPs and Facial Morphology in a Spanish Population. *Sci. Rep.* **2025**, *15*, 13826. [CrossRef]
106. Qian, W.; Zhang, M.; Wan, K.; Xie, Y.; Du, S.; Li, J.; Mu, X.; Qiu, J.; Xue, X.; Zhuang, X.; et al. Genetic Evidence for Facial Variation Being a Composite Phenotype of Cranial Variation and Facial Soft Tissue Thickness. *J. Genet. Genom.* **2022**, *49*, 934–942. [CrossRef]
107. Hopman, S.M.J.; Merks, J.H.M.; Suttie, M.; Hennekam, R.C.M.; Hammond, P. Face Shape Differs in Phylogenetically Related Populations. *Eur. J. Hum. Genet.* **2014**, *22*, 1268–1271. [CrossRef] [PubMed]
108. Yuan, M.; Goovaerts, S.; Vanneste, M.; Matthews, H.; Hoskens, H.; Richmond, S.; Klein, O.D.; Spritz, R.A.; Hallgrimsson, B.; Walsh, S.; et al. Mapping Genes for Human Face Shape: Exploration of Univariate Phenotyping Strategies. *PLoS Comput. Biol.* **2024**, *20*, e1012617. [CrossRef]
109. Liu, F.; van der Lijn, F.; Schurmann, C.; Zhu, G.; Chakravarty, M.M.; Hysi, P.G.; Wollstein, A.; Lao, O.; de Bruijne, M.; Ikram, M.A.; et al. A Genome-Wide Association Study Identifies Five Loci Influencing Facial Morphology in Europeans. *PLoS Genet.* **2012**, *8*, e1002932. [CrossRef] [PubMed]
110. Samuels, B.D.; Aho, R.; Brinkley, J.F.; Bugacov, A.; Feingold, E.; Fisher, S.; Gonzalez-Reiche, A.S.; Hacia, J.G.; Hallgrimsson, B.; Hansen, K.; et al. FaceBase 3: Analytical Tools and FAIR Resources for Craniofacial and Dental Research. *Development* **2020**, *147*, dev191213. [CrossRef]
111. Xiong, Z.; Dankova, G.; Howe, L.J.; Lee, M.K.; Hysi, P.G.; De Jong, M.A.; Zhu, G.; Adhikar, K.; Li, D.; Li, Y.; et al. Novel Genetic Loci Affecting Facial Shape Variation in Humans. *Elife* **2019**, *8*, e49898. [CrossRef] [PubMed]
112. Castagnola, M.J.; Medina-Paz, F.; Zapico, S.C. Uncovering Forensic Evidence: A Path to Age Estimation through DNA Methylation. *Int. J. Mol. Sci.* **2024**, *25*, 4917. [CrossRef]
113. Zhu, B.; Li, D.; Han, G.; Yao, X.; Gu, H.; Liu, T.; Liu, L.; Dai, J.; Liu, I.Z.; Liang, Y.; et al. Multiplexing and Massive Parallel Sequencing of Targeted DNA Methylation to Predict Chronological Age. *Front. Aging* **2025**, *6*, 1467639. [CrossRef]
114. Mathur, A.; Taurin, S.; Alshammary, S. New Insights into Methods to Measure Biological Age: A Literature Review. *Front. Aging* **2024**, *5*, 1395649. [CrossRef]

https://doi.org/10.3390/genes17010059

115. Maulani, C.; Auerkari, E.I. Age Estimation Using DNA Methylation Technique in Forensics: A Systematic Review. *Egypt. J. Forensic Sci.* **2020**, *10*, 38. [CrossRef]
116. Gerra, M.C.; Dallabona, C.; Cecchi, R. Epigenetic Analyses in Forensic Medicine: Future and Challenges. *Int. J. Leg. Med.* **2024**, *138*, 701–719. [CrossRef]
117. Bekaert, B.; Kamalandua, A.; Zapico, S.C.; Van De Voorde, W.; Decorte, R. Improved Age Determination of Blood and Teeth Samples Using a Selected Set of DNA Methylation Markers. *Epigenetics* **2015**, *10*, 922–930. [CrossRef]
118. Woźniak, A.; Heidegger, A.; Piniewska-Róg, D.; Pośpiech, E.; Xavier, C.; Pisarek, A.; Kartasińska, E.; Boroń, M.; Freire-Aradas, A.; Wojtas, M.; et al. Development of the VISAGE Enhanced Tool and Statistical Models for Epigenetic Age Estimation in Blood, Buccal Cells and Bones. *Aging* **2021**, *13*, 6459–6484. [CrossRef]
119. Marcante, B.; Marino, L.; Cattaneo, N.E.; Delicati, A.; Tozzo, P.; Caenazzo, L. Advancing Forensic Human Chronological Age Estimation: Biochemical, Genetic, and Epigenetic Approaches from the Last 15 Years: A Systematic Review. *Int. J. Mol. Sci.* **2025**, *26*, 3158. [CrossRef]
120. Onofri, M.; Delicati, A.; Marcante, B.; Carlini, L.; Alessandrini, F.; Tozzo, P.; Carnevali, E. Forensic Age Estimation through a DNA Methylation-Based Age Prediction Model in the Italian Population: A Pilot Study. *Int. J. Mol. Sci.* **2023**, *24*, 5381. [CrossRef]
121. Correia Dias, H.; Cunha, E.; Corte Real, F.; Manco, L. Age Prediction in Living: Forensic Epigenetic Age Estimation Based on Blood Samples. *Leg. Med.* **2020**, *47*, 101763. [CrossRef]
122. Refn, M.R.; Kampmann, M.L.; Morling, N.; Tfelt-Hansen, J.; Børsting, C.; Pereira, V. Prediction of Chronological Age and Its Applications in Forensic Casework: Methods, Current Practices, and Future Perspectives. *Forensic Sci. Res.* **2023**, *8*, 85–97. [CrossRef] [PubMed]
123. Kurdyukov, S.; Bullock, M. DNA Methylation Analysis: Choosing the Right Method. *Biology* **2016**, *5*, 3. [CrossRef] [PubMed]
124. De Chiara, L.; Leiro-Fernandez, V.; Rodríguez-Girondo, M.; Valverde, D.; Botana-Rial, M.I.; Fernández-Villar, A. Comparison of Bisulfite Pyrosequencing and Methylation-Specific qPCR for Methylation Assessment. *Int. J. Mol. Sci.* **2020**, *21*, 9242. [CrossRef]
125. Naue, J.; Hoefsloot, H.C.J.; Kloosterman, A.D.; Verschure, P.J. Forensic DNA Methylation Profiling from Minimal Traces: How Low Can We Go? *Forensic Sci. Int. Genet.* **2018**, *33*, 17–23. [CrossRef] [PubMed]
126. Manco, L.; Dias, H.C. DNA Methylation Analysis of ELOVL2 Gene Using Droplet Digital PCR for Age Estimation Purposes. *Forensic Sci. Int.* **2022**, *333*, 111206. [CrossRef] [PubMed]
127. Żarczyńska, M.; Żarczyński, P.; Tomsia, M. Nucleic Acids Persistence—Benefits and Limitations in Forensic Genetics. *Genes* **2023**, *14*, 1643. [CrossRef] [PubMed]
128. Wen, Y.; Liu, J.; Su, Y.; Chen, X.; Hou, Y.; Liao, L.; Wang, Z. Forensic Biogeographical Ancestry Inference: Recent Insights and Current Trends. *Genes Genom.* **2023**, *45*, 1229–1238. [CrossRef]
129. Than, K.Z.; Muisuk, K.; Woravatin, W.; Suwannapoom, C.; Srikummool, M.; Srithawong, S.; Lorphengsy, S.; Kutanan, W. Genetic Structure and Forensic Utility of 23 Autosomal STRs of the Ethnic Lao Groups From Laos and Thailand. *Front. Genet.* **2022**, *13*, 954586. [CrossRef]
130. Fondevila, M.; Phillips, C.; Santos, C.; Freire Aradas, A.; Vallone, P.M.; Butler, J.M.; Lareu, M.V.; Carracedo, Á. Revision of the SNPforID 34-Plex Forensic Ancestry Test: Assay Enhancements, Standard Reference Sample Genotypes and Extended Population Studies. *Forensic Sci. Int. Genet.* **2013**, *7*, 63–74. [CrossRef] [PubMed]
131. Zhang, S.; Bian, Y.; Chen, A.; Zheng, H.; Gao, Y.; Hou, Y.; Li, C. Developmental Validation of a Custom Panel Including 273 SNPs for Forensic Application Using Ion Torrent PGM. *Forensic Sci. Int. Genet.* **2017**, *27*, 50–57. [CrossRef]
132. Ruiz-Ramírez, J.; de la Puente, M.; Xavier, C.; Ambroa-Conde, A.; Álvarez-Dios, J.; Freire-Aradas, A.; Mosquera-Miguel, A.; Ralf, A.; Amory, C.; Katsara, M.A.; et al. Development and Evaluations of the Ancestry Informative Markers of the VISAGE Enhanced Tool for Appearance and Ancestry. *Forensic Sci. Int. Genet.* **2023**, *64*, 102853. [CrossRef]
133. Sun, K.; Yao, Y.; Yun, L.; Zhang, C.; Xie, J.; Qian, X.; Tang, Q.; Sun, L. Application of Machine Learning for Ancestry Inference Using Multi-InDel Markers. *Forensic Sci. Int. Genet.* **2022**, *59*, 102702. [CrossRef]
134. Kling, D.; Phillips, C.; Kennett, D.; Tillmar, A. Investigative Genetic Genealogy: Current Methods, Knowledge and Practice. *Forensic Sci. Int. Genet.* **2021**, *52*, 102474. [CrossRef]
135. Peterson, R.E.; Kuchenbaecker, K.; Walters, R.K.; Chen, C.Y.; Popejoy, A.B.; Periyasamy, S.; Lam, M.; Iyegbe, C.; Strawbridge, R.J.; Brick, L.; et al. Genome-Wide Association Studies in Ancestrally Diverse Populations: Opportunities, Methods, Pitfalls, and Recommendations. *Cell* **2019**, *179*, 589–603. [CrossRef]
136. Tan, M.; Tan, Y.; Jiang, H.; Xue, J.; Wu, Q.; Zheng, Y.; Liu, G.; Xiao, Y.; Lv, M.; Liao, M.; et al. Explainable Artificial Intelligence in Forensic DNA Analysis: Alleles Identification in Challenging Electropherograms Using Supervised Machine Learning Methods. *Forensic Sci. Int. Genet.* **2025**, *78*, 103289. [CrossRef]
137. Gaonkar, B.; Shinohara, R.T.; Davatzikos, C. Interpreting Support Vector Machine Models for Multivariate Group Wise Analysis in Neuroimaging. *Med. Image Anal.* **2015**, *24*, 190–204. [CrossRef]
138. Couronné, R.; Probst, P.; Boulesteix, A.L. Random Forest versus Logistic Regression: A Large-Scale Benchmark Experiment. *BMC Bioinform.* **2018**, *19*, 27. [CrossRef]

https://doi.org/10.3390/genes17010059

139. Ausmees, K.; Nettelblad, C. Achieving Improved Accuracy for Imputation of Ancient DNA. *Bioinformatics* **2023**, *39*, btac738. [CrossRef]
140. Mochurad, L.; Horun, P. Improvement Technologies for Data Imputation in Bioinformatics. *Technologies* **2023**, *11*, 154. [CrossRef]
141. Ausmees, K.; Sanchez-Quinto, F.; Jakobsson, M.; Nettelblad, C. An Empirical Evaluation of Genotype Imputation of Ancient DNA. *G3 Genes Genomes Genet.* **2022**, *12*, jkac089. [CrossRef] [PubMed]
142. Alharbi, W.S.; Rashid, M. A Review of Deep Learning Applications in Human Genomics Using Next-Generation Sequencing Data. *Hum. Genom.* **2022**, *16*, 26. [CrossRef] [PubMed]
143. Kolobkov, D.; Mishra Sharma, S.; Medvedev, A.; Lebedev, M.; Kosaretskiy, E.; Vakhitov, R. Efficacy of Federated Learning on Genomic Data: A Study on the UK Biobank and the 1000 Genomes Project. *Front. Big Data* **2024**, *7*, 1266031. [CrossRef] [PubMed]
144. Chen, J.; Chen, A.; Tao, R.; Zhu, R.; Zhang, H.; You, X.; Li, C.; Zhang, S. Solution to a Case Involving the Interpretation of Trace Degraded DNA Mixtures. *Int. J. Leg. Med.* **2024**, *138*, 2325–2330. [CrossRef]
145. Diepenbroek, M.; Bayer, B.; Anslinger, K. Pushing the Boundaries: Forensic DNA Phenotyping Challenged by Single-Cell Sequencing. *Genes* **2021**, *12*, 1362. [CrossRef]
146. Toom, V.; Wienroth, M.; M'Charek, A.; Prainsack, B.; Williams, R.; Duster, T.; Heinemann, T.; Kruse, C.; MacHado, H.; Murphy, E. Approaching Ethical, Legal and Social Issues of Emerging Forensic DNA Phenotyping (FDP) Technologies Comprehensively: Reply to "Forensic DNA Phenotyping: Predicting Human Appearance from Crime Scene Material for Investigative Purposes" by Manfred Kayser. *Forensic Sci. Int. Genet.* **2016**, *22*, e1–e4. [CrossRef] [PubMed]
147. Ogbogu, U.; Ahmed, N. Ethical, Legal, and Social Implications (ELSI) Research: Methods and Approaches. *Curr. Protoc.* **2022**, *2*, e354. [CrossRef] [PubMed]
148. García, Ó. Forensic Genealogy. Social, Ethical, Legal and Scientific Implications. *Span. J. Leg. Med.* **2021**, *47*, 112–119. [CrossRef]
149. Piraianu, A.I.; Fulga, A.; Musat, C.L.; Ciobotaru, O.R.; Poalelungi, D.G.; Stamate, E.; Ciobotaru, O.; Fulga, I. Enhancing the Evidence with Algorithms: How Artificial Intelligence Is Transforming Forensic Medicine. *Diagnostics* **2023**, *13*, 2992. [CrossRef]
150. Nikita, E.; Nikitas, P. On the Use of Machine Learning Algorithms in Forensic Anthropology. *Leg. Med.* **2020**, *47*, 101771. [CrossRef]
151. Guillen, M.; Lareu, M.V.; Pestoni, C.; Salas, A.; Carracedo, A. Ethical-Legal Problems of DNA Databases in Criminal Investigation. *J. Med. Ethics* **2000**, *26*, 266–271. [CrossRef]
152. Bernhardt, B.A.; Roche, M.I.; Perry, D.L.; Scollon, S.R.; Tomlinson, A.N.; Skinner, D. Experiences with Obtaining Informed Consent for Genomic Sequencing. *Am. J. Med. Genet. A* **2015**, *167*, 2635–2646. [CrossRef]
153. Hendriks, S.; Grady, C.; Ramos, K.M.; Chiong, W.; Fins, J.J.; Ford, P.; Goering, S.; Greely, H.T.; Hutchison, K.; Kelly, M.L.; et al. Ethical Challenges of Risk, Informed Consent, and Posttrial Responsibilities in Human Research with Neural Devices: A Review. *JAMA Neurol.* **2019**, *76*, 1506–1514. [CrossRef] [PubMed]
154. Ballantyne, K.N.; Summersby, S.; Pearson, J.R.; Nicol, K.; Pirie, E.; Quinn, C.; Kogios, R. A Transparent Approach: Openness in Forensic Science Reporting. *Forensic Sci. Int.* **2024**, *8*, 100474. [CrossRef]
155. Bollé, T.; Casey, E.; Jacquet, M. The Role of Evaluations in Reaching Decisions Using Automated Systems Supporting Forensic Analysis. *Forensic Sci. Int. Digit. Investig.* **2020**, *34*, 301016. [CrossRef]
156. Kayser, M.; Parson, W. Transitioning from Forensic Genetics to Forensic Genomics. *Genes* **2018**, *9*, 3. [CrossRef] [PubMed]
157. Mohsin, K. Artificial Intelligence in Forensic Science. *Int. J. Forensic Res.* **2023**, *4*, 172–173. [CrossRef]
158. Galante, N.; Cotroneo, R.; Furci, D.; Lodetti, G.; Casali, M.B. Applications of Artificial Intelligence in Forensic Sciences: Current Potential Benefits, Limitations and Perspectives. *Int. J. Leg. Med.* **2022**, *137*, 445–458. [CrossRef] [PubMed]
159. Sessa, F.; Esposito, M.; Cocimano, G.; Sablone, S.; Karaboue, M.A.A.; Chisari, M.; Albano, D.G.; Salerno, M. Artificial Intelligence and Forensic Genetics: Current Applications and Future Perspectives. *Appl. Sci.* **2024**, *14*, 2113. [CrossRef]

https://doi.org/10.3390/genes17010059

genes

MDPI

Article

Cardiac Genetic Variants in Sudden, Unexpected Death in Epilepsy: From Challenging DNA Extraction Methods to Updated NGS Panels for Improved Genetic Analysis

Alessia Bernini Di Michele [1], Valerio Onofri [2], Filomena Melchionda [1], Lucia Fiordelmondo [2], Eleonora Ciarimboli [2], Marco Palpacelli [2], Sara Sablone [3], Chiara Turchi [1,*] and Mauro Pesaresi [1]

[1] Section of Legal Medicine, Department of Biomedical Sciences and Public Health, Polytechnic University of Marche, Via Tronto, 60126 Ancona, Italy; a.bernini@pm.univpm.it (A.B.D.M.); f.melchionda@univpm.it (F.M.); m.pesaresi@univpm.it (M.P.)

[2] Legal Medicine Unit, A.O.U. Azienda Ospedaliero Universitaria delle Marche, 60126 Ancona, Italy; valerio.onofri@ospedaliriuniti.marche.it (V.O.); lucia.fiordelmondo@ospedaliriuniti.marche.it (L.F.); eleonora.ciarimboli@ospedaliriuniti.marche.it (E.C.)

[3] Section of Legal Medicine, Interdisciplinary Department of Medicine, University of Bari "Aldo Moro"-Bari Policlinico Hospital Giulio Cesare Square, 11, 70124 Bari, Italy; sara.sablone@policlinico.ba.it

* Correspondence: c.turchi@univpm.it

Abstract: Background/Objectives: SUDEP is the sudden, unexpected death of someone with epilepsy, and occurs mainly during sleep or at rest, or when the individual does not seem to have experienced a convulsive seizure. The cause of death in SUDEP is still unknown, and it may differ between cases. Cardiac factors are among the most prevalent causes observed in SUDEP. Therefore, within the forensic medicine framework, identifying well-known DNA markers involved in cardiac sudden and unexpected death would aid in understanding the cause of SUDEP, as well as in finding cardiac risk markers in patients with epilepsy. The purpose of this study was to identify any genetic variants by analyzing blood and formalin-fixed paraffin-embedded (FFPE) tissue samples, utilizing next-generation sequencing techniques. Methods: We investigated five cases of SUDEP that were examined at the Legal Medicine department of Ancona (Italy). Peripheral blood or FFPE cardiac tissues were collected, and different DNA extraction methods were performed. In particular, this study underlines a new extraction method from FFPE tissue, adapting the Casework kit for forensic application to our purpose. Later, about one hundred genes correlated to inherited cardiac diseases were sequenced through the Ion PGM System and Ion GeneStudio S5 Systems. Results: Bioinformatic analysis showed some genetic variants of unknown significance (VUS) on genes involved in SUDEP: RYR2, SCN8A, and AKAP9. Conclusions: As expected, very low coverage of the target base was observed for FFPE tissue samples because of the complexity of the biological material. Therefore, the presence of any significant variants in unamplified regions cannot be excluded in the FFPE samples. As suggested by the literature, the variants found in the blood samples are potentially associated with SUDEP.

Keywords: SUDEP; molecular autopsy; cardiac genes; next generation sequencing

1. Introduction

SUDEP is defined as a sudden, unexpected, witnessed or unwitnessed death in a non-traumatic or non-drowning manner, with or without evidence of a seizure—excluding

documented status epilepticus—in which there is no toxicological or anatomical cause of death [1]. Each year, more than 1 in 1000 people with epilepsy die from SUDEP. Most SUDEP cases are observed in young subjects (0–15 years old), and the incidence is higher in men (1.41/1000 person-years) than in women (0.96/1000 person-years) [2]. However, it is noted that the risk of SUDEP has been underestimated, especially in older people, regardless of sex [2]. These deaths occur mainly during sleep or at rest, and the individuals affected do not seem to experience convulsive seizures. The cause of death by SUDEP is still unknown, and it may differ between cases.

The overarching term SUDEP can be subdivided into four different categories: Definite, Definite Plus, Probably, and Possible; otherwise, if an alternate cause of death has been determined, the possibility that SUDEP is the cause of death is excluded (SUDEP Unlikely).

1. Definite SUDEP: a non-traumatic and non-drowning death in an individual with epilepsy, without a cause of death after postmortem examination.
2. Definite SUDEP Plus: includes the presence of a concomitant condition other than epilepsy, where death may be due to the combined effects of both epilepsy and the other condition.
3. Probably SUDEP: all the same criteria for Definite SUDEP are met, but no postmortem examination is performed.
4. Possible SUDEP: insufficient information is available regarding the death; postmortem examinations have not been carried out, and the SUDEP hypothesis cannot be ruled out [3–5].

Recent studies have extensively investigated the pathophysiology of SUDEP in different groups, proposing four main mechanisms for SUDEP: cardiac dysfunction, such as cardiac arrhythmias and other cardiac events; respiratory factors, such as seizure-induced pulmonary dysfunction; and cerebral and autonomic nervous system dysregulation. Other less frequent causes of SUDEP are anti-epileptic drugs; vagal nerve stimulation, which may induce bradycardia or cardiac arrest; and genetic factors, including mutations in several genes associated with an increased susceptibility to SUDEP [6]. Over 33% of these are related to mutations, leading to increased susceptibility to arrhythmia [7]. Cardiac factors such as channelopathies, cardiomyopathies, aortopathies, cardiac arrhythmias, and long QT syndrome (LQTS) are among the most involved elements in SUDEP. Therefore, within the forensic medicine framework, the well-known DNA markers involved in cardiac sudden and unexpected death would aid in understanding the cause of SUDEP and in finding cardiac risk markers in patients with epilepsy. The SUDEP research is supported by genetic analysis (so-called molecular autopsy) that can lead to the identification of variants with clinical significance related to the cause of death.

To date, few genes have been analyzed in genetic testing, although the implementation of next-generation sequencing (NGS) and the low cost of these high-throughput technologies are helping to identify new candidate genes. Few studies have examined possible genetic risk factors in SUDEP. One of the limiting factors is that quality DNA samples must be collected during the life of the patient or extracted from postmortem blood. Although there is increasing awareness of the importance of collecting blood samples in unexplained sudden death in order to perform post-mortem genetic testing of the main cardiac arrhythmia genes [8], it is not always suitable for laboratories [9]. As in our case, we had collected formalin-fixed paraffin-embedded (FFPE) tissue in the past years for further analyses, with no blood samples available. Bagnall et al. in 2017 [8] performed exome sequencing from degraded DNA derived from FFPE postmortem tissues, which identified a de novo *SCN1A* frameshift variant in a patient with SUDEP. This study shows the possibility of analyzing historical collections of postmortem fixed tissues from SUDEP

cases [8,9]. Another limitation of studies on SUDEP is the small number of cases. In fact, it is a rare event, and the largest genetic study of SUDEP was performed by Bagnall et al. in 2016 using exome sequencing-based analysis of 61 SUDEP cases [10].

In our forensic genetics laboratory, we analyzed two SUDEP cases in 2022 from FFPE heart tissues on a cardiac custom panel of 97 genes, and, more recently, we studied three other cases, two samples of whole blood and one sample of FFPE heart tissue, through an updated custom panel of 103 genes. We used a panel of cardiac genes because SUDEP was hypothesized to be caused by cardiac factors. In this study, we included not only samples of whole blood, but we also discussed the analysis of FFPE tissues, which were the only available biological matrices for some cases. Sometimes, it is common to store FFPE tissue for further analyses, since it can be stored for a longer time at room temperature at a lower cost. For this reason, we drew attention to the semi-automated DNA extraction method used for FFPE tissue and the results that we obtained.

2. Materials and Methods

In our research, we included five cases of SUDEP, renamed as sample 1, sample 2, sample 3, sample 4, and sample 5. In the study, two males and three females were included. All the subjects were epileptic patients treated with anti-epileptic drugs. In particular, sample 1 was a 31-year-old male who died in his sleep; sample 2 was a 47-year-old man with epilepsy under treatment; sample 3 was a 30-year-old woman with epilepsy and in drug treatment; sample 4 corresponded to a 56-year-old woman with cardiomyopathy who was HIV-positive; and finally, the most recent case of SUDEP, sample 5, was a 23-year-old young woman found unconscious lying in an apartment. For all cases, the toxicology tests revealed negative results for alcohol and psychoactive substances, and the anti-epileptic drugs present in the subjects in quantities were compatible with a therapeutic intake. Based on these findings, the coroner determined the cause of death to be attributable to Definite SUDEP for all cases, with the exception of sample 4, who suffered from cardiomyopathy and was classified as Definite Plus SUDEP, due to the appearance of fatal arrhythmia. The starting biological material was different: samples 1, 2, and 3 were FFPE heart tissue samples, and samples 4 and 5 were whole blood samples. Extraction of DNA from FFPE tissue is a critical step in molecular genetic testing. The area of the tissue was cut with a scalpel, and then the paraffin was eliminated, leaving only the tissue on the surface. This step facilitates slicing the tissue with the microtome without the interference of paraffin in the next step of extraction. Five to ten 5 μm thick slices were cut with the microtome, and a semi-automated DNA extraction method was performed following the "Promega Corporation, Revised 5/12, part #TB382" protocol of the Casework Kit (catalog number: AS1550, Promega, Madison, WI, USA) with the Maxwell® 16 Instrument (Promega). A total of 23 μL of Proteinase K solution and 180 μL of Casework Extraction Buffer was added, and samples were incubated at 70 °C overnight. The day after, 400 μL of lysis buffer was added, and the samples were ready for automated DNA extraction through the Maxwell 16 Instrument. DNA samples were eluted in 50 μL of elution buffer. The Casework Kit is usually used for challenging forensic samples, such as blood stains, semen stains, hair, cigarette butts, tissue samples, and trace DNA samples regularly encountered in forensic DNA analysis. It has also proven to be a good method for extracting DNA from FFPE tissue samples, since it reduces the number of steps and therefore also the risk that the different reagents can further degrade the DNA.

The DNA extraction method used for whole blood samples was performed through the Maxwell® CSC Genomic DNA Kit (catalog number: AS1850, Promega, Madison, WI, USA) by the Maxwell® CSC 48 instrument (Promega). The protocol was followed in all its

parts, considering an initial sample volume of 200 µL of whole blood and the volume of elution buffer of 200 µL. DNA extracted from FFPE tissue samples was quantified through a real-time PCR, using the Plexor® HY System kit (catalog number DC1001, Promega, USA). The instructions on the Plexor® HY System Protocol recommend using 2 µL of template DNA per reaction. DNA standards are in the range of 3.2 pg/µL to 50 ng/µL. Performing duplicate analysis of each sample DNA and averaging the quantitation results can reduce variability. Serial dilutions of the DNA standard were amplified in the same run as the unknown samples, and the results were used to generate a standard curve in the autosomal (fluorescein/GREEN) and Y (CALFluor® Orange 560/YELLOW, Berkeley, CA, USA) channels to determine the concentrations of unknown samples. It is necessary to include a no-template control (NTC) reaction for each set of reactions.

For blood samples, quantification was performed using the Qubit dsDNA HS (High Sensitivity) Assay kit (catalog number: Q32851, Thermo Fisher Scientific, Waltham, MA, USA), through the Qubit Instrument.

All the samples were then diluted, reaching a final concentration of 0.67 ng/µL for library preparation with Ion AmpliSeq™ Library Kit 2.0 (catalog number: 4475345, Thermo Fisher Scientific). A volume of 15 µL was aliquoted into the plate for library preparation with the Ion Chef System. The sequencing was then performed through the Ion PGM System for samples 1 and 2, sequenced in 2022 using a custom panel of 97 genes (V1) involved in cardiovascular diseases (18 genes of which were involved in SUDEP according to data collected in the literature). Samples 3, 4, and 5 were recently sequenced through Ion GeneStudio S5 Systems using an updated custom panel with 103 genes (V2), 21 of which are involved in SUDEP. The updated custom gene panel is shown in Supplementary Materials (Table S1). The genes added to the latest version were *DEPDC5*, *DTNA*, *GAA*, *PTPN11*, *SCN1A*, and *SCN8A*. In particular, *DEPDC5*, *SCN1A*, and *SCN8A* are involved in SUDEP. For data analysis, the Torrent Suite (v 5.12.3, TFS), the Integrative Genomics Viewer tool, the Alamut® Visual Plus software (v 1.9), and the Human Gene Mutation Database (HGMD) were used. We validated the NGS variants through Sanger sequencing as a gold-standard technique.

3. Results

The extraction methods used with FFPE heart tissue turned out to be quite efficient, since the concentration of DNA was higher than 0.67 ng/µL, as required for library preparation. Results collected by Qubit® and Real-Time PCR by Plexor® HY System are displayed in Table 1.

Table 1. Results of quantification by Qubit® and real-time PCR by Plexor® HY System.

Sample Name	Starting Material	C (ng/µL) by Qubit	C (ng/µL) by Real Time-PCR
Sample 1	10 slices of FFPE		0.7
Sample 2	5 slices of FFPE		1.2
Sample 3	8 slices of FFPE		5.7
Sample 4	200 µL of blood	27.2	
Sample 5	200 µL of blood	18.0	

As expected, very low coverage of the target base was observed for FFPE tissue samples as a result of the complexity of the biological material and the elaborate DNA extraction method. The average base coverage depth and the target base coverage are shown in Table 2. We have adopted the following criteria to discriminate the variants in

this study: a total depth at position > 100X for blood samples and >30X for FFPE tissue samples; AF > 0.45 for heterozygous; SNP Strand Bias < 0.6.

Table 2. This table shows the coverage analysis resulting from the Ion Torrent Suite software. The coverage of the 3 FFPE tissue samples (1, 2, and 3) is very low compared to the coverage of whole blood samples (4 and 5). For the evaluation of variants, we considered 30X as the target base coverage for FFPE tissue-derived DNA and 100X for blood-derived DNA.

Sample Name	% Base Reads on Target	Average Base Coverage Depth	Target Base Coverage at 30X	Target Base Coverage at 100X
Sample 1	38.59%	14.52	7.81%	-
Sample 2	34.59%	6.696	3.47%	-
Sample 3	45.50%	10.63	5.60%	-
Sample 4	95.23%	399.1	99.12%	97.46%
Sample 5	83.49%	271.6	98.76%	93.21%

Samples were then analyzed and the variants noted through wANNOVAR; subsequently, they were interpreted with the use of bioinformatics tools such as ClinVar, LOVD, CardioClassifier, Revel, and Cadd (Table 3).

Table 3. Variants found in the epilepsy-related sudden unexpected death cases through NGS analysis, with the updated panel (103 genes).

Sample Name	Gene	Chr	Start	End	Ref	Alt	Clinical Significance *
Sample 3	*MYBPC3*	chr11	47369430	47369430	G	C	Conflicting classifications of pathogenicity **
Sample 4	*ANK2*	chr4	114269433	114269433	A	G	Conflicting classifications of pathogenicity **
	DSG2	chr18	29078136	29078136	C	G	Conflicting classifications of pathogenicity **
	DSP	chr6	7585967	7585967	G	C	Conflicting classifications of pathogenicity **
	HCN4	chr15	73616159	73616159	C	T	Conflicting classifications of pathogenicity **
	RYR2	chr1	237972204	237972204	G	A	Uncertain Significance
	SCN8A	chr12	52115597	52115597	C	T	Uncertain Significance
Sample 5	*AKAP9*	chr7	91645538	91645538	A	T	Uncertain Significance
	DSP	chr6	7585967	7585967	G	C	Conflicting classifications of pathogenicity **

* Bioinformatic tools used for variant interpretation: ClinVar, LOVD, CardioClassifier, Revel, and Cadd (analysis was performed in August 2025). ** Conflicting classifications of pathogenicity refer to situations where the same genetic variant is described differently (e.g., as pathogenic or benign) by different experts or databases, leading to confusion about its potential to cause disease.

All the variants collected in Table 3 are different from each other; none of the samples share the same variants. Therefore, it is very difficult to make assumptions or draw conclusions for a diagnosis of SUDEP, since this does not allow us to define a typical genotype of an SUDEP case.

In particular, in Table 4, we have collected the variants with a relevant clinical significance possibly correlated to the cause of death. In detail, sample 4 resulted in two variants of unknown significance (VUS) on genes *RYR2* and *SCN8A*. Sample 5 resulted in one VUS on the *AKAP9* gene. All three variants are missense, and the variant allele frequency is shown in Table 4. Deepening the molecular significance of these three variants on gnomAD, we con-

cluded that the VUS on the *AKAP9* (NM_005751.5(AKAP9):c.3708A>T) gene is benign, the VUS on *SCN8A* (NM_001330260.2(SCN8A):c.1903C>T) is possibly damaging but predicted as tolerated, and, most interestingly, the VUS on *RYR2* (NM_001035.3(RYR2):c.14302G>A) is indicated as possibly damaging, with consequences on cardiovascular phenotype. All variants were confirmed by Sanger sequencing.

Table 4. A summary of the results of the analyses performed through IGV (Integrative Genome Viewer) and wANNOVAR. For FFPE tissue samples (1, 2, and 3), no variants of relevant clinical significance were observed. The interpretation of the variants followed the ACMG-AMP guidelines. MutationT@ster 2025 predicted the function of modified proteins.

Sample Name	Gene Region	dbSNP	Population Allele Frequency *	ACMG-AMP Classification	MutationT@ster 2025 Protein Function Prediction	Features of Protein at a Glance
Sample 4	NM_001035.3(RYR2):c.14302G>A p.(Val4768Ile)	rs775534249	0%	VUS: PM1 PM2 PP3	Deleterious	Amino acid sequence changed Protein features (might be) affected
	NM_001330260.2(SCN8A):c.1903C>T p.(Arg635Cys)	rs749983172	0%	VUS: PM2 PP2 BP4	Deleterious	Amino acid sequence changed Protein features (might be) affected
Sample 5	NM_005751.5(AKAP9):c.3708A>T p.(Glu1236Asp)	rs751002727	0.000036%	VUS: BP4 BP1 BP3 PM2	Undetermined/Benign	Amino acid sequence changed Protein features (might be) affected

* Population allele frequency from gnomAD genome.

4. Discussion

Performing a molecular autopsy on cases of SUDEP was challenging. The main limitation was the small cohort of SUDEP cases due to the rarity of the phenomenon. Hence, to try to broaden the case cohort, we also included in the study FFPE tissue samples from SUDEP cases collected in the past. We have developed a new method of DNA extraction from this complex biological matrix, despite knowing the low coverage in FFPE-derived DNA in NGS analysis. Complying with the results shown in this article, we assume that the choice of FFPE tissue samples prevented a well-conducted genetic analysis. This is due to the presence of formalin, which highly degrades the DNA molecule, leading to its fragmentation and the formation of cross-links. More recently, there has been a growing interest in extracting DNA from FFPE samples for genetic analysis. However, attempting to prepare DNA libraries for NGS from FFPE samples can be particularly challenging due to the effects of formalin fixation and paraffin embedding on the quality of DNA. The DNA extraction method shown in this article was found to be effective, accurate, and fast as a semi-automated method. Some strategies could be worked out from the beginning to overcome some issues, such as following some recommendations on FFPE tissue preparation. In particular, it has been demonstrated that after one day of formalin fixation, the level of DNA fragmentation and formation of cross-links increases in FFPE tissues [11]. Other strategies could be adopted to overcome FFPE tissue problems, such as using optimized pre-treatments like antigen retrieval and deparaffinization, as well as employing specialized extraction kits and technologies to enhance nucleic acid recovery and reduce degradation. The DNA extraction method by the Casework kit, described in this article, allows a reduction in the number of steps and therefore the risk that the different reagents could further degrade the DNA. For these reasons, FFPE tissue samples are usually more prone to errors and false positive variants in NGS analysis. Moreover, false negatives may occur due to the low coverage in FFPE-derived DNA. Therefore, the presence of additional significant variants in non-amplified regions in samples 1, 2, and 3

cannot be excluded. We can infer that for an NGS analysis, it would be better to use blood as a starting biological material in order to have a higher coverage of the target regions. In fact, blood samples 4 and 5 result in a higher coverage analysis. This allowed us to make a more thorough and complete analysis of the whole gene panel, leading to three VUS. The key variants found through NGS analysis and the clinical context of each case are displayed in Supplementary Table S2.

The variant NM_001035.3(RYR2):c.14302G>A in sample 4 was previously discussed in the literature [12–14] and classified as a VUS specifically involved in cardiac disease, such as cardiomyopathy [13] and catecholaminergic polymorphic ventricular tachycardia (CPVT) [12,13]. The deceased individual 4 had cardiomyopathy, and this VUS could explain the clinical picture. In particular, the *RYR2* gene encodes the cardiac ryanodine receptor 2 (RyR2), a major component of RyR2 channels, which mediate calcium release from the sarcoplasmic reticulum into the cytosol upon cell membrane depolarization. Defective closure of RyR2 channels results in intracellular calcium leakage, which leads to increased potential for delayed after-depolarizations and subsequent ventricular tachycardia. Mutations in the *RYR2* gene could lead to the most common form of CPVT. As suggested by the literature, *RYR2* mutations could lead to epilepsy and heart disease and are potentially associated with SUDEP [15]. The effect of the variant on protein function is classified as "Uncertain" in the MutationT@ster prediction tool, referring to the fact that the amino acid sequence change might affect the protein features. On Mutation Assessor, this variant has benign support.

The second variant, NM_001330260.2(SCN8A):c.1903C>T, in sample 4, is mentioned in the literature in one case of early infantile epileptic encephalopathy (early-infantile DEE) [14], a neurological disorder characterized by recurring seizures presenting within the first three months of life, progressive cerebral dysfunction, and low electrical brain activity interspersed with bursts of high spiked activity [16]. On MutationT@ster, the variant causes a deleterious protein with an uncertain prediction about the function. On Mutation Assessor, the variant is considered as benign moderate.

The variant NM_005751.5(AKAP9):c.3708A>T, in sample 5, was observed in the literature in Long QT Syndrome and Romano-Ward Syndrome [13], two inherited cardiac diseases that can be correlated with sudden death. Individual 5 was a young woman suffering from epilepsy and in drug treatment and was found lying on the floor of her apartment. Cardiac disease cannot be excluded. Referring to the prediction tools used, MutationT@ster classified the variant as undetermined/benign on the function of the protein, showing an uncertain prediction between different studies in the tool itself.

The three VUS found in this study raise another major problem in genetic analyses. These variants are, in fact, rare and still hold uncertain significance, often because they are related to scarce and poorly studied pathologies or phenomena. These variants need to be interpreted in further studies, since their significance is not certain. Functional tools show different interpretations as well. In order to interpret the correlation between the variant and the pathology in silico, a study is not sufficient; however, it could be suitable to perform experimental in vitro studies, such as RNA-sequencing and functional analysis [17].

5. Conclusions

In conclusion, for future studies, we would expand the cohort through multicenter collaborations and integrate genetic data with clinical information to improve interpretation and the genotype-phenotype correlation [18]. To increase the reliability of genetic analyses, we would suggest using the appropriate starting biological material to conduct an NGS analysis, i.e., whole blood rather than FFPE tissue, if available. However, the

DNA extraction protocol for FFPE tissue samples used in this study showed good results considering the type of biological matrix. The Casework kit (Promega) is usually used for challenging casework samples, such as in forensic analysis, and it proved adequate for the FFPE samples, too.

Moreover, the NGS custom gene panel may be updated in the future with other genes involved in cardiac disease and SUDEP, detecting additional significant variants if present. Further information on the found VUS in samples 4 and 5 will be provided in the future when functional studies will be conducted, bearing in mind that the interpretation of the found variants requires studies by a multidisciplinary team, including geneticists and clinical and forensic pathologists. It is also essential to perform a careful evaluation of the pathogenicity of the detected gene variants, and the combination of clinical information, pathological examination, and genetic testing through NGS can become a valid approach for SUDEP diagnosis, even in the absence of clinical appearance or typical gross pathology suggesting advanced inherited heart diseases [19].

Although silico instruments predict the possible pathogenicity and classification of some variants, they should not be used as the sole source of evidence to make a clinical assertion [9]. To ascertain the pathogenicity of the variants, studies on larger cohorts will be required. However, collecting a high number of SUDEP cases is a challenge due to the rarity of the event in the population. Molecular autopsy must become an inherent part of the post-mortem examination in cases classified as SUDEP. To date, molecular autopsy is not considered a routine examination, although recommended, which is why many pathologies, such as SUDEP, are underestimated. Moreover, this routine forensic practice should be combined with other clinical evaluations by a neuropathologist or cardiac pathologist for a more comprehensive clinical picture of SUDEP [18,20]. The molecular autopsy not only represents a diagnostic test to ascertain the causes of death of a deceased subject, but is also fundamental for the victim's family members. Genetic testing could also be performed for family members, who may be at-risk carriers of fatal cardiac disorders. A good interpretation of variants could help to identify the diagnosis or prognosis, preventing sudden death, including the avoidance of medications that may prolong the QT interval, taking antiarrhythmic drugs such as beta-blockers, and prophylactic interventions for possible lethal cardiac arrhythmias, such as implantable cardioverter defibrillators [8]. To best manage families, close interdisciplinary collaboration is essential [9].

Supplementary Materials: The following supporting information can be downloaded at https://www.mdpi.com/article/10.3390/genes16111272/s1: Table S1: The list of genes present in the updated panel used for analysis of samples 3, 4, and 5. A total of 103 genes (V2) were collected; 97 were also present in the past custom gene panel (V1). The genes added to the latest version were *DEPDC5*, *DTNA*, *GAA*, *PTPN11*, *SCN1A*, and *SCN8A*. In particular, *DEPDC5*, *SCN1A*, and *SCN8A* are involved in SUDEP. Table S2: Case Summary Table. It summarizes the most relevant findings (key variants and the clinical significance). V1: Gene Panel version 1 (97 genes), V2: Gene Panel version 2 (103 genes).

Author Contributions: Conceptualization, A.B.D.M., C.T. and M.P. (Mauro Pesaresi); methodology, A.B.D.M., F.M., L.F. and E.C.; software, V.O.; formal analysis, V.O.; investigation, C.T. and M.P. (Mauro Pesaresi); resources, M.P. (Marco Palpacelli), S.S. and M.P. (Mauro Pesaresi); data curation, V.O.; writing—original draft preparation, A.B.D.M.; writing—review and editing, F.M., L.F., E.C. and C.T.; visualization, M.P. (Mauro Pesaresi); supervision, C.T. and M.P. (Mauro Pesaresi); project administration, M.P. (Mauro Pesaresi); funding acquisition, C.T. All authors have read and agreed to the published version of the manuscript.

Funding: This research has received funding from the project Heal Italia—Project Code PE00000019, CUP I33C22006900006—funded under the National Recovery and Resilience Plan (NRRP), Mission 4 Component 2 Investment 1.3—Creation of "Extended Partnerships with Universities, Research Centers, and Companies for the Funding of Basic Research Projects"—Project "Health Extended Alliance for Innovative Therapies, Advanced Lab Research, and Integrated Approaches of Precision Medicine (HEAL ITALIA)" Call for tender No. 341 of 15 March 2022, and Concession Decree No. 0001559.11-10-2022 of Italian Ministry of University funded by the European Union—NextGenerationEU.

Institutional Review Board Statement: International ethical guidelines do not consider research on deceased individuals to be human-subject research requiring IRB/ethical approval. For these reasons, our institution did not require an ethics committee review or informed consent for this retrospective study on cadaveric specimens. However, we have ensured compliance with all relevant legal and ethical standards for handling human biological materials.

Informed Consent Statement: Ethical approval was not required for this study as it involved only deceased individuals and anonymized retrospective data. This study was conducted on tissue samples derived from judicial autopsies (forensic post-mortem examinations) carried out under authorization of the competent legal authority. According to Italian regulations, research involving exclusively cadaveric samples does not require approval by an ethics committee or informed consent, since no living human subjects are involved. In Italy, forensic autopsies are governed by the code of criminal procedure, which allows tissue sampling for investigative purposes without any family consent. The subsequent use of such autopsy-derived samples for scientific research is legally permissible as long as it complies with applicable laws. Moreover, all samples in our study were completely anonymized, and thus no person-identifiable information was used.

Data Availability Statement: The original contributions presented in this study are included in the article/Supplementary Materials. Further inquiries can be directed to the corresponding author.

Conflicts of Interest: The authors declare no conflicts of interest.

Abbreviations

The following abbreviations are used in this manuscript:

SUDEP	Sudden, Unexpected Death of Someone with Epilepsy
LQTS	Long QT Syndrome
NGS	Next-Generation Sequencing
FFPE	Formalin-Fixed Paraffin-Embedded
VUS	Variant of Unknown Significance
CPVT	Catecholaminergic Polymorphic Ventricular Tachycardia
IGV	Integrative Genome Viewer
Early-Infantile DEE	Early Infantile Epileptic Encephalopathy

References

1. Nashef, L. Sudden Unexpected Death in Epilepsy: Terminology and Definitions. *Epilepsia* **1997**, *38*, S6–S8. [CrossRef] [PubMed]
2. Sveinsson, O.; Andersson, T.; Carlsson, S.; Tomson, T. The Incidence of SUDEP. *Neurology* **2017**, *89*, 170–177. [CrossRef]
3. Nashef, L.; So, E.L.; Ryvlin, P.; Tomson, T. Unifying the Definitions of Sudden Unexpected Death in Epilepsy. *Epilepsia* **2011**, *53*, 227–233. [CrossRef]
4. Pathak, S.J.; Yousaf, M.I.K.; Shah, V.B. Sudden Unexpected Death in Epilepsy. Available online: https://www.ncbi.nlm.nih.gov/books/NBK559104 (accessed on 7 October 2025).
5. Harden, C.; Tomson, T.; Gloss, D.; Buchhalter, J.; Cross, J.H.; Donner, E.; French, J.A.; Gil-Nagel, A.; Hesdorffer, D.C.; Smithson, W.H.; et al. Practice Guideline Summary: Sudden Unexpected Death in Epilepsy Incidence Rates and Risk Factors: Report of the Guideline Development, Dissemination, and Implementation Subcommittee of the American Academy of Neurology and the American Epilepsy Society. *Epilepsy Curr.* **2017**, *17*, 180–187. [CrossRef]
6. Ruthirago, D.; Julayanont, P.; Karukote, A.; Shehabeldin, M.; Nugent, K. Sudden Unexpected Death in Epilepsy: Ongoing Challenges in Finding Mechanisms and Prevention. *Int. J. Neurosci.* **2018**, *128*, 1052–1060. [CrossRef]

7. Bagnall, R.D.; Crompton, D.E.; Semsarian, C. Genetic Basis of Sudden Unexpected Death in Epilepsy. *Front. Neurol.* **2017**, *8*, 348. [CrossRef] [PubMed]
8. Bagnall, R.D.; Ingles, J.; Yeates, L.; Berkovic, S.F.; Semsarian, C. Exome Sequencing–Based Molecular Autopsy of Formalin-Fixed Paraffin-Embedded Tissue after Sudden Death. *Genet. Med.* **2017**, *19*, 1127–1133. [CrossRef]
9. Coll, M.; Oliva, A.; Grassi, S.; Brugada, R.; Campuzano, O. Update on the Genetic Basis of Sudden Unexpected Death in Epilepsy. *Int. J. Mol. Sci.* **2019**, *20*, 1979. [CrossRef]
10. Bagnall, R.D.; Crompton, D.E.; Petrovski, S.; Lam, L.; Cutmore, C.; Garry, S.I.; Sadleir, L.G.; Dibbens, L.M.; Cairns, A.; Kivity, S.; et al. Exome-Based Analysis of Cardiac Arrhythmia, Respiratory Control, and Epilepsy Genes in Sudden Unexpected Death in Epilepsy. *Ann. Neurol.* **2016**, *79*, 522–534. [CrossRef]
11. Turashvili, G.; Yang, W.; McKinney, S.; Kalloger, S.; Gale, N.; Ng, Y.; Chow, K.; Bell, L.; Lorette, J.; Carrier, M.; et al. Nucleic Acid Quantity and Quality from Paraffin Blocks: Defining Optimal Fixation, Processing and DNA/RNA Extraction Techniques. *Exp. Mol. Pathol.* **2012**, *92*, 33–43. [CrossRef]
12. Richards, S.; Aziz, N.; Bale, S.; Bick, D.; Das, S.; Gastier-Foster, J.; Grody, W.W.; Hegde, M.; Lyon, E.; Spector, E.; et al. Standards and Guidelines for the Interpretation of Sequence Variants: A Joint Consensus Recommendation of the American College of Medical Genetics and Genomics and the Association for Molecular Pathology. *Genet. Med. Off. J. Am. Coll. Med. Genet.* **2015**, *17*, 405–424. [CrossRef]
13. Nykamp, K.; Anderson, M.; Powers, M.; Garcia, J.; Herrera, B.; Ho, Y.-Y.; Kobayashi, Y.; Patil, N.; Thusberg, J.; Westbrook, M.; et al. Sherloc: A Comprehensive Refinement of the ACMG–AMP Variant Classification Criteria. *Genet. Med.* **2017**, *19*, 1105–1117. [CrossRef] [PubMed]
14. Sarquella-Brugada, G.; Fernandez-Falgueras, A.; Cesar, S.; Arbelo, E.; Coll, M.; Perez-Serra, A.; Puigmulé, M.; Iglesias, A.; Alcalde, M.; Vallverdú-Prats, M.; et al. Clinical Impact of Rare Variants Associated with Inherited Channelopathies: A 5-Year Update. *Human Genet.* **2021**, *141*, 1579–1589. [CrossRef] [PubMed]
15. Ma, M.-G.; Liu, X.-R.; Wu, Y.; Wang, J.; Li, B.-M.; Shi, Y.-W.; Su, T.; Li, B.; Liu, D.-T.; Yi, Y.-H.; et al. RYR2 Mutations Are Associated with Benign Epilepsy of Childhood with Centrotemporal Spikes with or without Arrhythmia. *Front. Neurosci.* **2021**, *15*, 629610. [CrossRef] [PubMed]
16. Zuberi, S.M.; Wirrell, E.; Yozawitz, E.; Wilmshurst, J.M.; Specchio, N.; Riney, K.; Pressler, R.; Auvin, S.; Samia, P.; Hirsch, E.; et al. ILAE Classification and Definition of Epilepsy Syndromes with Onset in Neonates and Infants: Position Statement by the ILAE Task Force on Nosology and Definitions. *Epilepsia* **2022**, *63*, 1349–1397. [CrossRef] [PubMed]
17. Pesaresi, M.; Bernini Di Michele, A.; Melchionda, F.; Valerio, O.; Alessandrini, F.; Turchi, C. Sudden Cardiac Death and Channelopathies: What Lies behind the Clinical Significance of Rare Splice-Site Alterations in the Genes Involved? *Genes* **2024**, *15*, 1272. [CrossRef] [PubMed]
18. Whitney, R.; Sharma, S.; Jones, K.C.; RamachandranNair, R. Genetics and SUDEP: Challenges and Future Directions. *Seizure* **2023**, *110*, 188–193. [CrossRef] [PubMed]
19. Hata, Y.; Yoshida, K.; Kinoshita, K.; Nishida, N. Epilepsy-Related Sudden Unexpected Death: Targeted Molecular Analysis of Inherited Heart Disease Genes Using Next-Generation DNA Sequencing. *Brain Pathol.* **2016**, *27*, 292–304. [CrossRef] [PubMed]
20. Middleton, O.; Atherton, D.S.; Bundock, E.A.; Donner, E.J.; Friedman, D.; Hesdorffer, D.C.; Jarrell, H.S.; McCrillis, A.; Mena, O.J.; Morey, M.; et al. National Association of Medical Examiners Position Paper: Recommendations for the Investigation and Certification of Deaths in People with Epilepsy. *Epilepsia* **2018**, *59*, 530–543. [CrossRef] [PubMed]

genes

MDPI

Article

Forensic DNA Recovery from FFPE Tissue Using the Maxwell® RSC Xcelerate Kit: Optimization, Challenges, and Limitations

Dagmara Lisman [1,*], Andrzej Ossowski [1], Aleksandra Tołoczko-Grabarek [2], Mateusz Kozłowski [3] and Aneta Cymbaluk-Płoska [3]

[1] Department of Genomic and Forensic Genetics, Pomeranian Medical University in Szczecin, 70-111 Szczecin, Poland; andrzej.ossowski@pum.edu.pl
[2] Department of Pathomorphology, Pomeranian Medical University in Szczecin, University Clinical Hospital No. 2 in Szczecin, 70-111 Szczecin, Poland; aleksandra.toloczko.grabarek@pum.edu.pl
[3] Department of Reconstructive and Oncological Gynecology, Pomeranian Medical University in Szczecin, 70-111 Szczecin, Poland; mateusz.kozlowski@pum.edu.pl (M.K.); aneta.cymbaluk.ploska@pum.edu.pl (A.C.-P.)
* Correspondence: dagmara.lisman@pum.edu.pl

Abstract: Background/Objectives: Obtaining reliable DNA profiles from archival tissue preserved as formalin-fixed, paraffin-embedded (FFPE) samples remains a major challenge in both forensic and medical evaluations. The quality of DNA isolated from FFPE material is frequently compromised due to formalin-induced fragmentation and chemical modifications. These limitations are particularly relevant in cases of suspected medical malpractice related to cancer diagnosis or treatment, where retrospective molecular analyses may provide critical evidence. The aim of this study was to evaluate the performance of the Maxwell® RSC Xcelerate DNA FFPE Kit (Promega) in generating DNA profiles from archival FFPE tissue blocks of endometrial cancer and to identify the limitations associated with this approach. **Methods:** Archival FFPE blocks of endometrial cancer were analyzed using the Maxwell® RSC Xcelerate DNA FFPE Kit. DNA yield, purity, and degradation indices were assessed using standard real-time PCR-based quantification methods. Short tandem repeat (STR) profiling was performed with forensic genotyping kits, and the completeness, allele balance, and reliability of obtained profiles were evaluated. The obtained results were compared with reference quality thresholds commonly used in forensic practice. **Results:** The Maxwell® RSC Xcelerate Kit allowed for recovery of relatively high DNA yields with consistently low degradation indices, confirming good extraction efficiency from FFPE samples. Nevertheless, despite favorable quantitative values, the generation of complete STR profiles was often unsuccessful. Partial or incomplete profiles were frequent, characterized by allele dropout and imbalance, which substantially reduced their evidentiary value. These findings suggest that DNA fragmentation and fixation-related artifacts impair amplification efficiency and limit the usefulness of STR analysis. **Conclusions:** This study emphasizes the persistent challenges of DNA profiling from FFPE tissue in forensic-medical contexts. Although the Maxwell® RSC Xcelerate Kit demonstrated effective DNA recovery, the ability to generate complete and interpretable STR profiles remained limited. Further refinement of extraction protocols, as well as improved interpretative strategies, are required to enhance the reliability and evidentiary significance of molecular analyses based on archival FFPE material.

Keywords: formalin-fixed paraffin-embedded (FFPE); DNA degradation; short tandem repeats (STR); forensic genetics; DNA extraction

1. Introduction

Embedding tissues in paraffin (FFPE—Formalin-Fixed, Paraffin-Embedded) is the standard method for preparing histopathological samples, particularly in cancer diagnostics. One of the main objectives of this process is to preserve the tissue architecture and cellular morphology [1]. In routine histopathological procedures, the most commonly used fixative is 10% neutral-buffered formalin (NBF), which corresponds to a 4% aqueous solution of formaldehyde. Buffering, most often phosphate-based, ensures a neutral pH of around 7.0 [2]. In specialized studies, alternative variants of formalin may also be used, for example: 4% formaldehyde in PBS for immunohistochemistry, methacarn ("modified" formalin) for better preservation of lipid structures, or 4% paraformaldehyde (PFA) for molecular biology and electron microscopy. The choice of the fixative depends on the intended downstream application of the biological material [3].

Another reagent widely used in histopathological studies is paraffin. It stabilizes tissue structure, prevents morphological degradation, and enables long-term storage. Paraffin also protects tissues from mechanical damage—its hardened structure allows for precise sectioning of thin slices. Additionally, it minimizes structural alterations, ensuring that well-preserved tissues retain their cellular organization and histological details. An important aspect of paraffin embedding is the replacement of water and lipids—during embedding, tissues are dehydrated and infiltrated with paraffin, which stabilizes their structure. However, paraffin may also exert negative effects on tissues. It can cause cytoplasmic condensation, altering cellular appearance, and may contribute to DNA and RNA fragmentation, which complicates molecular analyses such as PCR or sequencing [4–6].

Formalin, on the other hand, preserves tissue by creating cross-links between proteins, preventing autolysis (self-destruction of cells) and tissue degradation. Paraffin complements this process by stabilizing tissue architecture, thereby allowing precise sectioning of ultrathin slices with a microtome for microscopic analysis. FFPE tissues are the gold standard in cancer diagnostics, enabling both classification and assessment of tumor aggressiveness [3,7,8]. Such preserved tissues can be stored for many years, allowing their re-analysis if needed, for example, in the context of additional genetic or immunohistochemical tests. This long-term stability is also crucial for retrospective studies, biomarker discovery, and clinical research [8,9].

The process of tissue fixation induces a series of chemical changes that affect DNA quality and integrity. Formalin, a solution of formaldehyde, forms cross-linking bonds between proteins and nucleic acids, which hinders DNA extraction and amplification [3]. The formation of methylene bridges between nitrogenous bases results in DNA fragmentation, leading to difficulties in obtaining complete genetic profiles. Moreover, prolonged storage in formalin enhances hydrolytic processes, causing further degradation of genetic material [10].

After fixation in formalin, tissue samples are embedded in paraffin, which protects the specimen from external factors but at the same time may hinder efficient DNA recovery [11]. Incomplete removal of formalin before paraffin embedding can result in further DNA degradation and fragmentation. The paraffinization process may also stabilize unwanted chemical bonds, which additionally complicates DNA extraction and reduces the efficiency of PCR amplification. As a result, FFPE material is often characterized by low amplification yield and an increased occurrence of artifacts in genetic analyses [12].

In forensic medicine and forensic genetics, FFPE tissues are used for identification analyses in situations where they constitute the only available biological material in criminal cases from many years ago, enabling examination even when other DNA sources have undergone degradation [13]. Post-mortem diagnostics also allow for the detection of

mutations associated with hereditary diseases, cancers, or other conditions that may have contributed to the cause of death. Their analysis can play a crucial role in cases involving medical malpractice, particularly when there is a need for a retrospective evaluation of the accuracy of a diagnosis, the applied treatment, or clinical decisions. This is especially important in assessing whether errors occurred during the preparation of histopathological samples, such as patient sample mix-ups or material contamination [14,15].

DNA can be recovered from formalin-fixed, paraffin-embedded (FFPE) tissues; however, the process is considerably more challenging than with fresh or frozen samples. Formalin induces DNA fragmentation and creates cross-links between proteins and nucleic acids, which can hinder both extraction and amplification. It leads to the formation of stable bonds between DNA and proteins, thereby reducing extraction efficiency [6,16]. In some cases, the amount of sample available may be small or insufficient to perform a complete analysis, requiring the use of optimized protocols, specialized extraction kits, and experienced laboratory personnel. FFPE preparations may also contain residual formalin, which introduces sequencing errors by generating mutational artifacts [17,18]. The short length of DNA fragments further limits the effectiveness of analytical methods, particularly those that rely on long amplicons, such as short tandem repeat (STR) analysis, commonly applied in forensic genetics. DNA quality in FFPE tissues is also strongly influenced by storage time and conditions; samples stored for many years often show additional degradation, which further complicates analysis [12,19].

Due to DNA degradation and potential histological artifacts, it is necessary to employ advanced analytical methods, such as molecular and immunohistochemical techniques [5]. A comprehensive evaluation requires an interdisciplinary approach, involving collaboration among pathologists, geneticists, and forensic experts. To minimize the inherent limitations of FFPE samples, various strategies have been developed to improve the quality of extracted DNA. One such strategy is the optimization of extraction procedures, including the use of protein-degrading enzymes (e.g., proteinase K) and modified DNA isolation protocols. Another is the use of amplification methods targeting small DNA fragments—such as short amplicon markers (miniSTRs)—which perform better with degraded DNA [5,20]. Next-generation sequencing (NGS) technologies also enable the analysis of highly degraded samples by employing specialized error-correction algorithms. Additionally, careful deparaffinization and limiting excessive exposure to formalin during sample preparation can improve DNA yield and quality [21].

There is a common misconception that the preparation of FFPE tissue completely destroys the DNA it contains. Nothing could be further from the truth. Although the DNA is certainly damaged and fragmented, it is not entirely lost. Formalin itself leads to the formation of methyl bridges and DNA crosslinking, which hinder subsequent isolation and analysis [22,23]. Prolonged fixation, combined with exposure to high temperatures during paraffin embedding, often results in chemical modifications of DNA, such as cytosine deamination to uracil, which may introduce sequencing errors [18,24]. This process also causes extensive crosslinking with proteins, further complicating the recovery of "pure" DNA.

Despite these limitations, FFPE tissues remain a viable source of DNA for identification studies, although the quality of the material is inherently restricted [13]. These protocols often include steps to reverse protein–DNA crosslinks while simultaneously shortening the extraction process. Enzymatic DNA repair, for example, through enzymes capable of reversing chemical modifications, can further enhance the quality of recovered DNA [18,20,25].

Another critical factor is avoiding excessively long fixation times in formalin (>24–48 h), which markedly increases DNA damage. The use of buffered formalin instead of unbuffered formalin also has a significant impact on DNA quality. Regular formalin is acidic (pH < 4),

leading to intense DNA degradation and higher rates of mutations, including cytosine-to-uracil deamination. Buffered formalin (commonly phosphate-buffered, pH ~ 7) stabilizes the environment, limiting hydrolysis and DNA fragmentation. Acidic conditions promote strong DNA–protein crosslinking, hindering subsequent extraction and increasing spontaneous DNA mutations (e.g., C > T transitions), which may interfere with genetic analyses. Buffered formalin reduces this process, allowing for the recovery of longer DNA fragments. DNA isolated from tissues fixed in buffered formalin may reach lengths of up to ~1 kb, compared to only 100–300 bp typically observed with unbuffered formalin. This substantially improves the usability of the material in molecular biology applications [3,18,26].

We have also observed these differences in our own molecular analyses. Material obtained from small regional hospitals, where unbuffered formalin was used for tissue fixation, consistently yielded inferior DNA results.

2. Material and Methods

The material used for the study consisted of FFPE tissues obtained from 25 patients diagnosed with advanced endometrial cancer. The material was collected during 2023/24. The study received approval from the Bioethics Committee of the Pomeranian Medical University (KB-006/49/2022 and KB/006/74/2024).

The studies are part of a project funded under the National Science Centre competition (grant number: 2024/08/X/NZ1/00695). All patients provided informed consent to participate in the study and for the scientific investigations resulting from this work.

The paraffin blocks were stored at room temperature for at least 30 min prior to sectioning (blocks that are too cold become brittle, while those that are too warm become soft). In cases of uneven block surfaces or oxidation, preliminary trimming was performed. The block was mounted on a microtome, ensuring that the cutting surface was perpendicular to the blade. Sections of 10 µm thickness were cut, as this is the standard thickness used for DNA analysis. Ten sections were placed into a sterile Eppendorf tube and stored at 4–8 °C until DNA isolation.

Archival FFPE blocks of endometrial cancer were obtained from the pathology archives. For each block, the exact archival time (years since fixation and embedding) was recorded in order to evaluate the potential effect of storage duration on DNA quality.

2.1. DNA Extraction

For all tumor samples, a minimum of 20% tumor cell content was required. Prior to DNA extraction, the percentage of tumor cells was assessed independently by two pathologists. The proportion of tumor cells was defined as the ratio of tumor cells to non-tumor cells, including normal stromal, epithelial, and lymphatic cells. Genomic DNA was extracted using the Maxwell® RSC Xcelerate DNA FFPE Kit (Promega, Mannheim, Germany).

The DNA isolation procedure using the Maxwell® RSC Xcelerate DNA FFPE Kit (Promega) is characterized by a high degree of automation, which significantly enhances both its efficiency and reproducibility. Following the initial sample preparation, including dewaxing and protease digestion, subsequent extraction steps are carried out in a fully automated manner on the Maxwell® RSC instrument. Samples are placed in single-use cartridges preloaded with the appropriate reagents, and running the dedicated program allows the isolation to be completed within approximately 30–60 min for up to 48 samples simultaneously. This technology considerably reduces manual handling time (hands-on time), while the resulting DNA isolates demonstrate high reproducibility and a lower risk of contamination compared to manual methods based on silica columns. Automated DNA isolation using the Maxwell® RSC Xcelerate DNA FFPE Kit therefore represents a fast, intuitive, and efficient solution, particularly suitable

for diagnostic and research laboratories where both high-quality nucleic acids and standardized analytical processes are essential.

2.2. DNA Quantification and Degradation Index

To assess the quality and quantity of DNA in the FFPE biological samples, the Quantifiler Trio DNA Quantification Kit (Thermo Fisher Scientific, Waltham, MA, USA) was used, following the manufacturer's protocol. This kit amplifies three target sequences: short fragments (80 bp)—total human DNA quantification, long fragments (214 bp)—DNA integrity assessment, and a sex marker (Y chromosome, 75 bp)—detection of male DNA. The Quantifiler Trio method is critical for the analysis of low-quality samples, such as those commonly encountered in forensic investigations, as it enables the optimal selection of subsequent analytical methods, including PCR or NGS.

The Degradation Index (DI) was calculated as the ratio of the quantity of long-fragment DNA to short-fragment DNA. A DI value > 1 indicates DNA fragmentation—the higher the value, the greater the degree of sample degradation.

2.3. STR Amplification

For amplification of Short Tandem Repeat (STR) markers, the GlobalFiler™ PCR Amplification Kit (Thermo Fisher Scientific, Waltham, MA, USA) was employed. This multiplex PCR kit allows for the simultaneous amplification of 24 STR markers and the sex-determining marker (amelogenin). Amplification was carried out according to the manufacturer's protocol. The GlobalFiler™ system enables the generation of DNA profiles even from low-quality and degraded samples, such as FFPE tissues. The method is characterized by high sensitivity, allowing amplification from as little as 0.1 ng of input DNA, while maintaining strong resistance to PCR inhibition.

2.4. Detection of PCR Products

Following amplification, the PCR products were separated by capillary electrophoresis on an Applied Biosystems 3500 Genetic Analyzer. Genetic profiles were analyzed and interpreted using GeneMapper™ ID-X Software v1.6 (Applied Biosystems, Foster City, CA, USA) with an analytical threshold of 100 RFU. Quality control measures included the evaluation of stutter peaks according to kit-specific thresholds GlobalFiler, (Thermo Fisher Scientific, Waltham, MA, USA), assessment of allele balance (heterozygote ratio 60:40), and identification of allele dropout. Negative controls were included in each run to monitor contamination.

3. Results

The chart (Figure 1) presents three key DNA quality parameters from FFPE samples:

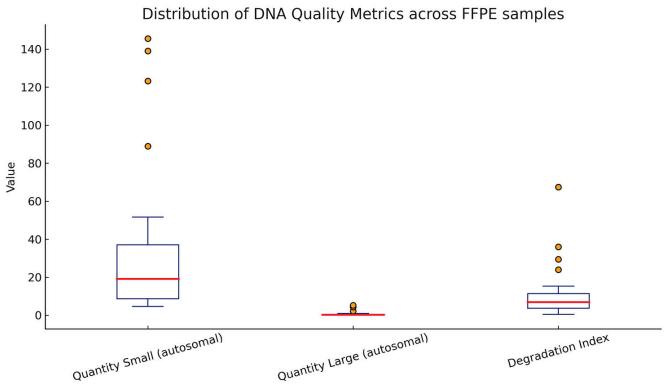

Figure 1. Distribution of degradation index and autosomal DNA quantities in FFPE samples.

Quantity Small (autosomal)—Values are relatively high, indicating that short DNA fragments amplify much better and are better preserved.

Quantity Large (autosomal)—Values are very low and scattered, confirming that long DNA fragments undergo degradation and have limited usefulness in STR analyses.

Degradation Index—the distribution is broad, with several outliers (>100), showing substantial variability in DNA quality among samples; a high DI indicates severe DNA degradation.

DNA from FFPE blocks is characterized by better amplification of short fragments, whereas longer ones are significantly degraded, which is reflected in high DI values.

3.1. Legend

IPC (Internal Positive Control): Ct values of ~27–28 are stable, indicating the absence of strong PCR inhibitors. This suggests that the issue is not inhibition but rather DNA degradation.

Large autosomal amplicon (~300 bp): very low DNA quantities (often <1 ng/μL).

Small autosomal amplicon (~80–100 bp): significantly higher DNA quantities in most samples.

Degradation Index (DI): calculated as the ratio of DNA quantity from the small amplicon to the large amplicon.

DI ~ 1–3 → DNA moderately preserved, full STR profiles are possible.

DI > 10 → DNA strongly degraded, only partial STR profiles expected.

DI > 50–100 → extreme degradation, requiring miniSTR or NGS target enrichment.

Samples with a low degradation index (DI 4–7) (Table 1) contained relatively well-preserved DNA, which makes it possible to obtain full or nearly full STR profiles, provided that the input material is sufficient.

Samples with a medium DI (15–40) (Table 1) indicated moderate DNA degradation. In such cases, there is a high probability of obtaining only partial STR profiles. Nonetheless, analysis is feasible, particularly when using markers with shorter amplicon lengths (miniSTRs) or alternatively SNP panels.

In contrast, samples with a very high DI ($\geq$80) (Table 1) exhibited severely degraded DNA. In these situations, conventional STR profiling usually fails or yields only trace results with a high risk of allele dropout. Therefore, advanced approaches such as miniSTRs, next-generation sequencing (NGS), or mitochondrial DNA analysis are required.

The results of DNA quantification from FFPE tissues demonstrated substantial quality limitations of the extracted genetic material. Elevated Degradation Index (DI) values, in some cases exceeding 100, clearly indicated a predominance of short DNA fragments accompanied by a pronounced scarcity of longer amplicons. These characteristics are typical for formalin-fixed, paraffin-embedded samples, in which DNA–protein cross-linking and fragmentation processes significantly compromise genomic integrity. Consequently, despite relatively high concentrations of short autosomal fragments, amplification of STR markers using the Global Filer kit was restricted to a limited number of loci with the shortest amplicons. The resulting STR profiles were therefore only partial and exhibited low evidential value. These findings suggest that in cases of severely degraded FFPE-derived DNA, alternative approaches such as mini-STRs, SNP panels, or mitochondrial DNA analysis, which rely on shorter amplicons, may provide more reliable and informative genetic data.

Table 1. Assessment of DNA concentration and Degradation Index (DI).

No.	Sample Name	Target Name	C_T Mean	Quantity Mean	Degradation Index
1	27338-23	T.IPC	27.28462982	-	-
	27338-23	T.Large Autosomal	28.03167725	0.191929743	51.59603119
	27338-23	T.Small Autosomal	23.33320999	9.902812958	51.59603119
2	780-24	T.IPC	27.39422417	-	-
	780-24	T.Large Autosomal	28.05417442	0.189387381	19.14279175
	780-24	T.Small Autosomal	24.87759399	3.625403166	19.14279175
3	24387-24	T.IPC	27.86660004	-	-
	24387-24	T.Large Autosomal	22.4848175	5.140621662	4.666538239
	24387-24	T.Small Autosomal	21.97338104	23.98890686	4.666538239
4	7622-23	T.IPC	27.42311668	-	-
	7622-23	T.Large Autosomal	26.39240265	0.507136106	18.29960823
	7622-23	T.Small Autosomal	23.43297958	9.280391693	18.29960823
5	47239-23	T.IPC	27.35767174	-	-
	47239-23	T.Large Autosomal	30.1026268	0.056239072	88.9747467
	47239-23	T.Small Autosomal	24.38232994	5.003857136	88.9747467
6	15330-24	T.IPC	27.6943512	-	-
	15330-24	T.Large Autosomal	25.44915199	0.887025833	5.82336092
	15330-24	T.Small Autosomal	24.33347511	5.165471554	5.82336092
7	27577-24	T.IPC	27.62685204	-	-
	27577-24	T.Large Autosomal	26.77074432	0.405258179	16.854599
	27577-24	T.Small Autosomal	23.90406418	6.830463886	16.854599
8	52934-23	T.IPC	27.72996712	-	-
	52934-23	T.Large Autosomal	31.37101936	0.026517242	23.76406479
	52934-23	T.Small Autosomal	27.56682968	0.630157471	23.76406479
9	816-24	T.IPC	27.65239334	-	-
	816-24	T.Large Autosomal	28.73755455	0.126309276	8.61333847
	816-24	T.Small Autosomal	26.72755241	1.087944508	8.61333847
10	2104-24	T.IPC	27.51393509	-	-
	2104-24	T.Large Autosomal	26.5255928	0.468639314	5.778486252
	2104-24	T.Small Autosomal	25.32598495	2.708025932	5.778486252
11	31954-23	T.IPC	27.62247467	-	-
	31954-23	T.Large Autosomal	27.56675911	0.252825886	36.40428925
	31954-23	T.Small Autosomal	23.44569206	9.203947067	36.40428925
12	3445-23	T.IPC	27.84559059	-	-
	3445-23	T.Large Autosomal	23.90898895	2.21006608	5.168225765
	3445-23	T.Small Autosomal	23.1138401	11.42212009	5.168225765
13	17486-24	T.IPC	28.19722366	-	-
	17486-24	T.Large Autosomal	31.04796028	0.032113694	15.91148281
	17486-24	T.Small Autosomal	27.88903999	0.510976493	15.91148281

Table 1. *Cont.*

No.	Sample Name	Target Name	C_T Mean	Quantity Mean	Degradation Index
14	18670-23	T.IPC	27.39790535	-	-
	18670-23	T.Large Autosomal	26.94467926	0.365558952	41.77180481
	18670-23	T.Small Autosomal	22.66760635	15.27005672	41.77180481
15	6180-24	T.IPC	27.63027191	-	-
	6180-24	T.Large Autosomal	31.10833549	0.030984785	145.5412598
	6180-24	T.Small Autosomal	24.54218292	4.509564877	145.5412598
16	1834-24	T.IPC	27.69294167	-	-
	1834-24	T.Large Autosomal	29.10348129	0.101680651	139.039566
	1834-24	T.Small Autosomal	22.78603172	14.13763428	139.039566
17	1754-23	T.IPC	28.40914917	-	-
	1754-23	T.Large Autosomal	30.97937202	0.033446159	36.38529587
	1754-23	T.Small Autosomal	26.55533028	1.21694839	36.38529587
18	11857-24	T.IPC	27.78021049	-	-
	11857-24	T.Large Autosomal	27.37384796	0.283452809	34.22826004
	11857-24	T.Small Autosomal	23.36468124	9.702096939	34.22826004
19	43248-24	T.IPC	28.07854462	-	-
	43248-24	T.Large Autosomal	29.62934685	0.074450895	37.04236221
	43248-24	T.Small Autosomal	25.29797173	2.757837057	37.04236221
20	6288-23	T.IPC	27.88058853	-	-
	6288-23	T.Large Autosomal	22.76756859	4.347402096	6.776962757
	6288-23	T.Small Autosomal	21.65751839	29.462183	6.776962757
21	5700-24	T.IPC	27.52523613	-	-
	5700-24	T.Large Autosomal	29.39518356	0.085535869	123.2788162
	5700-24	T.Small Autosomal	23.23667526	10.5447607	123.2788162
22	10623-24	T.IPC	27.41611862	-	-
	10623-24	T.Large Autosomal	26.42856407	0.496381819	13.13532639
	10623-24	T.Small Autosomal	23.97552681	6.52013731	13.13532639
23	55986-23	T.IPC	27.56273079	-	-
	55986-23	T.Large Autosomal	27.26762962	0.301872462	20.58268166
	55986-23	T.Small Autosomal	24.0496006	6.213344574	20.58268166
24	4415-24	T.IPC	27.99567986	-	-
	4415-24	T.Large Autosomal	22.76561165	4.352447987	8.263043404
	4415-24	T.Small Autosomal	21.35101891	35.96446609	8.263043404
25	15233-24	T.IPC	28.12033653	-	-
	15233-24	T.Large Autosomal	22.47094536	5.183064461	13.0022049
	15233-24	T.Small Autosomal	20.38585472	67.39126587	13.0022049

3.2. Forensic Relevance

In the case of samples with a low degradation index (DI), it is possible to obtain complete STR profiles that are fully compatible with identification systems such as CODIS

and ESS [27–29]. Such profiles provide high discriminatory power and enable unambiguous personal identification as well as reliable database comparisons.

However, in severely degraded samples, conventional STR typing often fails due to allele dropout, preferential amplification of shorter loci, and reduced overall information content. In such cases, the application of modern SNP panels analyzed by next-generation sequencing (NGS) becomes essential. SNP markers offer significant advantages in the analysis of degraded DNA because they can be targeted with very short amplicons (60–100 bp), increasing the likelihood of successful amplification from fragmented material [30–32]. Moreover, SNPs provide additional utility in kinship testing and ancestry inference, expanding their forensic value beyond classical STR-based identification.

NGS further enhances this approach by allowing the simultaneous multiplexed analysis of hundreds to thousands of SNPs, combined with bioinformatic algorithms that correct for damage-induced artifacts typical of FFPE and other archival samples. This makes SNP/NGS-based analysis a powerful complementary strategy in forensic casework, especially when working with archival histopathological blocks or highly degraded biological material [33–36].

The number of detected STR alleles was compared across FFPE-derived DNA samples. The bar chart illustrates the allelic recovery per sample, highlighting differences in amplification success and the variability in STR profile completeness (Figure 2).

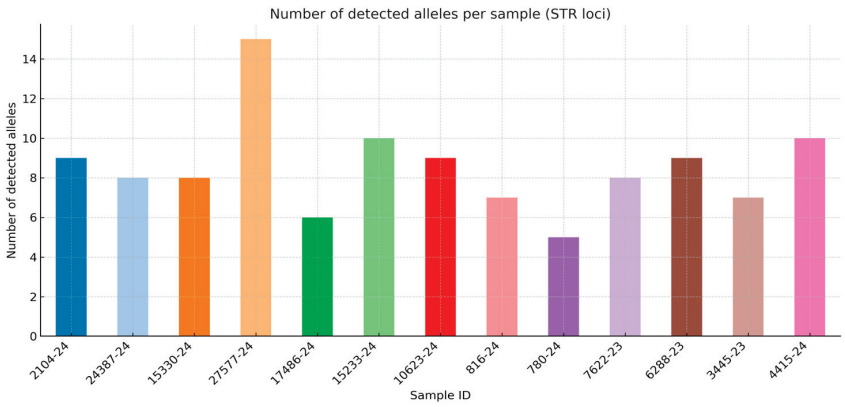

Figure 2. Number of successfully amplified STR alleles per FFPE sample.

The STR profiles obtained from the analyzed FFPE samples (Tables 2 and 3) exhibited considerable variability in terms of completeness and amplification quality.

Table 2. Results of amplification using the GlobalFiler individual identification system (Applied Biosystems).

Locus/Sample	2104-24	24387-24	15330-24	27577-24	17486-24	15233-24	10623-24
D3S1358	15,16	14,16	16,18	16,17	15,16	16,17	14,16
vWA	14,15	15,17	14,16	15,16	15,17	17,18	14,18
D16S539	13	-	-	12,13	-	13	-
CSF1PO	-	-	-	12,13	-	-	-
TPOX	-	-	-	8	-	12	-
INS/DEL	-	-	-	-	-	-	-
AMELO	XX	XX	XX	XX	XX	XX	XX
D8S1179	14,16	12,13	14,15	12,13,14,15	12,13	11,16	10,13
D21S11	30,30.2	29,31.2	28,29	31.2,33.2	-	30	32.2

Table 2. *Cont.*

Locus/Sample	2104-24	24387-24	15330-24	27577-24	17486-24	15233-24	10623-24
D18S51	15	16	19	13,14	-	14,15	-
DYS391	-	-	-	-	-	-	-
D2S441	10,14	10,11	11,14	11,13,14	11,14	14	10,14
D19S433	14,15.2	13,14	15	12,13	12,15	12,15	14,16
TH01	9.3	9.3	-	9.3	-	9,9.3	9,9.3
FGA	21,25	19	22	22,23	22	22	21
D22S1045	14,16	12,15	16	12,15	16	11	15
D5S818	9,10	10,12	11,12	9,11,12,13	12,13	12,13	12,13
D13S317	-	11	9,10	9,11	-	8,10	-
D7S820	8	9,10	9,11	7.3,10	-	-	10
SE33	-	24.2	-	14,20	-	-	-
D10S1248	14,16	15,17	13,16	13,17	12,13	14	14,15
D1S1656	13,14	12,14	12,17.3	-	16	15,17.3	16,17.3
D12S391	-	16,22	-	22	21	17.3,21	23
D2S1338	-	-	-	19	-	16	-
Locus/Sample	816-24	780-24	7622-23	6288-23	3445-23	4415-24	
D3S1358	14	13,16	15	15,18	15,17	16	
vWA	17	17	15,18	15,18	14,16	16,17	
D16S539	-	-	13	11	-	12	
CSF1PO	11	-	-	-	-	10,11	
TPOX	-	-	-	-	-	-	
INS/DEL	-	-	-	-	-	-	
AMELO	XX	XX	XX	XX	XX	XX	
D8S1179	10,12	10,14	10,13	13,14	10,14	10,14	
D21S11	29,32.2	-	30,32.2	29,30	33.2	29,31.2	
D18S51	16,17	-	-	13,15	16	-	
DYS391	-	-	-	-	-	-	
D2S441	10,11	10,14	11.3,14	10,11	10,11	10,11	
D19S433	13,15	14,15	15,16.2	12,16.2	14.2,15	14,15	
TH01	7,9.3	6	9.3	9	9.3	7,9	
FGA	22	23	23,24	20,21	24	21,22,23	
D22S1045	14,16	16	11,12	14,17	11,15	16,17	
D5S818	11,13	11,12	10,12	12,13	9,12	11,12	
D13S317	10,13	8,10	-	9,13	8,10	8,10	
D7S820	-	10	9	8,11	11	8,12	
SE33	-	-	-	-	-	29.2,30.2	
D10S1248	14,17	13,14	13,16	13,16	13,14	14,15	
D1S1656	18.3	14,16	16.3,17.3	11,17	13,15	14,16.3	
D12S391	-	-	20	18	17	-	
D2S1338	-	-	-	16	-	-	

Table 3. Summary of STR Profile Completeness—FFPE Samples.

Sample Name	Number of STR Loci	Profile Status	Recommendation
2104-24	18	Complete profile	Suitable for STR-based identification
24387-24	19	Complete profile	Suitable for STR-based identification
15330-24	17	Complete profile	Suitable for STR-based identification
27577-24	18	Complete profile	Suitable for STR-based identification
17486-24	16	Complete profile	Suitable for STR-based identification
15233-24	14	Partial profile	Potential identification, validation recommended
10623-24	17	Complete profile	Suitable for STR-based identification
816-24	10	Partial profile	Useful for exclusion or SNP comparison
780-24	9	Partial profile	Suitable for SNP or mtDNA analysis
7622-23	11	Partial profile	Applicable for kinship comparisons
3445-23	7	Fragmented profile	Re-isolation/miniSTR suggested
4415-24	6	Fragmented profile	Incomplete, mtDNA may be considered
6288-23	7	Fragmented profile	Unusable as is, consider SNP/mtDNA

Analysis of the STR profiles derived from FFPE material revealed substantial heterogeneity in both completeness and data quality. In some cases, relatively rich profiles were obtained, encompassing a dozen or more markers (e.g., 2104-24, 27577-24, 6288-23, 4415-24), which may be applicable in both individual identification and kinship analysis. However, in certain samples, the presence of more than two alleles in a single locus was observed (e.g., D8S1179 and D5S818 in sample 27577-24, FGA in sample 4415-24), which may reflect formalin-induced artifacts or indicate potential DNA mixtures.

A considerable number of samples yielded only partial profiles, with extensive allele dropout and single alleles present in heterozygous loci. Examples include samples in which the number of identified markers was very limited (e.g., 17486-24, 15233-24, 780-24, 3445-23). Such results considerably limit their usefulness for individual identification, but they may still provide supportive information in genealogical and kinship analyses.

In summary, STR profiles obtained from FFPE samples were, in most cases, fragmentary and burdened with interpretational uncertainty due to allele dropout and the occurrence of additional alleles. Only a few samples allowed for the generation of profiles with potential individual identification value. In forensic practice, such results are primarily applicable in kinship analyses. Full exploitation of FFPE-derived DNA requires alternative approaches, such as miniSTRs, SNP panels analyzed by next-generation sequencing (NGS), or mitochondrial DNA analysis, which are better suited for highly degraded genetic material.

For the remaining samples, no amplification of STR markers was obtained, which is fully consistent with the DNA quantification results. The elevated Degradation Index (DI) values indicated the presence of only short DNA fragments, with a near-complete absence of longer sequences required for amplification of STR loci. Consequently, despite PCR being performed under standard conditions, no detectable signals corresponding to genetic markers were observed, reflecting the insufficient quantity of intact DNA capable of successful amplification. These findings confirm that in cases of severely degraded FFPE-derived material, conventional STR systems may yield no informative results, and alternative approaches targeting shorter amplicons, such as mini-STRs, SNP panels, or mitochondrial DNA analysis, should be considered.

From a forensic perspective, STR profiles obtained from FFPE tissues carry limited value for direct individual identification. Complete profiles, suitable for database comparisons in CODIS or ESS, were achieved only in rare cases. More commonly, partial profiles were recorded, prone to interpretational errors associated with allele dropout, additional alleles, and low signal quality. Nevertheless, even fragmentary results may represent a valuable source of information in kinship analysis, especially when compared with profiles obtained from related individuals.

As mentioned above, FFPE material demonstrates significant limitations in conventional STR profiling, and its usefulness for individual identification remains restricted. Nevertheless, in forensic practice, such samples may still provide value in genealogical and kinship investigations, particularly when complemented by analytical strategies specifically designed for highly degraded DNA. Approaches employing reduced amplicon size or alternative genetic targets can mitigate the effects of fragmentation, thereby enhancing the reliability of the obtained results and supporting the interpretation of data derived from formalin-fixed tissues.

4. Discussion

DNA profiling from FFPE samples is associated with numerous challenges, including DNA degradation, low extraction efficiency, and potential sequencing artifacts. Nevertheless, the development of new technologies and analytical approaches, including the application of artificial intelligence and alternative techniques, opens up new possibilities for improving the quality and reliability of results obtained from this type of material.

Analysis of Short Tandem Repeats (STRs) from FFPE (formalin-fixed, paraffin-embedded) samples represents an important tool in forensic genetics [19], molecular diagnostics [37,38], retrospective studies [39], and personalized therapy selection [40]. Nevertheless, this type of biological material poses a number of analytical challenges, which are also evident in the obtained results.

In the analyzed profiles, frequent data loss was observed in certain loci (e.g., CSF1PO, TPOX, DYS391, D2S1338, SE33), reflecting DNA fragmentation and allelic dropout. This phenomenon, typical for degraded DNA, may lead to misinterpretation of heterozygotes as homozygotes. Irregular amplification in loci such as SE33 or FGA further highlights the challenges of working with FFPE-derived DNA. Despite these limitations, most samples yielded 10–12 informative loci, which remains sufficient for comparative and identification purposes, although optimization strategies (e.g., miniSTRs, repeated amplifications) are required to improve reliability.

Many researchers emphasize the problem of DNA degradation in FFPE samples. Comparative studies have shown that FFPE-derived DNA is of lower quality and shorter fragment length than cryopreserved samples, with significantly reduced yields [3,36]. Moreover, fixation-induced artifacts, such as cytosine deamination to thymine, can introduce sequencing errors and compromise data accuracy [22,41]. To address these challenges, novel approaches, including AI-assisted methods such as the SmartPath system, have been proposed to optimize tissue selection for macrodissection, thereby improving DNA recovery and sample purity [42].

The obtained results highlight the need for particular caution when interpreting STR profiles that include fewer than 15 loci. The literature indicates that as the number of recovered markers decreases, the discriminatory power of the profile is significantly reduced, while the risk of misinterpretation increases due to phenomena such as allele dropout, drop-in, or artifacts associated with DNA degradation [43]. Partial profiles, especially from degraded material, may still contain useful information; however, they

require complementary statistical analysis, such as calculating the Likelihood Ratio (LR) or the Combined Probability of Inclusion/Exclusion (CPI/CPE), which enables an objective assessment of the evidential value of the obtained data [44,45].

It should also be emphasized that despite numerous technical limitations and the risk of artifacts, FFPE tissues may represent the only available source of DNA in a range of forensic contexts. This is particularly relevant in cases of human identification, where archival histopathological samples may be the only preserved material [1]. In inheritance disputes, archival paraffin blocks can provide the sole means of obtaining the DNA profile of a deceased person in order to resolve questions of succession. Likewise, in cases of missing persons or suspected medical malpractice, FFPE material serves as a valuable source of information, enabling retrospective genetic analysis. Publications addressing the use of paraffin-embedded samples in forensic investigations clearly indicate that, despite the technical challenges associated with DNA degradation, this approach holds significant practical value and is increasingly supplemented with miniSTR, SNP, and next-generation sequencing (NGS) analyses. These complementary approaches allow for improved recovery of genetic information from highly degraded material, enhance the discriminatory power of partial profiles, and provide additional layers of evidence that can strengthen forensic and clinical interpretations, particularly in retrospective or otherwise challenging cases [4,8,35,46].

Despite its limitations, the forensic significance of FFPE tissues remains considerable—particularly in cases where no other sources of DNA are available. Modern approaches, such as miniSTR, qPCR, and Next Generation Sequencing, together with advances in bioinformatics, substantially improve the analysis of FFPE-derived DNA. These methods help to overcome the limitations associated with degradation and fragmentation, thereby increasing the reliability and evidential value of the results in forensic and clinical contexts.

Our study also demonstrates the practical advantages of the Maxwell® RSC Xcelerate DNA FFPE Kit. The system is automated, user-friendly, and time-efficient, enabling the simultaneous extraction of up to 48 samples. These features make it attractive for forensic and clinical laboratories that process larger sample sets, offering reproducibility and reduced risk of contamination compared to manual protocols.

In conclusion, while DNA from FFPE material remains technically challenging due to degradation and fixation artifacts, its forensic and clinical relevance is considerable—particularly when no other sources of DNA are available. The integration of modern approaches, including miniSTRs, qPCR, NGS, and bioinformatics pipelines, significantly improves the reliability and evidential value of FFPE-derived profiles. The tested automated extraction kit further enhances workflow efficiency, supporting its potential role in routine applications.

5. Conclusions

1. FFPE tissues can be effectively utilized in STR profiling; however, this requires a careful approach for result validation and protocol optimization. Critical steps include the use of optimized DNA extraction methods, quality assessment of DNA prior to PCR, and cautious interpretation of results due to potential dropout and artifact occurrence.
2. The utility of FFPE samples depends primarily on the degradation index (DI), the number of amplified loci, and DNA concentration. Samples with DI < 10 and a concentration > 5 ng/μL can be used for full STR analysis, whereas for samples with DI > 50, alternative approaches such as SNP analysis, miniSTR, or mtDNA analysis should be considered.

3. DNA profiling from FFPE tissues in forensic practice carries inherent risks due to DNA degradation, but it can still provide valuable information when no other sources are available.
4. Our study indicates that the Maxwell® RSC Xcelerate DNA FFPE Kit provides a convenient and efficient tool for DNA isolation from formalin-fixed, paraffin-embedded tissues. The automation of the process, the capacity to isolate up to 48 samples simultaneously, and high reproducibility make it an attractive solution for forensic and clinical laboratories, even though the obtained STR profiles are often partial and require careful interpretation.

Author Contributions: Conceptualization, D.L. and A.O.; methodology, D.L.; validation, D.L., A.C.-P. and A.T.-G.; formal analysis, A.O. and A.C.-P.; investigation, D.L.; resources, D.L., A.C.-P. and A.T.-G.; data curation, D.L., M.K., A.T.-G. and A.C.-P.; writing—original draft preparation, D.L.; writing—review and editing, D.L.; visualization, D.L.; project administration, D.L. and A.C.-P.; funding acquisition, D.L. All authors have read and agreed to the published version of the manuscript.

Funding: This research was funded by National Science Centre in Poland competition, grant number 2024/08/X/NZ1/00695.

Institutional Review Board Statement: The study was conducted in accordance with the Declaration of Helsinki and approved by the Institutional Review Board Pomeranian Medical University in Szczecin (KB-006/49/2022 and KB-006/74/2024, 16 November 2022).

Informed Consent Statement: Informed consent was obtained from all subjects involved in the study.

Data Availability Statement: The detailed data and electropherograms supporting the findings of this study are available from the corresponding author upon reasonable request (email: dagmara.lisman@pum.edu.pl).

Acknowledgments: The authors have reviewed and edited the output and take full responsibility for the content of this publication.

Conflicts of Interest: The authors declare no conflicts of interest. The funders had no role in the design of the study; in the collection, analyses, or interpretation of data; in the writing of the manuscript; or in the decision to publish the results.

References

1. Kassab, M.; Jehanzaib, M.; Başak, K.; Demir, D.; Keles, G.E.; Turan, M. FFPE++: Improving the quality of formalin-fixed paraffin-embedded tissue imaging via contrastive unpaired image-to-image translation. *Med. Image Anal.* **2024**, *91*, 102992. [CrossRef]
2. Snyder, J.M.; Radaelli, E.; Goeken, A.; Businga, T.; Boyden, A.W.; Karandikar, N.J.; Gibson-Corley, K.N. Perfusion with 10% neutral-buffered formalin is equivalent to 4% paraformaldehyde for histopathology and immunohistochemistry in a mouse model of experimental autoimmune encephalomyelitis. *Vet. Pathol.* **2022**, *59*, 498. [CrossRef] [PubMed]
3. Srinivasan, M.; Sedmak, D.; Jewell, S. Effect of Fixatives and Tissue Processing on the Content and Integrity of Nucleic Acids. *Am. J. Pathol.* **2002**, *161*, 1961–1971. [CrossRef]
4. Gilbert, M.T.P.; Haselkorn, T.; Bunce, M.; Sanchez, J.J.; Lucas, S.B.; Jewell, L.D.; Van Marck, E.; Worobey, M.; Volff, J.-N. The Isolation of Nucleic Acids from Fixed, Paraffin-Embedded Tissues–Which Methods Are Useful When? *PLoS ONE* **2007**, *2*, e537. [CrossRef]
5. Oba, U.; Kohashi, K.; Sangatsuda, Y.; Oda, Y.; Sonoda, K.-H.; Ohga, S.; Yoshimoto, K.; Arai, Y.; Yachida, S.; Shibata, T.; et al. An efficient procedure for the recovery of DNA from formalin-fixed paraffin-embedded tissue sections. *Biol. Methods Protoc.* **2022**, *7*, bpac014. [CrossRef]
6. Shi, S.-R.; Datar, R.; Liu, C.; Wu, L.; Zhang, Z.; Cote, R.J.; Taylor, C.R. DNA extraction from archival formalin-fixed, paraffin-embedded tissues: Heat-induced retrieval in alkaline solution. *Histochem. Cell Biol.* **2004**, *122*, 211–218. [CrossRef]
7. Thavarajah, R.; Mudimbaimannar, V.K.; Elizabeth, J.; Rao, U.K.; Ranganathan, K. Chemical and physical basics of routine formaldehyde fixation. *J. Oral Maxillofac. Pathol.* **2012**, *16*, 400. [CrossRef]

8. Likhithaswamy, H.R.; Madhushankari, G.S.; Selvamani, M.; Kumar, K.P.M.; Kokila, G.; Mahalakshmi, S. Assessing the quality of long-term stored tissues in formalin and in paraffin-embedded blocks for histopathological analysis. *J. Microsc. Ultrastruct.* **2022**, *10*, 23–29. [CrossRef] [PubMed]
9. Ludyga, N.; Grünwald, B.; Azimzadeh, O.; Englert, S.; Höfler, H.; Tapio, S.; Aubele, M. Nucleic acids from long-term preserved FFPE tissues are suitable for downstream analyses. *Virchows Arch.* **2012**, *460*, 131–140. [CrossRef] [PubMed]
10. Lu, K.; Ye, W.; Zhou, L.; Collins, L.B.; Chen, X.; Gold, A.; Ball, L.M.; Swenberg, J.A. Structural characterization of formaldehyde-induced cross-links between amino acids and deoxynucleosides and their oligomers. *J. Am. Chem. Soc.* **2010**, *132*, 3388–3399. [CrossRef]
11. Vitošević, K.; Todorović, M.; Slović, Ž.; Varljen, T.; Matić, S.; Todorović, D. DNA isolated from formalin-fixed paraffin-embedded healthy tissue after 30 years of storage can be used for forensic studies. *Forensic Sci. Med. Pathol.* **2021**, *17*, 47–57. [CrossRef]
12. Reid, K.M.; Maistry, S.; Ramesar, R.; Heathfield, L.J. A review of the optimisation of the use of formalin fixed paraffin embedded tissue for molecular analysis in a forensic post-mortem setting. *Forensic Sci. Int.* **2017**, *280*, 181–187. [CrossRef]
13. Ullah, S.; Garg, R.K.; Noor, F. DNA perspectives of fixed and paraffin embedded human tissues as resource materials for the identification. *Egypt. J. Forensic Sci.* **2017**, *7*, 23. [CrossRef]
14. A Alzahrani, S.; Alswaimil, N.F.; Alammari, A.M.; Al Saeed, W.H.; Menezes, R.G. Postmortem Genetic Testing in Sudden Unexpected Death: A Narrative Review. *Cureus* **2023**, *15*, e33728. [CrossRef]
15. Latimer, R.; MacLeod, H.; Dellefave-Castillo, L.; Macaya, D.; Hart, T.R. Postmortem Genetic Testing Is an Increasingly Utilized Tool in Death Investigation. *Acad. Forensic Pathol.* **2022**, *12*, 129. [CrossRef]
16. Geisenberger, C.; Chimal, E.; Jurmeister, P.; Klauschen, F. A cost-effective and scalable approach for DNA extraction from FFPE tissues. *Biol. Methods Protoc.* **2025**, *10*, bpaf003. [CrossRef] [PubMed]
17. A Steiert, T.; Parra, G.; Gut, M.; Arnold, N.; Trotta, J.-R.; Tonda, R.; Moussy, A.; Gerber, Z.; Abuja, P.M.; Zatloukal, K.; et al. A critical spotlight on the paradigms of FFPE-DNA sequencing. *Nucleic Acids Res.* **2023**, *51*, 7143. [CrossRef] [PubMed]
18. Do, H.; Dobrovic, A. Sequence Artifacts in DNA from Formalin-Fixed Tissues: Causes and Strategies for Minimization. *Clin. Chem.* **2015**, *61*, 64–71. [CrossRef]
19. Zhang, J.; Li, L.; Bai, X.; Zhang, Z.; Yuan, L. DNA quality and STR success rate in different formalin-fixed tissues. *Int. J. Leg. Med.* **2024**, *139*, 995–1003. [CrossRef]
20. Meizarini, A.; Puteri, A.; Yasan, Y.D.R.; Hussaini, H.M. Optimization of proteinase K incubation protocol duration during DNA extraction from oral squamous cell carcinoma FFPE samples. *Dent. J.* **2023**, *56*, 233–237. [CrossRef]
21. Cazzato, G.; Caporusso, C.; Arezzo, F.; Cimmino, A.; Colagrande, A.; Loizzi, V.; Cormio, G.; Lettini, T.; Maiorano, E.; Scarcella, V.S.; et al. Formalin-fixed and paraffin-embedded samples for next generation sequencing: Problems and solutions. *Genes* **2021**, *12*, 1472. [CrossRef]
22. Guo, Q.; Lakatos, E.; Al Bakir, I.; Curtius, K.; Graham, T.A.; Mustonen, V. The mutational signatures of formalin fixation on the human genome. *Nat. Commun.* **2022**, *13*, 4487. [CrossRef]
23. Yun, B.H.; Guo, J.; Turesky, R.J. Formalin-Fixed Paraffin-Embedded Tissues—An Untapped Biospecimen for Biomonitoring DNA Adducts by Mass Spectrometry. *Toxics* **2018**, *6*, 30. [CrossRef] [PubMed]
24. Kim, S.; Park, C.; Ji, Y.; Kim, D.G.; Bae, H.; van Vrancken, M.; Kim, D.-H.; Kim, K.-M. Deamination Effects in Formalin-Fixed, Paraffin-Embedded Tissue Samples in the Era of Precision Medicine. *J. Mol. Diagn.* **2017**, *19*, 137–146. [CrossRef] [PubMed]
25. Essawy, M.M.; Campbell, C. Enzymatic Processing of DNA–Protein Crosslinks. *Genes* **2024**, *15*, 85. [CrossRef] [PubMed]
26. Koshiba, M.; Ogawa, K.; Hamazaki, S.; Sugiyama, T.; Ogawa, O.; Kitajima, T. The Effect of Formalin Fixation on DNA and the Extraction of High-molecular-weight DNA from Fixed and Embedded Tissues. *Pathol. Res. Pract.* **1993**, *189*, 66–72. [CrossRef]
27. Bhoyar, L.; Mehar, P.; Chavali, K. An overview of DNA degradation and its implications in forensic caseworks. *Egypt. J. Forensic Sci.* **2024**, *14*, 15. [CrossRef]
28. Gill, P.; Fereday, L.; Morling, N.; Schneider, P.M. The evolution of DNA databases-Recommendations for new European STR loci. *Forensic Sci. Int.* **2006**, *156*, 242–244. [CrossRef]
29. Schneider, P.M. tHe eSS loCi Expansion of the European Standard Set of DNA Database Loci-the Current Situation. 2009. Available online: https://www.promega.com/-/media/files/resources/profiles-in-dna/1201/expansion-of-the-european-standard-set.pdf?utm_source=chatgpt.com (accessed on 21 August 2025).
30. Kidd, K.K.; Pakstis, A.J.; Speed, W.C.; Grigorenko, E.L.; Kajuna, S.L.; Karoma, N.J.; Kungulilo, S.; Kim, J.-J.; Lu, R.-B.; Odunsi, A.; et al. Developing a SNP panel for forensic identification of individuals. *Forensic Sci. Int.* **2006**, *164*, 20–32. [CrossRef]
31. Kidd, K.K.; Speed, W.C.; Pakstis, A.J.; Furtado, M.R.; Fang, R.; Madbouly, A.; Maiers, M.; Middha, M.; Friedlaender, F.R.; Kidd, J.R. Progress toward an efficient panel of SNPs for ancestry inference. *Forensic Sci. Int. Genet.* **2014**, *10*, 23–32. [CrossRef]

32. Eduardoff, M.; Santos, C.; de la Puente, M.; Gross, T.; Fondevila, M.; Strobl, C.; Sobrino, B.; Ballard, D.; Schneider, P.; Carracedo, Á.; et al. Inter-laboratory evaluation of SNP-based forensic identification by massively parallel sequencing using the Ion PGM™. *Forensic Sci. Int. Genet.* **2015**, *17*, 110–121. [CrossRef] [PubMed]
33. Parson, W.; Ballard, D.; Budowle, B.; Butler, J.M.; Gettings, K.B.; Gill, P.; Gusmão, L.; Hares, D.R.; Irwin, J.A.; King, J.L.; et al. Massively parallel sequencing of forensic STRs: Considerations of the DNA commission of the International Society for Forensic Genetics (ISFG) on minimal nomenclature requirements. *Forensic Sci. Int. Genet.* **2016**, *22*, 54–63. [CrossRef]
34. Terrado-Ortuño, N.; May, P. Forensic DNA phenotyping: A review on SNP panels, genotyping techniques, and prediction models. *Forensic Sci. Res.* **2024**, *10*, owae013. [CrossRef]
35. Stelloo, E.; Meijers, R.W.; Swennenhuis, J.F.; Allahyar, A.; Hajo, K.; Cangiano, M.; de Leng, W.W.; van Helvert, S.; Van der Meulen, J.; Creytens, D.; et al. Formalin-Fixed, Paraffin-Embedded–Targeted Locus Capture: A Next-Generation Sequencing Technology for Accurate DNA-Based Gene Fusion Detection in Bone and Soft Tissue Tumors. *J. Mol. Diagn.* **2023**, *25*, 758–770. [CrossRef]
36. Bonnet, E.; Moutet, M.-L.; Baulard, C.; Bacq-Daian, D.; Sandron, F.; Mesrob, L.; Fin, B.; Delépine, M.; Palomares, M.-A.; Jubin, C.; et al. Performance comparison of three DNA extraction kits on human whole-exome data from formalin-fixed paraffin-embedded normal and tumor samples. *PLoS ONE* **2018**, *13*, e0195471. [CrossRef]
37. Okojie, J.; O'neal, N.; Burr, M.; Worley, P.; Packer, I.; Anderson, D.; Davis, J.; Kearns, B.; Fatema, K.; Dixon, K.; et al. DNA Quantity and Quality Comparisons between Cryopreserved and FFPE Tumors from Matched Pan-Cancer Samples. *Curr. Oncol.* **2024**, *31*, 2441–2452. [CrossRef]
38. Daş, T.; Buğra, A.; Buğra, A.K. Evaluation of histopathological findings of cardiac deaths in forensic autopsies. *Ir. J. Med. Sci.* **2022**, *191*, 937–944. [CrossRef] [PubMed]
39. Viljoen, R.; Reid, K.M.; Mole, C.G.; Rangwaga, M.; Heathfield, L.J. Towards molecular autopsies: Development of a FFPE tissue DNA extraction workflow. *Sci. Justice* **2022**, *62*, 137–144. [CrossRef]
40. Inoue, F.; Sone, K.; Toyohara, Y.; Takahashi, Y.; Kukita, A.; Hara, A.; Taguchi, A.; Tanikawa, M.; Tsuruga, T.; Osuga, Y. Targeting Epigenetic Regulators for Endometrial Cancer Therapy: Its Molecular Biology and Potential Clinical Applications. *Int. J. Mol. Sci.* **2021**, *22*, 2305. [CrossRef]
41. Do, H.; Dobrovic, A. Dramatic reduction of sequence artefacts from DNA isolated from formalin-fixed cancer biopsies by treatment with uracil-DNA glycosylase. *Oncotarget* **2012**, *3*, 546–558. [CrossRef] [PubMed]
42. Osinski, B.L.; BenTaieb, A.; Ho, I.; Jones, R.D.; Joshi, R.P.; Westley, A.; Carlson, M.; Willis, C.; Schleicher, L.; Mahon, B.M.; et al. Artificial intelligence-augmented histopathologic review using image analysis to optimize DNA yield from formalin-fixed paraffin-embedded slides. *Mod. Pathol.* **2022**, *35*, 1791–1803. [CrossRef]
43. Gill, P.; Whitaker, J.; Flaxman, C.; Brown, N.; Buckleton, J. An investigation of the rigor of interpretation rules for STRs derived from less than 100 pg of DNA. *Forensic Sci. Int.* **2000**, *112*, 17–40. [CrossRef] [PubMed]
44. Bieber, F.R.; Buckleton, J.S.; Budowle, B.; Butler, J.M.; Coble, M.D. Evaluation of forensic DNA mixture evidence: Protocol for evaluation, interpretation, and statistical calculations using the combined probability of inclusion. *BMC Genet.* **2016**, *17*, 125. [CrossRef] [PubMed]
45. Gill, P.; Brenner, C.H.; Buckleton, J.S.; Carracedo, A.; Krawczak, M.; Mayr, W.R.; Morling, N.; Prinz, M.; Schneider, P.M.; Weir, B.S.; et al. DNA commission of the International Society of Forensic Genetics: Recommendations on the interpretation of mixtures. *Forensic Sci. Int.* **2006**, *160*, 90–101. [CrossRef] [PubMed]
46. Gouveia, G.R.; Ferreira, S.C.; Siqueira, S.A.; Pereira, J. Nucleic Acids Extraction from Formalin-Fixed and Paraffin-Embedded Tissues. In *Nucleic Acids—From Basic Aspects to Laboratory Tools*; IntechOpen Limited: London, UK, 2016. [CrossRef]

genes

MDPI

Article

DNA Transfer Between Items Within an Evidence Package

Yong Sheng Lee * and Christopher Kiu-Choong Syn

DNA Profiling Laboratory, Biology Division, Health Sciences Authority, 3 Biopolis Drive, Synapse, 03-14/15, Singapore 138623, Singapore; christopher_syn@hsa.gov.sg
* Correspondence: lee_yong_sheng@hsa.gov.sg; Tel.: +65-6684-2050

Abstract: Background/Objectives: Advancements in DNA profiling have made it possible to retrieve intact DNA profiles from increasingly minute biological samples. This increased sensitivity in DNA detection has highlighted crucial considerations to be made when handling and packing items from the crime scene to minimize potential contamination from either direct or indirect transfer of DNA. To investigate potential DNA transfer between items stored within the same evidence package, we conducted a simulation study with items commonly encountered during forensic casework. **Methods:** Participants were grouped in pairs, each of them handling the same type of item to simulate the activity conducted at the crime scene. The items were then collected from each pair of participants and stored in the same evidence package for 4 to 5 days. To evaluate the basal DNA transfer between items within the same package, the packed items were not subjected to friction, force, or long-distance movement in this study. **Results:** We have observed the occurrence of DNA transfer on 39% of the studied items inside the package, which changed the source attribution of the DNA profiles for 10% of the recovered samples. Our results showed that the types of items were associated with the number of transferred alleles and the amount of DNA recovered, while no association was found between the number of transferred alleles and the amount of DNA on the studied items. **Conclusions:** Taken together, the results from this study reiterate the importance of packing each item from the crime scene separately, especially when packing items together may impact the interpretation of source attribution.

Keywords: forensic DNA; DNA transfer; touch DNA; evidence packaging

1. Introduction

Biological samples with low levels of DNA have sometimes been referred to as "trace DNA" as their specific source cannot be determined, or "touch DNA" as "touching" is assumed to be the activity that left these samples behind.

DNA deposited by "touch" is often assumed to come from cells sloughed off from the outermost layer of skin [1]. Attributed to the active process of desquamation, an adult human can shed as many as 1000 cells/cm^2/hour in a continuous manner, leading to the loss of up to 1 billion corneocytes from the body each day [2].

Despite the large number of shed cells, the recovery of full DNA profiles from fingerprints, a typical source of touch DNA, was first demonstrated only in 1997 in the seminal paper by Van Oorschot and Jones [3]. Even with this ground-breaking discovery and the subsequent progress in touch DNA studies, it was still challenging to apply earlier DNA profiling technologies to solve criminal cases involving touch DNA.

This challenge likely arose due to a combination of two aspects of touch DNA. Firstly, most of the shed cells may be anucleate, as the outermost layer of the epidermis consists of fully differentiated keratinocytes which have lost their nuclei during the keratinization process [4]. Therefore, detectable DNA may only come from a limited number of nucleated epithelia, free nuclei from degraded cells, and cell-free DNA. Secondly, the amount of DNA deposited onto an item through touching or handling can be affected by various factors, such as duration of contact, nature of contact, and the shedder status of an individual. These factors may explain the wide range of touch DNA—from 0 ng to 75 ng—that has been reported to be recovered from items after regular use by an individual [5] and the difficulty in obtaining an interpretable profile from touch DNA with quantities at the lower range. With recent improvements in DNA profiling technologies, such as the use of newer DNA analysis kits and genetic analyzer platforms, the sensitivity of DNA detection and the probability of obtaining interpretable DNA profiles from touch DNA samples have been dramatically enhanced.

However, these improvements in DNA analysis would also lead to the detection of small amounts of transferred DNA unrelated to the crime, such as background DNA deposited by activities prior to the crime or other DNA introduced through secondary DNA transfer. Nonetheless, this transferred DNA would complicate inferences that can be drawn from the DNA evidence. Hence, it is also necessary to address the probability of DNA transfer when evaluating the DNA evidence.

DNA transfer can occur when two items are placed together with direct contact. This may happen during the evidence collection process when multiple items from the crime scene are packed and transported together. Previous studies have reported the possibility of DNA transfer from a packed item to the interior of the evidence packaging, as well as between items stored within the same package [6]. However, several of these studies only examined DNA transfer using biological fluids with high levels of DNA, such as blood and saliva, while other studies involving touch DNA only evaluated the DNA transfer from the packed item to the interior of the packaging, but not amongst the items themselves [7].

In this study, we have assessed the occurrence of DNA transfer between two items that had been packed within the same package, a scenario that can occur during the handling and packing of evidence items by law enforcement. This study was conducted in response to a real operational issue, which led to a need to inform both law enforcement and the courts what can happen when exhibits are packed and stored together. As such, we focused on evaluating the basal rate of DNA transfer when items were packed together instead of mimicking the friction, temperature, and movement involved during long-distance transport of the packaged items from the crime scene to the laboratory.

2. Materials and Methods

2.1. Preparation of Mock Casework Items

Nine types and a total of 94 items commonly encountered in casework were used in this study (Table 1). These items were divided into two groups to study DNA transfer pertaining to touch DNA and/or saliva. All items, except paper and cigarette butts, were rendered 'DNA-free' by soaking in 1 g/L sodium hypochlorite for 2 h, followed by soaking in ultrapure water (Milli-Q water; 18.2 MΩ·cm resistivity) (Merck Millipore, Burlington, MA, USA) for 4 h.

To assess if DNA was present on the items prior to conducting this study, the surfaces of randomly selected items for each type, except cigarette butts, were swabbed and processed as described in Section 2.3. Additionally, one 15 × 11 cm paper envelope, three 24 × 16 cm paper envelopes, and one 31 × 21 cm paper envelope, which were used as packaging

for the mock casework items, were also randomly selected, and the interior surfaces of these paper envelopes were swabbed and processed as described in Section 2.3.

Table 1. List of different types of items used in this study. Number of each item in groups A and B, and the way they were used.

Item	N	Way of Use	Note
Group A			
Cotton glove	16	Worn for whole day for ≥2 days	Interior of glove facing out when placed in envelope
Latex glove	6	Worn for ≥1 h	Interior of glove facing out when placed in envelope
Lighter	10	Held for 1 min and rolled the wheel at least 3 times every hour for 6 h	
Paper	10	Wrote 3 sentences on it (landscape) and folded it twice, with each fold bringing shorter ends to each other, unfolded, and pressed down on the table (blank side in contact with the table) to mimic a debt collector pressing the paper onto the door of the debtor's house before fixing it with adhesive tape.	Folded form when placed in envelope
Plastic straw for drug packing	10	Cut and heat sealed	
Re-sealable bag	6	Touched ≥ 5 times within a day	
Syringe	10	Opened cap and plunged 3 times, then capped back	
Group B			
Cigarette butt	10	Held as when smoking	Provided by participants after smoking
Plastic straw for drinking	16	Used to drink beverage	
Total	94		

2.2. Experimental Design

This study sought to examine the occurrence of DNA transfer between casework items that may have been packed together into a single package (graphically summarized in Figure 1).

Two identical items (e.g., gloves) were allocated to a pair of participants. Each of the 43 participants independently used their allocated item in a manner that could mimic its utility in a crime event (Table 1). The items were then collected from the pair of participants and placed into a single envelope package for 4 or 5 days.

In this design, each participant is concurrently a "user" (i.e., participant had direct contact/handling of one item) and a "partner" (i.e., participant's DNA was transferred to the other item through co-placement of both items in a common package).

DNA samples were separately collected from all exposed surfaces of each item via 'double-swabbing' with wet and dry sterile cotton swabs, with the exception of cigarette butts. For cigarette butts, 1 cm from the unburnt end of the tipping paper was cut. All samples were collected 4 days after they were placed in the envelope package, except for all latex gloves, 10 cotton gloves, and 6 plastic straws for drinking, which were collected 5 days after being placed in the envelope package. The swabs and cuttings from cigarette butts were stored in microcentrifuge tubes at −21 °C prior to extraction.

Informed consent was obtained from each participant involved in this study, and DNA profiles were obtained from each individual as references. This study has been approved

by the Domain Specific Review Board of the National Healthcare Group, Ministry of Health, Singapore.

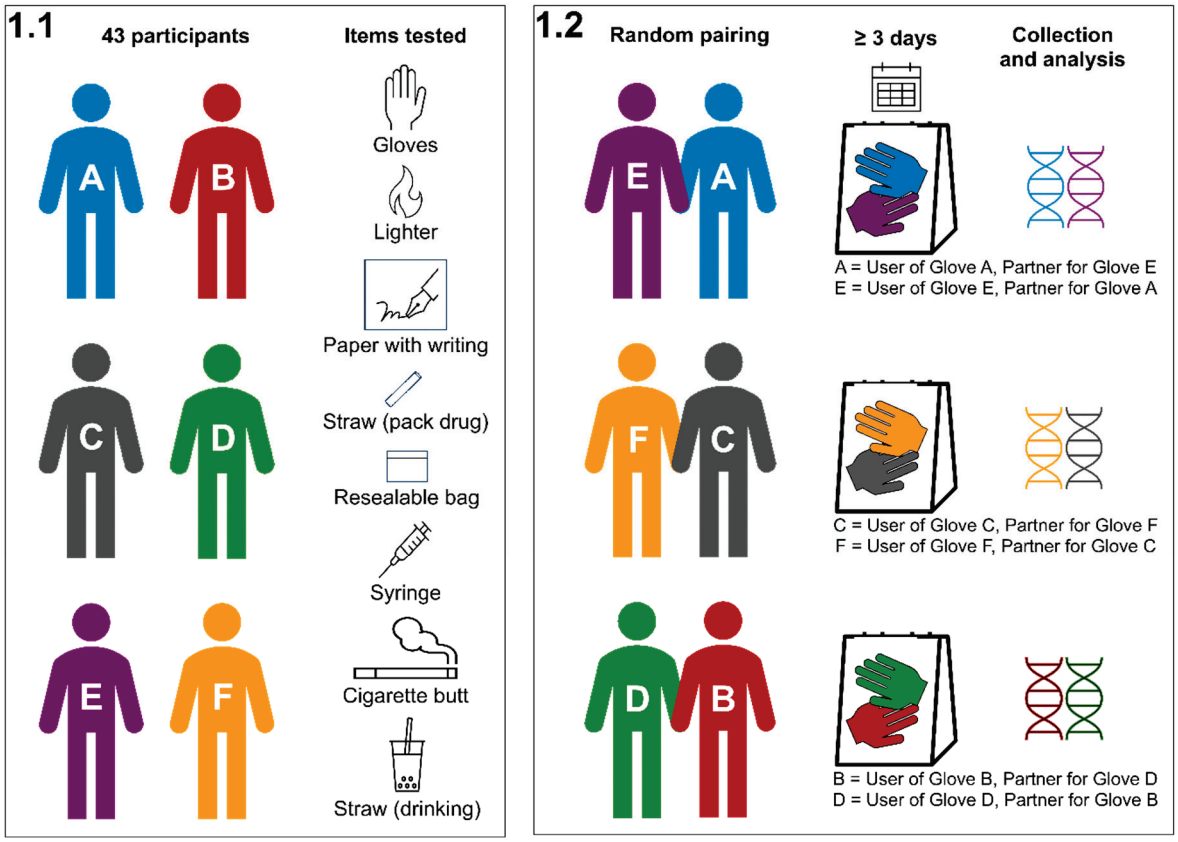

Figure 1. Experimental design for studying possible DNA transfer between items packed within a single evidence package. (1.1) Participants were requested to individually handle a list of commonly encountered casework items to simulate handling at a crime scene. The items included gloves, plastic straws used for packing drugs, lighters, paper with writing, syringes, cigarette butts, and plastic straws used for drinking. (1.2) After handling, each participant was randomly paired with another participant, with whom they had no contact before and after the item handling. As per the illustration above, two gloves, one from each participant, were collected and placed together into one envelope to mimic multiple items packed into a single evidence package. The items were kept together for 4 or 5 days before the DNA was collected from the items and analyzed. Each participant is simultaneously deemed a "user" and a "partner" in each of the experiments, with the "user" being defined as having direct contact with the item (e.g., glove) and as a "partner" as having only indirect contact with the item. For example, Contributor A (blue) is a "user" of Glove A since he has directly worn and used the glove. On the other hand, Contributor A is a "partner" for Glove E (purple) as he had no direct contact with Glove E, and any traces of Contributor A's DNA on Glove E would only be possible through DNA transfer from Glove A to E during storage within the same evidence packaging. For resealable bags, straws (touch), paper, and syringes, participants were requested to refrain from washing their hands at least 1 h before the experiment to ensure that as much DNA as possible would be deposited on the items.

2.3. DNA Processing

DNA extraction was performed using the DNA IQ™ Casework Extraction Kit and the DNA IQ™ Casework Pro Kit on a Maxwell® FSC instrument (Promega Corporation, Seoul, Republic of Korea) as per the manufacturer's protocol [8,9]. DNA yield was estimated using Quantifiler® Trio DNA Quantification kit (Applied Biosystems, Warrington, UK) on the QuantStudio™ 7 Flex Real-Time PCR System (Applied Biosystems, Singapore) as

per the manufacturer's protocol [10,11]. STR-PCR amplification was performed (29 cycles) with a GlobalFiler™ PCR Amplification kit (Applied Biosystems, Warrington, UK), as per the manufacturer's protocol [12], using 1 ng input DNA or a maximum of 15 µL DNA extract. Capillary electrophoresis was performed on the 3500 xL Genetic Analyzer (Applied Biosystems, Ibaraki, Japan) with 3 µL of amplified product injected at 1.2 kV for 24 s. Results were analyzed using GeneMapper® ID-X v1.2 software.

2.4. Profile Analyses

DNA profiles were interpreted with an analytical threshold of 110 RFU, a stochastic threshold of 535 RFU, and the number of contributors determined based on the method used by Szkuta et al. [13]. DNA profiles of the contributors were deemed reportable only if they met the laboratory's minimum reporting criteria of 16 alleles before the likelihood ratio (LR) was calculated using EuroForMix v3.2. The DNA mixture profiles were deemed to have major and minor contributors when EuroForMix deconvolution showed the major contributor proportion to be at least 75% of the total DNA contribution. DNA profiles with four or more contributors were deemed uninterpretable, and no LR was calculated.

Interpreted profiles were then compared with the reference profiles of the participants. Alleles detected were first attributed to the "user" participant who had directly used the item, followed by the paired "partner" participant whose item had been co-placed into the same packaging. Alleles that could not be attributed to either the "user" or the "partner" were termed as foreign alleles.

2.5. Statistical Analyses

A Kruskal–Wallis test was performed on the association between item type and the above-mentioned variables. p-value < 0.05 was considered statistically significant. Post-hoc analysis (Dunn's Test) was also performed, followed by Bonferroni Correction.

3. Results

3.1. DNA Recovery from Different Types of Items and Biological Materials

A total of 94 samples were recovered from nine types of items (Table 1). These items were divided into two groups based on the different biological materials recovered. Touch DNA was collected from items in Group A (cotton gloves, latex gloves, lighters, paper, plastic straws for drug packing, resealable bags, and syringes) while a mix of both saliva and touch DNA was concurrently collected from items in Group B (cigarette butts and plastic straws for drinking).

The amount of DNA recovered from the various types of items is shown in Figure 2. Touch DNA recovered from items in Group A ranged from 0 ng to 32 ng, with a median of 3 ng. In comparison, items in Group B yielded more DNA, with the median DNA amount recovered from cigarette butts and plastic drinking straws being 30 ng and 2.5 ng, respectively.

3.2. Recovery of Alleles That Could Be Attributed to the "User" and the "Partner"

The occurrence of DNA transfer between the two items within the same package was observed in a total of 37 items (39% of the total number of items) (Table 2). To evaluate this transfer, the number of alleles attributed to either the "user" or the "partner" was compared (Figure 3).

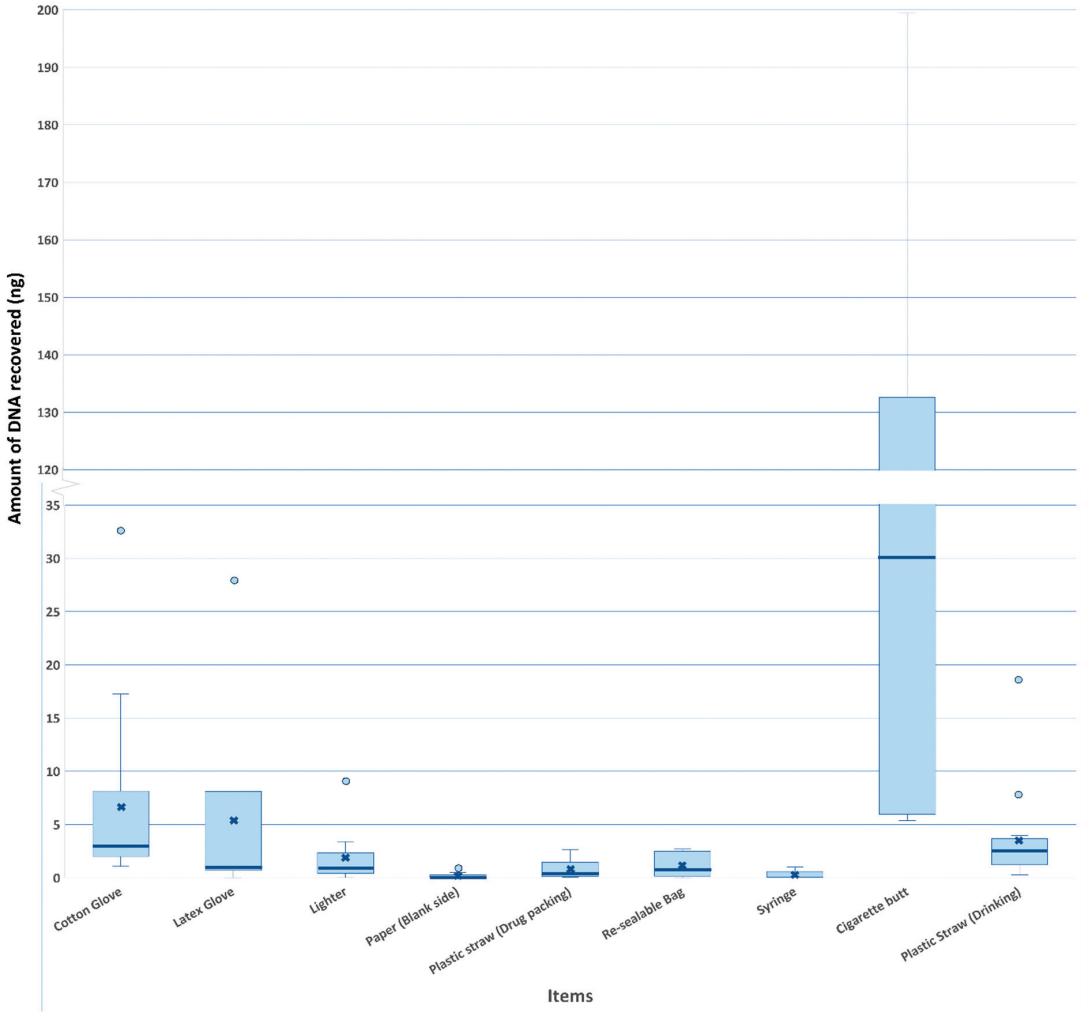

Figure 2. Amount of DNA recovered from different types of items. DNA quantities from nine items and the respective mean (represented by bold x), median (bold line), and outlier (blue circle).

Table 2. Number of items with at least one allele that could be attributed to the "partner". Count and percentage of each item type from Group A (items with touch DNA) and Group B (items with both touch DNA and saliva) with one or more alleles that could be attributed to the "partner".

Group	Item Type	Count (% of Total Number of Each Item Type)
A	Cotton glove (n = 16)	14 (88%)
	Latex glove (n = 6)	4 (67%)
	Lighter (n = 10)	1 (10%)
	Paper (n = 10)	2 (20%)
	Plastic straw for drug packing (n = 10)	0 (0%)
	Resealable bag (n = 6)	5 (83%)
	Syringe (n = 10)	2 (20%)
B	Cigarette butt (n = 10)	2 (20%)
	Plastic straw for drinking (n = 16)	7 (44%)

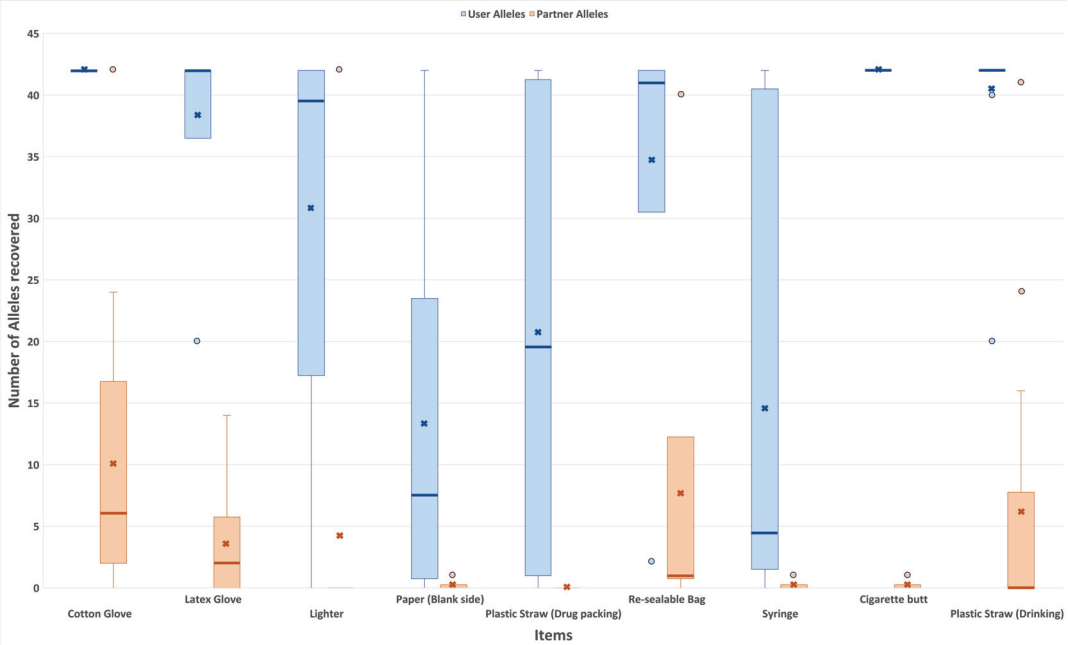

Figure 3. Number of DNA alleles recovered from different types of items. Number of "user" and "partner" alleles observed on nine items and the respective mean (represented by bold x), median (bold line), and outlier (blue circle and orange circle).

It was observed that the number of alleles that can be attributed to the "user" was generally in the higher range of 20 alleles and above for all the studied items (Figure 3). In contrast, it was observed that the number of alleles that can be attributed to the "partner" was generally lower than 20 alleles, except for the outliers seen in those samples collected from cotton gloves, lighters, resealable bags, and plastic straws for drinking.

Significant differences were found in the amount of DNA, number of alleles attributed to the "user", and number of alleles attributed to the "partner" among different types of items (Table 3).

Table 3. Items with significant differences in the amount of DNA, number of alleles attributed to "user" or number of alleles attributed to "partner" after Kruskal–Wallis test and post-hoc analysis (Dunn's Test) with Bonferroni Correction.

Category of Comparison	Item (A)	Item with Significant Difference with Item (A)
Amount of DNA	Cotton glove	Paper
		Plastic straw for drug packing
		Syringe
	Cigarette butt	Lighter
		Paper
		Plastic straw for drug packing
		Resealable bag
		Syringe
	Plastic straw for drinking	Paper
		Syringe

Table 3. *Cont.*

Category of Comparison	Item (A)	Item with Significant Difference with Item (A)
Number of alleles attributed to "user"	Cotton glove	Paper
		Plastic straw for drug packing
		Syringe
	Cigarette butt	Paper
		Plastic straw for drug packing
		Syringe
	Plastic straw for drinking	Paper
		Plastic straw for drug packing
		Syringe
Number of alleles attributed to "partner"	Cotton glove	Lighter
		Paper
		Plastic straw for drug packing
		Syringe
		Cigarette butt

3.3. Interpretation of DNA Profiles

All the DNA profiles were subsequently interpreted, and the interpretation results are shown in Table 4. Reportable DNA profiles were obtained from a total of 72 items (77%). The majority of these profiles were attributed to the "user" (62 out of 72 items—86%); it should, however, be noted that only 33 (53%) of them were single-source, while the remaining 29 (47%) exhibited additional alleles that could be attributed to the "partner". However, based on our laboratory criterion of a minimum of 16 alleles for reporting, the recovery rate of reportable DNA profiles from the "partner" was relatively low at 10% (Table 4; 1 attributed to the "partner" plus 8 attributed to a mix of the "user" and the "partner" making up 9 out of 94 items).

Table 4. Interpretation results of DNA profiles. Count and percentage of the reportable, not reportable, and uninterpretable profiles. Reportable profiles were further classified into sub-categories depending on attribution.

Interpretation	Count of Sample
Reportable	72 (76.6%)
• Attributed to the "user"	62
• Attributed to the "partner"	1
• Mix of the "user" and the "partner"	8
• Mix of the "user" and foreign person	1
Not reportable	21 (22.3%)
Uninterpretable	1 (1.1%)

The source attribution of reportable DNA profiles recovered from different types of items is detailed in Table 5. A total of eight DNA mixtures comprising "partner" and "user" alleles were recovered from four cotton gloves, one resealable bag, and three plastic straws for drinking, while one DNA profile attributed to the "partner" was recovered from a lighter. Interestingly, one DNA mixture was recovered from a plastic straw for drug packing, whereby alleles of a foreign person were found together with the "user".

Table 5. Attribution of reportable DNA profiles from items grouped by different types. Count and percentage of profile attribution for each item type.

Item Type	Attributed to the "User"	Attributed to the "User" and the "Partner"	Attributed to the "Partner"	Attributed to the "User" and Foreign Person
Cotton glove (n = 16)	11 (69%)	4 (25%)		
Latex glove (n = 6)	6 (100%)			
Lighter (n = 10)	8 (80%)		1 (10%)	
Paper (n = 10)	3 (30%)			
Plastic straw for drug packing (n = 10)	4 (40%)			1 (10%)
Resealable bag (n = 6)	4 (67%)	1 (17%)		
Syringe (n = 10)	3 (30%)			
Cigarette butt (n = 10)	10 (100%)			
Plastic straw for drinking (n = 16)	13 (81%)	3 (19%)		

For items directly handled by "users", a total of 71 "users" could be included as single contributors or major contributors. The allele counts ranged from 18 to 42 with likelihood ratio (LR) values between 3.15×10^5 and 9.3×10^{35}, respectively. In contrast, for items that had not been directly handled by the "partner", 9 "partners" could be included as major or minor contributors. In these cases, the allele counts (16 to 42) and LR values (3.83×10^4 to 3.01×10^{27}) were generally lower. As expected, the majority (64 out of 71) of the "user" LRs were in the quintillions or higher, while only a minority (three out of nine) of the "partner" LRs exceeded the quintillion mark. Nevertheless, the allele counts and LR values of the "partner" still provided strong evidence to support their inclusion as a contributor (Supplementary Materials).

4. Discussion

4.1. The Amount of DNA Does Not Correlate with the Number of Transferred Alleles

In this study, the amounts of DNA recovered from cigarette butts were the highest among the items, which was possibly due to saliva (with high levels of DNA) being deposited onto the cigarette butts. Although saliva was likely present on the plastic straw for drinking, relatively low levels of DNA were obtained. This could possibly be attributed to the duration of direct contact between the cigarette butts and the mouth of the participant being longer than that of the straws, which may have led to the deposition of higher amounts of biological samples on the cigarette butts. Another factor could be the porosity of the cigarette butt, possibly absorbing/trapping the DNA, unlike the straw, where the DNA could have been easily wiped off. It should also be noted that DNA extraction of cigarette butts and plastic straws was different in that DNA was extracted directly from cigarette butt paper, vis-à-vis plastic straws, where the DNA extraction was indirect (i.e., from the wet-dry swabs of the straw). As such, the DNA extraction efficiency

from the cigarette butts may also be higher, thereby giving rise to a higher DNA yield. Although a much higher amount of DNA was recovered from the cigarette butt than from the rest of the items, the number of transferred alleles (alleles attributed to the "partner") between the cigarette butts in the same package was observed to be similar to that from the lighters and plastic straw for drug packing (Figure 3), from which only a relatively low amount of DNA was recovered (Figure 2). As such, no obvious correlation between the amount of DNA and the number of transferred alleles could be determined, which suggested that DNA transfer between items may occur in similar ways regardless of the amount of DNA present.

4.2. DNA Transfer Between Different Types of Items

Our results showed that the majority of the reportable DNA profiles could be attributed to the "user", which is expected as direct contact with or handling of an item may deposit more DNA onto it than that from the secondary DNA transfer in the setting of our study.

For five types of items—cotton gloves, latex gloves, lighters, resealable bags, and plastic straws for drinking—the number of alleles that could be attributed to the "partner" (between 0 and 24 alleles, except for the outliers) was comparable with the range of transferred alleles detected in a previous study [6]. With respect to cigarette butts, Goray et al. reported observing 1–5 transferred alleles in 37.9% of the samples and 6–10 transferred alleles in 62.1% of the samples [6]. In comparison, our study showed fewer transferred alleles between the cigarette butts, possibly because our study only assessed the basal DNA transfer with shorter distance movement of the evidence package, while the settings in their study involved longer distance movement, friction, and force. A similar low transfer rate was observed by Thornbury et al. [14] when they studied DNA transfer without contact from dried biological materials on different objects. For all objects subjected to tapping action, the highest transfer rate of saliva was one out of six, while no transfer of touch DNA was observed.

The number of transferred alleles between plastic straws for drinking was observed to be higher than that of the cigarette butts, which indicated that DNA transfer may be more likely to occur between non-porous surfaces than porous surfaces, in corroboration with a previous report [15].

In the study by Stella et al. [7], where non-porous polyvinyl chloride (PVC) capped tubes were used to mimic real exhibits, 100% (three out of three tubes) of saliva and 0% (zero out of three tubes) of touch DNA were transferred from one part of the tube to another part of the tube through the interior of the package as the intermediate surface. Their results contrasted with our study involving items often encountered in crime casework—19% (3 out of 16 plastic straws for drinking) of saliva were transferred to the paired items, and 25% (4 out of 16 cotton gloves), 10% (1 out of 10 lighters), and 17% (1 out of 6 resealable bags) of touch DNA was transferred to the paired items. The difference could likely be attributed to the amount of saliva/touch DNA used in their study. In the case of saliva, Stella et al had used 100 µl (roughly two droplets) of saliva to spot the tube, which would be substantially more than what would remain on a straw used for drinking. With respect to the touch DNA, Stella et al. had participants rub an area on the tube with a fingertip, which would likely have deposited less biological material compared to our study, where participants handled a larger surface area, e.g., wearing a glove for hours, holding a lighter while rolling the wheel, and using a syringe.

In general, there were significant differences in the amount of DNA recovered, as well as the number of alleles attributed to the "user" and "partner" amongst the different types

of items used in this study. This suggests that item type may be associated with the number of transferred alleles between two items.

4.3. DNA Transfer Within the Same Package Could Be a Potential Source of Contamination

In this study, DNA transfer between the two items within the same evidence package was observed in 39% of the recovered samples (Table 2; 37/94 samples). Although the majority of the interpretable DNA profiles obtained could be attributed to the "user", 46% of these profiles also contained additional alleles that could be attributed to the "partner" (although it was below our laboratory reporting threshold). Moreover, the number of transferred alleles in this study may be underestimated as shared alleles can exist between the "user" and the "partner". In this respect, adoption of massively parallel sequencing (MPS) techniques (compared to traditional STR genotyping via capillary electrophoresis techniques) may enable better distinction between the "user" and "partner" in a mixed DNA sample even if they share the same number of STR repeats [16,17]. Nevertheless, these results indicate that secondary DNA transfer within the same evidence package can be a real source of contamination in criminal casework. In addition, other factors commonly encountered during the evidence collection process may further increase the probability of DNA transfer within the package, such as long-distance movement and friction amongst the items packed together [18].

4.4. DNA Transfer May Further Interfere with Downstream DNA Profile Interpretation

Transfer of DNA between two items can alter the DNA profile and consequently impact the interpretation of source attribution. The impact of DNA transfer occurring within the evidence package on the interpretation of source attribution in our study was evaluated. While the interpretation of source attribution was unaffected for most of the 72 items with reportable DNA profiles, likely a reflection of the generally low levels of DNA being transferred, there were changes in the interpretation of source attribution for nine items, a non-trivial 12.5% (Table 6). This represents 10% of the items (Table 6; 9/94 samples) and indicates that DNA transfer can indeed influence the interpretation of source attribution, especially when the initial DNA on the item is in minute quantities. Additionally, any further DNA lost from these minute quantities due to transfer may impede our attempt to obtain an interpretable DNA profile from the item.

Table 6. Changes in DNA profile interpretation of source attribution caused by DNA transfer. Count of the number of items for each of the three different ways the interpretation of source attribution has been altered by DNA transfer.

Number of Items	Expected Profile If No DNA Transfer	Observed Profile
1	Not reportable single-source profile of the "user" but less than 16 alleles	"partner" being the major contributor
3	Essentially a single-source profile of the "user"	"user" and "partner" being approximately equal co-contributors
5	Essentially a single-source profile of the "user"	"user" being the major contributor and "partner" being the minor contributor

This issue of influence on the interpretation of source attribution may be addressed by evaluative reporting, which is a recent trend in DNA transfer studies [19–21]. Our present study shares similarities in the investigation of the frequency of detecting the person of interest, such as the "user" and "partner". Such frequencies may then be used towards evaluating the likelihood of direct and indirect transfer when items have been packed together, though it should be noted that scenarios involving different items packed together may require further studies.

Furthermore, the current study was focused on the basal rate of DNA transfer between items packed together, as it was in response to an operational issue and the need to inform both law enforcement and the courts what can happen when exhibits of the same type are packed and stored together. As such, it does not address variables such as friction between items, environmental temperature, and movement of items within the package during long-distance transport of the packaged items from the crime scene to the laboratory. It also does not address the issue of the directionality of DNA transfer between different types of items packed in the same package.

5. Conclusions

The present study highlighted the general DNA recovery and the number of "user" and "partner" alleles from the different types of items. With more questions being raised in courts about DNA transfer, e.g., activities that can lead to DNA deposition, quantities of DNA deposited, and associated probabilities of the deposited DNA being detectable, it is timely and relevant to assess the impact of DNA transfer occurring when multiple evidential items are packed in a common package. This study showed that DNA transfer was observed on 39% of the items (refer to Section 4.3 for details) that had been packed together, with 10% of the items (refer to Section 4.4 for details) having altered interpretations (e.g., 'false inclusion' on the source attribution). As such, laboratories and law enforcement agencies would benefit from procedures guiding the individual packaging of each evidence item to reduce the risk of secondary DNA transfer within an evidence package, leading to an inaccurate source attribution. One approach may be to pack each evidence item separately unless the items were found to already be in contact with each other upon discovery. Another approach could be to collect DNA from the evidence items at the crime scene itself to minimize potential DNA transfer while transporting the evidence items to the laboratory.

Supplementary Materials: The following supporting information can be downloaded at: https://www.mdpi.com/article/10.3390/genes16080894/s1. Refer to Excel spreadsheet S1: Table of Raw Data.

Author Contributions: Conceptualization: Y.S.L. and C.K.-C.S.; formal analysis: Y.S.L.; writing—original draft: Y.S.L.; writing—review and editing: Y.S.L. and C.K.-C.S. All authors have read and agreed to the published version of the manuscript.

Funding: This research received no external funding.

Institutional Review Board Statement: This study was conducted in accordance with the Declaration of Helsinki, and the protocol has been approved by the Domain Specific Review Board (DSRB) of the National Healthcare Group (NHG), Ministry of Health, Singapore on 4 December 2024. The NHG DSRB reference number for this study is 2024-4384.

Informed Consent Statement: Informed consent was obtained from each participant involved in this study, and DNA profiles were obtained from each individual as references.

Data Availability Statement: Raw electropherograms are not available due to restrictions on privacy, legal, or ethical reasons.

Acknowledgments: The authors would like to thank Li Yen Candy Lee and Jiayu Tan for their roles in the conceptualization of this study; Nurul Insyirah Binte Ishak, Marlene Abdul Mugni, Hui Wen Yeo, and Sabrina Binte Mustaffa for their assistance in the execution of the experimental plans. We would also like to express our appreciation to all volunteers for their participation in this study.

Conflicts of Interest: The authors declare no conflicts of interest, financial or otherwise.

References

1. Wiegand, P.; Kleiber, M. DNA typing of epithelial cells after strangulation. *Int. J. Legal Med.* **1997**, *110*, 181–183. [CrossRef]
2. Roberts, D.; Marks, R. The determination of regional and age variations in the rate of desquamation: A comparison of four techniques. *J. Investig. Dermatol.* **1980**, *74*, 13–16. [CrossRef]
3. van Oorschot, R.A.; Jones, M.K. DNA fingerprints from fingerprints. *Nature* **1997**, *387*, 767. [CrossRef]
4. Bragulla, H.H.; Homberger, D.G. Structure and functions of keratin proteins in simple, stratified, keratinized and cornified epithelia. *J. Anat.* **2009**, *214*, 516–559. [CrossRef]
5. Meakin, G.; Jamieson, A. DNA transfer: Review and implications for casework. *Forensic Sci. Int. Genet.* **2013**, *7*, 434–443. [CrossRef]
6. Goray, M.; van Oorschot, R.A.; Mitchell, R.J. DNA transfer within forensic exhibit packaging: Potential for DNA loss and relocation. *Forensic Sci. Int. Genet.* **2012**, *6*, 158–166. [CrossRef]
7. Stella, C.J.; Meakin, G.E.; van Oorschot, R.A.H. DNA transfer in packaging: Attention required. *Forensic Sci. Int. Genet. Suppl. Ser.* **2022**, *8*, 303–305. [CrossRef]
8. Promega Corporation. DNA IQTM Casework Pro Kit for Maxwell® 16 Technical Manual Part# TM332, Revised 11/11.
9. Promega Corporation. Maxwell® FSC Instrument Operating Manual TM462 Revised 8/17.
10. Applied Biosystems. QuantStudio™ 6/7 Flex Real Time PCR System, Getting Started Guide, Rev A, 2013.
11. Applied Biosystems. Quantifiler™ HP and Trio DNA Quantification Kits, User Guide, 2017.
12. Applied Biosystems. GlobalFiler™ PCR Amplification Kit, User Guide, July 2016.
13. Szkuta, B.; Ballantyne, K.N.; van Oorschot, R.A.H. Transfer and persistence of DNA on the hands and the influence of activities performed. *Forensic Sci. Int. Genet.* **2017**, *28*, 10–20. [CrossRef]
14. Thornbury, D.; Goray, M.; van Oorschot, R.A.H. Indirect DNA transfer without contact from dried biological materials on various surfaces. *Forensic Sci. Int. Genet.* **2021**, *51*, 102457. [CrossRef]
15. Goray, M.; Mitchell, R.J.; van Oorschot, R.A. Investigation of secondary DNA transfer of skin cells under controlled test conditions. *Leg. Med.* **2010**, *12*, 117–120. [CrossRef]
16. Gettings, K.B.; Kiesler, K.M.; Faith, S.A.; Montano, E.; Baker, C.H.; Young, B.A.; Guerrieri, R.A.; Vallone, P.M. Sequence variation of 22 autosomal STR loci detected by next generation sequencing. *Forensic Sci. Int. Genet.* **2016**, *21*, 15–21. [CrossRef]
17. Neste, C.V.; Nieuwerburgh, F.V.; Hoofstat, D.V.; Deforce, D. Forensic STR analysis using massive parallel sequencing. *Forensic Sci. Int. Genet.* **2012**, *6*, 810–818. [CrossRef]
18. Goray, M.; Eken, E.; Mitchell, R.J.; van Oorschot, R.A. Secondary DNA transfer of biological substances under varying test conditions. *Forensic Sci. Int. Genet.* **2010**, *4*, 62–67. [CrossRef]
19. van Oorschot, R.A.H.; Meakin, G.E.; Kokshoorn, B.; Goray, M.; Szkuta, B. DNA Transfer in Forensic Science: Recent Progress towards Meeting Challenges. *Genes* **2024**, *12*, 1766. [CrossRef]
20. Cahill, A.; Volgin, L.; van Oorschot, R.A.H.; Taylor, D.; Goray, M. Where did it go? A study of DNA transfer in a social setting. *Forensic Sci. Int. Genet.* **2024**, *73*, 103101. [CrossRef]
21. Taylor, D.; Volgin, L.; Kokshoorn, B. Accounting for site-to-site DNA transfer on a packaged exhibit in an evaluation given activity level propositions. *Forensic Sci. Int. Genet.* **2024**, *73*, 103122. [CrossRef]

genes

Article

An Upper Bound on the Power of DNA to Distinguish Pedigree Relationships

Maarten Kruijver

Institute of Environmental Science and Research, Auckland 1142, New Zealand; maarten.kruijver@esr.cri.nz

Abstract: Background/Objectives: Dense genetic marker panels are increasingly used in kinship analysis for the identification of distant relatives. As more markers are available, it is possible to pinpoint IBD segments more precisely and more reliably, ultimately approaching close to continuously observed IBD. This study investigates the evidential value obtained for discrimination between common pedigree relationships if IBD is observed continuously across the autosomal genome without error. In the continuous case, the evidential value is limited only by the pedigree relationship and the recombination rates. **Methods:** We conducted simulations to generate IBD segments across the autosomal genome for individuals with defined pedigree relationships. The evidential value for relationship discrimination was then calculated exactly from the underlying model, assuming no genotyping error and full genome coverage. **Results:** The simulations show that the ability to distinguish pedigree relationships quickly diminishes as relationships become more distant. First cousins can be distinguished from second cousins with 99.9% accuracy which drops to 94% when distinguishing second and third cousins. Relationships with the same expected degree of relatedness can be discriminated using continuously observed IBD, although the effectiveness decreases with more distant relationships. **Conclusions:** Continuous IBD observation establishes a theoretical upper bound on the power to distinguish relationships if a large but finite number of markers is used. The findings provide a benchmark for evaluating kinship analyses based on finite genetic marker panels.

Keywords: identity by descent; kinship; relationship testing; investigative genetic genealogy

1. Introduction

The use of DNA to estimate family relationships is commonplace in areas ranging from animal conservation and crop improvement to paternity testing and missing persons identification [1]. There is a long history of using independent genetic markers and comparing the likelihood of the observations under two alternative hypotheses, dating at least back to Essen-Möller [2,3]. More recently, the use of dense SNP marker panels and direct-to-consumer genetic testing [4,5] has enabled the identification of more distant relatives, broadening the scope of applications to large-scale genetic genealogy. On a smaller scale, these methods have also been adopted in criminal investigations [6,7].

The move from a small number of genetic markers usually residing on different chromosomes to dense panels that contain many markers on the same chromosome has required changes to the way the genetic data are interpreted statistically [8–10]. Markers on the same chromosome can be inherited together, which complicates the calculation of pedigree likelihoods [11]. At a more fundamental level, there is increased awareness that the level of relatedness is not just described by the pedigree but can be seen as varying

continuously throughout the genome if viewed as the distance to their most recent common genetic ancestor at that location [12]. Although a pedigree-based notion of relatedness is the most widely used one in everyday life, it is not always the most useful definition in other contexts. For example, in medical studies realised relatedness may be more relevant than pedigree-based relatedness when considering genetic factors that influence disease risk or treatment response [13]. That notwithstanding, the current work adopts the pedigree perspective motivated by the relevance to human identification. Specifically, we ask the question: *how well can the different pedigree relationships be distinguished using genetic data from two persons*? To shed light on this question, we consider an idealised setting in which it is possible to observe identity by descent (IBD) continuously along the autosomal genome for a pair of persons. In practice, it is only possible to observe identity by state (IBS) for discrete genetic data, and this can be further complicated by genotyping errors. Because a segment can only be IBD if it is IBS, we may view relationship testing based on genetic marker data as an inferential problem with incomplete information, where the full information is IBD observed for a continuous genome. As a consequence, the power of discrimination of a procedure based on continuously observed IBD serves as an upper bound on what could be achieved in practice.

To answer the central question of this work, we simulate large numbers of samples of continuously observed IBD for various pedigree relationships. IBD is observed for two persons and these persons are assumed to not be related otherwise than through the pedigree. Based on the simulated data, we estimate how informative the data are for distinguishing relationships (e.g., first versus second cousins) by studying the empirical likelihood ratio distributions [14] and related summary statistics. These likelihood ratios are calculated using an exact likelihood model for the IBD segments. Both the simulations and calculations make use of the **ibdsegments** package for **R** [15]. The code that generates the results presented in the article is available online (https://github.com/mkruijver/an_upper_bound_paper_data accessed on 31 March 2025).

The power to distinguish pedigree relationships is assessed in several ways. When comparing two specific relationships, denoted as H_1 and H_2, the (log) likelihood ratio distributions for H_1 true and H_2 true show how well the relationships can be distinguished based on the data. If the curves have little overlap, then there is strong discriminative power. Numerical summaries are also given. Rates of misleading evidence, $\Pr(\mathrm{LR} > 1|H_2)$ and $\Pr(\mathrm{LR} < 1|H_1)$, inform us how often the evidence from the data is misleading rather than informative. The median LR's for H_1 true and H_2 true inform us how strongly the data typically support the correct hypothesis. If the rate of misleading evidence is small and the median LR of the H_1 true distribution is large, it is possible to reliably distinguish H_1 and H_2. Further, we estimate the accuracy of a classifier that assigns H_1 when $\mathrm{LR} \geq 1$ and H_2 otherwise. If H_1 and H_2 are equally probable, then the accuracy is the average of one minus the rates of misleading evidence. The accuracy is a single number that summarises how well relationships can be distinguished. Besides the power to distinguish pairs of relationships, we also investigate the power to identify the correct relationship from a set of more than two relationships.

Many previous studies have investigated the power of DNA to distinguish pedigree relationships if a certain set of markers or specific methodology is used. For example, Tillmar and Kling recently compared the performance of several SNP kits when used with different statistical methods [10]. In contrast, we directly study the information content of the IBD distribution, establishing an upper bound on the potential performance of any method. As far as we are aware, this is the first attempt to directly apply an exact likelihood-based approach to observations of continuous IBD segments. The modelling approach and

assumptions are, however, fairly standard. Specifically, we adopt Haldane's model for recombination [16] which assumes that crossovers occur according to a Poisson process along the genetic map, and we use sex-averaged recombination rates to simplify calculations. This approach has been widely used in variants of the Lander–Green algorithm [17,18]. The application to modelling continuous IBD goes back to Donnelly [19], who provided results about the probability of sharing some DNA for different pedigree relationships, effectively envisioning today's investigative genetic genealogy [20]. The current work does not only consider the probability of sharing some DNA but extends to a complete model for IBD segment observations.

2. Materials and Methods

2.1. Pedigree Relationships and IBD

We discuss several pairwise pedigree relationships (e.g., half-siblings, first cousins, etc.). Following the notation of [21], $\mathcal{P}$ denotes a pedigree, and a pairwise relationship between pedigree members a and b is a triple $(a, b, \mathcal{P})$. At any point on the genome, each pedigree founder can be assigned two founder haplotype labels representing two homologous chromosomes. Two pedigree members are said to be IBD1 at a location on a chromosome if they inherited the same founder haplotype. If the pedigree members share two founder haplotypes, then we say they are IBD2 (or double IBD), and if they do not share anything, then they are IBD0.

Several pedigree relationships were studied. Figure 1 illustrates some relationships and their abbreviations. In particular, we refer to the following relationships:

- Linear relationships: These are relationships between a person and their parent, grandparent (abbreviated GP), great-grandparent (abbreviated GGP), and so on. Beyond the GGP, these relationships are abbreviated as G^{n}GP with $n = 2, 3, \ldots$. The GP relationship is referred to as a linear relationship of degree 2, so G^{n}GP is a linear relationship of degree $n + 2$.
- Cousin relationships: These are relationships between linear descendants of two full siblings. First cousins are labelled 1C, second cousins 2C, and so on. Removal is indicated by the number and the letter R such that first cousins once removed becomes 1C1R. The full sibling relationship could be considered 0th cousins but this relationship is excluded from this study to simplify the analysis by considering the IBD status to be binary (0 or 1).
- Avuncular relationships: These are relationships between a person and (descendants of) a child of their full sibling. The uncle–nephew relationship is abbreviated as N. Great-nephew is abbreviated as GN. For $n \geq 2$, this relationship is abbreviated as G^{n}N.
- Half-cousin relationships: These are linear descendants of two half-siblings. These relationships are prefixed with the letter H, for example, H1C2R stands for half first cousins twice removed.

The ability to distinguish pedigree relationships based on genetic marker data relies on IBD [22]. For a given pedigree relationship, the expected proportion of a chromosome that is IBD can be computed. For example, full siblings are expected to share approximately 50% of their autosomal genome IBD on average: about 25% as IBD2 (both alleles identical by descent), 50% as IBD1 (one allele shared), and 25% as IBD0 (no alleles identical by descent). The realised quantities are different as a consequence of Mendelian inheritance and recombination [23]. For example, it is possible that full siblings are not IBD on one chromosome, while on another chromosome, they are partly IBD1 and partly IBD2.

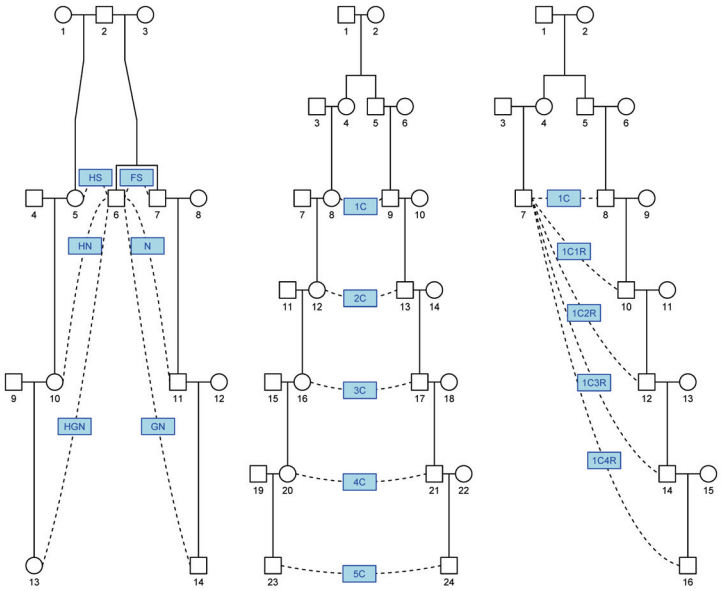

Figure 1. Common pedigree relationships. The left-hand side shows half-siblings (abbr. HS) (5, 6) and full siblings (abbr. FS) (6, 7). Descendants of the full siblings are the nephew (abbr. N) (6, 11) and great-nephew (abbr. GN) (6, 14). The corresponding half-relationships are HN (6, 10) and HGN (6, 13). The middle pedigree illustrates cousin relationships 1C (first cousins) up to 5C (fifth cousins), i.e., pairs of linear descendants of the full siblings (4, 5). The right-hand side illustrates cousin relationships with removal, e.g., 1C1R stands for first cousins once removed.

2.2. Relatedness Inference

In a recent review, Kling et al. discuss various approaches to infer genetic relationships between two or more persons [7]. The authors broadly distinguish two categories of approaches. The exploratory approaches aim to estimate one or more summary statistics from genetic data that are informative of the degree of relatedness or relationship. This category covers a wide range of approaches ranging from counting the number of shared alleles at STR loci [24] or estimating the kinship coefficient using dense SNP data (e.g., [25,26]) to directly identifying IBD segments using dense [27] or relatively sparse marker sets [28] and considering their length and/or count [29].

Kling et al. also discuss likelihood ratio approaches where the probability of the observed data under one hypothesis is compared to the probability of the observed data under another hypothesis. Likelihood ratio approaches are widely used in paternity testing [30] and other kinship testing using small panels of mostly independent markers [31]; however, these approaches are still emerging for use with denser marker panels for which the population genetic modelling is more complex [32].

Likelihood ratio approaches can make use of all available data to quantify the evidence for one hypothesis versus a second one [14]. The summary statistics produced in exploratory approaches are generally not sufficient to convey all the information that is informative of the data-generating hypothesis. This means that efficiency may be lost when these exploratory approaches are applied to discriminate between two pedigree relationships instead of a likelihood ratio-based approach that models all the data. In practice, likelihood ratio approaches are sensitive to model misspecification and measurement error, for instance when population genetic assumptions are not met or measurements are unreliable, which may cause increased rates of misleading evidence [33,34]. A practical benefit of exploratory approaches is that these may be more amenable to the use of statistics that can be estimated robustly, for instance when genotyping error or population genetics

are complicating factors. The distinction between exploratory approaches and likelihood ratio approaches is blurred by score-based likelihood ratio approaches in which likelihood ratios are assigned based on summary statistics, or scores, instead of the raw data.

2.3. Continuous IBD

We briefly sketch how computations and simulations involving continuous IBD are implemented in the **ibdsegments** package. Further details are available in the package documentation and the references therein. We applied a likelihood ratio approach where the data are continuously observed IBD segments without error. We viewed the chromosome as a continuum and assumed Haldane's model of recombination [16] with equal recombination rates for males and females. For a given pedigree relationship, the IBD state at a point on a continuous chromosome of length L centiMorgan (cM) is a random variable $(X_t, t \geq 0)$ taking values in a finite set S of identity states for $0 \leq t \leq L$. In the remainder, we keep the exposition simple and in line with investigative genetic genealogy practice by considering only the two identity states IBD0 and IBD1: $S = \{0, 1\}$. The algorithms and software used support other choices for the set S of identity states as well. For example, one could also chose the three states IBD0 to IBD2, the nine condensed, or the fifteen detailed identity states [35]. The current work was restricted to IBD0 and IBD1, so the IBD state could be conveniently viewed as an indicator variable, which simplified the methodology. Because the full sibling relationship had an IBD2 probability greater than zero, it was not considered.

2.3.1. IBD Vector and the Hidden Markov Model

Applying Haldane's model for recombination, the IBD process can be seen as a continuous-time Hidden Markov Model [36], where the observed variable is X_t. The hidden component is the binary IBD vector V_t that tracks for each meiosis whether the grandpaternal or grandmaternal haplotype segment is passed down. See Figure 2 for a schematic illustration of the relationship between X_t and V_t. This setup is also the basis for the widely used Lander–Green algorithm [17].

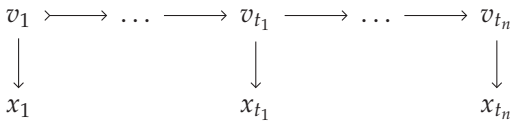

Figure 2. Hidden Markov Model relating the continuously observed IBD state (X_t) to the underlying hidden pedigree IBD state (V).

For a pedigree with n_{nf} non-founders, there are $2 \times n_{nf}$ meioses tracked by the IBD vector, so V_t has length $2 \times n_{nf}$. Because each element of the vector is binary (0 or 1), there are $2^{2 \times n_{nf}} =: n_v$ possible IBD vectors. Thus, the state space of the Hidden Markov Model has n_v elements and can be identified with the integers $0, \ldots, n_v - 1$. Note that in practice, the size of the state space can be reduced by exploiting symmetries [37,38] which further complicates implementation details. Crossovers for individual meioses have inter-arrival times with $\lambda = 0.01$ crossovers per cM. It follows that the transition intensity q_{ab} from state a to state b of the whole IBD vector with $a, b \in 0, \ldots, n_v - 1$ is:

$$q_{ab} = \begin{cases} -\sum_{c \neq a} q_{ac}, & \text{if } a = b, \\ 0.01, & \text{if Hamming}(a, b) = 1, \\ 0, & \text{otherwise,} \end{cases}$$

where Hamming(a, b) denotes the Hamming distance between the binary representations of integer states a and b (i.e., the number of bits by which they differ). The transition intensity q_{ab} represents the instantaneous rate of transitioning from IBD state a to state b. The rate $q_{ab} = 0.01$ applies only when the binary representation of a and b differ by exactly one bit, i.e., differ by one crossover in the pedigree. The diagonal entries q_{aa} are chosen so that each row of the intensity matrix sums to zero as is required for a continuous-time Markov process.

2.3.2. Simulating Continuous IBD

For all but the simplest pedigree relationships, the IBD process (X_t) cannot be easily analysed using standard probability distributions. Although individual meioses yield exponential inter-arrival times for crossovers, the joint effect of crossovers throughout the pedigree leads to non-standard IBD segment length distributions. However, it is possible to simulate large numbers of realisations of X_t at little computational cost by simulating the individual crossovers represented in V_t and determining X_t from V_t. The **ibdsegments** package was used to simulate Mendelian inheritance and crossover for the 22 autosomes. The simulation procedure worked by randomly flipping bits of the unobserved IBD vector with exponential inter-arrival times. A sex-averaged genetic map [39] was used with Haldane's model for recombination events [16]. For example, Table 1 shows data obtained from the result of a simulation for a pair of first cousins at a chromosome of length 100 cM. There are 4 non-founders in the pedigree, so there are 8 meioses and $2^8 = 256$ possible IBD vectors. Each row of **(a)** shows a segment for which the IBD state does not change. The underlying IBD vector (V_t) is shown in **(b)**. Note that while the table shows a realisation of the simulation for a single chromosome, the simulations in this study comprised 22 chromosomes of different lengths.

Table 1. Example of simulated IBD segments for a pair of first cousins on a chromosome of length 100 cM. **(a)** shows IBD segments only, while **(b)** shows the full IBD vector as both integer indices and their corresponding binary representations.

(a) Simulated IBD Segments Only			
Start (cM)	**End (cM)**	**Length (cM)**	**IBD State (X_t)**
0.00	5.06	5.06	1
5.06	29.06	24.00	0
29.06	93.94	64.88	1
93.94	100.00	6.06	0
(b) Unobserved IBD vector represented by an integer and the binary representation			
Start (cM)	**End (cM)**	**Length (cM)**	**IBD vector (V_t)**
0.00	5.06	5.06	47: [0 0 1 0 1 1 1 1]
5.06	26.69	21.63	63: [0 0 1 1 1 1 1 1]
26.69	27.81	1.12	191: [1 0 1 1 1 1 1 1]
27.81	29.06	1.25	183: [1 0 1 1 0 1 1 1]
29.06	47.96	18.90	167: [1 0 1 0 0 1 1 1]
47.96	49.91	1.96	175: [1 0 1 0 1 1 1 1]
49.91	78.40	28.49	167: [1 0 1 0 0 1 1 1]
78.40	93.94	15.54	135: [1 0 0 0 0 1 1 1]
93.94	100.00	6.06	199: [1 1 0 0 0 1 1 1]

2.3.3. Expectation and Variance of Total IBD

For many relationships, the single point probability distribution of (X_t)—also referred to as identity coefficients—is reproduced in textbooks, and software tools are available to compute it for any relationship [40]. We denote the three identity coefficients for IBD0,

IBD1, and IBD2 as κ_0, κ_1, and κ_2, that is $\kappa_1 = \Pr(\text{IBD1})$. In the **ibdsegments** package, these identity coefficients can be computed for arbitrary pairs of pedigree members. The package uses a brute-force algorithm that exhaustively iterates through all possible, equally probable IBD vectors. For each vector, founder haplotype labels are dropped through the pedigree to determine if the identity state is realised and the probability has to be incremented.

In the current work, we were also interested in the full stochastic process $(X_t, t \geq 0)$ observed continuously over $t \in [0, L]$ with X_t taking values 0 and 1 corresponding to the IBD0 and IBD1 states. For a chromosome of length L, we defined total IBD, T, as the combined length of all IBD1 segments on the chromosome:

$$T = \int_0^L I_{\{X_t=1\}} \, \mathrm{d}t, \tag{1}$$

where I_A denotes the indicator function that is 1 for A and 0 otherwise. The expectation and variance of T can be relatively easily computed. Since $\Pr(X_t = 1)$ does not depend on t, we may write the expected value of T as the product of κ_1 and L:

$$\mathrm{E}(T) = \int_0^L \kappa_1 \, \mathrm{d}t = \kappa_1 L. \tag{2}$$

The variance of T can be calculated as $\mathrm{Var}(T) = \mathrm{E}(T^2) - \mathrm{E}(T)^2$, where the term $\mathrm{E}(T^2)$ depends on the joint distribution X_u, X_v for $0 \leq u, v \leq L$. In Haldane's model of recombination, this distribution depends only on the distance $|u - v|$, so we may compute the variance of T by double numerical integration of the two-locus IBD probability [41–43].

$$\mathrm{E}(T^2) = \int_0^L \int_0^L I_{\{X_u=X_v=1\}} \, \mathrm{d}v \, \mathrm{d}u = \int_0^L \int_0^L \kappa_{11}(|u - v|) \, \mathrm{d}v \, \mathrm{d}u, \tag{3}$$

where $\kappa_{11}(|u - v|)$ denotes the two-locus IBD probability for loci separated by $|u - v|$ cM.

When more than one chromosome is considered, we denote the total IBD across the chromosomes as T_+. The chromosomes are assumed to be independent so expectations and variances can be summed.

2.3.4. Probability of No IBD: $\Pr(T = 0)$

Computing the probability of no IBD across a chromosome, $\Pr(T = 0)$, requires more elaborate calculations involving the IBD process. $\Pr(T = 0)$ can be written as

$$\Pr(T = 0) = \Pr(X_t = 0, \forall t \in [0, L]). \tag{4}$$

The IBD vector has to only take on values for which the observed IBD state is 0; however, neither the state nor the number of state transmissions (recombination events) are observed. The probability $\Pr(T = 0)$ can be computed by conditioning on the number of recombination events in the pedigree—Poisson-distributed—and then enumerating all possible paths that are compatible with no IBD:

$$\Pr(X_t = 0, \forall t \in [0, L]) = \sum_{k=0}^{\infty} \Pr(N = k) \Pr(X_t = 0, \forall t \in [0, L] | N = k) \tag{5}$$

$$= \sum_{k=0}^{\infty} \Pr(N = k) \sum_{v_0, \ldots, v_k \in V^0} p_{v_0} \prod_{j=1}^{k} p_{v_{j-1}, v_j}, \tag{6}$$

where

- $\Pr(N = k) = \exp(-\lambda)\lambda^k/k!$ since the number of recombination events in the pedigree is Poisson-distributed, $N \sim \text{Poisson}(\lambda)$, with $\lambda = 0.01 \times L \times 2n_{nf}$, where n_{nf} is the number of non-founders in the pedigree.
- The sum over k can be truncated after a finite value $k_{\max}$. Choosing the $1 - \epsilon$-quantile of the Poisson distribution ensures the truncation error is smaller than ϵ.
- V^0 is the set of paths for which the IBD state remains 0.
- p_{v_0} denotes the prior probability $\Pr(V_0 = v_0)$ of starting in v_0. This probability equals $1/n_v$ where n_v is the number of IBD vectors.
- p_{v_{j-1},v_j} is shorthand for $\Pr(V_j = v_j | V_{j-1} = v_{j-1})$.

In practice, explicitly enumerating all possible paths that are compatible with no IBD and summing over those is not feasible. Instead, the forward algorithm [44] is used to efficiently compute the probability of the observed sequence under the Hidden Markov Model. Although the IBD vector at each position is unobserved, only the states in V^0 are considered in the computation. The forward algorithm recursively computes, for each discrete step m, the probability of being in each compatible hidden state given the observations up to time m. Let $\alpha_m(v) = \Pr(V_m = v, \text{ all observed IBD states up to } m \text{ are } 0)$ for $v \in V^0$. Then, the forward recursion is given by:

$$\alpha_0(v) = 1/n_v, \quad \text{for } v \in V^0,$$

$$\alpha_m(v) = \sum_{u \in V^0} \alpha_{m-1}(u) p_{u,v}, \quad \text{for } v \in V^0,$$

where $p_{u,v} = \Pr(V_t = v \mid V_{t-1} = u)$ is the transition probability from u to v. This transition probability is $1/n_{nf}$ if u and v differ by one bit and zero otherwise. The recursion proceeds up to $k_{\max}$. Finally, the probability of observing no IBD across the entire chromosome is obtained by summing over the forward probabilities:

$$\Pr(X_t = 0, \forall t \in [0, L]) = \sum_{k=0}^{k_{\max}} \Pr(N = k) \sum_{v \in V^0} \alpha_k(v). \tag{7}$$

2.3.5. Likelihoods for IBD Segments

Computing the likelihood of a realisation of the continuous IBD process (such as displayed in Table 1) is approached similarly. As in the previous section, the key idea is to use the forward algorithm to efficiently sum over all unobserved IBD vectors that are compatible with the observed IBD segments. Let $t_1, \ldots, t_n$ be the endpoints of the n segments, and let x_i denote the IBD status of the segment ending at t_i. The likelihood of the segment observations can be computed iteratively for each segment where the IBD vector is captured in the probability of V_t at the start of the segment. Writing v_{i-} for the unobserved state at the start of segment i,

$$\Pr(\mathbf{x}, \mathbf{t}) = \Pr(x_1, t_1, \ldots, x_n, t_n | H) \tag{8}$$

$$= \Pr(x_1, t_1 | H) \prod_{i=2}^{n} \Pr(x_i, t_i | x_1, \ldots, x_{i-1}, t_1, \ldots, t_{i-1}, H) \tag{9}$$

$$= \prod_{i=1}^{n} \sum_{v_{i-} \in S^{x_i}} \Pr(x_i, t_i | v_{i-}, H) \Pr(v_{i-} | x_1, \ldots, x_{i-1}, t_1, \ldots, t_{i-1}, H). \tag{10}$$

The probabilities $\Pr(x_i, t_i | v_{i-}, H)$ are computed analogous to the method of the previous section by summing over the forward probabilities. The probabilities of v_{i-} are also obtained from the forward pass. Finally, since chromosomes are assumed to be independent,

the likelihood ratio for a whole genome observation is the product of likelihood ratios per chromosome.

2.3.6. Likelihood Ratios for IBD Segments

After simulating many realisations of the continuous IBD process for all considered pedigree relationships, we may compute likelihood ratios for the simulated data where H_1 is one relationship and H_2 is another. This yields an empirical distribution of likelihood ratios for H_1 true and H_2 true. Kernel density estimates of the $\log_{10}$ likelihood ratios are shown in a plot, and numerical summaries are also provided.

We also considered the power to distinguish between more than two relationships. In this scenario, likelihood ratios are computed for hypothesis pairs of the form where H_1 is a relationship and H_2 is all other relationships in the set under consideration. For example, when considering the relationships GP, HS, and N, we may have the proposition pair:

$$H_1 : \text{HS}, \tag{11}$$

$$H_2 : \overline{\text{HS}} = \text{GP}, \text{N}. \tag{12}$$

Assuming equal prior probabilities for all alternatives, the likelihood ratio is then

$$\text{LR} = \frac{\Pr(E|H_1)}{\Pr(E|H_2)} = \frac{\Pr(E|H_{\text{HS}})}{\Pr(E|H_{\overline{\text{HS}}})} = \frac{\Pr(E|H_{\text{HS}})}{1/2 \times \Pr(E|H_{\text{GP}}) + 1/2 \times \Pr(E|H_{\text{N}})}, \tag{13}$$

where E denotes the whole-genome continuous IBD segment observations.

2.4. Exploring IBD and Segment Count Distributions

As a first experiment towards answering the main question posed in this work, we proceeded by establishing an overview of which relationships could be distinguished reliably on the basis of summary statistics of IBD sharing. For a set of relationships, the following summary statistics were computed:

- κ_1: the probability of (single) IBD at any point.
- The expectation and standard deviation of T_+ (total IBD), the combined length (cM) of all IBD segments.
- The expectation and standard deviation of the segment count.
- $\Pr(T_+ = 0)$: the probability of not sharing any autosomal DNA across the 22 chromosomes.
- The expectation and standard deviation of N_0, the number of chromosomes for which there is no IBD.

These statistics were exactly computed. Relationships with large differences in the summary statistics were relatively easily distinguished. However, these summary statistics did not contain all the information contained in the IBD process, and there were relationships that were distinguishable based on the full data but not based on T_+. To illustrate this, we simulated 100,000 realisations of continuous IBD for all pedigree relationships and plotted the empirical distributions of the following:

- Segment count: the number of IBD segments across the autosomal genome.
- T_+ (total IBD): the combined length (cM) of all IBD segments.

2.5. Empirical LRs for Distinguishing Relationships Using Continuous IBD

The main question of this work was directly investigated by studying likelihood ratio distributions for continuously observed IBD. The following scenarios were investigated. First, the power to distinguish relationships with different κ_1 was investigated for

- Linear relationships;
- Cousin-type relationships.

Secondly, the power to distinguish relationships with identical κ_1 was investigated for $\kappa_1 = 1/2, 1/4, 1/8$.

3. Results

3.1. Exploring Total IBD and Segment Count

The complete pattern of IBD sharing for a pedigree relationship is described by a complex stochastic process. Fortunately, a large part of the story can be understood by studying simple summary statistics. Table 2 shows κ_1, the moments of T_+, the moments of the segment count, $\Pr(T_+ = 0)$, and the moments of N_0 for various relationships. We made several high-level observations:

- Close relationships (larger κ_1) could be reliably distinguished from distant relationships (smaller κ_1) because the distributions of total IBD were well separated.
- As the relationships became more distant, the total expected IBD decreased while the standard deviation increased relative to the expected value. This means that the distributions of total IBD had more overlap as relationships became more distant.
- Relationships with identical κ_1 had the same expected total IBD. For example, relationships with $\kappa_1 = 1/2$ included GP, N, and HS, and these were all expected to share 1696 cM. However, their IBD distributions were not the same as evidenced by differences in the standard deviations. Thus, it may be possible to distinguish these relationships based on data beyond total IBD, such as segment count.
- The differences in IBD distributions between relationships with the same κ_1 decreased quickly as relationships became more distant. The standard deviation of total IBD, Pr(total IBD = 0) and the expected value and standard deviation of the number of chromosomes without IBD all showed a similar trend of convergence within the groups of relationships with the same κ_1. It was therefore not possible to reliably distinguish higher-order relationships with the same κ_1.
- Many cousin-type relationships such as 2C and 1C2R could not be distinguished because the IBD distributions were identical. Donnelly [19] considered cousin-type relationships of the type "sth cousins t times removed" where $s \geq 1$ and $t \geq 0$ and showed that the IBD distribution depended on $2s + t$.
- For higher-order relationships, there was a substantial probability that no DNA was shared at all. For fifth cousins, there was about a 69% probability of not sharing DNA. For fourth cousins, this probability was about 30%.

Segment count is a useful statistic to distinguish relationships when the expected total IBD is identical. Figure 3 shows box plots of total IBD and segment count for 100,000 simulations of continuous IBD for the studied pedigree relationships. The figure demonstrates the extra resolution gained from considering the number of segments on top of total IBD. In particular, we observed the following:

- GP, HS, and N (all with $\kappa_1 = 1/2$) had mostly overlapping total IBD distributions but could be distinguished based on segment count.
- GGP, HN, GN, and 1C (all with $\kappa_1 = 1/4$) had mostly overlapping total IBD distributions and partly overlapping distributions of segment count.
- There appeared to be limited information in the segment count for distinguishing relationships with κ_1 smaller than, say, $1/4$.
- As relationships become more distant, both the distributions of total IBD and segment count became highly skewed.

Table 2. IBD distributions summarised for common pedigree relationships.

Relationship	κ_1	Total IBD (cM)		Segment Count		$\Pr(T_+ = 0)$	$N_{T_i=0}$	
		Expected	S.d.	Expected	S.d.		Expected	S.d.
GP	1/2	1695.68	243.48	27.96	3.38	4.455×10^{-22}	2.67	1.51
HS	1/2	1695.68	188.64	44.91	4.44	8.326×10^{-37}	0.80	0.86
N	1/2	1695.68	174.35	53.39	4.94	2.091×10^{-43}	0.49	0.68
GGP	1/4	847.84	196.31	22.46	4.02	2.264×10^{-12}	6.80	2.13
HN	1/4	847.84	173.26	30.94	4.99	1.512×10^{-15}	5.03	1.93
GN	1/4	847.84	167.35	35.17	5.56	1.828×10^{-16}	4.61	1.87
1C	1/4	847.84	148.60	39.41	5.24	1.148×10^{-21}	2.95	1.55
G^2GP	1/8	423.92	139.15	15.47	3.89	1.903×10^{-7}	11.07	2.31
H1C	1/8	423.92	127.39	19.71	4.61	9.641×10^{-9}	9.74	2.29
G^2N	1/8	423.92	124.22	21.83	5.05	3.854×10^{-9}	9.37	2.27
1C1R	1/8	423.92	115.34	23.95	5.02	1.425×10^{-10}	8.16	2.22
G^3GP	1/16	211.96	94.45	9.85	3.36	0.0001	14.66	2.18
H1C1R	1/16	211.96	87.97	11.97	3.86	2.860×10^{-5}	13.79	2.24
G^3N	1/16	211.96	86.14	13.03	4.16	1.808×10^{-5}	13.52	2.25
2C	1/16	211.96	81.46	14.09	4.19	4.761×10^{-6}	12.76	2.28
G^4GP	1/32	105.98	63.05	5.99	2.72	0.0050	17.33	1.90
H2C	1/32	105.98	59.33	7.05	3.05	0.0025	16.80	1.97
G^4N	1/32	105.98	58.22	7.58	3.25	0.0019	16.62	2.00
2C1R	1/32	105.98	55.62	8.11	3.29	0.0011	16.18	2.05
G^5GP	1/64	52.99	41.86	3.52	2.12	0.0460	19.14	1.57
H2C1R	1/64	52.99	39.66	4.05	2.33	0.0322	18.84	1.64
G^5N	1/64	52.99	38.98	4.32	2.46	0.0283	18.73	1.66
3C	1/64	52.99	37.49	4.58	2.49	0.0211	18.49	1.71
G^6GP	1/128	26.49	27.80	2.03	1.61	0.1702	20.30	1.25
H3C	1/128	26.49	26.47	2.29	1.75	0.1415	20.14	1.30
G^6N	1/128	26.49	26.04	2.42	1.83	0.1321	20.07	1.32
3C1R	1/128	26.49	25.17	2.56	1.86	0.1144	19.94	1.36
G^7GP	1/256	13.25	18.51	1.15	1.21	0.3653	21.02	0.97
H3C1R	1/256	13.25	17.70	1.28	1.30	0.3319	20.93	1.01
G^7N	1/256	13.25	17.42	1.34	1.35	0.3200	20.89	1.02
4C	1/256	13.25	16.90	1.41	1.37	0.2979	20.82	1.05
G^8GP	1/512	6.62	12.37	0.64	0.89	0.5674	21.44	0.74
H4C	1/512	6.62	11.87	0.71	0.95	0.5400	21.39	0.77
G^8N	1/512	6.62	11.69	0.74	0.99	0.5296	21.37	0.78
4C1R	1/512	6.62	11.38	0.77	1.00	0.5110	21.34	0.80
G^9GP	1/1024	3.31	8.30	0.35	0.66	0.7293	21.69	0.56
H4C1R	1/1024	3.31	7.99	0.39	0.70	0.7109	21.66	0.58
G^9N	1/1024	3.31	7.87	0.40	0.72	0.7037	21.65	0.59
5C	1/1024	3.31	7.68	0.42	0.73	0.6912	21.63	0.60

As a final exploratory remark, we further illustrate differences between the IBD distributions of GP, HS, and N on a single chromosome. Assume that two persons are IBD at the start of a chromosome and consider the probability density function of the length of the segment, i.e., the distance until a recombination event disrupts the IBD. Figure 4 shows this probability density function (left) and the corresponding hazard rate [45,46] (right). For a continuous random variable with density $f(x), x \geq 0$ and distribution function $F(x) = \Pr(X \leq x)$, the hazard rate is $h(x) = \frac{f(x)}{1-F(x)} = \frac{f(x)}{S(x)}$, where $S(x) = 1 - F(x)$ is the survival function. The hazard rate represents the instantaneous rate at which two individuals switch from being IBD to not IBD, given that they were IBD up to that specific point on the chromosome. In our simulations, we observed the following:

- For HS, IBD occurred if and only if the shared parent passed down the same DNA to both offspring. Two meioses could break the IBD, so the segment length followed an $\text{Exp}(0.02)$ distribution with a constant hazard rate of 0.02.

- For GP, only one meiosis broke the IBD, so the segment length followed an $\mathrm{Exp}(0.01)$ distribution with a constant hazard rate of 0.01.
- For N, there were two cases. Either the parent and uncle (who are siblings) were double IBD or single IBD. If they were double IBD, then it did not matter whether the grandpaternal or grandmaternal segment was transmitted from the parent to the nephew (this did not break the segment); however, two meioses broke the segment, yielding a hazard rate of 0.02. In the single IBD case, there were three meioses that broke the segment, and the hazard rate was 0.03. Both cases were equally probable at the start of the segment, so the hazard rate was 0.025. However, as the segment progressed, the double IBD could become a single IBD and vice versa without breaking the segment. Over longer segment lengths, the probability of being in the double IBD state increased, which slightly reduced the hazard rate.

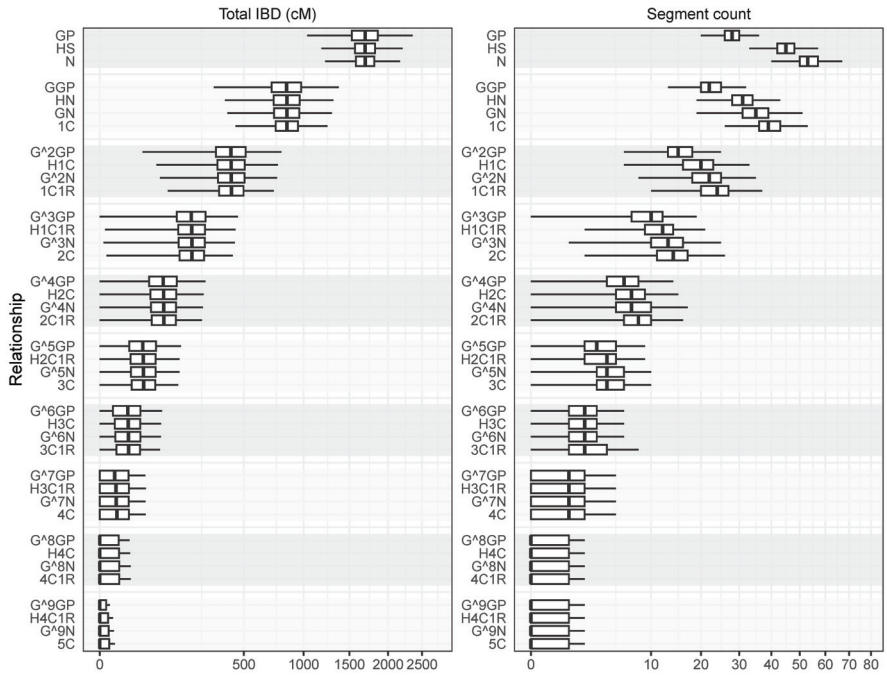

Figure 3. Realised total IBD (cM) and segment count for 100,000 simulations of pedigree relationships. Some relationships with the same expected degree of IBD such as N, GP, and HS can be distinguished based on segment count. As relationships become more distant, segment count quickly becomes less useful to distinguish between relationships with the same expected degree of IBD sharing.

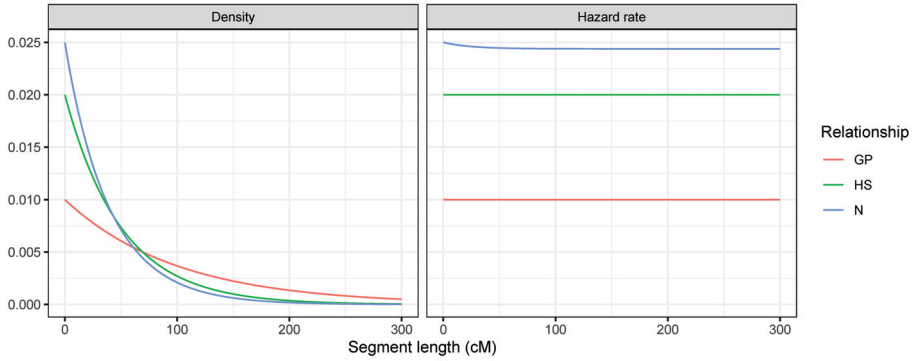

Figure 4. Segment length distributions at the start of a chromosome for three relationships with $\kappa_1 = 0.5$: grandparent–grandchild, half-siblings, and uncle–nephew.

3.2. Distinguishing Linear Relationships Using Continuous IBD

First, likelihood ratio distributions are presented for distinguishing linear relationships of degree d and $d+1$ for $d = 2, \ldots, 5$ based on continuous IBD. Note that $d = 2$ is the grandparent relationship, and $d = 5$ is the great-great-great-grandparent relationship. Figure 5 shows kernel density estimates of the log likelihood ratio distributions for H_1 true and H_2 true for $d = 2, \ldots, 5$. As expected, the curves for H_1 true and H_2 true had more overlap as d increased, indicating that these relationships were less distinguishable. When distinguishing between grandparents and great-grandparents, likelihood ratios were often in the millions or more for H_1 true, although the range was substantial. Distinguishing great-grandparents ($d = 3$) from great-great-grandparents ($d = 4$) was harder, with likelihood ratios typically in the hundreds or thousands when H_1 was true (the median was just under 200). Further numerical summaries are presented in Table 3. Notably, the accuracy decreased from 98% when distinguishing second- and third-degree linear relationships to 77% when distinguishing linear relationships of fifth and sixth degree.

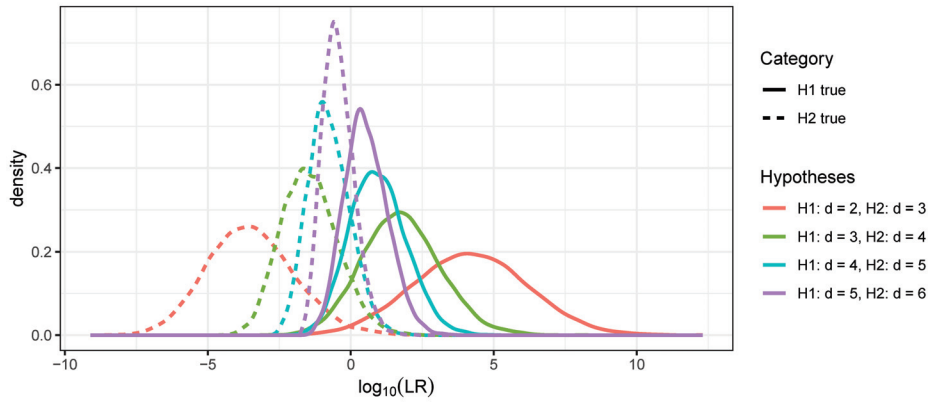

Figure 5. Kernel density estimates of 10,000 draws from LR distributions for distinguishing linear relationships of order d and $d+1$ for H_1 true (solid curves) and H_2 true (dashed curves).

Table 3. Summary of 10,000 draws from LR distributions for distinguishing between linear relationships of order d and $d+1$.

H_1	H_2	H_{true}	$\Pr(\text{LR} > 1)$	$\Pr(\text{LR} < 1)$	Median log LR	Accuracy
$d = 2$	$d = 3$	H_1	0.9837	0.0163	4.1709	0.983
		H_2	0.0177	0.9823	−3.5500	
$d = 3$	$d = 4$	H_1	0.9069	0.0931	1.7197	0.9123
		H_2	0.0824	0.9176	−1.4897	
$d = 4$	$d = 5$	H_1	0.8337	0.1663	0.9137	0.8397
		H_2	0.1544	0.8456	−0.8139	
$d = 5$	$d = 6$	H_1	0.7545	0.2455	0.4865	0.7743
		H_2	0.2060	0.7940	−0.4883	

3.3. Distinguishing Cousin Relationships Using Continuous IBD

Figure 6 shows boxplots of 10,000 draws from the LR distributions for distinguishing between cousin relationships of degree one to five. Boxplots were used instead of density estimates, because there were many samples with no IBD segments at all, especially for fifth cousins, which caused a point mass in the LR distribution. The boxplots show that first cousins could be distinguished from second cousins with LRs often in the billions in favour of the correct relationship. Distinguishing second cousins from third cousins

was considerably harder with LRs typically in the hundreds or thousands. A numerical summary of the same data is presented in Table 4. The table shows that the rate of misleading evidence increased sharply for higher-degree cousins. There was about a 6% chance of misleading evidence when distinguishing second and third cousins. This increased to 30% when distinguishing fourth from fifth cousins.

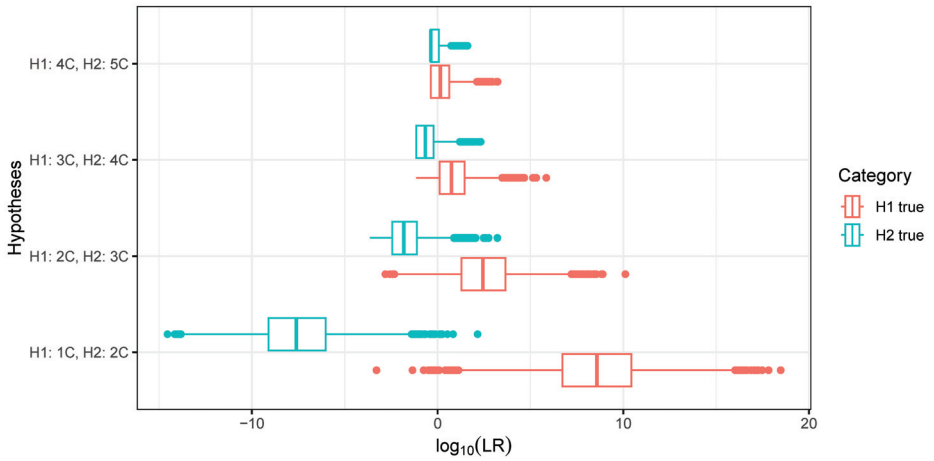

Figure 6. Boxplots of 10,000 draws from likelihood ratio distributions for distinguishing between sth and $(s+1)$th cousins for H_1 true and H_2 true.

Table 4. Summary of 10,000 draws from LR distributions for distinguishing between cousin relationships.

H_1	H_2	H_{true}	$\Pr(\text{LR} > 1)$	$\Pr(\text{LR} < 1)$	Median log LR	Accuracy
1C	2C	H_1	0.9986	0.0014	8.5754	0.9990
		H_2	0.0007	0.9993	−7.6095	
2C	3C	H_1	0.9342	0.0658	2.4376	0.9421
		H_2	0.0501	0.9499	−1.8169	
3C	4C	H_1	0.7770	0.2230	0.7456	0.8119
		H_2	0.1532	0.8468	−0.6617	
4C	5C	H_1	0.7009	0.2991	0.1516	0.6980
		H_2	0.3049	0.6951	−0.3655	

3.4. Distinguishing Relationships with Identical κ_1

It is well known that the total IBD length is informative of the degree of the relationship. It is not clear how much information there is in the IBD segments besides their combined length, especially when it comes to distinguishing relationships with the same κ_1. Likelihood ratio distributions for distinguishing relationships with $\kappa_1 = 1/2$, $\kappa_1 = 1/4$, and $\kappa_1 = 1/8$ are presented in Figure 7. Numerical summaries are provided in Table 5. For each set of relationships with identical expected total IBD (identical κ_1), 100,000 random samples of the likelihood ratio distributions were taken for H_1 true and H_2 true. H_1 was a relationship (e.g., GP), and H_2 was the complement of this relationship within the set of relationships with the same κ_1. For example, for H_1 : GP, the complement would be $H_2 : \overline{GP} = \{\text{HS}, \text{N}\}$. The alternatives in the composite hypothesis received equal weight in the likelihood of H_2.

Figure 7 and Table 5 demonstrate clearly that the power to discriminate relationships with the same κ_1 quickly diminished as the degree of the relationships increased. The accuracy decreased and the rates of misleading evidence increased with the degree of the

relationships. Second-degree relationships ($\kappa_1 = 1/2$) could be distinguished especially well. The GP relationship was often distinguished from the others (HS and N) with likelihood ratios in the millions or more; the median was 4.8 on a $\log_{10}$ scale. There was less information in the IBD process for distinguishing HS and N. This was also apparent from Figure 3, which showed that the segment count distribution of HS and N had considerable overlap. Note that the $\log_{10}$ likelihood ratio curves looked jagged, especially for GP (H_1 true) and HS (both H_1 true and H_2 true). This was not an effect of the small sample size but was caused by point masses in the chromosome-wise likelihood ratio distributions. For the GP relationship, the expected number of chromosomes with no IBD was 2.67, and the standard deviation was 1.51 (see Table 2).

Third-degree relationships $\kappa_1 = 1/4$ were less distinguishable than first-degree relationships. Again, the linear relationship (GGP) was most distinguishable from the rest; however, the accuracy for this relationship dropped to 94%, down from over 99% for second-degree relationships. There was little power to discriminate fourth-degree relationships $\kappa_1 = 1/8$. The linear relationship (G^2GP) was most separate from the others and could be distinguished with an accuracy of only 84%. The median $\log_{10}$ LR for that relationship was less than one for the H_1 true samples.

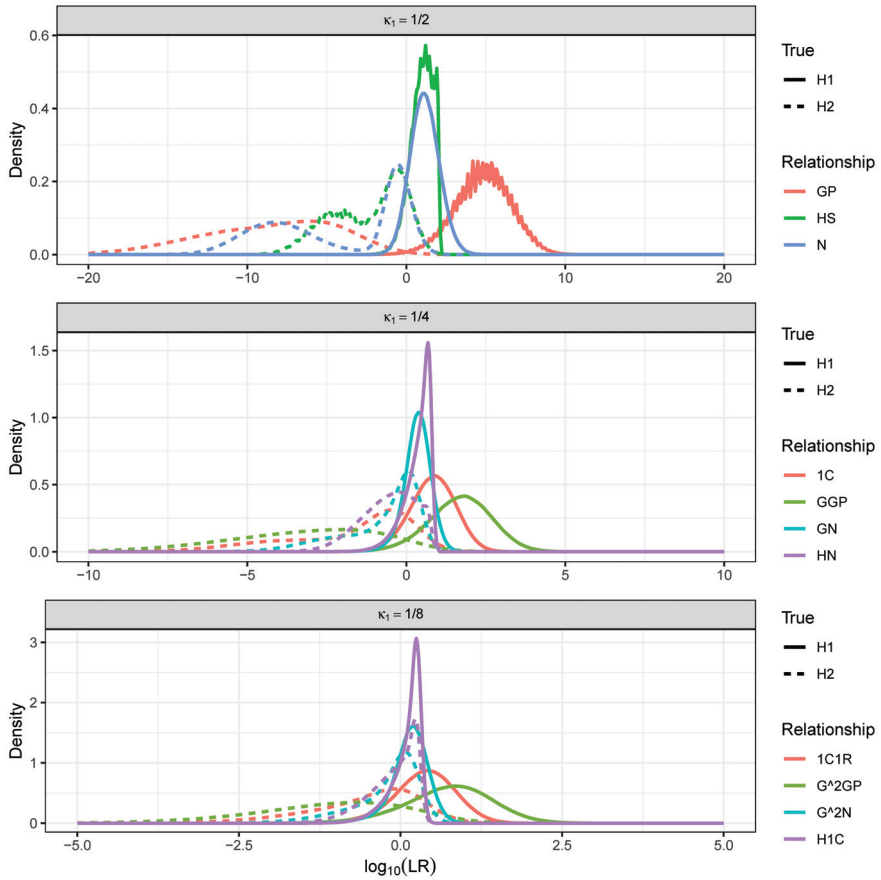

Figure 7. Density estimates of likelihood ratio distributions for distinguishing relationships with identical κ_1 for H_1 true and H_2 true. For each value of κ_1 and each relationship, likelihood ratios comparing H_1 (the relationship) and H_2 (another relationship with the same κ_1) were sampled (1,000,000 of each).

Table 5. Numerical summaries of random samples from LR distributions (H_1 true and H_2 true) for distinguishing relationships of the same degree. For each value of κ_1 and each relationship, likelihood ratios comparing H_1 (the relationship) and H_2 (another relationship with the same κ_1) were sampled (1,000,000 of each).

κ_1	H_1	H_2	H_{true}	$\Pr(\text{LR} > 1)$	$\Pr(\text{LR} < 1)$	Median log LR	Accuracy
1/2	GP	$\overline{\text{GP}}$	H_1	0.9944	0.0056	4.7944	0.9946
			H_2	0.0052	0.9948	−8.1254	
1/2	HS	$\overline{\text{HS}}$	H_1	0.9082	0.0918	1.0630	0.8823
			H_2	0.1436	0.8564	−1.7842	
1/2	N	$\overline{\text{N}}$	H_1	0.9023	0.0977	1.1379	0.8849
			H_2	0.1324	0.8676	−2.5758	
1/4	1C	$\overline{\text{1C}}$	H_1	0.8761	0.1239	0.8497	0.8509
			H_2	0.1742	0.8258	−1.1190	
1/4	GGP	$\overline{\text{GGP}}$	H_1	0.9503	0.0497	1.7242	0.9385
			H_2	0.0734	0.9266	−2.9268	
1/4	GN	$\overline{\text{GN}}$	H_1	0.8197	0.1803	0.3703	0.7465
			H_2	0.3267	0.6733	−0.3335	
1/4	HN	$\overline{\text{HN}}$	H_1	0.8213	0.1787	0.4690	0.7637
			H_2	0.2938	0.7062	−0.4700	
1/8	1C1R	$\overline{\text{1C1R}}$	H_1	0.7938	0.2062	0.3913	0.7510
			H_2	0.2918	0.7082	−0.3773	
1/8	G^2GP	$\overline{\text{G}^2\text{GP}}$	H_1	0.8637	0.1363	0.7782	0.8390
			H_2	0.1856	0.8144	−0.9586	
1/8	G^2N	$\overline{\text{G}^2\text{N}}$	H_1	0.7409	0.2591	0.1702	0.6578
			H_2	0.4253	0.5747	−0.0693	
1/8	H1C	$\overline{\text{H1C}}$	H_1	0.7375	0.2625	0.1660	0.6346
			H_2	0.4683	0.5317	−0.0322	

4. Discussion

Our results demonstrated that the ability to distinguish pedigree relationships quickly diminished as relationships became more distant. For example, first cousins could be distinguished from second cousins with 99.9% accuracy, second from third with 94% accuracy, and this dropped to 81% when distinguishing third from fourth cousins. We demonstrated that there was useful information in the IBD distribution beyond the total length of shared segments. This additional information could be used to distinguish relationships with the same degree. This was effective for distinguishing second-degree relationship. Grandparents could be separated from half-siblings and nephews with over 99% accuracy. There was less power to distinguish half-siblings and nephews. As the degree of the relationships increased, there was less information in the shared segments that could be used to distinguish relationships of the same degree. Half-nephews and grand-nephews were distinguished from other third-degree relationships with only 75% accuracy. First cousins could be distinguished with 85% accuracy and great-grandparents with 94% accuracy. There was very little information to distinguish the different fourth-degree relationships.

The results of this study provide an upper bound on the power for distinguishing relationships if IBD is observed continuously and without error. The upper bound of what is achievable in practice using dense SNP panels is lower. As relationships become more distant, the IBD segments become shorter and increasingly hard to detect.

Several simplifying assumptions were made in this study. Notably, sex-averaged crossover rates were used to simplify the calculations. It is well known that recombination rates are higher for female meioses than for males. For close relationships, this fact could be used to inform if DNA is more likely to be inherited via the paternal or maternal line. Further, we assumed Haldane's model of recombinations, which assumes the absence of chiasma interference.

In future work, the simplifying modelling assumptions may be relaxed. There is also scope to investigate the use of IBD on the X chromosome. As far as we are aware, the evidential value of IBD segments on the X chromosome has not been quantified for distinguishing pedigree relationships. Finally, we mention that the current work only considered IBD for two pedigree members at a time. A natural generalisation would be to consider the problem of identifying the most likely relationship on the basis of IBD between more than two pedigree members. For example, given a pedigree with persons a and b, one could ask where person c would fit best in the pedigree given identified IBD segments between c and a and c and b.

Funding: This research received no external funding.

Institutional Review Board Statement: Not applicable.

Informed Consent Statement: Not applicable.

Data Availability Statement: The code to generate plots and tables is available from https://github.com/mkruijver/an_upper_bound_paper_data (accessed on 23 April 2025).

Conflicts of Interest: The author declares no conflicts of interest.

References

1. Skare, Ø.; Sheehan, N.; Egeland, T. Identification of distant family relationships. *Bioinformatics* **2009**, *25*, 2376–2382. [CrossRef] [PubMed]
2. Essen-Moller, E. Die Beweiskraft der Ahnlichkeit im Vaterschaftsnachweis-theoretische Grundlagen. *Mitteilungen Anthropol. Ges. Wien* **1938**, *68*, 9–53.
3. Egeland, T.; Mostad, P.F. Statistical genetics and genetical statistics: A forensic perspective. *Scand. J. Stat.* **2002**, *29*, 297–307. [CrossRef]
4. Glynn, C.L. Bridging disciplines to form a new one: The emergence of forensic genetic genealogy. *Genes* **2022**, *13*, 1381. [CrossRef] [PubMed]
5. Martins, M.F.; Murry, L.T.; Telford, L.; Moriarty, F. Direct-to-consumer genetic testing: An updated systematic review of healthcare professionals' knowledge and views, and ethical and legal concerns. *Eur. J. Hum. Genet.* **2022**, *30*, 1331–1343. [CrossRef]
6. Erlich, Y.; Shor, T.; Pe'er, I.; Carmi, S. Identity inference of genomic data using long-range familial searches. *Science* **2018**, *362*, 690–694. [CrossRef]
7. Kling, D.; Phillips, C.; Kennett, D.; Tillmar, A. Investigative genetic genealogy: Current methods, knowledge and practice. *Forensic Sci. Int. Genet.* **2021**, *52*, 102474. [CrossRef]
8. Weir, B.S.; Anderson, A.D.; Hepler, A.B. Genetic relatedness analysis: Modern data and new challenges. *Nat. Rev. Genet.* **2006**, *7*, 771–780. [CrossRef]
9. Henn, B.M.; Hon, L.; Macpherson, J.M.; Eriksson, N.; Saxonov, S.; Pe'er, I.; Mountain, J.L. Cryptic distant relatives are common in both isolated and cosmopolitan genetic samples. *PLoS ONE* **2012**, *7*, e34267. [CrossRef]
10. Tillmar, A.; Kling, D. Comparative Study of Statistical Approaches and SNP Panels to Infer Distant Relationships in Forensic Genetics. *Genes* **2025**, *16*, 114. . [CrossRef]
11. Balding, D.J.; Bishop, M.; Cannings, C. *Handbook of Statistical Genetics*; John Wiley & Sons: Hoboken, NJ, USA, 2008.
12. Speed, D.; Balding, D.J. Relatedness in the post-genomic era: Is it still useful? *Nat. Rev. Genet.* **2015**, *16*, 33–44. [CrossRef] [PubMed]
13. Rousset, F. Inbreeding and relatedness coefficients: What do they measure? *Heredity* **2002**, *88*, 371–380. [CrossRef] [PubMed]
14. Meester, R.; Slooten, K. *Probability and Forensic Evidence: Theory, Philosophy, and Applications*; Cambridge University Press: Cambridge, UK, 2021.

15. R Core Team. *R: A Language and Environment for Statistical Computing*; R Foundation for Statistical Computing: Vienna, Austria, 2024.
16. Lange, K. *Mathematical and Statistical Methods for Genetic Analysis*; Springer: Berlin/Heidelberg, Germany, 2002; Volume 488.
17. Lander, E.S.; Green, P. Construction of multilocus genetic linkage maps in humans. *Proc. Natl. Acad. Sci. USA* **1987**, *84*, 2363–2367. [CrossRef]
18. Kruglyak, L.; Lander, E.S. Faster multipoint linkage analysis using Fourier transforms. *J. Comput. Biol.* **1998**, *5*, 1–7. [CrossRef] [PubMed]
19. Donnelly, K.P. The probability that related individuals share some section of genome identical by descent. *Theor. Popul. Biol.* **1983**, *23*, 34–63. [CrossRef] [PubMed]
20. Edge, M.D.; Coop, G. Donnelly (1983) and the limits of genetic genealogy. *Theor. Popul. Biol.* **2020**, *133*, 23–24. [CrossRef]
21. Vigeland, M.D. *Pedigree Analysis in R*; Academic Press: Cambridge, MA, USA, 2021.
22. Thompson, E.A. Identity by Descent: Variation in Meiosis, Across Genomes, and in Populations. *Genetics* **2013**, *194*, 301–326. [CrossRef]
23. Hill, W.G.; Weir, B.S. Variation in actual relationship as a consequence of Mendelian sampling and linkage. *Genet. Res.* **2011**, *93*, 47–64. [CrossRef]
24. Balding, D.J.; Krawczak, M.; Buckleton, J.S.; Curran, J.M. Decision-making in familial database searching: KI alone or not alone? *Forensic Sci. Int. Genet.* **2013**, *7*, 52–54. [CrossRef]
25. Manichaikul, A.; Mychaleckyj, J.C.; Rich, S.S.; Daly, K.; Sale, M.; Chen, W.M. Robust relationship inference in genome-wide association studies. *Bioinformatics* **2010**, *26*, 2867–2873. [CrossRef]
26. Gorden, E.M.; Greytak, E.M.; Sturk-Andreaggi, K.; Cady, J.; McMahon, T.P.; Armentrout, S.; Marshall, C. Extended kinship analysis of historical remains using SNP capture. *Forensic Sci. Int. Genet.* **2022**, *57*, 102636. [CrossRef] [PubMed]
27. Durand, E.Y.; Eriksson, N.; McLean, C.Y. Reducing pervasive false-positive identical-by-descent segments detected by large-scale pedigree analysis. *Mol. Biol. Evol.* **2014**, *31*, 2212–2222. [CrossRef]
28. Snedecor, J.; Fennell, T.; Stadick, S.; Homer, N.; Antunes, J.; Stephens, K.; Holt, C. Fast and accurate kinship estimation using sparse SNPs in relatively large database searches. *Forensic Sci. Int. Genet.* **2022**, *61*, 102769. [CrossRef] [PubMed]
29. Bettinger, B. The shared cM project: A demonstration of the power of citizen science. *J. Genet. Geneal* **2016**, *8*, 38–42.
30. Gjertson, D.W.; Brenner, C.H.; Baur, M.P.; Carracedo, A.; Guidet, F.; Luque, J.A.; Lessig, R.; Mayr, W.R.; Pascali, V.L.; Prinz, M.; et al. ISFG: Recommendations on biostatistics in paternity testing. *Forensic Sci. Int. Genet.* **2007**, *1*, 223–231. [CrossRef]
31. Amorim, A.; Crespillo, M.; Luque, J.A.; Prieto, L.; Garcia, O.; Gusmão, L.; Aler, M.; Barrio, P.A.; Saragoni, V.G.; Pinto, N. Formulation and communication of evaluative forensic science expert opinion—A GHEP-ISFG contribution to the establishment of standards. *Forensic Sci. Int. Genet.* **2016**, *25*, 210–213. [CrossRef]
32. Kling, D.; Mostad, P.; Tillmar, A. FamLink2–A comprehensive tool for likelihood computations in pedigrees analyses involving linked DNA markers accounting for genotype uncertainties. *Forensic Sci. Int. Genet.* **2025**, *74*, 103150. [CrossRef]
33. Kruijver, M. Characterizing the genetic structure of a forensic DNA database using a latent variable approach. *Forensic Sci. Int. Genet.* **2016**, *23*, 130–149. [CrossRef]
34. Ramos, D.; Gonzalez-Rodriguez, J. Reliable support: Measuring calibration of likelihood ratios. *Forensic Sci. Int.* **2013**, *230*, 156–169. [CrossRef]
35. Thompson, E. Gene identities and multiple relationships. *Biometrics* **1974**, *30*, 667–680. [CrossRef]
36. Cox, D.R. *The Theory of Stochastic Processes*; Routledge: London, UK, 2017.
37. Abecasis, G.R.; Cherny, S.S.; Cookson, W.O.; Cardon, L.R. Merlin—Rapid analysis of dense genetic maps using sparse gene flow trees. *Nat. Genet.* **2002**, *30*, 97–101. [CrossRef] [PubMed]
38. Ingolfsdottir, A.; Gudbjartsson, D. Genetic linkage analysis algorithms and their implementation. In *Transactions on Computational Systems Biology III*; Springer: Berlin/Heidelberg, Germany, 2005; pp. 123–144. [CrossRef]
39. Halldorsson, B.V.; Palsson, G.; Stefansson, O.A.; Jonsson, H.; Hardarson, M.T.; Eggertsson, H.P.; Gunnarsson, B.; Oddsson, A.; Halldorsson, G.H.; Zink, F.; et al. Characterizing mutagenic effects of recombination through a sequence-level genetic map. *Science* **2019**, *363*, eaau1043. [CrossRef] [PubMed]
40. Vigeland, M.D. Relatedness coefficients in pedigrees with inbred founders. *J. Math. Biol.* **2020**, *81*, 185–207. [CrossRef] [PubMed]
41. Guo, S.W. Proportion of genome shared identical by descent by relatives: Concept, computation, and applications. *Am. J. Hum. Genet.* **1995**, *56*, 1468.
42. Guo, S.W. Variation in genetic identity among relatives. *Hum. Hered.* **1996**, *46*, 61–70. [CrossRef]
43. Vigeland, M.D. Two-locus identity coefficients in pedigrees. *G3* **2023**, *13*, jkac326. [CrossRef]
44. Rabiner, L.R. A tutorial on hidden Markov models and selected applications in speech recognition. *Proc. IEEE* **1989**, *77*, 257–286. [CrossRef]

45. Cox, D.R. Regression models and life-tables. *J. R. Stat. Soc. Ser. B (Methodol.)* **1972**, *34*, 187–202. [CrossRef]
46. Klein, J.P.; Moeschberger, M.L. *Survival Analysis: Techniques for Censored and Truncated Data*; Springer Science & Business Media: Berlin/Heidelberg, Germany, 2006.

MDPI AG
Grosspeteranlage 5
4052 Basel
Switzerland
Tel.: +41 61 683 77 34

Genes Editorial Office
E-mail: genes@mdpi.com
www.mdpi.com/journal/genes

Academic Open
Access Publishing

mdpi.com

ISBN 978-3-7258-8846-7